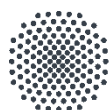


Cooperative Polymerization Catalysis of *O*-Heterocyclic Monomers



University of Stuttgart
Germany

Von der Fakultät Chemie der Universität Stuttgart
zur Erlangung der Würde eines
Doktors der Naturwissenschaften (Dr. rer. nat.)
genehmigte Abhandlung

vorgelegt von
Patrick Walther
aus Rutesheim

Hauptberichter: Prof. Dr. M. R. Buchmeiser

- 1. Mitberichter:** Prof. Dr. S. Laschat
- 2. Mitberichter:** Prof. Dr. B. Hauer

Tag der mündlichen Prüfung:
04.11.2020

Institut für Polymerchemie der Universität Stuttgart
2020

*„Most people say that it is the intellect which makes a great scientist.
They are wrong: it is character.“ – Albert Einstein*

This work was carried out from January 2017 to March 2020 at the Institute of Polymer Chemistry (University of Stuttgart, Germany) under the supervision of Dr. S. Naumann and Prof. Dr. M. R. Buchmeiser.

Selbstständigkeitserklärung

Hiermit versichere ich, die vorliegende Arbeit mit dem Titel *Kooperative Polymerisationskatalyse von O-Heterozyklischen Monomeren* selbständig verfasst, keine anderen als die angegebenen Quellen benutzt und alle wörtlich oder sinngemäß aus anderen Werken übernommenen Aussagen als solche gekennzeichnet zu haben. Das elektronische Exemplar stimmt mit den anderen Exemplaren überein.

Stuttgart, den 16. November 2020

Declaration of Authorship

I hereby assure that I have independently written the present work with the title *Cooperative Polymerization Catalysis of O-Heterocyclic Monomers*, that I have not used any other sources than those indicated, and that I have marked as such all statements taken literally or analogously from other works. The electronic copy agrees with the other copies.

Stuttgart, 16 November 2020

Acknowledgements

Zunächst gilt mein Dank meinem Doktorvater *Herrn Prof. Dr. M. R. Buchmeiser* und meinem Betreuer *Herrn Dr. S. Naumann*, die es mir ermöglichten diese Doktorarbeit anzufertigen. Vor allem für die herausragenden Arbeitsbedingungen, die Möglichkeit an zahlreichen Tagungen teilzunehmen und dort Poster zu präsentieren, die Unterstützung bei der Anfertigung von Publikationen, sowie für den stets fairen und aufrichtigen gegenseitigen Umgang möchte ich mich besonders bedanken. Ebenfalls möchte ich mich bei *Prof. Dr. S. Laschat* und *Prof. Dr. B. Hauer* für die Übernahme des Zweitgutachtens bzw. des Prüfungsvorsitzes bedanken.

Dank gebührt auch *Dongren Wang*, der unzählige MALDI-ToF MS Spektren gemessen hat und auf den immer Verlass war, wenn man bei der Instandhaltung eines Geräts nichtmehr weiterwusste.

Ich möchte mich ganz herzlich bei allen ehemaligen und aktuellen Mitgliedern der Arbeitskreise *Naumann* und *Buchmeiser* bedanken, die meine Promotion zu einer unvergesslichen Zeit gemacht haben. Begonnen mit *Iris*, für das kontinuierliche Testen meiner Fähigkeiten im Beseitigen von Horkruxen, für das Korrekturlesen dieser Arbeit und für selbstlose Hilfe in allen Belangen. *Kai*, der so weit wie möglich geflüchtet ist und trotzdem immer für Joggingsimulationen zur Stelle war. *Melita*, mit der meine synthetischen Fähigkeiten (untermalt von Backstreet Boys) zu Höchstformen aufliefen. Dem höchstwahrscheinlich narkoleptischen *Hagen*, für unzählige überhagende Backabende im Onese. *Flex*, für garantiert gute Stimmung in Labor und Büro, sowie für die tägliche Dosis Literaturrecherche. *Felix* für das agieren als Personal Trainer, andorianischer Zwerg und das Gewähren von Back-Asyl. Seiner Durchlauchtheit *Jonas*, gelegentlicher Trainingspartner, der immer alles bei Klimmzügen und Freundschaften gibt. *Mathé*, die Gabel Gottes, für Binokel- und Backabende sowie für kompetente Beratung in Synthesefragen. *Alex*, für rege Diskussionen über neue Chapter, inklusive detailgenauer Analyse und Aufstellung von Theorien. *Philipp*s (des macht garnix), *Julian* (Tschorle), *Alina*, *Charly*, *Ayla* und dem Rest der feierwütigen Bande. Ihr seid alle das Herz des AKs, bleibt so wie ihr seid und lernt endlich die Kaffeemaschine zu leeren :). Danke an meine betreuten Studenten *Annabelle* („sooooo“), *Ivan* (alles klar Chef), *Nils* und *Tamara* für die entspannte Zusammenarbeit.

Vielen Dank auch an meine Kommilitonen *Asli*, *Pascal* und *Manne*, für einen wöchentlichen Grund der Mensa zu entfliehen und die neuesten Infos auszutauschen. Besonders bedanken möchte ich mich bei meiner ehemaligen Stufe – *Turner*, *Ebu*, *Schaber*, *Luther*, *Bohne*, *Voke*, *Ox*, *Schami*, *Fabse*, *Johann*, *Nasti*, *Alena*, *Viki*, *Vanessa*, *Sofia*, *Nina*, *Kerstin*, *Ela*, vielen Dank für Feierabendbierchen, alljährliche Ausflüge und die Freundschaft über all die Jahre.

Zu guter Letzt möchte ich mich bei *meiner Familie* bedanken, deren vollste Unterstützung mich auch in schwierigen Zeiten immer wieder motiviert hat. Ebenfalls danke ich in diesem Zuge *Annika*. Ich hätte mir keinen besseren Corona-buddy wünschen können, danke für deine Wertschätzung und Unterstützung.

Table of Contents

Acknowledgements	VII
Table of Contents	IX
List of Abbreviations	XI
Objective	XV
Kurzfassung	XVII
Abstract	XXIII
Summary	XXIX
1. Theory and Background	
1.1. Ring-Opening Polymerization	3
1.1.1. Introduction.....	3
1.1.2. Thermodynamic Considerations	4
1.1.3. Kinetic Considerations	12
1.1.4. General Polymerization Mechanisms of ROP	20
1.2. Lewis Pair Polymerization.....	26
1.2.1. Historical Remarks	26
1.2.2. Introduction.....	27
1.2.3. Lewis Pair catalysed Polymerizations	30
1.3. N-Heterocyclic Olefins	39
1.3.1. Introduction.....	39
1.3.2. Synthetic Methods, Rationale of Design and Distinctive Features of NHOs	40
1.3.3. Catalytic Transformations Mediated by NHOs.....	45
1.3.4. N-Heterocyclic Olefins as Ligands in Complexes	51
2. Ring-Opening Polymerization of Lactones	
2.1. Introduction	59
2.2. Mechanisms.....	60
2.2.1. Coordination – Insertion Mechanism	60
2.3. Initiators	61
2.3.1. Metal Alkoxides	61

2.3.2.	Well-Defined Metal Complexes.....	63
2.3.3.	Organocatalysts	66
2.3.4.	Enzymes.....	70
2.3.5.	Other Initiating Systems	71
2.3.6.	Polymerizations mediated by Lewis Pairs	72
2.4.	Publications.....	77
3.	Ring-Opening Polymerization of Epoxides	
3.1.	Introduction	147
3.2.	Catalytic Systems.....	149
3.2.1.	Oxyanionic ROP	149
3.2.2.	Coordination Polymerization	151
3.2.3.	Activated Monomer Mechanism	154
3.2.4.	N-Heterocyclic Carbenes	155
3.2.5.	N-Heterocyclic Olefins.....	157
3.2.6.	Phosphazenes.....	158
3.2.7.	Double Metal Cyanide Catalysis.....	159
3.2.8.	Cationic Systems	162
3.3.	Publications.....	163
4.	Appendix	
4.1.	References.....	191

List of Abbreviations

[M] _{eq}	<i>Monomer Concentration at Equilibrium</i>
2-VP.....	<i>2-Vinylpyridine</i>
ACE.....	<i>Activated Chain-End</i>
AGE.....	<i>Allyl Glycidyl Ether</i>
AM.....	<i>Activated Monomer</i>
AN.....	<i>Acceptor Number</i>
aNHC.....	<i>Abnormal NHC</i>
aROP.....	<i>Anionic Ring-Opening Polymerization</i>
BBL.....	<i>β-Butyrolactone</i>
BnOH.....	<i>Benzyl Alcohol</i>
BO.....	<i>Butylene Oxide</i>
c.....	<i>Crystalline</i>
C _{exo}	<i>Exocyclic Carbon Atom</i>
CL.....	<i>ε-Caprolactone</i>
cROP.....	<i>Cationic Ring-Opening Polymerization</i>
DABCO.....	<i>1,4-Diazabicyclo[2.2.2]octane</i>
DBU.....	<i>1,8-Diazabicyclo(5.4.0)undec-7-ene</i>
DMAP.....	<i>4-Dimethylaminopyridine</i>
DMC.....	<i>Double Metal Cyanide</i>
DP.....	<i>Degree of Polymerization</i>
DP _n	<i>Number Average Degree of Polymerization</i>
DPP.....	<i>Diphenyl Phosphate</i>
EAM.....	<i>Enzyme-Activated Monomer</i>
EC.....	<i>Ethylene Carbonate</i>
ECH.....	<i>Epichlorohydrine</i>
EISA.....	<i>Evaporation-Induced Self-Assembly</i>
Et ₂ O.....	<i>Diethyl Ether</i>
FIA.....	<i>Flouride Ion Affinity</i>
FLP.....	<i>Frustrated Lewis Pair</i>
GBL.....	<i>γ-Butyrolactone</i>

GEI	<i>Global Electrophilicity Index</i>
GPC-MALLS.....	<i>Gel Permeation Chromatography - Multiangle Laserlight Scattering</i>
<i>h</i>	<i>Planck Constant</i>
HIA	<i>Hydride Ion Affinity</i>
HMDS.....	<i>Hexamethyldisilazide</i>
HOTf.....	<i>Trifluoromethanesulfonic Acid</i>
HSAB.....	<i>Hard and Soft Acids and Bases</i>
IL	<i>Ionic Liquid</i>
IMes.....	<i>1,3-bis(2,4,6-trimethylphenyl)imidazol-2-ylidene</i>
K	<i>Equilibrium Constant</i>
k_b	<i>Boltzman Constant</i>
K_D	<i>Equilibrium Constant of Dissociation</i>
KH.....	<i>Potassium Hydride</i>
l	<i>Liquid</i>
LA.....	<i>Lewis Acid</i>
LAC	<i>Lactide</i>
LB.....	<i>Lewis Base</i>
LPP	<i>Lewis Pair Polymerization</i>
MA	<i>Maleic Anhydride</i>
MALDI-ToF MS.....	<i>Matrix Assisted Light Desorption Ionization - Time of Flight</i>
MeI	<i>Methyl Iodide</i>
MEP	<i>Molecular Electrostatic Potential</i>
Mes ^F ₂ BF.....	<i>Bis[2,4,6-tris-(trifluoromethyl)phenyl]boron Fluoride</i>
NCA	<i>N-Carboxy Anhydride</i>
NH ₄ BF ₄	<i>Ammonium Tetrafluoroborate</i>
NHO.....	<i>N-Heterocyclic Olefin</i>
PA	<i>Proton Affinity</i>
PDL.....	<i>ω-Pentadecalactone</i>
PE.....	<i>Polyethylene</i>
PEG	<i>Polyethylene Glycol</i>
PEO.....	<i>Polyethylene Oxide</i>
PET	<i>Polyethylene Terephthalate</i>
PMP	<i>1,2,2,6,6-Pentamethylpiperidine</i>
PO	<i>Propylene Oxide</i>

PP.....	<i>Polypropylene</i>
PPO.....	<i>Polypropylene Oxide</i>
PVC.....	<i>Polyvinylchloride</i>
ROMP.....	<i>Ring-Opening Metathesis Polymerization</i>
ROP.....	<i>Ring-Opening Polymerization</i>
R_p	<i>Polymerization Rate</i>
rROP.....	<i>Radical Ring-Opening Polymerization</i>
SDAs.....	<i>Structure-Directing Agents</i>
SEC.....	<i>Size-Exclusion Chromatography</i>
sIMes.....	<i>1,3-bis(2,4,6-trimethylphenyl)-4,5-dihydroimidazol-2-ylidene</i>
Sn(Oct) ₂	<i>Tin(II)-2-Ethylhexanoate</i>
S _N Ar.....	<i>Nucleophilic Substitution in Aromatic Systems</i>
T_c	<i>Ceiling Temperature</i>
T_f	<i>Floor Temperature</i>
T_g	<i>Glass-Transition Temperature</i>
THF.....	<i>Tetrahydrofuran</i>
T_i	<i>Temperature of Inversion</i>
TON.....	<i>Turn-Over-Number</i>
TPT.....	<i>1,3,4-Triphenyl-4,5-dihydro-1H-1,2,4-triazol-5-ylidene</i>
VL.....	<i>δ-Valerolactone</i>
α	<i>Fraction of Free Ions</i>

Objective

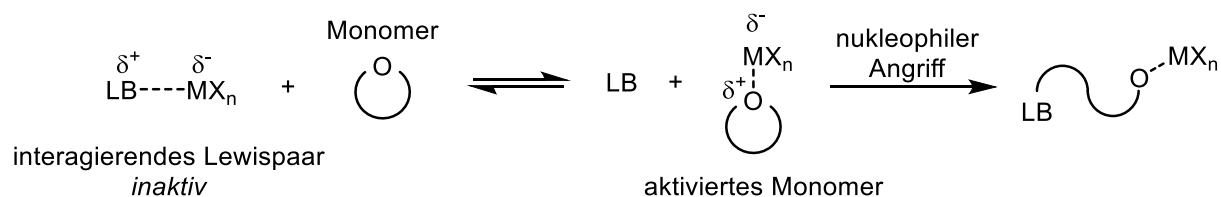
Polymeric materials, colloquially referred to as plastics, have long since established themselves in everyday life, to a point where the current age is referred to as “the age of plastics”. Indeed, with a scale of about 360 million metric tons in world-wide annual production,¹ the plastic industry easily places itself amongst the major industries world-wide. Its ubiquitous products range from so-called commodity plastics (polyolefins like polyethylene, polypropylene or polyvinylchloride), to more specialized polymers or engineered plastics like polyesters and polyamides. A significant proportion of the latter is generated *via* ring-opening polymerization (ROP),¹ paradigmatically exemplified by the preparation of Nylon®-6. This polyamide is synthesized by the ROP of ϵ -caprolactam, a seven-membered lactam, which was first reported as early as 1938. The process of understanding the underlying kinetics and mechanisms of ROP, however, continues to this day. This also entails the development of novel procedures and catalytic systems for other cyclic monomers. The prime challenge for the ROP of cyclic monomers, as also true for any other chemical transformation, is to develop a cheap catalytic system with broad applicability, that is also readily available and easily tunable. Of course, this poses a major task which will most likely not conclusively be resolved for years to come. Nevertheless, one promising approach to address multiple of the above-mentioned issues, is to apply dual catalysis. In such a setup, several components interact in a cooperative manner to achieve the desired chemical transformation, in this case polymerization. The purpose of this work was to contribute to the cooperative polymerization catalysis of *O*-heterocyclic monomers by the application of so-called *N*-heterocyclic olefins (NHOs), assisted by simple Lewis Acids (LAs) to form a dual catalytic setup. This combination utilizes the Lewis acidity to coordinate onto heterocyclic monomers, which decreases their electron density and renders them susceptible to nucleophilic attacks by either the NHO or an initiator. Both the structure of the LA and the NHO play a pivotal role in affecting the electronic situation of the monomer and the resulting nucleophilic attack. This presents oneself with a tool to directly influence not only polymerization kinetics and

¹ Source: Plastics – The facts 2019, page 14.
https://www.plasticseurope.org/application/files/1115/7236/4388/FINAL_web_version_Plastics_the_facts2019_14102019.pdf (accessed 17.01.2020).

copolymerization parameters, but also the underlying polymerization mechanism itself. It was thus envisioned, that by screening different LAs and NHO combinations, a conclusive study of the fundamental influences could be obtained, leading to a better understanding of the structure-effect relationship in the described catalytic system. To realize this, different NHOs were designed and synthesized according to literature-known procedures. LAs of varying structure, ranging from inorganic, mono- and polyvalent salts like LiCl, MgCl₂ or YCl₃ to organic salts like KHMDS (HMDS = Hexamethyldisilazide) were examined as potential cocatalysts.

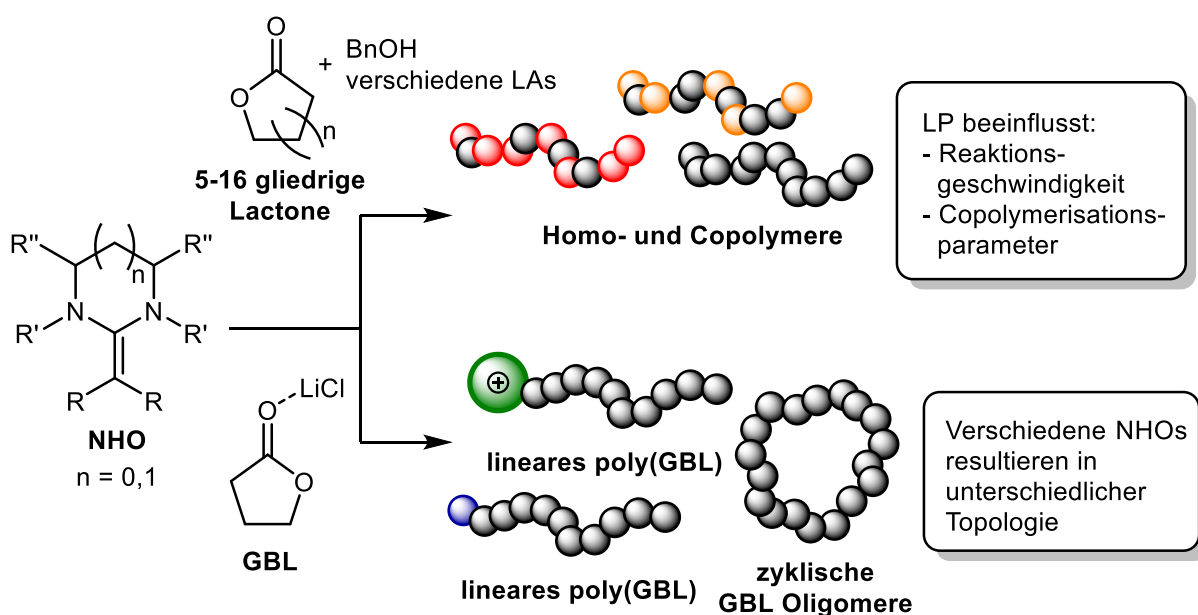
Kurzfassung

Die Technik der ringöffnenden Polymerisation (ROP) kann zur Polymerisation eines breiten Monomerspektrums eingesetzt werden. Neben zyklischen Alkanen und Alkenen sind es vor allem die heteroatomaren, zyklischen Monomere wie Ether (Epoxide), Ester (Lactone) oder Amide (Lactame), die Kunststoffe mit faszinierenden Materialeigenschaften hervorbringen. Jedoch stellen explizit diese Heteroatome die verwendeten Katalysatorsysteme vor Herausforderungen während der Polymerisation. Deshalb werden oft hochspezialisierte Katalysatoren eingesetzt, die auf die spezifischen Anforderungen des jeweiligen Monomers angepasst wurden. Es wäre daher erstrebenswert ein Katalysatorsystem zu entwickeln, welches in der Lage ist mehrere Monomerklassen effizient zu polymerisieren, ohne dabei gravierende Änderungen am System vornehmen zu müssen. Hier bietet sich das Konzept der dualen Katalyse an, welches zwei (oder mehr) katalytisch aktive Substanzen enthält, die unabhängig voneinander ausgetauscht werden können. Die dadurch erreichte Flexibilität erlaubt es, durch marginale Änderungen das System an neue Monomere und Monomerklassen anzupassen.² Das in dieser Arbeit entwickelte System besteht aus einer Lewis-Base (LB) in Form eines *N*-heterozyklischen Olefins (NHO), einem optionalen Initiator (Benzylalkohol, BnOH) und einer simplen Lewis-Säure (LA) wie z.B. LiCl, MgCl₂ oder YCl₃. Die LA fungiert hierbei als monomeraktivierende Spezies, während das NHO die Polymerisation initiiert (entweder über Aktivierung des Initiators oder direkt). Dieses Konzept der dual katalysierten Polymerisation (Schema 1)³ wurde in einem ersten Projekt dazu verwendet, verschiedene Lactone zu (co)polymerisieren (γ -Butyrolacton (GBL, 5-gliedrig), δ -Valerolacton (VL, 6-gliedrig), ϵ -Caprolacton (CL, 7-gliedrig), ω -Pentadecalacton, (PDL, 16-gliedrig)).⁴ Die Co- und Homopolymerisation verlief problemlos (z.B. PDL: 85 - 97 % Umsatz, PDL-*co*-GBL:



Schema 1: Konzept der Lewispaar Polymerisation (LPP). Das System steht in einem Gleichgewicht zwischen einer inaktiven Spezies, dem interagierenden Lewispaar (LP) (links), und der monomeraktivierten Spezies (Mitte), welches den nukleophilen Angriff begünstigt (rechts).

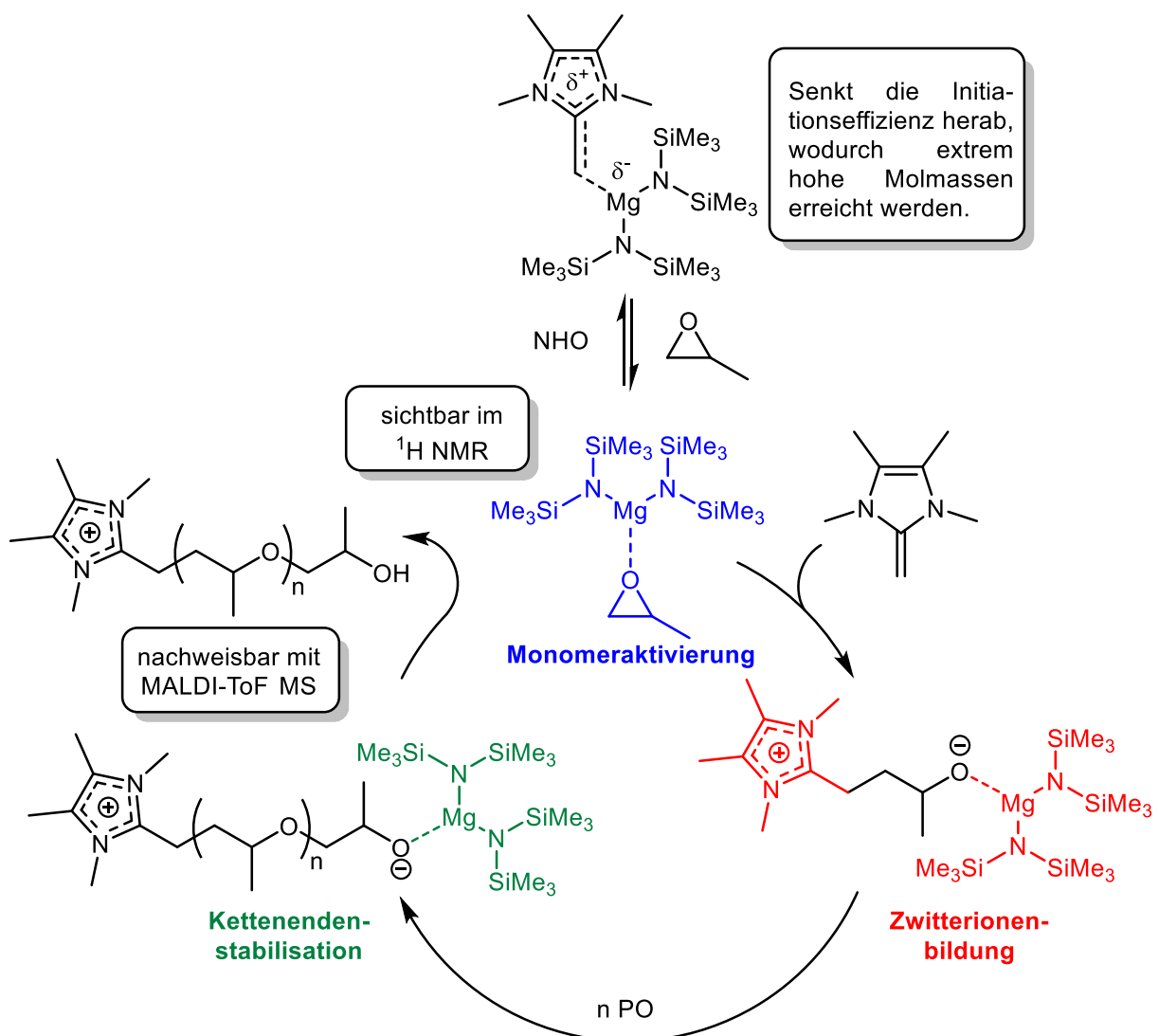
15 - 50 % Umsatz, bis zu 22 % GBL-Gehalt im Copolymer laut ^{13}C NMR Analysen). Hierbei werden die Polymerisationsgeschwindigkeit und Copolymerisationsparameter maßgeblich vom verwendeten LP beeinflusst wurden (Geschwindigkeiten: 0 bis >80 % Umsatz nach 15 min; Parameter: 7 - 50 % PDL Einbau in einem PDL-*c*-CL Copolymer je nach LA). Bemerkenswerterweise gelang sogar die Copolymerisation von GBL mit dessen Comonomeren bei erhöhten Temperaturen (100 °C), obwohl die Homopolymerisation von GBL eine extrem niedrige „Ceiling-Temperatur“ (T_c ; -136 °C bei 1 M) besitzt.⁵ Die niedrige T_c , zusammen mit der Tatsache, dass der Ringschluss eines propagierenden, geöffneten GBLs thermodynamisch stark begünstigt ist, ist der Grund, weshalb GBL bis vor kurzem dafür berüchtigt war, nicht polymerisierbar zu sein. Dass geeignete Methoden sich jedoch auf die „superbasische“ Reaktivität von Phosphazenen beschränkten, motivierte uns, das hier präsentierte Katalysatorsystem auf dessen Fähigkeit Homopolymere aus GBL herzustellen, zu untersuchen (Schema 2).⁶ LA-freie Ansätze die bei -36 °C in Substanz mit NHO und BnOH als Initiator durchgeführt wurden, führten zu einem Umsatz von bis zu 70 % von GBL, mit katalytischen Produktivitäten (turn-over number, TONs) von 140 - 230. Jedoch zeigten MALDI-ToF MS Messungen, dass ein großer Teil des generierten Polymers zyklische Strukturen aufwies. Die Bildungstendenz dieser zyklischen Polymere konnte durch Verwendung von



Schema 2: In dieser Arbeit entwickelter, dualkatalytischer Ansatz zur Lactonpolymerisation. Für exakte NHO Strukturen, siehe Scheme 5 und Scheme 7.

Lithiumsalzen (LiX, X = Cl, I, OTf) abgeschwächt werden. Des Weiteren waren drei verschiedene Polymerisationsmodi adressierbar, wenn kein protischer Initiator (BnOH) verwendet wurde. a) Stark nukleophile NHOs (z.B. 1,3,4,5-Tetramethyl-2-Methylidenimidazol) bilden nach einem direkten nukleophilen Angriff ein stabiles Zwitterion, welches in einer inhärent kationisierten NHO-basierten Endgruppe im Polymer resultiert. b) Weniger nukleophile NHOs mit sterisch anspruchsvollen Substituenten (1,3-Dimesityl-2-Methylidentetrahydropyrimidin) bilden noch immer Zwitterionen; durch den sterischen Anspruch ist die NHO-basierte Endgruppe jedoch anfällig für Substitutionen, was eine makrozyklische poly(GBL) Topologie begünstigt. c) Stark basische, sterisch gehinderte NHOs (1,3,4,5-Tetramethyl-2-Isopropylidenimidazol) deprotonieren GBL, wodurch ein Enolat gebildet wird welches wiederum eine „traditionelle“ anionische Polymerisation initiiert. Generell ordneten sich die molaren Massen der generierten Polymere im niederen polymeren, bzw. hohen oligomeren Bereich ein ($1000 - 9000 \text{ g}\cdot\text{mol}^{-1}$, GPC), wobei LA-freie Ansätze signifikant höhere Umsätze erreichten als solche mit Lithiumsalz. Diese Resultate suggerierten bereits, dass das entwickelte dualkatalytische System bei gleichbleibender Effizienz auf ein breites Monomerspektrum anwendbar ist. Deshalb wurden als nächste Monomere substituierte Epoxide verwendet, deren Polymerisationen starke Einschränkungen in Bezug auf Nebenreaktionen, Reaktionsgeschwindigkeiten und Molmassen aufwiesen.⁷ Obwohl die NHO-basierte anionische Polymerisation bereits zu einer Reduktion der Nebenreaktionen führte blieb der erhoffte Durchbruch in Molmassen und Reaktionsgeschwindigkeiten bislang aus.⁸ Hier versprach der zwitterionische Mechanismus, der bereits in der Lactonpolymerisation erfolgreich angewandt werden konnte, Abhilfe zu schaffen: Frühe, nicht optimierte Versuche zeigten, dass eine direkte Ringöffnung eines aktivierten Propylenoxids (PO) durch einen NHO möglich ist (die Aktivierung wurde hierbei durch Wasserstoffbrückenbindungen mit BnOH erreicht). Da dies dem Ansatz der dualen Katalyse schon sehr nahekommt, wurde vermutet, dass es möglich ist speziell diesen Reaktionsmechanismus mit einem geeigneten LP zu adressieren. Dies war in der Tat unter der Verwendung von Magnesium(bis-hexamethyldisilazid) ($\text{Mg}(\text{HMDS})_2$) möglich, wodurch Polyether mit Molmassen von bis zu $10^6 \text{ g}\cdot\text{mol}^{-1}$ (bestimmt über Gelpermeationschromatographie, GPC) hergestellt werden konnten.⁹ Die Darstellung von Molmassen dieser Größenordnung durch die ROP von PO war bislang nicht möglich. Realisierbar wurde das durch die extrem starke Aktivierung

des Monomers durch $\text{Mg}(\text{HMDS})_2$, welche sich in einer signifikanten Tieffeldverschiebung der Monomersignale um ca. 0.60 ppm im ^1H NMR Spektrum äußern. Auch das charakteristische Kopplungsmuster im ^1H NMR Spektrum von $\text{Mg}(\text{HMDS})_2$ änderte sich quantitativ: Die beiden Singulets, welche durch die in Lösung vorliegende dimere Spezies von $\text{Mg}(\text{HMDS})_2$ verursacht werden, verschwanden und das breite Signal der monomeren Spezies wurde zu einem scharfen Singulett, welches um ca. 0.15 ppm in Richtung Tieffeld verschoben wurde. Um den Mechanismus aufzuklären wurden niedermolekulare PPO Proben synthetisiert und mittels MALDI-ToF MS analysiert. Dies erlaubte es, NHO-basierte

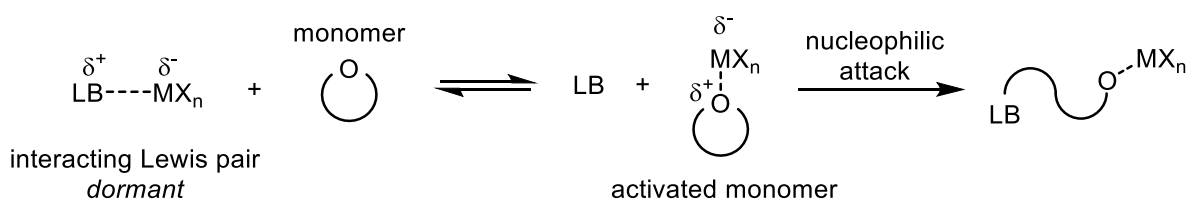


Schema 3: Postulierter Polymerisationsmechanismus von PO. Das LP $\text{NHO}/\text{Mg}(\text{HMDS})_2$ entfernt freies NHO aus der Polymerisationsmischung, wodurch die Initiations-effizienz herabgesenkt wird, was zu einem höheren effektiven Verhältnis von $\text{NHO}:\text{Monomer}$ führt. Das Monomer wird durch die Aktivierung mittels $\text{Mg}(\text{HMDS})_2$ anfällig für den nukleophilen Angriff des NHO s (blau), was zu NHO -basierten Endgruppen und einer Zwitterionenbildung führt (rot). Während der Polymerisation ist es wahrscheinlich, dass die LA sich in räumlicher Nähe zum propagierenden Kettenende aufhält, wodurch dessen Basizität herabgesenkt wird und Nebenreaktionen unterdrückt werden (grün).

Endgruppen zu verifizieren wobei die gefundenen Massen exzellent mit den berechneten übereinstimmten. Zusätzlich waren die hergestellten Proben immer noch mittels MALDI-ToF MS nachweisbar, obwohl das Natriumsalz während der Probenvorbereitung nicht zugesetzt wurde. Dies deutete stark auf eine inhärent geladene Spezies hin, welches sich mit der postulierten NHO-basierten Endgruppe decken würde. Diese Resultate ermöglichten, einen zwitterionischen Polymerisationsmechanismus zu postulieren (Schema 3). Um die Grenzen des katalytischen Systems auszuloten, wurde das Monomerspektrum um Butylenoxid (BO) und Allylglyzidylether (AGE) erweitert. In Bezug auf BO wurde eine deutlich herabgesenkte Reaktivität im Vergleich zu PO beobachtet, welche dem Verhalten von NHO-basierten BO Organopolymerisationen ähnelt^{8b} und Polymere mit einer molekularen Masse von 7000 - 21000 g·mol⁻¹ in Substanz generiert. Im Gegenteil dazu zeigt AGE eine vergleichbare Reaktivität zu PO, wobei Molmassen in derselben Größenordnung erhalten wurden. Ebenso konnten Copolymere generiert werden, wobei mittels ¹H/¹³C NMR Analysen kein Gradient nachgewiesen werden konnte, was auf die Bildung eines statistischen Copolymers hindeutet.

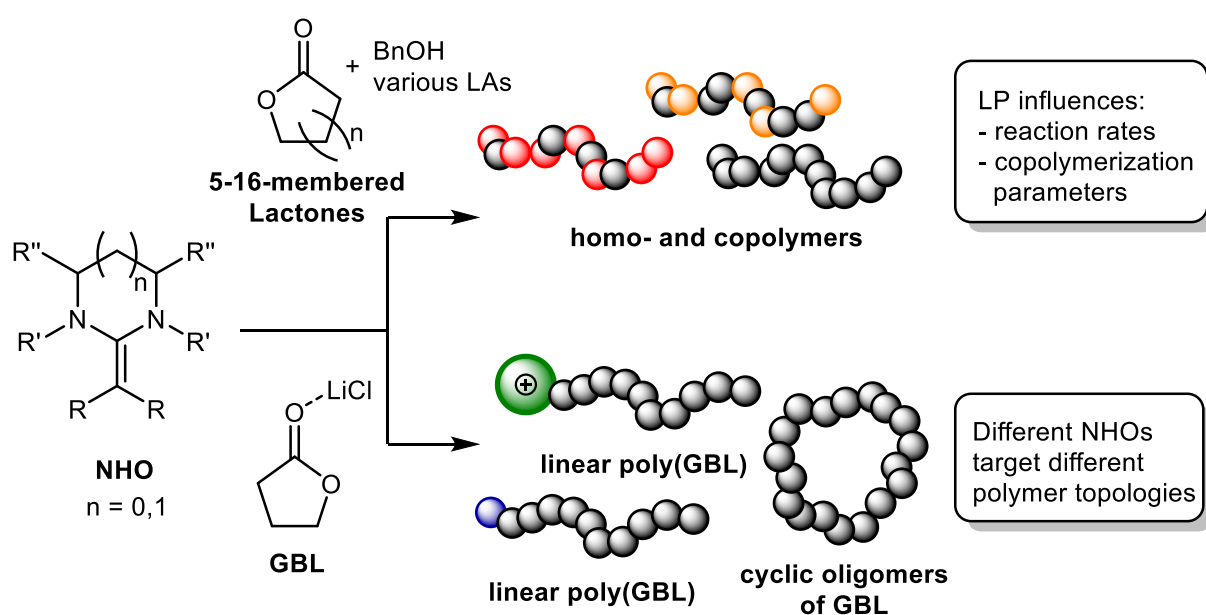
Abstract

An abundant range of polymers with intriguing material properties is accessible through the ring-opening polymerization (ROP) of cyclic, heteroatomic monomers. However, the pronounced electronegativity of these heteroatoms poses multiple challenges embodied by highly reactive intermediates or propagating chain ends. Thus, catalytic systems are often highly specialized setups that are only applicable to a fraction of available monomers. It would therefore be most desirable to develop a catalytic system, capable of polymerizing different monomer classes with only minuscule changes, while maintaining its efficiency. Here, the so-called dual catalysis offers a promising approach: since the catalytic setup is composed of two (or more) catalytically active compounds, both can be exchanged independently to address the demands of different monomers and even monomer classes.² In this work, the development of a catalytic system capable of polymerizing *O*-heterocyclic monomers (i.e. lactones and epoxides) is presented. The catalytic setup consists of a Lewis Base (LB), which is embodied by an *N*-heterocyclic olefin (NHO). The polymerizations were conducted together with simple Lewis Acids (LAs), such as LiCl, MgCl₂ or YCl₃, and, if needed, an initiator bearing a hydroxy moiety (i.e. benzyl alcohol, BnOH). This places the polymerization setup in the context of Lewis pair polymerizations (LPPs),³ whereby the LA acts as a monomer activating species and the LB (together with the initiator) initiates the polymerization (Scheme 1). In a first project,⁴ this setup was then subjected to multiple lactones (γ -butyrolactone (GBL, 5-membered), δ -valerolactone (VL, 6-membered), ϵ -caprolactone (CL, 7-membered) and ω -pentadecalactone (PDL, 16-membered)). The co- and homopolymerizations proceeded smoothly (e.g. PDL: 85 - 97 % conversion, PDL-*co*-GBL: 15 - 50 % conversion, up to 22 % GBL content according to ¹³C NMR spectroscopy), whereby the polymerization rates and copolymerization parameters



Scheme 1: General approach of Lewis pair polymerization (LPP). Note the equilibrium between the dormant, interacting Lewis pair (left) and the dissociated, monomer-activated species (middle) which facilitates the nucleophilic attack (right).

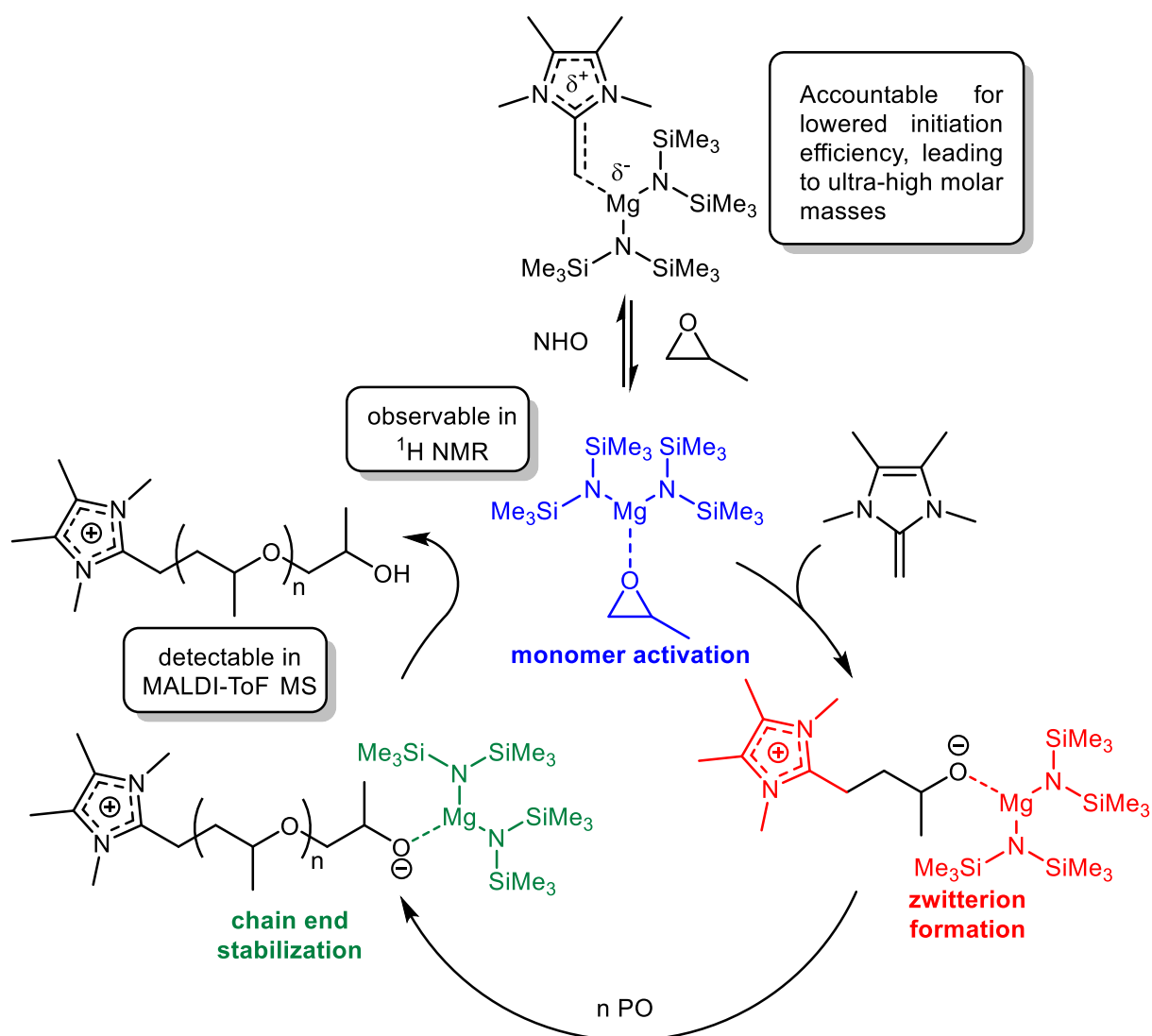
were significantly modulated by the applied LP (rates: 0 to >80 % conversion after 15 min; parameters: 7 to 50 % PDL incorporation in a PDL-*co*-CL copolymer, depending on the LA). Notably, the copolymerization of GBL with its comonomers succeeded even at elevated temperatures (100 °C), even though the homopolymerization of GBL requires an ultra-low ceiling temperature (T_c , -136 °C at 1 M).⁵ This, together with the fact, that the ring-closure of a propagating GBL-species back to its monomeric form is thermodynamically strongly favored, made GBL notorious for its non-polymerizability until recently. Since suitable methods to polymerize GBL *via* ROP are scarce and limited to “superbasic” mechanisms based on phosphazenes, this spurred us to investigate the ability of the catalytic setup presented herein to homopolymerize GBL.⁶ Metal-free polymerizations conducted at -36 °C in bulk, with NHO and BnOH as initiator, succeeded to convert up to 70 % of GBL into polymers, with turnover numbers (TONs) ranging from 140 - 230. However, a pronounced fraction of the polymer was determined to be cyclic by MALDI-ToF MS analyses. This was mitigated by applying lithium salts (LiX, X = Cl, I, OTf) as cocatalysts. Furthermore, without a protic initiator (BnOH) three different modes of operation were addressable during polymerization: a) highly nucleophilic NHOs (i.e. 1,3,4,5-tetramethyl-2-methylidene imidazole) form stable zwitterionic species *via* a direct nucleophilic attack of the NHO onto the monomer, resulting in an inherently charged, NHO-derived end group in the polymer.



Scheme 2: Dual catalytic approach to lactone polymerizations presented in this work. For exact NHO structures see Scheme 5 and Scheme 7.

b) Less nucleophilic, sterically encumbered NHOs (1,3-dimesityl-2-methylidene tetrahydropyrimidine) will still form zwitterions; however, the NHO-derived end group is susceptible to substitution, favoring a macrocyclic poly(GBL) topology. c) Strongly basic, sterically hindered NHOs (1,3,4,5-tetramethyl-2-isopropylidene imidazole) will deprotonate GBL and form enols, since a nucleophilic attack cannot be realized. This ensues a “traditional” anionic polymerization, initiated by enolized GBL. Overall, the resulting poly(GBL) ranged from low polymeric to high oligomeric molar masses ($1000 - 9000 \text{ g}\cdot\text{mol}^{-1}$, GPC), while metal-free setups achieved significantly higher conversions than those including lithium salts. These findings already suggested, that the herein presented dual catalytic setup is applicable to a broad range of monomers while retaining an excellent efficiency. This prompted us to refocus on substituted epoxides, a monomer class that suffered from severe limitations regarding side reactions, reaction rates and molar masses.⁷ NHO-based anionic polymerization was already able to foreclose side reactions,⁸ however the significant improvement of reaction rates and molar masses remained out of grasp. The zwitterionic polymerization mechanism, addressed during lactone polymerization, was regarded as a promising approach in this context. During preliminary studies, a high-molecular “impurity” was observed during the initial stages of the anionic polymerization. This was attributed to a nucleophilic attack of the NHO onto the monomer, which was slightly activated by H-bonding of the initiator (BnOH). As this already very much resembles the approach of dual catalysis, it was envisioned that it would be possible to exclusively address this zwitterionic mechanism by applying a suitable LP. Indeed, this was the case for various NHOs in combination with magnesium(hexamethyldisilazide) ($\text{Mg}(\text{HMDS})_2$), which succeeded in the preparation of poly(propylene oxide) (PPO) with molar masses up to $10^6 \text{ g}\cdot\text{mol}^{-1}$ as determined by gel permeation chromatography (GPC)/lightscattering.⁹ The molecular weights accessible using the catalytic system presented herein are unprecedented for polyethers derived from ROP of PO. This can be attributed to the strong monomer activation achieved by $\text{Mg}(\text{HMDS})_2$, which is observable by ^1H NMR analyses and is expressed by a significant downfield-shift of the monomer signals of about 0.60 ppm. Furthermore, the characteristic coupling pattern of $\text{Mg}(\text{HMDS})_2$ in the ^1H NMR spectrum also changed quantitatively: the two singlets corresponding to its dimeric species in solution disappeared, while the broad singlet of its monomeric species sharpened and experienced a downfield-shift of

about 0.15 ppm. In order to further elucidate the underlying mechanism, low-molecular weight PPO samples were prepared for MALDI-ToF MS analyses. This abetted us to verify NHO-derived end groups, with excellent fit of found and calculated masses. In addition, the prepared samples were also detectable in MALDI-ToF MS analyses, despite omitting a sodium salt during the sample preparation. This strongly hints towards an inherently charged species, as would be the case for the proposed NHO-derived end group. With these findings, we were able to propose a zwitterionic mechanism for PO polymerization (Scheme 3). The limitations of the catalytic system were mapped out by switching monomers from PO to butylene oxide

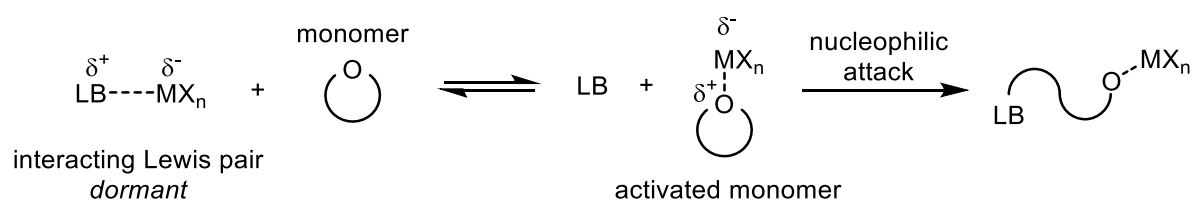


Scheme 3: Proposed polymerization mechanism of PO. The LP NHO/Mg(HMDS)₂ removes free NHO from the polymerization mixture, decreasing initiation efficiency which leads to a higher apparent NHO:monomer ratio. The monomer is rendered susceptible to nucleophilic attack via activation by Mg(HMDS)₂ (blue), leading to NHO-derived end groups and a zwitterion-formation (red). During the polymerization, the LA is likely in close proximity to the negative charge of the propagating chain end, reducing its basicity and thus mitigating side reactions (green).

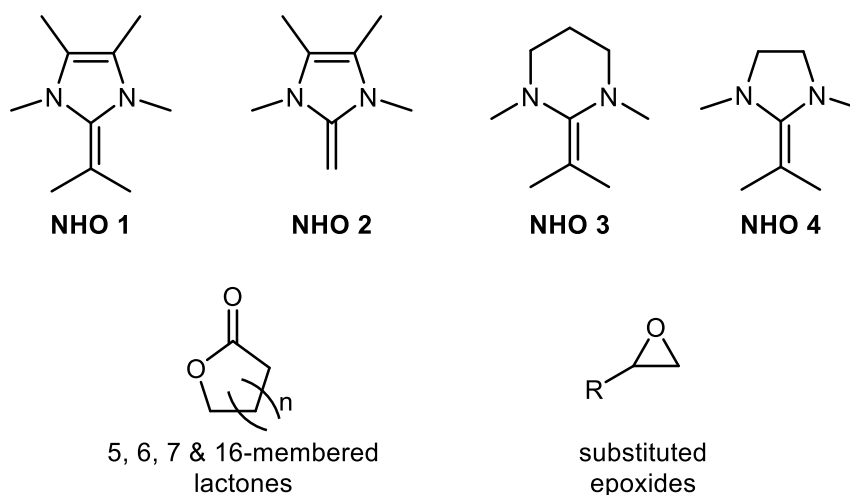
(BO) and allyl glycidyl ether (AGE). Regarding BO, a significantly reduced reactivity was observed when compared to PO, mirroring the behavior of NHO-based BO organopolymerization,^{8b} and generating polymers in bulk with molar masses ranging from 7000 - 21000 g·mol⁻¹. In contrast to BO, AGE displayed a reactivity similar to PO, with molecular weights in the same order of magnitude. Copolymerization reactions also succeeded in generating a random copolymer with no apparent gradient, as evidenced by ¹H/¹³C NMR analyses.

Summary

The technique of ring-opening polymerization (ROP) renders an abundant range of monomers accessible for polymerization. Amongst cyclic alkanes and alkenes, especially compounds containing heteroatoms such as cyclic ethers, esters, or amides give polymers with often intriguing material properties. However, specifically these heteroatoms frequently pose challenges during polymerization; their increased electronegativity often results in highly reactive intermediates or propagating species, which in turn promote side reactions and impair control over the reaction. Here, the approach of dual catalysis, embodied by the so-called Lewis pair polymerization (LPP)³ offers mitigation to these issues. *Via* a cooperative interaction between a Lewis Acid (LA)/Base (LB)-pair, the overall control over the reaction is increased, which results in higher reactivity, chemo- or regioselectivity and the inhibition of undesired side reactions. This is achieved by a complex interplay of LA and LB, whereby the LA will activate the polar monomer through coordination, facilitating the nucleophilic attack by the LB (Scheme 4). This dual catalytic setup benefits from another merit: since both components are independently adjustable, the versatile scope of this setup even encompasses different monomer classes, as presented herein. Moreover, this work aims to substantiate the broad monomer scope, and to gain further insights into the structure-reactivity relationship of different LPs and monomers. Therefore, several monomer classes and LP combinations, consisting of *N*-heterocyclic olefins (NHOs, LBs) and simple LAs, were addressed and their polymerizability was evaluated, whereby all monomers incorporated an oxygen-derived moiety in their cyclic structure (Scheme 5). Although neglected for almost three decades,¹⁰ NHOs represent a class of highly reactive, versatile and readily accessible organic molecules, whose efficiency as organic

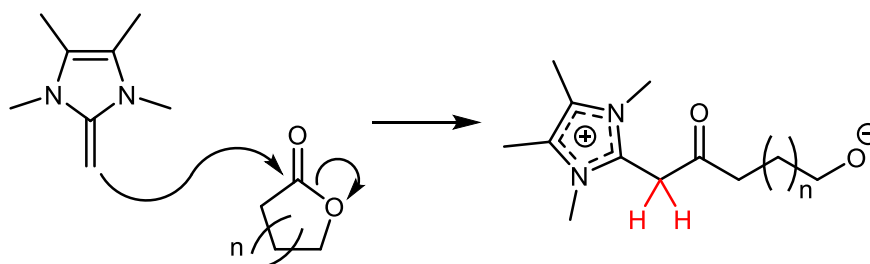


Scheme 4: General approach of Lewis pair polymerization (LPP). Note the equilibrium between the dormant, interacting Lewis pair (left) and the dissociated, monomer-activated species (middle) which facilitates the nucleophilic attack (right).



Scheme 5: chemical structure of typical NHOs applied in this study (top). *O*-heterocyclic monomers probed for polymerizability in this work (bottom).

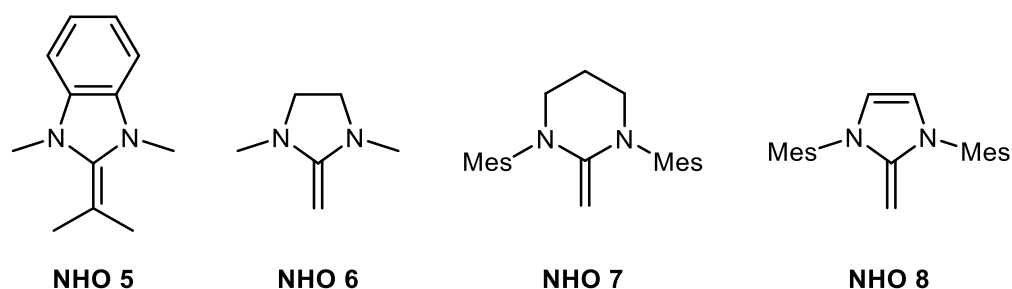
catalysts was only recently (re)discovered.^{2c, d, 8a, 11} One of their most striking features is the possibility to directly modify the reactive center, the exocyclic carbon atom, in a straightforward manner. Furthermore, changing from a saturated backbone (NHO 4, Scheme 5) to an unsaturated, imidazolium-derived heterocyclic structure (NHOs 1, 2, Scheme 5), brings about another conspicuous change: if an imidazolium-derived NHO is protonated, the charge delocalization will lead to an aromatization of the heterocycle, acting as a strong driving force and thus increasing overall reactivity of these compounds.¹² This was taken into consideration while designing NHOs for their herein intended use. For lactones, only NHOs with a dimethyl-substitution on their exocyclic carbon atom were deemed rewarding. This dimethyl-substitution precluded the direct nucleophilic attack of the NHO onto the monomer, which would result in undesired side-reactions like proton transfers *via* the formation of a zwitterionic species (Scheme 6).^{11g} During the initial studies presented in this work, a profound effect of the catalytic system (comprised of NHO, BnOH as co-initiator and LA) could be observed when subjected to lactone monomers: for the 16-membered ω -pentadecalactone (PDL), depending on the applied LP, about 95 % conversion could be achieved within an hour at a catalyst loading of 1 mol.-%, while retaining good control over the reaction ($D_M = 1.64$, $M_n = 23$ kDa). Intriguingly, control reactions without LA did not entail any monomer conversion over the monitored reaction time of 4 h. An exception from this was NHO 1 (Scheme 5), whose basicity appears to be high enough (*vide supra*) to deprotonate this lactone and form enolates, initiating polymerization (conv.: 40 %, $D_M = 1.52$, $M_n = 15$ kDa). Continuing



Scheme 6: Direct nucleophilic attack of the NHO onto a lactone monomer. Note the acidic protons (red) resulting from the formation of a zwitterionic species that are susceptible to deprotonation, resulting in the deactivation of this molecule. $n = 1, 2, 3, 12$.

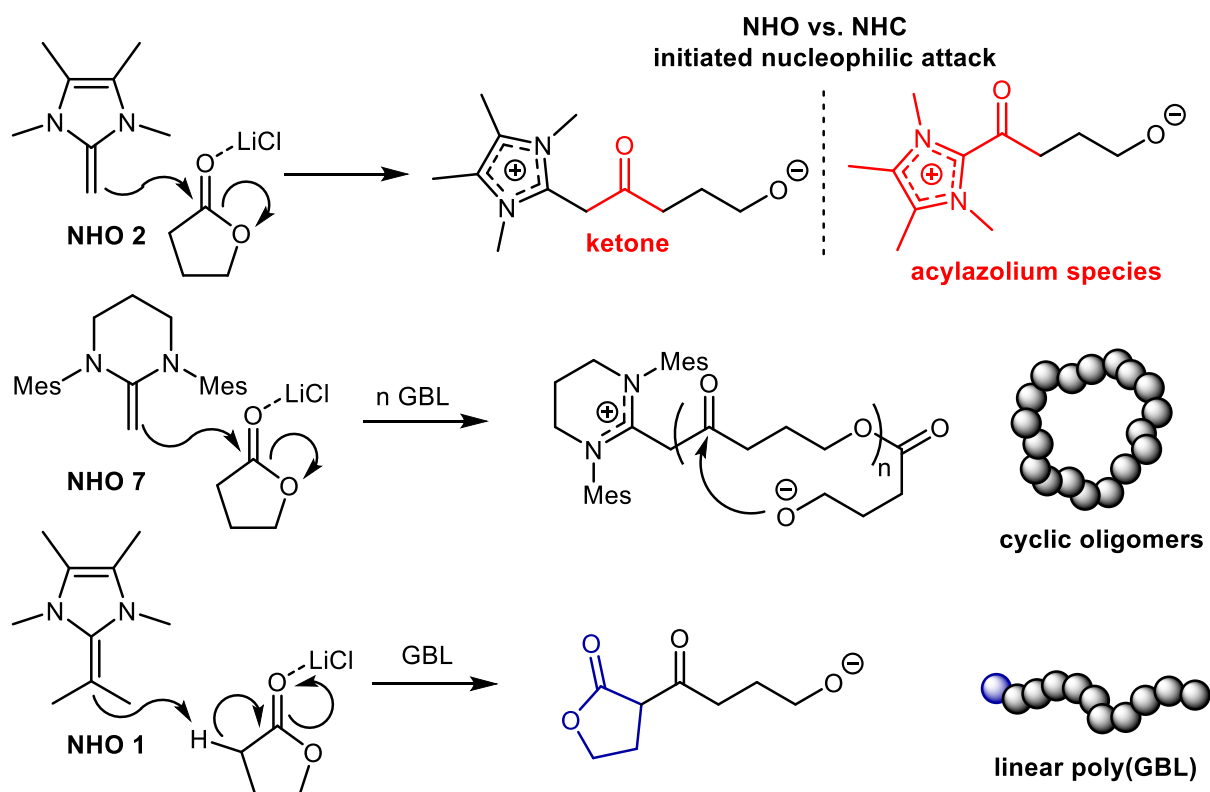
the efforts, the copolymerization of PDL with other lactones was investigated. Excitingly, not only did the copolymerization proceed very well-behaved ($D_M = 1.3$ - 2.1), even the copolymerization parameters could directly be influenced by simply changing the applied LA. Employing the tetrahydropyrimidine-derived NHO 3, the copolymerization of PDL and ϵ -caprolactone (CL) resulted in an incorporation of PDL between 7 % (LA = ZnI_2) and 50 % (LA = MgI_2). ^{13}C NMR analysis suggested a random copolymer structure in all experiments, while near quantitative conversion (97 %) was still retained after 4 h. Moving to δ -valerolactone (VL), this picture drastically changed: at 110 °C, only a sluggish conversion of the monomer mixture was observed, most probably attributable to the increased equilibrium concentration of VL at elevated temperatures.¹ Nevertheless, after applying a temperature step (8 h at 50 °C, then 24 h at 110 °C) during the reaction, a random copolymer structure could be realized using the LP NHO 3/ YCl_3 . Finally, to map out the limits of this catalytic setup concerning lactones, focus was shifted to γ -butyrolactone (GBL), a monomer that until recently was notorious for its non-polymerizability.^{5, 13} The copolymerization with PDL, CL and VL proceeded in a well-behaved manner and, again, showed to be strongly dependent on the applied LP. Once more, NHO 3 proved to be the most suitable NHO, and together with LiCl was able to incorporate 20 % GBL into a PDL-GBL copolymer, as determined by ^{13}C NMR. Strikingly, despite GBL's ultra-low ceiling temperature (T_c) of -136 °C (1 M),⁵ this incorporation was achieved at 100 °C during 24 h, again demonstrating the efficiency of dual catalysis. These intriguing findings spurred us to further investigate not only GBL as a comonomer, but rather the polymerization of GBL itself. As *Chen et al.*^{5, 13c, f} have shown, there is compelling reason to do so: polymers derived from GBL possess exciting material properties depending on their architecture (linear or cyclic), as they have proven to be fully thermally recyclable, as well as readily degradable. Furthermore, GBL itself can be acquired from renewable resources and is likely to

remain an abundantly available and cheap monomer. However, catalytic systems capable of achieving this feat remain scarce and often highly specialized, which is why an adaptable and readily accessible system as presented herein would be most desirable. Due to the difficulty of this task, the scope of the applied NHOs was drastically broadened. NHOs from Scheme 5 were complemented by NHOs depicted in Scheme 7, including saturated NHOs (NHOs 3, 4, 6, 7), imidazolium-derived structures (NHOs 1, 2, 5, 8), as well as compounds with a dimethyl-substitution on the exocyclic carbon atom (NHOs 1, 3, 4, 5). Furthermore, two compounds with *N,N'*-dimesityl-substitution (NHOs 7, 8) were investigated, to explore the effect of steric demand on the heterocyclic nitrogen atoms. In order to remain beneath T_c , polymerizations were conducted in bulk at -36 °C inside the glove box. Interestingly, the organocatalysis of GBL initiated with benzyl alcohol (BnOH) entailed conversion of the monomer to a noteworthy degree: the saturated NHO 3 emerged as the best organocatalyst, with 68 % conversion after 24 h ($M_n = 5.9$ kDa, $\mathcal{D}_M = 2.1$). However, truly surprising behavior was observed when investigating the effect of dual catalysis on the polymerization of GBL. A quick screening revealed LiCl as the most potent LA for this setup. Most probably, this was attributable to the reduced stability of Li/NHO-LP, which was still able to dissociate even at these reduced temperatures and enabled initiation. Nevertheless, it quickly became clear that depending on the LP, the polymerization mechanism itself could directly be influenced by applying a setup without additional initiator. Together with MALDI-ToF MS end group analyses, three different modes of operation could be identified (Scheme 8): firstly, a direct nucleophilic attack of imidazolium-derived NHO 2 was observed; this highly nucleophilic NHO¹² can stabilize the resulting positive charge along its now-aromatic heterocycle, and the resulting ketone functionality is much more stable



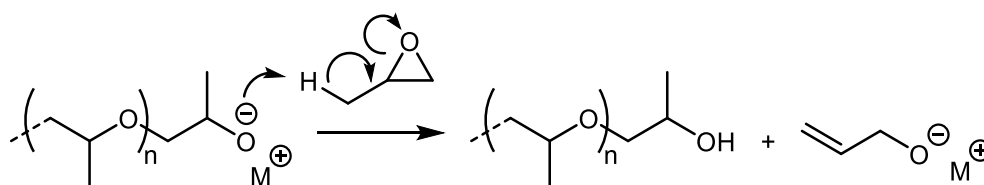
Scheme 7: Additional NHOs for the polymerization study of GBL. Mes = 2,4,6-trimethylphenyl.

towards nucleophilic attacks than e.g. acylazolium species resulting from an NHC mediated direct initiation (Scheme 8, top). Secondly, switching to a saturated NHO with increased steric demand on the nitrogen atoms (NHO 7), resulted in a significant change in polymer architecture, albeit in only low yield. Though the initiation mechanism remained the same, no NHO-terminated species were observable, instead found masses suggested a cyclic structure. Since no enolate formation was evident at low conversions which would entail the same mass, this suggested that macrocyclization ensued due to cleavage of the NHO moiety (Scheme 8, middle). This is readily understandable, if one takes the above-mentioned characteristics of this NHO into account: the resulting positive charge cannot be stabilized to the same extent as imidazolium-derived structures, due to the saturated nature of the heterocycle. Furthermore, together with the steric congestion induced by the two mesityl groups, these features render this NHO a good leaving group that can readily be substituted by back-biting of the propagating chain-end.



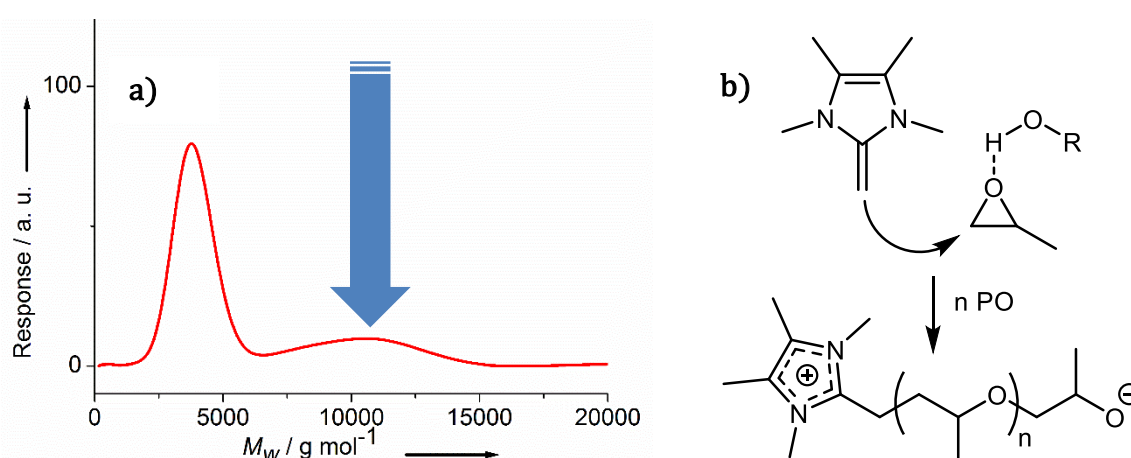
Scheme 8: Different modes of operation for GBL polymerization mediated by NHO/LiCl. Depicted are the key steps, which give the respective microstructures. Top: zwitterionic initiation *via* direct nucleophilic attack of NHO 2, the resulting ketone functionality is resistant to NHO-cleavage compared to NHC-derived acylazolium-species; a zwitterionic polymerization entails, resulting in linear poly(GBL). Middle: cyclic oligomers can be obtained *via* a direct initiation by NHO 7; however, due to its low capacity to delocalize the resulting positive charge and its increased sterical demand, this NHO moiety is susceptible to nucleophilic substitution, forming cyclic oligomers of GBL. Bottom: the highly basic, but non-nucleophilic NHO 1 deprotonates GBL to form an enolate species, which initiates an anionic polymerization, resulting in linear poly(GBL).

However, it must also be mentioned that at higher conversions, enolate formation was observed, hinting at an equilibrium between nucleophilic attack and proton abstraction. Finally, when applying the highly basic, non-nucleophilic NHO 1 without additional initiator, solely enolate-formation was detected by ^1H NMR spectroscopy and confirmed *via* MALDI-ToF MS measurements. The high basicity, however, not only emerges from the good conjugation and ensuing delocalization of the positive charge, but is also driven by sterics; the dimethyl-substitution on the exocyclic carbon forces the heterocycle out of plane, resulting in a distortion of the cycle and subsequent retardation of conjugation.¹² Upon protonation this ring strain can be relieved, thus acting as an additional driving force and increasing basicity. Recapitulating these findings, it was shown that dual catalysis is a promising approach for the polymerization of a broad range of lactones, that can readily be adjusted to the specific demands of the chosen monomers. By judicious choice of the applied LA, copolymerization parameters and polymerization kinetics were directly influenced. On the other side, adapting the NHO structure enabled the manipulation of polymerization mechanisms. Yet, especially the NHO/LA-mediated polymerization of a challenging lactone like GBL, still has much room for improvement, as the obtained molar masses and conversions still remained short of established phosphazene systems.^{5, 13c} Since these findings demonstrated an activity rivalling those of the most active LPs, another application was envisioned: the challenging ROP of substituted epoxides such as propylene oxide (PO).¹⁴ Polyethers in general (e.g. polyethylene oxide, PEO, polypropylene oxide, PPO) have a multitude of applications, ranging from hydrogels for drug-delivery¹⁵ to mesoporous carbons,¹⁶ solid-state electrolytes¹⁷ and triblock-copolymers comprised of $\text{PEO}_n - \text{PPO} - \text{PEO}_n$ (so-called “pluronics”).¹⁸ Yet, molar masses still remained impaired to roughly 10 kDa by occurring side-reactions, embodied by so-called transfer-to-monomer processes that result in allylic end groups (Scheme 9). It was shown that the application of NHOs can mitigate these shortcomings to some degree. Together with an alcohol initiator, a well-controlled polymerization can be achieved, with full control over end groups and virtually perfect molecular weight distributions (\mathcal{D}_M 1.02 – 1.07).^{8a, 19} However, molar masses were fully exploited at 12 kDa at most, with reaction times of several days not being uncommon. Clearly, there was room for improvement in this context. Food for thought actually came from an early, non-optimized system; the organopolymerization of PO applying NHO 2 and BnOH as initiator was always



Scheme 9: Transfer-to-monomer side-reactions typically present in metal alkoxide catalysts, that impair chain-growth and limit molar masses. The resulting allyl-terminated alkoxide can initiate polymerization, leading to allylic end-groups.

accompanied by a high-molecular weight impurity, that was attributed to a direct initiation by the NHO (Scheme 10).^{8a} Hence, it was envisioned to overcome the low molar masses by readjusting the system to solely promote the initiation by direct nucleophilic attack. However, simply omitting the alcohol initiator resulted in no conversion at all – an indication, that the monomer was activated by H-bonding of the alcohol moiety. This activation already very much resembles the approach of dual catalysis – a monomer activated by a cocatalyst, that is in turn initiated by a nucleophilic LB. In order to facilitate this mode of operation, the monomer activation must be achieved by a non-protic LA to foreclose side reactions. Thus, various non-protic LAs were screened without success, with one prime exception: magnesium bis(hexamethyldisilazide) ($\text{Mg}(\text{HMDS})_2$) was such a potent cocatalyst, that the polymerization which usually proceeds over a span of multiple days, reached completion in approximately five minutes. NMR analysis revealed full conversion, and an unusually high molar mass was detected in size-exclusion chromatography (SEC) ($M_n = 61 \text{ kDa}$, $D_M = 1.47$). Another intriguing feature of this setup was its turbulent, notably exothermic polymerization, which probed us to perform further reactions in



Scheme 10: a) SEC trace of a polymer derived from NHO 2 + BnOH. Note the high molecular weight impurity indicated by the arrow. b) Proposed initiation mechanism responsible for creating high molecular weight impurities, together with resulting polymer structure.^{8a}

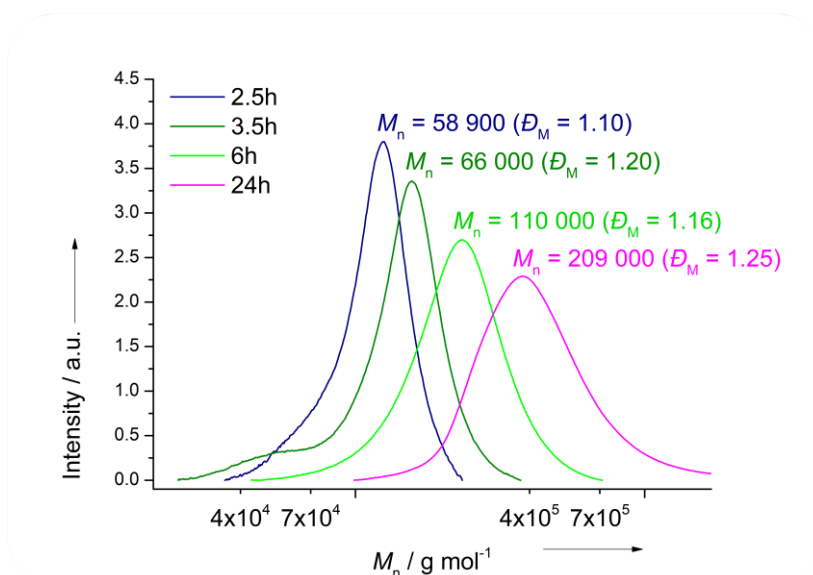


Figure 1: SEC traces of various polymerization setups consisting of NHO 2/Mg(HMDS)₂/PO 1:20:5000 after different reaction times at -36 °C in 5 M pentane. Noted molar masses were already offsetted against a compensation value determined by lightscattering SEC measurements (GPC-MALLS).

higher dilution at lowered temperatures (-36 °C). After optimization of reaction parameters, this enabled us to realize molar masses of up to 1 MDa (= 10⁶ g·mol⁻¹) depending on the applied LP, with a good correlation of molar mass vs. time (Figure 1). Encouraged by achieving these unprecedented molar masses, we then strived to elicit the underlying mechanism. This was realized *via* NMR studies with various compositions (Mg(HMDS)₂/PO and NHO/Mg(HMDS)₂), as well as MALDI-ToF MS

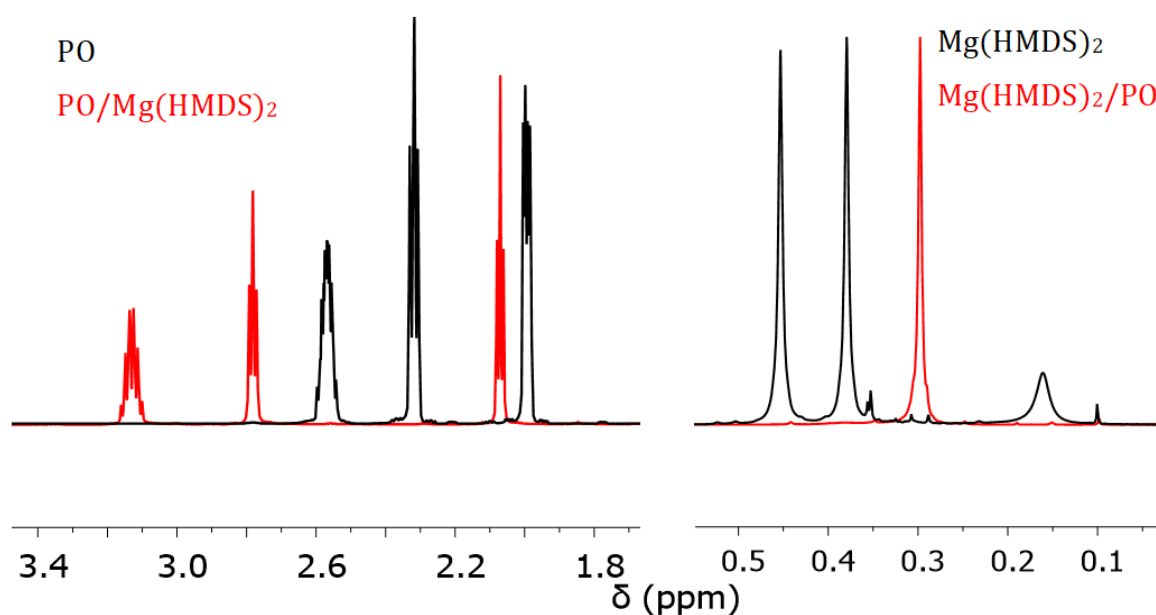
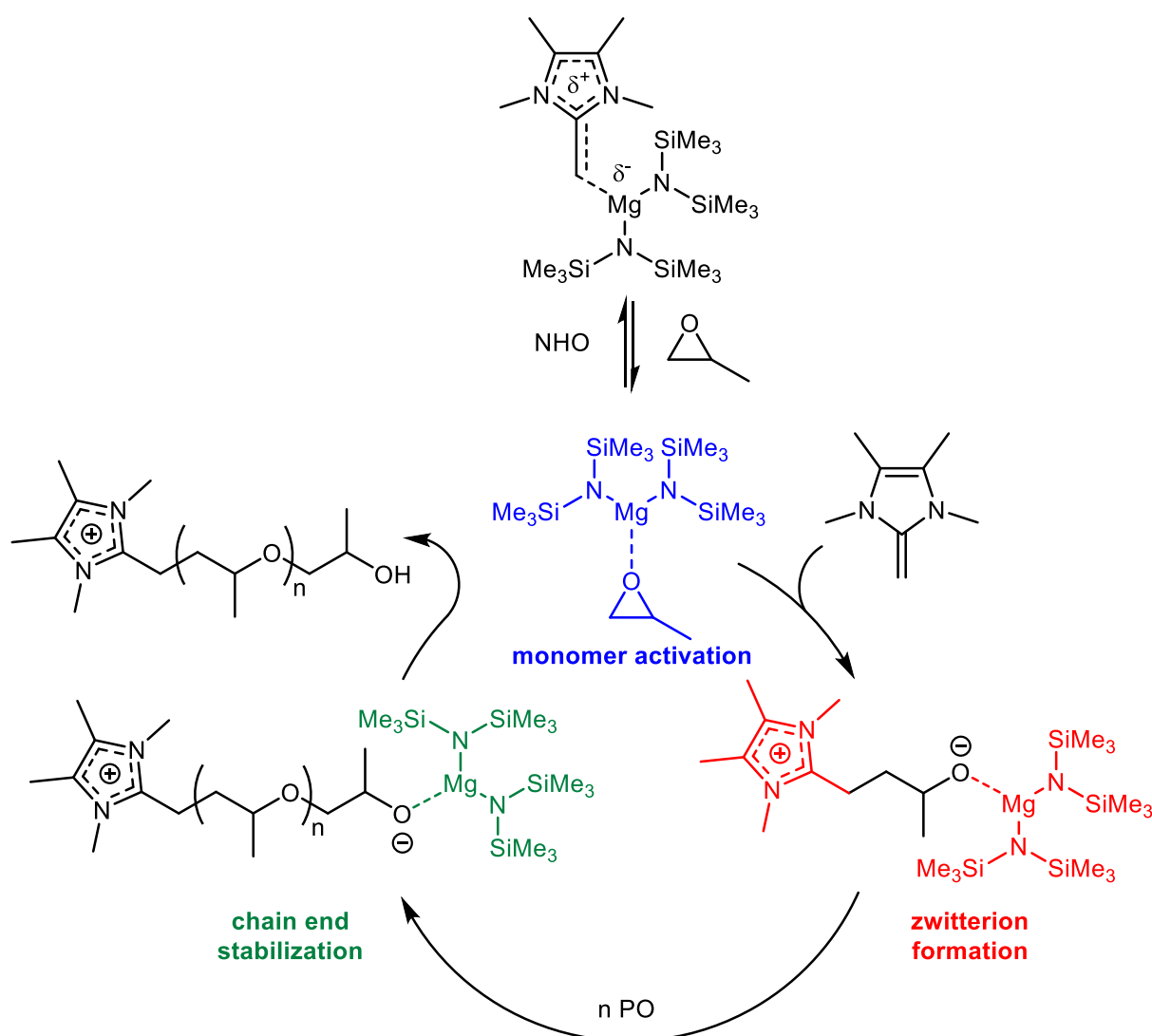


Figure 2: Black: original NMR spectra of the starting materials PO (left) and Mg(HMDS)₂ (right). Red: resulting NMR spectra of a mixture of PO 1:1 Mg(HMDS)₂. Note the stark shift for PO signals (left) and the change of coupling pattern of Mg(HMDS)₂ (right).

analyses of specifically prepared low molecular weight samples. The findings were captivating: as depicted in Figure 2 (left side), the characteristic signals for the cyclic protons of PO were strongly shifted downfield (about 0.5 ppm, compare red vs. black spectrum), while the distinctive signals resulting from an equilibrium between monomeric and dimeric $\text{Mg}(\text{HMDS})_2^{20}$ (Figure 2 right side, black) changed into a singlet that also experienced a shift (Figure 2, right side, red). This quantitative effect strongly hinted towards a monomer activation, that could almost be described as complex formation; however, the isolation of this complex failed so far. It is abundantly clear, that such a powerfully activated monomer is highly susceptible to a nucleophilic attack, which in this case is accomplished by NHOs, resulting in positively charged end groups that should be detectable by MALDI-ToF MS measurements. This was indeed the case, and the mass spectra showed perfect fits for NHO-derived end groups of the measured polymers, no matter whether measured with additional sodium, or not; which is again another strong indication that a zwitterionic polymerization mechanism is indeed at play here. These findings abetted us to propose an alternative polymerization mechanism (Scheme 11). Here, $\text{Mg}(\text{HMDS})_2$ is proposed to fulfill three separate roles: a) complexation of the NHO, whereby the resulting complex represents a dormant species that removes free NHO from the polymerization mixture, which decreases initiation efficiency and thus increases resulting molecular weights. b) Monomer activation *via* complexation, which renders the monomer susceptible for nucleophilic attack, facilitating ring-opening and initiating polymerization; c) stabilization of the propagating chain end that bears a negative charge, mitigating side reactions like transfer-to-monomer. Since this system represents one of the most reactive setups, it was envisioned it might overcome the kinetic limitations in epoxide chemistry; already butylene oxide (BO) is extraordinarily hard to polymerize using conventional systems. However, applying this setup, BO was readily polymerized in bulk at 60 °C for 2 h, reaching a conversion of 89 % and a molecular weight of 7 kDa ($\bar{M}_w = 2.5$). Higher molar masses were also realizable at -36 °C after 72 h ($\bar{M}_n = 21$ kDa, $\bar{M}_w = 2.1$). Furthermore, this setup proved to be just as active for allyl glycidyl ether (AGE) as it is for PO, which is why the copolymerization of these two monomers was investigated. It was shown that monomer consumption occurred unselectively, yielding a random copolymer. The observed intact allylic side groups highlight the chemoselectivity of this LP polymerization. This also permits for subsequent cross-linking or post-



Scheme 11: Proposed mechanism of zwitterionic PO polymerization using NHO/Mg(HMDS)₂ LPs. The pre-equilibrium of an NHO/Mg(HMDS)₂ complex is cleaved by a PO molecule, which is then activated (blue) and susceptible to nucleophilic attack by a free NHO. This forms a zwitterion with an NHO-derived end group on one side and a propagating oxanion on its tail (red), which is likely to be stabilized by a Mg(HMDS)₂ molecule. Propagation will then take place, mediated by Mg(HMDS)₂ which reduces the basicity of the propagating chain end *via* coordination (green), until no monomer is left and/or the reaction is quenched.

functionalization, possibly leading to materials with intriguing material properties that were so far inaccessible by conventional methods.

The above stated results, be it with lactones or epoxides, substantiate the versatility of LP polymerization methods. Albeit the herein presented system denotes but a small fraction of the nearly unlimited possible LB/LA-combinations, its reactivity is comparable to e.g. phosphazene-based LPs, that achieved impressive feats in polymerizations lately.^{3, 5, 13c, d, 21} However, the ready availability (LAs described in this work can be bought, NHOs are typically accessible in a 2-3 step, literature-known synthesis) at comparably low costs more than makes up for the slightly attenuated reactivity compared to phosphazenes. Furthermore, LAs like MgCl₂ are neither toxic, nor explosive or combustible, simplifying handling to a

significant degree. Various insights could be obtained in this work: when copolymerizing lactones, depending on the LA, copolymerization parameters and polymerization kinetics were directly influenced. This constitutes a remarkably practicable way to adjust material properties like melting points or glass transition temperatures. On the other hand, regarding GBL, changing the structure of the NHO promotes different polymer microstructures; that way, cyclic, linear and positively charged, linear polymer structures were accessible. These findings also underline, that the ideal LP has yet to be established for GBL, in order to increase molecular weights and yields of the polymerization. Nevertheless, taking the versatility of NHO structures and abundance of possible LP combinations into account, it is most likely that improvements can be achieved shortly. After having surpassed the current limitations of epoxide polymerization in terms of both, molecular weight and speed, the question arises what issues remain unresolved with polyether synthesis. When consulting the literature, it quickly becomes apparent that there are only very few catalytic systems capable of generating isotactic poly(PO) of reasonable molecular weight.²² This remains unique to highly specialized catalysts, with impressive ligand systems that are arduously designed and synthesized. In this regard, it would be most desirable if the catalytic system presented herein was also able to induce tacticity during polymerization. One could either achieve this *via* a chain-end-control mechanism, which would require the modification of the LA to have an influence on stereoregularity. Alternatively, one could approach this issue by modifying the NHO structure to control the subsequent insertion of a monomer unit. However, despite best efforts, this issue remains out of grasp for an NHO/LA-based dual catalytic system, and the required modifications to the systems are just as elusive up to now. Nevertheless, the prowess of this setup for epoxide polymerization persists, and for the same reasons as stated above, is likely to be developed even further in the future. Overall speaking, this work provided some valuable insights into NHO-mediated cooperative catalysis with LAs, while also mapping out its current limitations, thus offering various starting points for future research efforts. Mechanistic investigations have been conducted to further elucidate accessible modes of operation and to increase the understanding of NHO reactivity. After all, it is of prime importance to grasp the changes necessary in NHO structure to induce a specific reactivity, otherwise one would just depend on serendipity to find a suitable NHO for an envisioned reaction.

1. Theory and Background

1.1. Ring-Opening Polymerization

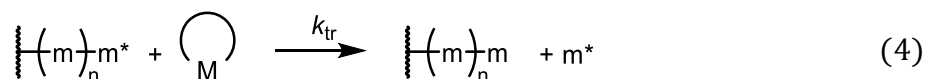
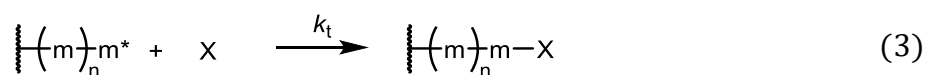
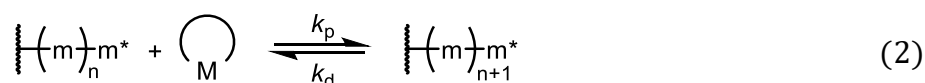
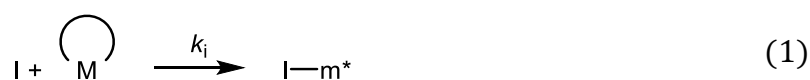
1.1.1. Introduction

Literature provides an excellent compilation of all aspects of ring-opening polymerization (ROP), including an overview over the monomer classes accessible by this technique.^{1, 2c, 3-4, 6-8, 9a, 11g, 19, 21b, 23} These monomer classes encompass e.g. cyclic carbohydrates (saturated and unsaturated), ethers, esters, carbonates, sulphides, siloxanes and lactams. In this chapter, the basic concepts of ROP are outlined. In view of the comprehensive data set reported in the above-mentioned references, only a brief summary of issues relevant to this thesis will be discussed at this point.

ROP transforms the cyclic monomer structure into a linear, cross-linked or macrocyclic structure during polymerization. The respective polymerization mechanism is dependent on the monomer and catalyst/initiator system, and encompasses ionic, coordination, metathetic, radical and enzymatic methods. A further mechanistic distinction is possible between an active chain-end and activated monomer mechanism, whereas the latter is the approach followed in this thesis. A more detailed look at the general mechanisms in ROP is provided in chapter 1.1.4. The catalytic systems applicable for ROP are just as versatile as their monomers: depending on the desired material properties and/or the challenges posed by the respective monomer, the systems range from simple alkali metals or metal alkoxides,²⁴ to highly specialized catalysts with imposing ligand systems.^{22b, 25} It is important to note, that especially the propagation is in general reversible, resulting in the prerequisite to shift the monomer-macromolecule equilibrium to the macromolecular side. This is no easy feat, since particularly the depropagation reaction of macromolecules derived from 5- and 6-membered monomers is thermodynamically favored. Thus, it is important to understand the underlying thermodynamic and kinetic restrictions present in ROP, which will be outlined in chapter 1.1.2 and 1.1.3.

1.1.2. Thermodynamic Considerations

As mentioned in chapter 1.1.1, special focus has to be placed on the reversibility of the (de-)propagation reaction. This is expressed by high monomer concentrations at the equilibrium of polymerization during the reaction, caused by a high rate constant of depropagation (k_d). Therefore, the equilibrium monomer concentration $[M]_{eq}$ was introduced as a measure of thermodynamic polymerizability.²⁶ A general depiction of possible reactions during ROP is given in Scheme 12. These consist of initiation, where an initiator reacts with a monomer molecule (Scheme 12, equation 1), forming an active species ($-m^*$), and propagation, where the active species adds another monomer (Scheme 12, equation 2). Each of those reactions possesses their respective rate constants, forming a complex interplay of thermodynamic and kinetic relationships. Termination and transfer-to-monomer reactions (Scheme 12, equations 3 and 4), are side reactions apparent in ROP. For idealized, living polymerizations, the rate constants of the termination and transfer reactions are equal to zero ($k_{t,tr} = 0$, Scheme 12). However, molar masses and end groups can only be controlled when $k_i \geq k_p$ (Scheme 12, equations 1 and 2). The general polymerizability of a given monomer is related to the sign of the free enthalpy of polymerization (ΔG_p , equation 5). Polymerization is only possible, if $\Delta G_p(xy) < 0$ applies; however, $\Delta G_p(xy)$ is dependent on the monomer and polymer states (x and y) to such an extent, where the polymerizability may depend on the solvent used. Another way to express the free enthalpy of polymerization is as sum of standard free enthalpy of polymerization (ΔG_p^0), together with a term related to instantaneous monomer molecules and growing macromolecules (equation 6), obtained from the



Scheme 12: General polymerization steps present in ROP. I = initiator, m^* = active species, X = termination agent, M = monomer. $k_{i,p,d,t,tr}$ = rate constants of initiation, propagation, depropagation, termination and transfer-to-monomer, respectively. Scheme modified from literature.¹

$$\Delta G_p(xy) = \Delta H_p(xy) - T\Delta S_p(xy) \quad (5)$$

$$\Delta G_p = \Delta G_p^0 + RT \cdot \ln \left(\frac{\left[\left[\text{---} \left(\text{---} \right)_n \text{---} \right]_{m^*} \right]}{[M] \left[\left[\text{---} \left(\text{---} \right)_n \text{---} \right]_{m^*} \right]} \right) \quad (6)$$

law of mass action. R hereby denotes the gas constant. According to *Flory*, the reactivity of an active center, located on a sufficiently long macromolecular chain, is independent of its degree of polymerization (DP). This, together with the relation $\Delta G_p^0 = \Delta H_p^0 - T\Delta S_p^0$, leads to equation 7. At equilibrium ($\Delta G_p = 0$), $[M]_{\text{eq}}$ assumes a value determined by ΔH_p^0 , ΔS_p^0 and T (equations 8 and 9).

$$\Delta G_p = \Delta H_p^0 - T(\Delta S_p^0 + R \cdot \ln([M])) \quad (7)$$

$$\ln([M]_{\text{eq}}) = \frac{\Delta H_p^0}{RT} - \frac{\Delta S_p^0}{R} \quad (8)$$

$$[M]_{\text{eq}} = e^{\frac{\Delta H_p^0}{RT} - \frac{\Delta S_p^0}{R}} \quad (9)$$

If $[M]_0 > [M]_{\text{eq}}$, then polymers of various number average degrees of polymerization (DP_n) can be generated, depending on the ratio of $\frac{[M]_0 - [M]_{\text{eq}}}{\Sigma(\dots m_n^*)}$. However, shorter oligomeric chains ($DP_n \leq 20$) do not conform to *Flory's* assumption, which must be considered (equation 10 and 11):

$$\ln \left(\frac{DP_n}{DP_n - 1} \cdot [M]_{\text{eq}} \right) = \frac{\Delta H_p^0}{RT} - \frac{\Delta S_p^0}{R} \quad (10)$$

$$[M]_{\text{eq}} = \frac{DP_n - 1}{DP_n} \cdot e^{\frac{\Delta H_p^0}{RT} - \frac{\Delta S_p^0}{R}} \quad (11)$$

Plotting the \ln of equation 10 versus the reciprocal temperature is a method to determine ΔH_p^0 (slope) and ΔS_p^0 (intercept) from experimentally determined $[M]_{\text{eq}}$ values. Another typical option is to measure the combustion and specific heat of the monomer and corresponding polymer. The thus-determined values for ΔH_p^0 and ΔS_p^0 allow for an estimation of $[M]_{\text{eq}}$, which is especially useful if $[M]_{\text{eq}} \approx 0$. Several conclusions can be drawn from equation 7: a) if the standard enthalpy is lower than zero ($\Delta H_p^0 < 0$), and the standard entropy of polymerization is larger than zero ($\Delta S_p^0 > 0$), polymerization is possible at any given temperature. b) Polymerization is

impossible, if $\Delta H_p^0 > 0$ and $\Delta S_p^0 < 0$. c) Monomers, for which $\Delta H_p^0, \Delta S_p^0 < 0$ is true, are polymerizable up to a so-called ceiling temperature (T_c). d) Likewise, if $\Delta H_p^0, \Delta S_p^0 > 0$ applies to monomers, the polymerization is feasible down to a floor temperature (T_f). The respective expression to calculate those temperatures is denoted in equation 12.

$$T_{c,f} = \frac{\Delta H_p^0}{\Delta S_p^0 + R \cdot \ln([M]_0)} \quad (12)$$

One of the major driving forces for the polymerization of cyclic compounds is the release of ring-strain. This strain can be caused by various effects, such as the distortion of bond angles or the stretching or compression of a bond. Furthermore, the repulsion between eclipsed hydrogen atoms and non-bonding interactions between substituents is the cause for angular, conformational or trans-annular strain. In this context, if specific monomer-polymer-solvent interactions can be neglected, ΔH_p serves as a measure of ring-strain. This leads to the conclusions, that i) the higher the ring-strain, the lower the resulting $[M]_{eq}$ and ii) polymerization is only possible, if $|\Delta H_p|$ is larger than $-T \cdot \Delta S_p$, since most polymerizations are accompanied by an entropy decrease due to the loss of translational degrees of freedom. However, 5- and 6-membered alkanes and ethers feature the least ring-strain, ultimately precluding polymerization in some cases, since hypothetical $[M]_{eq}$ are well above any possible $[M]_0$. This is expressed by the relatively high $[M]_{eq}$ of cyclopentane and tetrahydrofuran (THF). The introduction of a sulfur atom or a carbonyl group in a 5-membered ring, however, precludes high-polymer formation, either due to the increased atomic radius of the sulfur atom, or due to a decrease in the number of bond oppositions of the sp^2 -hybridized carbonyl moiety. In contrast to this, the introduction of an ester functionality in a 6-membered ring introduces ring-strain due to the planar nature, making lactone polymerizations readily feasible (except for the 5-membered γ -butyrolactone (GBL), see chapter 2). An increase in ring-size generally leads to a decrease in ring-strain, which entails an increased polymerization entropy. This can be explained by the higher flexibility of the resulting polymer chains, resulting in an entropy-driven polymerization. The same rules also apply for ring-opening metathesis polymerization (ROMP). However, a detailed look at ROMP will be omitted in the context of this thesis - a descriptive quote by R.H. Grubbs shall suffice: "... the most favorable conditions for a successful ROMP is to use the highest monomer concentration at the lowest temperature possible."²⁷

Since the considerations mentioned hitherto relate to idealized systems, one must be aware of their limitations and distinctions from non-idealized conditions. For one, ΔH_p^0 and ΔS_p^0 depend substantially on the states of the monomer and polymer, due to phase transition enthalpies and entropies. For example, for liquid (l) ω -pentadecalactone (PDL), ΔH_p^0 has been determined to be $3 \text{ kJ}\cdot\text{mol}^{-1}\cdot\text{K}^{-1}$, while ΔH_p^0 of crystalline (c) PDL was ascertained as $-39 \text{ kJ}\cdot\text{mol}^{-1}\cdot\text{K}^{-1}$. Likewise, standard polymerization entropies differ for the respective states ($\Delta S_p^0(\text{PDL}_{(l)}) = 23 \text{ J}\cdot\text{mol}^{-1}\cdot\text{K}^{-1}$ and $\Delta S_p^0(\text{PDL}_{(c)}) = -86 \text{ J}\cdot\text{mol}^{-1}\cdot\text{K}^{-1}$).²⁸ Furthermore, ΔS_p^0 determined at different standard conditions (e.g. $1 \text{ mol}\cdot\text{L}^{-1}$ and weight fraction = 1) cannot be directly compared and must be recalculated. Also, as can be deduced from equation 12, $T_{c,f}$ are directly dependent on the initial monomer concentration $[M]_0$.

As briefly mentioned, the discussion above is based on various assumptions: a) the polymerization is carried out in a homogeneous medium. b) Neglect of monomer-polymer-solvent interactions. c) Only polymers with high molar masses are formed. Of course, deviations from these assumptions occur when moving from observing an idealized system, to the observation of a system under realistic conditions. These shall be concisely discussed hereafter. For heterogeneous systems (e.g. the polymerization of Lactide (LAC)), an apparent decrease of $[M]_{\text{eq}}$ can be achieved by aging the living polymerization mixture below the melting point of poly(LAC) (PLA). This entails a crystallization of PLA, which reduces the volume of the liquid phase, and in turn increases $[M]$ above $[M]_{\text{eq}}$. Thus, $[M]_{\text{eq}}$ is not actually decreasing, but rather the molar fraction of M is. Using this technique, LAC polymerizations can be continued to entail a virtually complete monomer consumption, as $[M]$ is repeatedly increased above $[M]_{\text{eq}}$. Moving to monomer-polymer-solvent interactions, the ROP of THF serves as prime example to discuss the involved changes. Since monomeric THF possesses a higher nucleophilicity than poly(THF), the polymerization is strongly dependent on the monomer-solvent interactions. The energy-loss of these interactions concomitant with the polymerization can only be partially compensated by solvent-polymer interactions, which leads to an increase of $[M]_{\text{eq}}$ with increasing strength of monomer-solvent interactions. For THF, it was found that $[M]_{\text{eq}}$ increases for a given $[M]_0$ in order of the following solvents: $\text{CCl}_4 (4.0 \text{ mol}\cdot\text{L}^{-1}) < \text{C}_6\text{H}_6 (4.3 \text{ mol}\cdot\text{L}^{-1}) < \text{CH}_2\text{Cl}_2 (5.6 \text{ mol}\cdot\text{L}^{-1}) < \text{CH}_3\text{NO}_2 (6.0 \text{ mol}\cdot\text{L}^{-1})$.²⁹ As the Flory-Huggins-Equation dictates, the reactivity of an active center located on a polymer chain of sufficient

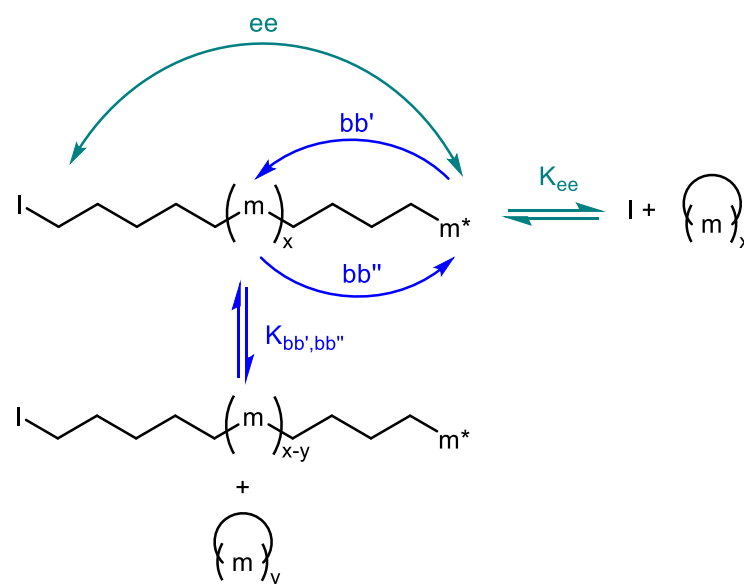
length, is independent of its DP. However, this also means, that this is not the case for shorter polymer chains or oligomers that are present during the beginning of the polymerization. In fact, the equilibrium constants (K) differ for the first few (~ 20) monomer additions, due to an influence of the last added monomer unit on the active center ($K_{p0-p20} > K_{pi}$). Furthermore, oligomerization also affects $[M]_{eq}$ in a way, that it increases for higher oligomers ($[THF]_{eq} = 1 - 4.3 \text{ mol}\cdot\text{L}^{-1}$ for $DP_n = 1-15$).³⁰ This is also true for polymerizations conducted in the vicinity of $T_{c,f}$: despite no high-polymer formation is possible, oligomerization can be achieved even for GBL (DP up to 10 with $\text{Al}(\text{O}^i\text{Pr})_3$).^{13a} Poly(GBL)-formation (M_n up to $3.5\cdot 10^3 \text{ g}\cdot\text{mol}^{-1}$) can also be observed when applying high pressures ($2\cdot 10^4 \text{ bar}$).³¹ This is in accordance with the T_c - pressure relationship predicted by the *Clausius-Clapeyron* equation (equation 13):

$$\ln T_c(p) = \ln T_c(p = 1 \text{ bar}) + \frac{V_P - V_M}{\Delta H_p^0} \cdot p \quad (13)$$

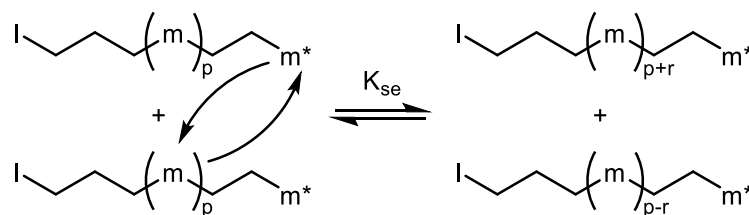
The term $V_P - V_M$ corresponds to the volumes of the polymer and monomer, respectively. This term is typically negative, since a molar volume contraction occurs in a vast majority of polymerizations during the reaction. Thus, T_c experiences a significant increase when applying high pressures, ultimately making the formation of low molar mass polymers of GBL possible.

Another deviation from idealized systems is the occurrence of side-reactions, embodied by macrocyclization and segmental exchange reactions (scrambling, leading to a broadening of D_M). Since the same reactive groups are present in both polymer and monomer, these reactions severely limit the control over polymer synthesis. There are various possible ways to form macrocycles during polymerization, as depicted in Scheme 13. Back-biting occurs *via* a nucleophilic attack onto different positions along the polymer chain. In anionic and coordinative polymerizations, the active center typically attacks a repeating unit along the chain, forming a macrocyclic species (Scheme 13, top, blue, bb'). In cationic processes, the repeating unit performs the nucleophilic attack on the propagating species to form macrocycles (Scheme 13, top, blue, bb''). Both processes can also perform end-to-end-cyclization reactions (Scheme 13, top, green, ee). The same rules apply for segmental

Back Biting



Segmental Exchange (Scrambling)

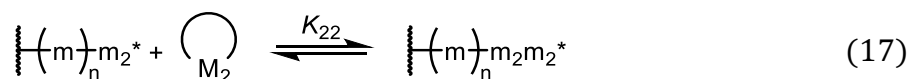
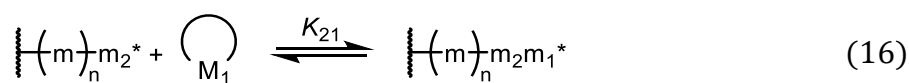
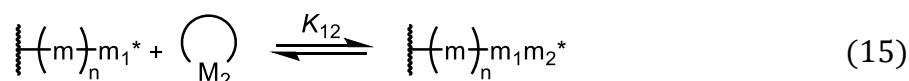
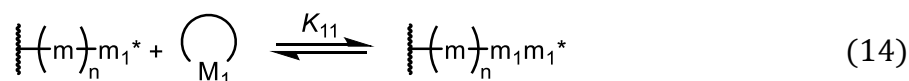


Scheme 13: Possible side-reactions during ROPs. Top: back-biting can occur either through a nucleophilic attack of the active species onto a repeating unit along the chain (bb' , blue, present with anionic and coordinative polymerizations), or *via* a nucleophilic attack of the repeating unit onto the active species (bb'' , blue, present in cationic processes). The same applies for an end-to-end-cyclization (ee , green); both processes lead to macrocyclization. Bottom: segmental exchange reactions resulting in a broadening of \mathcal{D}_M . Scheme adapted from literature.¹

exchange reactions depicted in Scheme 13, bottom, leading to a broadening of \mathcal{D}_M . Following theoretical considerations based on the Jacobson-Stockmeyer theory, the equilibrium concentration of a macrocycle containing y repeating units of $\cdots -m -\cdots$ ($[M(y)]_{eq}$) in a Θ -solvent was determined to be proportional to $y^{-\frac{5}{2}}$.³² This means, that $[M(y)]_{eq}$ decreases monotonically with increasing ring-size of the corresponding macrocycle, and also, that $[M(y)]_{eq}$ is temperature-independent for non-strained cycles. Furthermore, the propagation and depropagation of larger cyclics entails an enthalpy change that is roughly equal to zero. This has been specifically shown for cyclic CL oligomers but is generally accepted for reactions that feature a ring-chain-equilibrium.^{32b} Since the formation of macrocycles deteriorates material properties, they are considered as a contamination and are especially undesired with functional polymers. Thus, the critical concentration of macrocycles ($\sum y[M(y)]_{eq}$) is a

parameter of technical relevance, denoting the concentration of monomer that will eventually be converted to macrocycles.

Now that the thermodynamic basics for homopolymerizations of cyclic monomers have been briefly summarized, it is of interest to also discuss the thermodynamic requirements of copolymerizations. Just as in homopolymerization, $\Delta G_{co} = 0$ is a necessary (but not sufficient) requirement for the occurrence of a thermodynamic equilibrium. Under the assumption, that the preceding repeating unit has no influence on homo- and cross-propagation equilibria constants, four reversible reactions exist in a two-component-system (Scheme 14, equations 14-17). This simplified diad model is sufficiently accurate for many copolymerization systems, since the influence that a repeating unit can exert on its vicinity is rather limited.



Scheme 14: Reversible propagation reactions present in a two-component copolymerization, under the assumption that the preceding repeating unit has no influence on the respective equilibria constants. Scheme adapted from literature.¹

Following equations 14-17, the respective equilibrium concentrations can be calculated using equation 18 (exemplified for monomer 1 (M_1)):

$$[M_1]_{eq} = \frac{[\dots -m_1 m_1^*]_{eq}}{K_{11} [\dots -m_1^*]_{eq}} \quad (18)$$

Finally, this leads to the conclusion that $[M_1]_{eq,copo} < [M_1]_{eq,homo}$. This can readily be explained considering the fact, that cross-propagation reduces the concentration of $\dots -m_n m_n^*$ -centers. Furthermore, it is also possible to correlate $[M_1]_{eq,copo}$ with the degree of polymerization (equation 19), given that the formation of heterodiads is preferred ($K_{12}K_{21} > K_{11}K_{22}$ and $[M_1]_0[M_2]_0 > (K_{12}K_{21})^{-1}$). This also enables the possibility to predict $[M_1]_{eq,copo}$ even if the homopolymerization of the respective

$$[M_1]_{\text{eq,copo}} = \frac{1 - DP_{n(M_1)}}{K_{11} DP_{n(M_1)}} \quad (19)$$

monomer is impossible.

To conclude the thermodynamic considerations, influences on polydispersities of ROPs shall concisely be discussed. The molar mass distribution of equilibrium polymerizations ranges from narrowly dispersed polymers derived from three- and four-membered monomers ($1 < \mathcal{D}_M \leq 1.25$, equation 20) to rather broad expected distributions of larger rings ($\mathcal{D}_M = 2$, equation 21). The deviation for three- and four-membered monomers is caused by the irreversibility of propagation, since these monomers possess a significant ring-strain, making ring-closure during depropagation essentially impossible. However, despite taking propagation and depropagation equilibria into account for larger rings, the observed polydispersities are often significantly lower than 2 (e.g. poly(LAC): $\mathcal{D}_M < 1.15$). This is the case, since the equilibria at which polymerizations are stopped are, in fact, incomplete: to reach $\mathcal{D}_M = 1.99$ (which equals to quantitative conversion), it would take 100-fold longer than to reach 99.9 % conversion.³³ Thus, a Poisson-like molar mass distribution can be achieved, when stopping the reaction during its kinetically controlled period. Side-reactions, like the above-discussed scrambling and macrocyclizations broaden \mathcal{D}_M ; however, segmental exchange reactions apparent in reversible polymerizations can interestingly still fulfil criteria of a living polymerization.

$$\mathcal{D}_M = \frac{DP_w}{DP_n} = 1 + \frac{1}{DP_n} \quad (20)$$

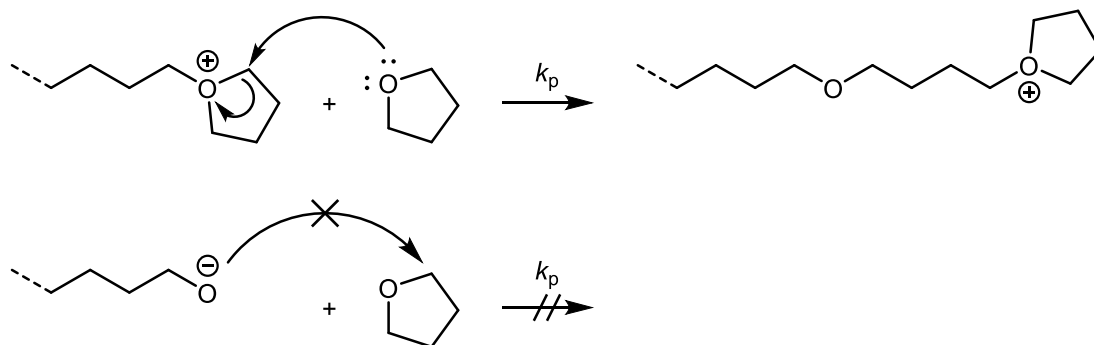
$$\mathcal{D}_M = \frac{DP_w}{DP_n} = 2 - \frac{1}{DP_n} \quad (21)$$

1.1.3. Kinetic Considerations

In contrast to the thermodynamic criteria for polymerizability discussed in chapter 1.1.2, the kinetic criterion to facilitate propagation is related to the molar free enthalpy of activation (ΔG_p^\ddagger). Since ΔG_p^\ddagger represents an energy barrier during propagation, this term exclusively attains positive values in theory. However, in realistic systems this value may also assume negative values, hinting to a system that is more complex than simple macromolecular chain growth. The resulting rate constant of propagation (k_p) can be determined *via* equation 22:

$$k_p = \frac{k_b T}{h} \cdot e^{-\frac{\Delta G_p^\ddagger}{RT}} = \frac{k_b T}{h} \cdot e^{-\frac{\Delta H_p^\ddagger}{RT} + \frac{\Delta S_p^\ddagger}{R}} \quad (22)$$

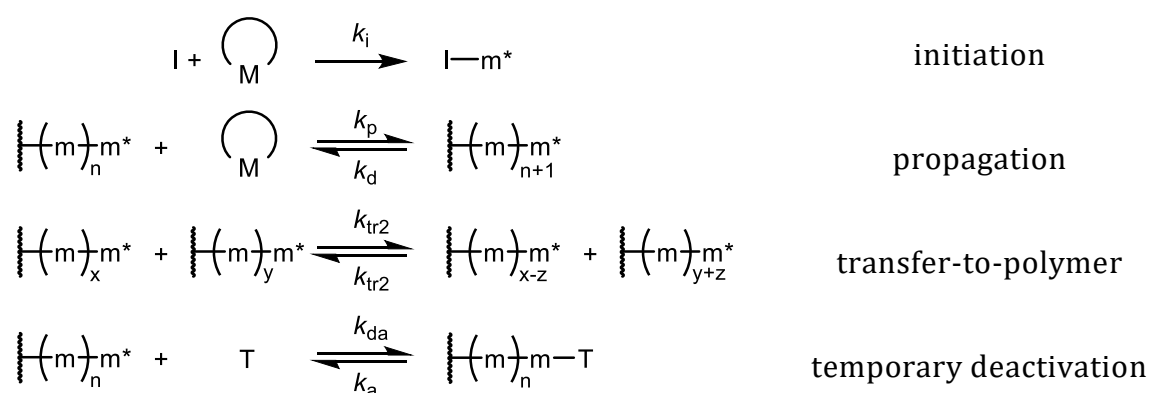
with k_b , h , ΔH_p^\ddagger , ΔS_p^\ddagger respectively denote the Boltzman constant, Planck constant, enthalpy and entropy of activation. As mentioned before, the fulfilment of thermodynamic requirements is a necessity for polymerization but is not sufficient. This can be illustrated when considering the ROP of THF (Scheme 15). Theoretically, two possible modes of operation exist: a cationic pathway, as well as an anionic pathway. However, only the cationic polymerization of THF has been established so far. This becomes abundantly clear when taking the underlying mechanism into consideration. With a cationic propagation mechanism, the C-O-bond of an activated, cyclic ether moiety must be cleaved by the nucleophilic attack of a monomer. This is readily achieved, and polymerizations can be conducted in e.g. methylene chloride (Scheme 15, top).³⁴ On the other hand, if one tries to imagine an anionic pathway, it quickly becomes obvious that in order to achieve a ring-opening of the monomer, the C-O-bond of a stable ether moiety would have to be cleaved. This step features a



Scheme 15: Two theoretical pathways of THF polymerization. Top: well-established cationic pathway, where the C-O-bond of an activated monomer is cleaved. Bottom: theoretical anionic pathway, precluded by the high stability of the unactivated ether moiety, resulting in a high ΔG_p^\ddagger .

significantly high ΔG_p^\ddagger , or rather a high ΔH_p^\ddagger value due the substantial ether bond-strength, resulting in a low k_p and precluding anionic polymerization (Scheme 15, bottom). Thus, it is insufficient to only consider thermodynamic polymerizability as a measure of a monomer's reactivity. Differences in predicted vs. observed reactivity can also result from back-reactions, as is the case for GBL: its depropagation is significantly faster than its propagation, resulting in no observable propagation (with selected exceptions). Another trend manifesting itself in lactone polymerization is the tendency of a reduced reactivity with increasing ring-size. This can be attributed to a higher ΔH_p^\ddagger , caused by a reduction in ring-strain and thus an increase in the lactone's overall stability. However, this dependence is inverted in enzyme-catalysed ROP of lactones, due to the rate-determining step being the lactone-enzyme complex formation. Since the active centers of enzymes are hydrophobic in nature, this complex formation is facilitated by an increase in hydrophobicity of the lactone, which increases with its ring-size.^{28a}

The first anionic ROP to fulfil living criteria was the ROP of ethylene oxide (EO), developed by *Flory* in 1940.³⁵ During that time, he determined the molar mass ratio to be dependent on the molar ratio of monomers vs. initiator ($[EO]_0 - [EO] / [I]_0$), while the generated poly(EO) possessed a Poisson molar mass distribution, hinting to the absence of irreversible transfer and termination reactions. However, not only processes without side-reactions fulfil the criteria of living polymerizations. As long as the system exclusively provides macromolecules capable of growth and $k_a \geq k_p$ are true, the kinetic criteria of living polymerizations may be met (Scheme 16).



Scheme 16: Side-reactions that may be present during living ROPs. $k_{i,p,d,tr2,da,a}$ are the rate constants of initiation, propagation, depropagation, transfer-to-polymer, deactivation and activation, respectively. Note that despite temporary deactivation, the polymerization may still fulfil criteria for living polymerizations, as long as the system only provides macromolecules capable of growth and $k_a \geq k_p$.

The polymerization rate (R_p) of a system incorporating only rapid initiation, reversible propagation and a single type of active center can be determined using equation 21, assuming that k_p is independent of DP_n :

$$R_p = -\frac{d[M]}{dt} = k_p \Sigma [m_n^*][M] - k_d \Sigma [m_n^*] \quad (21)$$

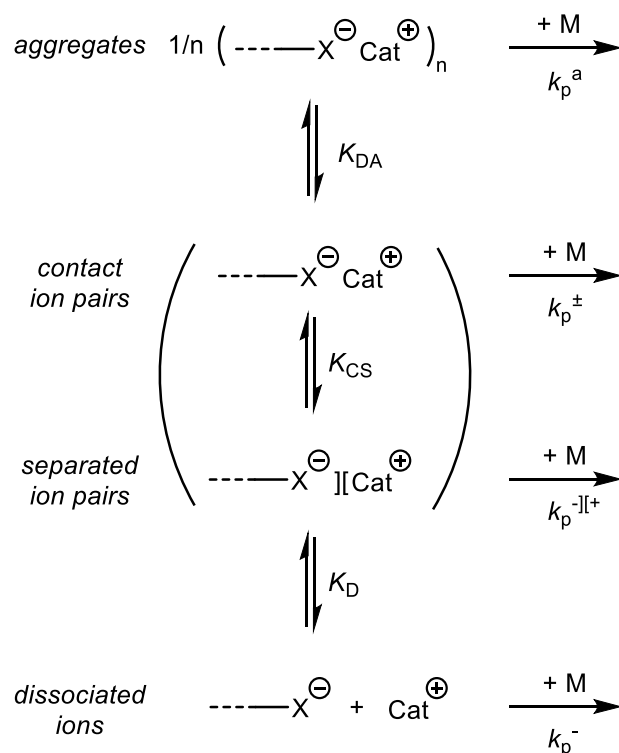
This equation can be transformed into the well-known semilogarithmic dependence of monomer concentration on the reaction time *via* integration (equation 22):

$$\ln \frac{[M]_0 - [M]_{eq}}{[M] - [M]_{eq}} = k_p \Sigma [m_n^*] t = k_p [I]_0 t \quad (22)$$

The term $[M]_{eq}$ only needs to be considered in cases of larger cyclics, since $[M]_{eq} \approx 0$ for three- and four-membered rings. Also, it is important to note that the $[M]_{eq}$ value determined under identical conditions as the polymerization must be used, since otherwise significant errors might occur as has been the case for THF polymerizations.³⁶ As expected for a living polymerization, the DP_n is a linear function of monomer conversion (if $k_i \geq k_p$ is true), and can be described as $DP_n = \frac{[M]_0 - [M]}{[I]_0}$. Thus, both above-mentioned correlations are used as a criterion of polymerization livingness: if the plots of $\ln \frac{[M]_0 - [M]_{eq}}{[M] - [M]_{eq}}$ vs. t and DP_n (or M_n) vs. $\frac{[M]_0 - [M]}{[M]_0}$ exhibit linearity from the very beginning, this strongly hints towards the absence of chain termination and a rapid and quantitative initiation. Likewise, a slow initiation typically results in an acceleration (positive curvature) for the kinetic, and in a deceleration (negative curvature) for the molar mass evolution, respectively. However, a slow initiation does not entail a significant broadening of \mathcal{D}_M ($\mathcal{D}_M \leq 1.4$ for $\frac{k_p}{k_i} \geq 10^3$); it rather leads to the molar mass being uncontrollable. Furthermore, termination reactions also cause a decrease in the polymerization rate and result in a negative curvature of the kinetic plot but will not affect the linearity of the molar mass evolution plot. Both arguments were combined into a single equation by *Penczek* et al., and the linearity of its plot vs. t is both a necessary and sufficient criterion for the livingness of a polymerization (equation 23).³⁷

$$-\ln\left(1 - \frac{[I]_0}{[M]_0 - [M]_{\text{eq}}} \cdot DP_n\right) = k_p [I]_0 t \quad (23)$$

In order to fully understand the polymerization process, it is necessary to determine the chemical structure of the active centers. However, in the case of ionic polymerizations, this encompasses a multitude of different species, such as aggregates, contact ion pairs, separated ion pairs and fully dissociated ions. Each of these species possess their respective rate constant of propagation, while being interlocked in equilibria with differing equilibrium constants that allow interconversion (Scheme 17). This forms a complex picture that needs to be considered when elucidating polymerization processes. Over the time underlying effects have been studied to maintain control over the reaction. For example, the formation of aggregates can be eliminated with crown ethers as additives or polar solvents as reaction medium, greatly increasing polymerization rates.³⁸ Also, in ionic polymerizations, the fraction of free ions (α) plays a pivotal role in influencing the absolute rate constants of polymerization. α is directly dependent on the equilibrium constant of dissociation (K_D) and the total concentration of ionic



Scheme 17: Ionic species occurring during ionic ROPs. Note the equilibria connecting these species, making interconversion possible.

species. In an anionic ROP with fast initiation, the latter is equal to the initial concentration of the initiator ($[I]_0$). This leads to equation 24 to determine α , whereby equation 24 simplifies to equation 25 if $\frac{[I]_0}{K_D} \gg 1$ is true. The absolute rate constants of polymerization (k_p^- and k_p^\pm) can in turn be determined through consecutive measurements of the apparent rate constant k_p for varying degrees of α (i.e. by changing $[I]_0$), and subsequently plotting k_p vs. α . The intercept hereby yields k_p^\pm , while the slope gives ($k_p^- - k_p^\pm$). Finally, the rate constants are connected *via* equation 26:

$$\alpha = \frac{K_D}{2[I]_0} \left(\sqrt{1 + 4 \frac{[I]_0}{K_D}} - 1 \right) \quad (24)$$

$$\alpha = \sqrt{\frac{K_D}{[I]_0}} \quad (25)$$

$$k_p = k_p^\pm + (k_p^- - k_p^\pm) \sqrt{\frac{K_D}{[I]_0}} \quad (26)$$

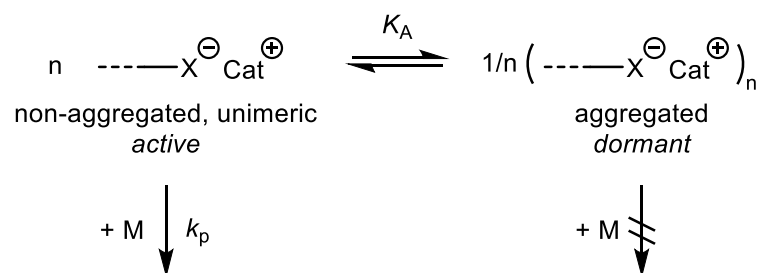
As can be deduced from equation 26, dissociated ions typically possess the highest rate constant of propagation, followed by the rate constants of ion pairs and lastly the rate constant of aggregates. For polymerizations conducted in THF without an additional cation-complexing agent, K_D is typically low, resulting in active centers being present in the form of ion pairs. An interesting phenomenon here is the so-called temperature of inversion (T_i). Below T_i , macroion pairs actually possess a higher reactivity than free macroions. This is due to the activation enthalpy of macroion pairs being lower than that of macroions, which is caused by the specific solvation shell of macroions, that first must be broken. This solvation shell becomes more perfect the lower the polymerization temperature is, leading to the above-described effect. For cationic processes, this picture changes drastically: K_D is typically significantly higher and increases proportionally with the polarity of the solvent used. The reason for this difference is the localized charge of the heteroatom in anionic polymerizations, while with cationic processes, the charge is distributed amongst the surrounding carbon atoms.³⁹ Furthermore, the rate constants of

polymerization of free ions and ion pairs in cationic processes are about the same ($k_p^+ \approx k_p^\pm$), since a) the cation is small while the counter-anion is large, leading to weak coulombic interactions. b) 90 % of the cationic charge is located not on the heteroatom, but on the adjacent carbon atoms, which also means that the counterion is not located in the direct vicinity of the active center, eliminating the need to significantly separate the counterion from it in order to facilitate propagation.

Growing/dormant species equilibria, represented by the temporary deactivation reaction depicted in Scheme 16, have also been observed in living ROP. In cationic processes, the dormant species is generated from a reaction of ion pair counterions (e.g. CH_3SO_3^- , CF_3SO_3^- or ClO_4^-) with the onium cation on the active center, generating a covalent bond. It is readily understandable, that the resulting covalent bond possesses a significantly lowered reactivity compared to the active species, which is why it is of utmost importance to understand how these species are formed and how one can influence their generation. In the cationic living ROP of THF, the temporary deactivation leads to a reversible ester formation, while the concentrations of macroesters and -ion pairs strongly depend on the polarity of the solvent used: in CCl_4 for example, almost no ions are present, while virtually no covalent species are being formed when using CH_3NO_2 .³⁹⁻⁴⁰ Given that both the ionic and covalent species operate simultaneously during a polymerization, the apparent rate constant is comprised of the absolute rate constants of ionic propagation (k_p^i) and covalent propagation (k_p^c), while taking the proportions of ionic (β) and covalent species ($1-\beta$) into account (equation 27). The reactivity of ionic species is about three orders of magnitude higher than that of covalent species and is thus virtually exclusively responsible for the propagation of the polymerization.

$$k_p = \beta \cdot k_p^i + (1 - \beta) \cdot k_p^c \quad (27)$$

The underlying mechanism generating dormant species differs for anionic and coordinative ROP vs. cationic processes. In cationic processes, one also must account for aggregates of ion pairs and covalent species, that both have been proven to be essentially unreactive.⁴¹ Hence, the only species participating in macromolecular chain growth are non-aggregated, unimeric species. Thus, Scheme 18 provides an appropriate overview of reactions that need to be considered for determining the



Scheme 18: Pertinent reaction scheme for kinetic considerations in anionic/coordinative ROPs with dormant/active center equilibria.

$$\ln r_p = \ln k_p \cdot (m \cdot K_A)^{-\frac{1}{m}} + \frac{1}{m} \cdot \ln [I]_0 \quad (28)$$

$$r_p^{1-m} = -m \cdot K_A k_p^{1-m} + k_p [I]_0 r_p^{-m} \quad (29)$$

dormant-active center kinetics. The corresponding kinetic equations provide two useful dependences according to literature (equations 28 and 29).^{41c, d} r_p hereby reads as $r_p = \frac{d[M]}{dt} \cdot \frac{1}{[M]} = t^{-1} \cdot \ln \frac{[M]_0}{[M]}$. $[I]_0$ corresponds to the starting initiator concentration, which is, given that the correct living polymerization conditions are chosen, equivalent to the total concentration of active (dormant and growing) centers. *Via* equation 28, the degree of aggregation (m) can be calculated after determining the experimental data (r_p and $[I]_0$). A value of $m = 1$ hereby represents a propagation on one type of active center, that is formed quantitatively from an initiator. $m < 1$ in turn corresponds to species that aggregate into species of lower reactivity (equation 28, $r_p \sim [I]_0^{1/m}$). However, plotting r_p vs. $[I]_0$ will only give the product of K_A and k_p and cannot be used to determine both values separately. If the degree of aggregation is known, separate determination of K_A and k_p is possible *via* equation 29. It can conclusively be argued, that K_A depends on a multitude of factors, such as the chemical structure and polarity of the monomer, initiator, as well as on reaction parameters like solvent, temperature and concentrations. For example, for the polymerization of CL initiated by diethyl aluminum ethanolate (Et_2AlOEt), k_p and K_A were shown to decrease with increasing dielectric constant of the solvents ($r_p(\text{C}_6\text{H}_6) > r_p(\text{THF}) > r_p(\text{CH}_3\text{CN})$).^{41e} However, when increasing $[I]_0$ up to $0.1 \text{ mol}\cdot\text{L}^{-1}$, the measured r_p -values were almost equal. This shows that the generation of unreactive aggregates increases with increasing concentration, whereby this effect is more prominent for less-polar solvents. Also, it appears that the most polar solvent CH_3CN is able to break down aggregates, while C_6H_6 and THF still possess equilibria between non-aggregated and aggregated species. This is counterintuitive to the

above-mentioned low k_p for THF and CH₃CN, since retarded aggregate formation should lead to an increase in non-aggregated, active species and thus increase k_p . Yet, an inverted reactivity has been observed. When considering the increased solvating power of THF and CH₃CN, this phenomenon can be readily explained: an improved solvation of growing chain-ends will necessarily lead to an increase in ΔH_p^\ddagger , since the formed complex is more stable than when using less-polar solvents. Thus, specific solvation effects seem to prevail over electrostatic field effects, leading to the observed decrease of k_p , despite increasing solvating power and polarity of the solvent. Furthermore, not only active chain-ends can undergo aggregation. It is also known for initiators like aluminum triisopropoxide (Al(O^{*i*}Pr)₃) to exist in an active-dormant species equilibrium. In the case of Al(O^{*i*}Pr)₃, this is embodied by its trimeric and tetrameric aggregates, where it was shown that exclusively trimeric aggregates initiated the polymerization of CL.⁴²

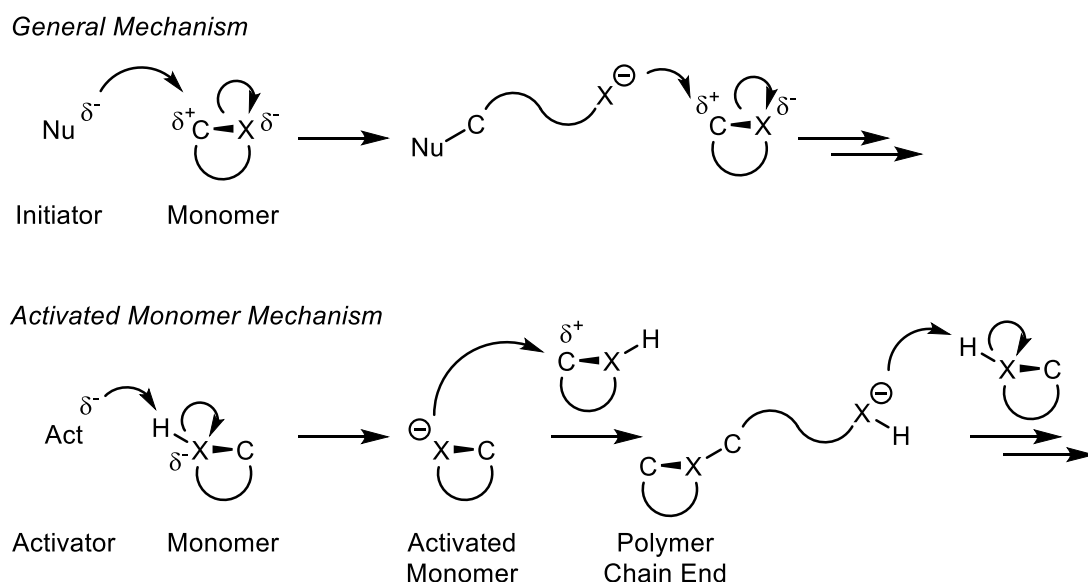
This concludes the concise summary of thermodynamic and kinetic considerations in scope of this thesis. The discussed phenomena however reveal the pivotal role of thermodynamic and kinetic considerations in understanding polymerization mechanisms, and ultimately to perform a controlled ROP yielding the desired material properties and microstructures. Of course, the herein provided overview only scratches the surface of kinetic and thermodynamic phenomena, and an encompassing encyclopedia is abundantly offered in literature.^{1, 7, 26b, 43}

1.1.4. General Polymerization Mechanisms of ROP

The abundance of heterocyclic monomers of differing chemical structures offers a remarkable variety of applicable polymerization mechanisms in ROPs. These processes shall be summarized in this chapter, whereby the applied technique of Lewis Pair Polymerization (LPP) will be discussed in more detail in chapter 1.2.

1.1.4.1. Anionic ROP

Ring-opening induced through a nucleophilic attack from an initiator can be classified as anionic ROP (aROP), since an anionic species is generated in the process (Scheme 19, top). The prerequisite for a monomer to be polymerizable *via* an aROP mechanism is the existence of a polarized bond (in Scheme 19 (top) depicted as wedged bond), which is susceptible to nucleophilic attack. Prime examples are cyclic esters, carbonates, amides, urethanes or phosphates which can readily be converted into their corresponding polymers. If the monomer features a three-membered ring structure, less-nucleophilic moieties become addressable using aROP, due to the ring-strain induced decrease in ΔH_p^\ddagger . Congeners polymerizable through this effect are e.g. three-membered ethers, amines or thioethers. Traditionally, the propagation then proceeds *via* a nucleophilic attack of the active chain-end to a monomer.

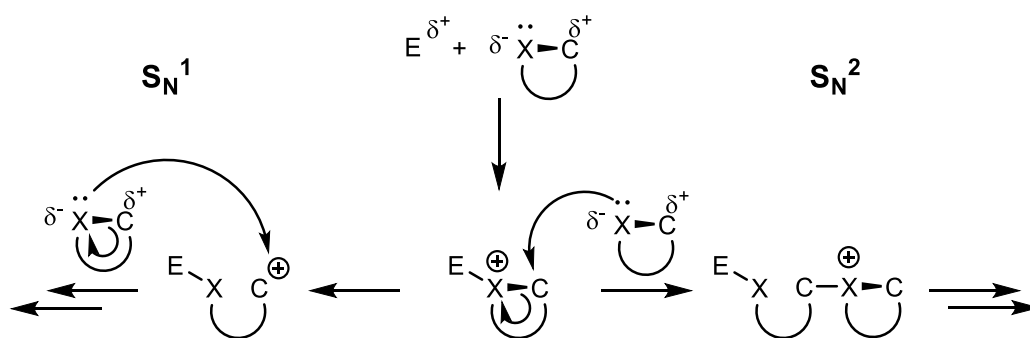


Scheme 19: Mechanisms present during anionic ROP (aROP). Top: general mechanism, where an initiator performs a nucleophilic attack on a polarized bond (wedged) in the monomer, leading to an anionic propagating species. Bottom: activated monomer mechanism, where an activator activates a monomer (i.e. *via* deprotonation), prior to the now activated monomer initiating ring-opening *via* nucleophilic attack on a polarized (wedged) bond of a non-activated monomer. Subsequently, the generated propagating species will activate another monomer to reform the initiating species. Propagation then proceeds *via* nucleophilic attack of the initiating species on the polymer chain end. Wedged bonds symbolize the polarized nature of the bond.

However, due to the highly reactive nature of the propagating chain end, this process typically suffers from back-biting side-reactions. Monomers like CL or PO are converted to polymers using this traditional approach of aROP. In contrast to this, the activated monomer mechanism (Scheme 19, bottom) achieves propagation in a different manner: firstly, the monomer is activated by an activator *via* e.g. deprotonation, generating an activated monomer species which in turn performs a nucleophilic attack on another monomer. This generates a highly basic species, which can abstract a proton from a monomer and regenerates the activated monomer. Propagation then proceeds *via* a nucleophilic attack of the activated monomer on the polymer chain end. This activated monomer mechanism can be used to mitigate the occurrence of side-reactions, since no highly reactive polymer chain end is generated. The polymerization of ϵ -caprolactam, a seven-membered lactam, is an industrially relevant process utilizing the activated monomer mechanism (e.g. preparation of Nylon®). However, side-reactions still govern the polymerization of this specific monomer and to date no living anionic polymerization has been developed.

1.1.4.2. Cationic ROP

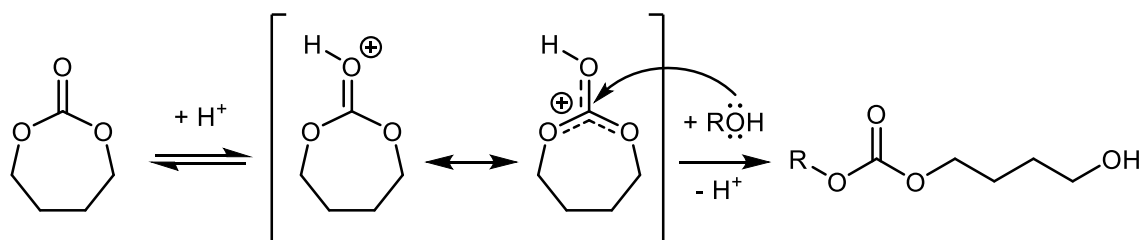
In cationic ROP (cROP), an electrophilic initiator (E) is used to generate the initiating species, much resembling the activated monomer mechanism of aROP. A prerequisite for this is, that the monomer heteroatom bears a free electron pair which can perform the nucleophilic attack on the initiator. There are generally two different modes of operation possible during traditional cROPs, one being an S_N^1 mechanism (Scheme 20, left), while the other proceeds *via* an S_N^2 mechanism (Scheme 20, right). Which of those processes dominates depends on the stability of the generated cationic



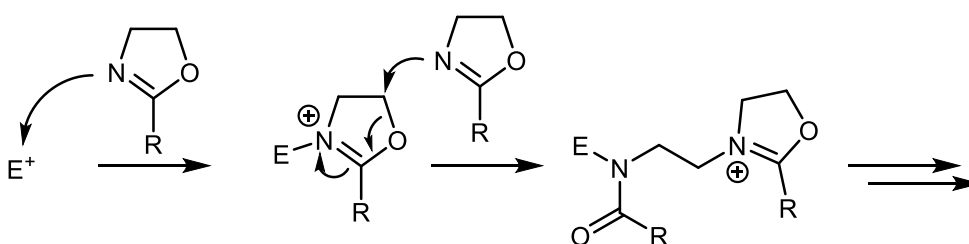
Scheme 20: Two modes of operation present during cationic ROPs (cROPs). Left: S_N^1 mechanism, predominately occurring if substituent effects stabilize the cationic center during polymerization. Right: S_N^2 mechanism, where the nucleophilic attack and the ring-opening occur concertedly. Wedged bond = polarized.

species. If the cationic center is sufficiently stabilized (e.g. by substituent effects (+I/M)), the S_N1 process is likely to predominate during the polymerization. Likewise, an activated monomer mechanism can occur during cROPs, as exemplified in the cROP of seven-membered butylene carbonate (Scheme 21, top). The activation hereby frequently proceeds *via* protonation of a monomer leading to the formation of the activated monomer bearing a cationic charge. Subsequently, the activated monomer is attacked by an initiator (e.g. an alcohol), performing the ring-opening and regenerating the proton to enable the *de novo* formation of the activated monomer. Propagation then proceeds *via* nucleophilic attack of the polymer chain end on the activated monomer, while the resulting polymer features an initiator-derived end group. Another powerful tool of cROP is the so-called isomerization polymerization, whereby a functional group in the monomer isomerizes during the polymerization process, forming a thermodynamically favored moiety. Using this isomerization as driving force, such polymerizations proceed smoothly and are free of back-biting reactions, as exemplified in the isomerization cROP of oxazolines (Scheme 21, bottom).⁴⁴ Here, the oxazoline monomer attacks an electrophilic initiator to form the

Activated Monomer cROP



Isomerization cROP

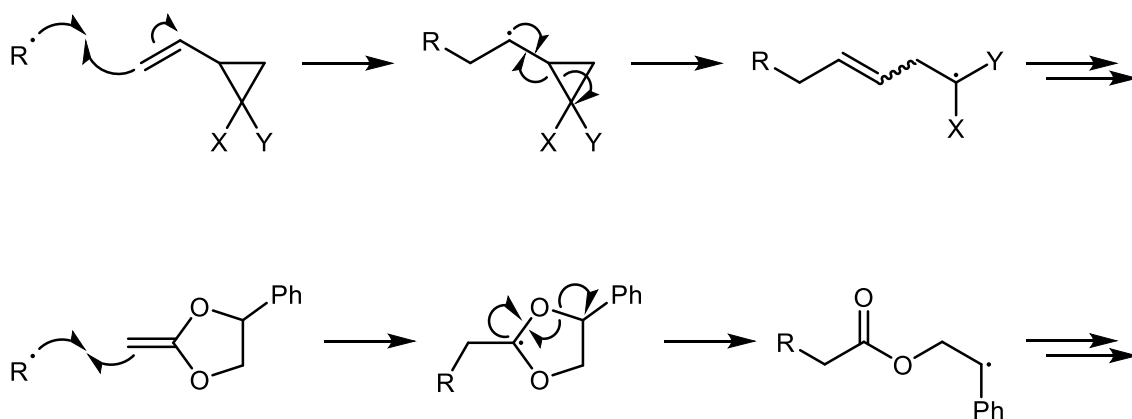


Scheme 21: Activated cROP of butylene carbonate (top). Activation is achieved *via* protonation of the monomer, generating a cationically charged species which is susceptible to nucleophilic attack by an initiator. Bottom: isomerization cROP of a substituted oxazoline, which first performs a nucleophilic attack on the initiator generating the corresponding iminium cation. This is then attacked by a monomer, to perform a concerted ring-opening and isomerization, yielding an amide-bearing side-group in the corresponding polymer.

corresponding iminium cation. The iminium cation is then in turn attacked by another monomer, which is accompanied by a concerted ring-opening and isomerization. The cyclic imino ester moiety is hereby transformed into an amide side chain of the growing polymer. This latter approach allows for the application of unique monomers, specifically designed to undergo isomerization during polymerization, such as spiro-orthoesters or dithiocarbonates.⁴⁵

1.1.4.3. Radical ROP

The main difference between the radical ROP (rROP) and other mechanisms discussed hitherto, manifests in the chemical nature of the functional groups present. While both in aROP and cROP processes, the existence of highly polarized functional groups is a premise for the required heterolytic bond cleavage, this is not the case for rROPs. Here, the homolytic bond cleavage generates a radical that can be stabilized by well-established processes originating from organic chemistry. Two typical approaches are depicted in Scheme 22: firstly, a substituted vinyl cyclopropane monomer is polymerized (top). The vinyl bond hereby acts as radical acceptor, forming a secondary radical which is subsequently transformed into a radical stabilized by substituents through the formation of an internal olefin.⁴⁶ On the bottom of Scheme 22, the terminal olefin of a ketene acetal acts as radical acceptor, initially generating a tertiary radical. Through the formation of a thermodynamically favored ester moiety, this radical is then transformed into a secondary radical stabilized through the mesomeric interactions with the phenyl substituent.⁴⁷ These rROP



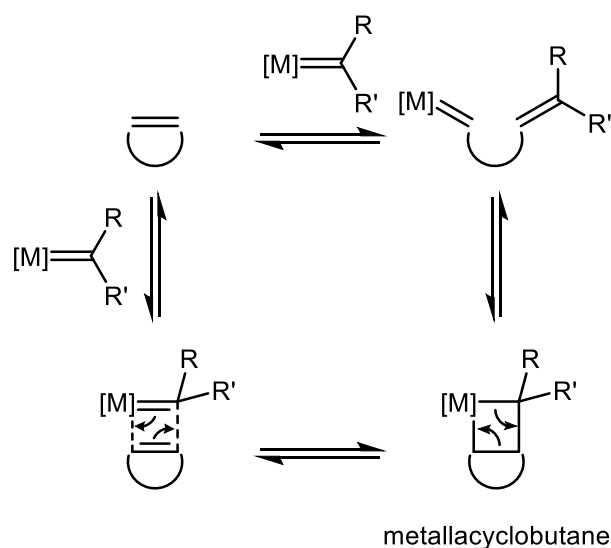
Scheme 22: Exemplary radical ROP (rROP) processes of monomers bearing vinyl moieties. Top: rROP of a substituted vinyl cyclopropane, generating a tertiary radical stabilized by substituents through the formation of an internal olefin. Bottom: rROP of a ketene acetal, forming a thermodynamically favored ester moiety and a secondary radical stabilized by mesomeric interactions with a phenyl substituent.

processes are a viable approach to polymers bearing functional groups, that are not accessible through traditional polymerization of vinyl monomers. Furthermore, this approach offers the possibility to perform copolymerizations with other, non-cyclic vinyl monomers, conceivably generating hydrolysable and photodegradable polymers from e.g. acrylates.⁴⁸

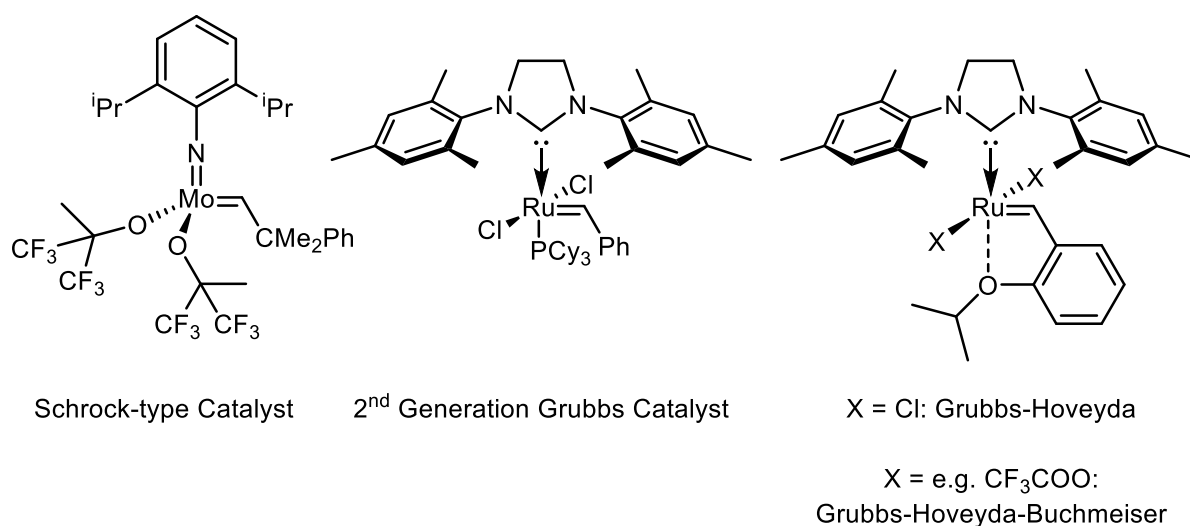
1.1.4.4. Ring-Opening Metathesis Polymerization

Another method to polymerize cyclic olefins is embodied by the ring-opening metathesis polymerization (ROMP). However, as this polymerization's mechanism is based on olefin metathesis, monomers are concomitantly joined during the polymerization process *via* 2+2 cycloaddition reactions, without an apparent charge or radical being present during propagation (Scheme 23). ROMP transfers mono-, bi- or multicyclic olefins into the corresponding polymers *via* a polyinsertion process that is triggered by a transition metal alkylidene. As the resulting polymer still possesses one double bond per repeating unit, back-biting reactions leading to macrocycle formation must be considered as well. The extent of this side-reaction heavily depends on multiple factors, such as temperature, monomer concentration, *cis/trans* configuration of the resulting double bond along the polymer backbone, solvent, reaction time and steric bulk of the applied monomer. Also, whether the monomer is condensed into a multicyclic ring-system affects the extent of back-biting. Furthermore, it needs to be stressed that generally every step of a ROMP process is reversible (Scheme 23). Hence, the equilibrium needs to be shifted to favour polymerization in order to generate high-polymers. Here, the release of the monomer's ring-strain or the formation of low-molecular-weight side products like ethylene are typically used as additional driving force of the polymerization.^{23c} Together with multiple contributions from other groups, the contributions of *R.R. Schrock* and *R.H. Grubbs* must be specifically mentioned in this context, as their work played a pivotal role in gaining important insights into metathesis chemistry and was awarded with the Nobel Prize for chemistry in 2005. Their work led to the design of well-defined ROMP initiators, that quickly outrivalled the state-of-the-art systems at that time, and has been comprehensively reviewed in literature (Scheme 24).^{23c, 49} The development of novel initiator systems based on well-defined transition metal catalysts with pre-formed alkylidenes continues to this day, and significant progress has been made. High-performance initiators are now able to address issues like regio-

and stereoselectivity, latency of the initiating system, induce tacticity in the resulting polymer, are able to perform metathesis reactions under biphasic conditions or even specifically address macrocyclization over polymerization.⁵⁰ This intense research interest will guarantee further progress in both polymer and materials science, and will ensure that ROMP stays an essential part of ROPs.



Scheme 23: Reaction scheme of ring-opening metathesis polymerization (ROMP). Since all steps are generally reversible, ROMP can be seen as an inverse ring-closing metathesis (RCM). ROMP is triggered *via* a transition metal alkylidene, that undergoes a 2+2 cycloaddition to form a metallacyclobutane, a species typical for metathesis reactions. Finally, the metallacyclobutane undergoes a 2+2 cycloreversion to finalize the insertion of the monomer into the existing olefinic bond. Scheme adapted from literature.¹

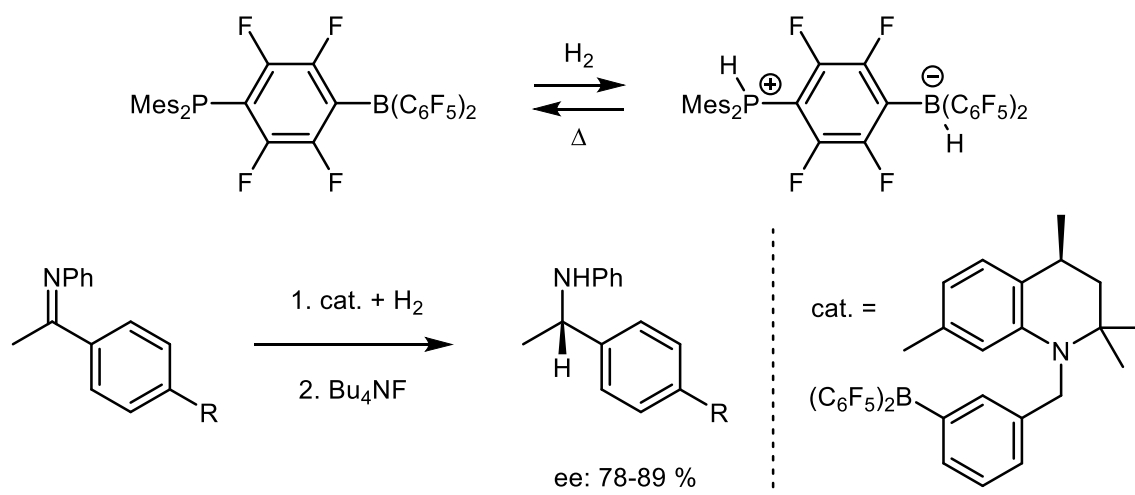


Scheme 24: Typical olefin metathesis catalysts. *Schrock*-type catalysts employ Mo(VI) and W(VI) metal centers supported by alkoxide and imido ligands, while *Grubbs* catalysts feature Ru(II) carbenoid complexes. Alteration of the 2nd generation *Grubbs* Catalysts with a chelating isopropoxybenzylidene ligand gives access to *Grubbs-Hoveyda* (X = Cl) and *Grubbs-Hoveyda-Buchmeiser* (X = e.g. CF₃COO) catalysts.⁵¹

1.2. Lewis Pair Polymerization

1.2.1. Historical Remarks

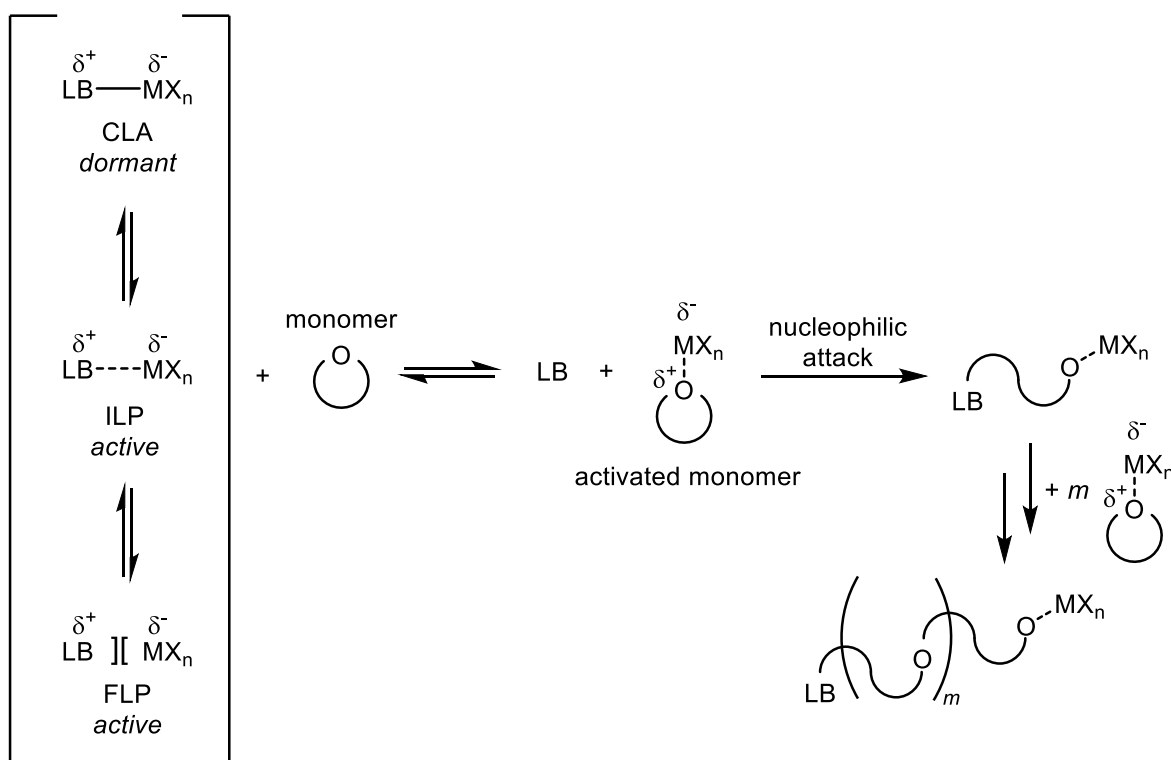
The concept of Lewis acidity and basicity dates back to the initial rationale first postulated by Lewis.⁵² This now universally accepted theory classifies electron-accepting and -donating molecules as acids and bases, respectively, to describe dative donor-acceptor adducts. Henceforth, this principle was a fundamental part of main-group chemistry, formed the basis of coordination chemistry of transition metals and was pervasive in a multitude of both stoichiometric and catalytic transformations of organic chemistry.⁵³ About a decade ago, the scope of Lewis adducts has been supplemented by a novel class of compounds, so-called “frustrated Lewis Pairs” (FLPs). Seminal contributions by *Stephan* and co-workers have coined the definition of FLPs as “bulky Lewis acids (LAs) and bases (LBs) which are sterically precluded from forming simple Lewis adducts” (selected examples given in Scheme 25).⁵⁴ These compounds possess an astonishing chemical reactivity, that was previously often unique to transition-metal complexes: from small molecule activation (H_2 , CO_2 , N_2O), to reactions with alkenes and alkynes or even catalytic hydrogenation, FLPs cover a broad range of chemical transformations.⁵⁵ It was only a matter of time, until polymerization catalysis would also be included in this list. Here, it was the inspiring work of *Chen* and co-workers that established the first highly active FLP-catalysed polymerization of substituted acrylates in 2010, employing sterically encumbered LBs together with $\text{Al}(\text{C}_6\text{F}_5)_3$ as LA.⁵⁶ These findings sparked the research interest in this field, and culminated into an encompassing selection of Lewis pair mediated polymerization catalyses, that shall be concisely summarized in this chapter.



Scheme 25: Selected reactions to demonstrate diverse FLP reactivity.^{55a}

1.2.2. Introduction

Lewis Pair Polymerization (LPP) defines itself as a process, that harnesses the cooperativity of a LA and LB to achieve and control the various steps of polymerization, namely monomer activation, chain initiation, propagation, termination and transfer reactions.³ Hereby, the polar nature of the monomer is a premise for the applicability of LPP, since a key step of LPPs is the coordination of the LP onto the monomer. The difference between other types of polymerizations (e.g. zwitterionic, anionic, cationic or coordination polymerization) lies in the auxiliary relationship of the LP: both components participate in the respective steps of the polymerization process, unlike being simple additives as is the case with the other techniques. This polymerization method provided significant enhancements to already existing systems and is applicable to a broad range of polar monomers while being able to achieve high activity, control or livingness. Even full chemo- and/or regioselectivity can be accomplished using the technique of LPP. Since the first report in 2010,⁵⁶ the scope of applicable LPs has extended beyond FLPs and encompasses also classical Lewis adducts (CLAs) and loosely bound LPs (interacting



Scheme 26: Concept of Lewis Pair Polymerization (LPP). Note the different LP species (CLA, ILP, FLP), that often interconvert *via* equilibria governed by various factors (e.g. solvent, temperature). After coordination to the monomer is achieved, the activated monomer will be attacked by a LB to accomplish initiation. Propagation will then proceed with other activated monomer species to form the final polymer. The propagating chain end is likely to be stabilized by the LA.

Lewis Pairs, ILPs). When subjected to an eligible monomer, the LP will coordinate onto it to form an activated monomer, which is susceptible to initiation. Propagation is then achieved by incorporating other activated monomer species (Scheme 26). From this general mechanism, it is evident that the respective strength of LA and LB are essential in determining the efficiency of the catalytic setup. IUPAC recommends that the respective Lewis strengths should be determined using equilibrium constants, or in form of the corresponding Gibbs free energies of adduct formation with a specific reference.³ However, there are no full-range, absolute and consistently quantitative scales for Lewis acidity or basicity, due to the complex acid-base interactions that are furthermore limited by the respective choice of reference.³ NMR spectroscopy is used by two of the most common methods (*Childs* and *Gutmann-Beckett*) employed to determine the strength of LAs. Both methods apply specific reference compounds and determine the spectroscopic shift when a LA coordinates to the reference. *Childs* et al. hereby use ¹H NMR measurements and crotonaldehyde as LB reference, while standardizing the scale on the chemical shift of the crotonaldehyde - BBr₃ complex.⁵⁷ Gutmann and Beckett have demonstrated that using triethylphosphine oxide as a reference and following the shifts in ³¹P NMR spectroscopy upon complexation, is a convenient method to determine so-called acceptor numbers (ANs), by defining two arbitrary points with *n*-hexane (AN = 0) and SbCl₅ (AN = 100).⁵⁸ Other, computational methods, prove especially useful for short-lived or decomposing LAs. Here, the Lewis acidity is calculated in the gas phase against a reference, whereby the negative enthalpy of formation is being considered (e.g. fluoride ion affinity (FIA) or hydride ion affinity (HIA)).⁵⁹ As of recently, *Stephan* et al. use global electrophilicity indices (GEI, $\omega = \mu^2 \cdot (2\eta)^{-1} = \chi^2 \cdot (2\eta)^{-1}$ with μ being the chemical potential, χ representing electronegativity and η embodying the chemical hardness) as a metric to gauge Lewis acidity in a timely manner.⁶⁰ For LBs, another parameter is equally important: nucleophilicity, or rather, the balance between basicity and nucleophilicity heavily dictates chemical reactivity in LB-mediated polymerizations. To quantify base strength, Brønsted basicity is still a widely applied concept as its reference acid is the most commonly encountered acid H⁺. Hence, the well-recognized equilibrium constant p*K*_A can be used to assess Lewis basicity, and encompassing p*K*_A-tables of a multitude of compounds in various solvents have been published in literature (see cited literature and references therein³). Another computational method to compare the basicity of organic

compounds is the proton affinity (PA).⁶¹ PAs are the negative of the enthalpy change of a protonation reaction in the gas phase, and are thus an expeditious method to compare the basicity of compounds that otherwise cannot (or only arduously) be determined. Furthermore, the molecular electrostatic potential (MEP) can be used to visualize nucleophilicity and basicity. Here, a probe (H^+) is subjected along the surface of a molecule, whereby the dipole moment, electronegativity and partial charges affect it, resulting in either attractive or repulsive forces. The respective strength of the forces can then be employed to generate a “heat map” of nucleophilicity and basicity of a compound, which provides significant insights in chemical reactivity.¹² As outlined above (Scheme 17 and Scheme 26), the structure in solution is crucial to an LP’s reactivity. This poses a challenge when employing CLAs that are for example embodied by simple inorganic LAs like $AlCl_3$, as their structure in solution is often polycentric. Typically, additional energy must be provided to break up these aggregates and transform them into active species. This is most likely accompanied by complex equilibria that enable interconversion between the species, where each possesses their respective rate constants. Also, due to these equilibria, the Lewis acidity might be attenuated, as the equilibrium constant of LA-monomer-adduct formation is detrimentally affected. Yet, there still exists a vast abundance of such examples, with one of the most well-recognized being the Ziegler-Natta polymerization of olefins.⁶² Here, $TiCl_3$ together with Et_2AlCl forms a heterogeneous, polymeric catalytic system with multiple possible ways of activation, capable of generating isotactic PP. This inherent complexity spurred researchers to develop well-defined single-site catalysts, in order to elucidate the underlying mechanism of Ziegler-Natta polymerizations, ultimately leading to an enhanced understanding and improved control and stereoselectivity. In context of LPs, it is interesting to consider whether there exists a definite boundary between CLAs, ILPs and FLPs. Earlier, the understanding of LP chemistry dictated, that the individual reactivities of LAs and LBs will be quenched upon forming a CLA. Hence, FLPs and CLAs were considered as two distinct species that possess fundamentally different reactivities. This was reconceived by *Stephan* et al., proving that Verkade’s base forms a spectroscopically stable CLA with $B(C_6F_5)_3$, while still being able of small molecule activation.⁶³ Also, an LP consisting of 2,6-lutidine and BMe_3 favours a CLA at low temperatures, while re-entering an equilibrium with the dissociated LA/LB form in solution and featuring enough reactivity to heterolytically cleave dihydrogen and ring-open THF.⁶⁴

1.2.3. Lewis Pair catalysed Polymerizations

A strong indicator, that a multicomponent catalytic system should be placed in the context of LP mediated polymerizations, is that no polymer formation can be observed in the absence of one of the components. This hints to a close liaison between catalytically active elements, that goes beyond of one being simply an additive to modulate reactivity or control. The first of such highly active systems was introduced in 2010 by *Chen* et al., using the highly Lewis acidic and sterically encumbered LA $\text{Al}(\text{C}_6\text{F}_5)_3$ in combination with LB featuring high steric demand, to polymerize substituted (cyclic and linear) acrylates (Figure 3).⁵⁶ This system generated FLPs of varying catalytic activity, with the most active being the $\text{IMes}\cdot\text{Al}(\text{C}_6\text{F}_5)_3$ LP ($\text{TOF} > 48000 \text{ h}^{-1}$, $M_n = 26.6 \text{ kg}\cdot\text{mol}^{-1}$, $D_M = 1.77$). Interestingly, NHC-based LPs investigated in this study also formed a CLA at room temperature in benzene, emphasizing the importance of the assembling sequence of the system. It was thus necessary, to preform an activated monomer species by adding $\text{Al}(\text{C}_6\text{F}_5)_3$ to the monomer, and subsequently add the LB to generate a zwitterionic active species (Scheme 27, A). Further encompassing mechanistic studies revealed a bimetallic mechanism operating during propagation (Scheme 27, B).⁶⁵ Here, the zwitterionic active species will perform a nucleophilic attack on another LA-activated monomer, liberating one LA molecule that can thus again act as a monomer activator. Furthermore, the authors identified yet another even more active LP for the polymerization of MMA. $\text{Al}(\text{C}_6\text{F}_5)_3$ together with the phosphazene superbases ${}^t\text{Bu-P}_4$

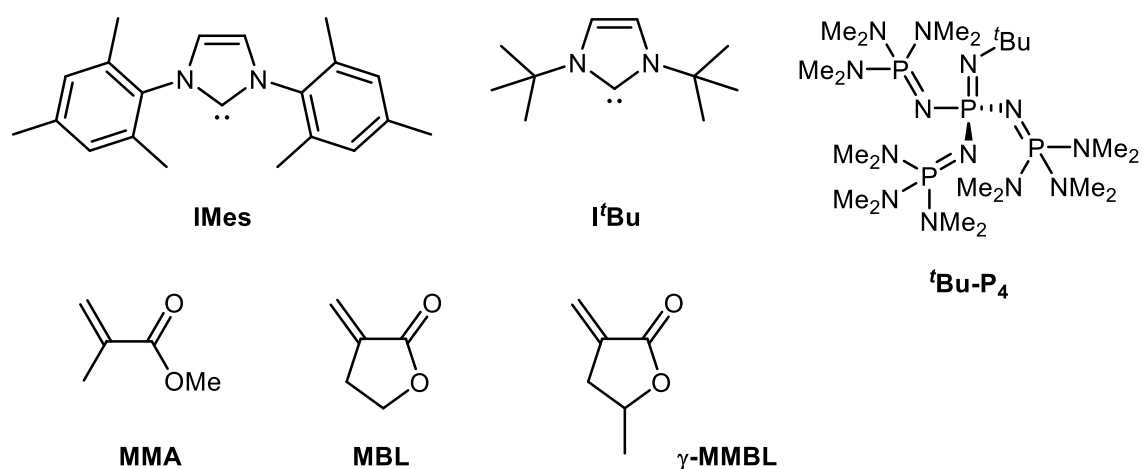
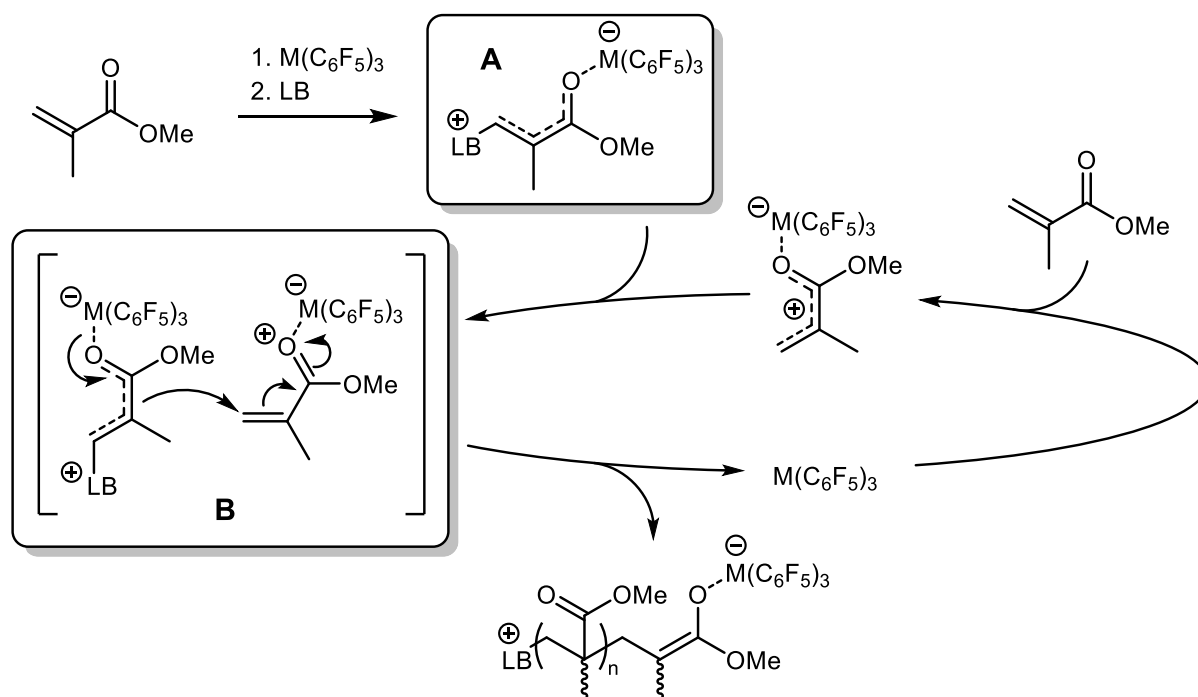
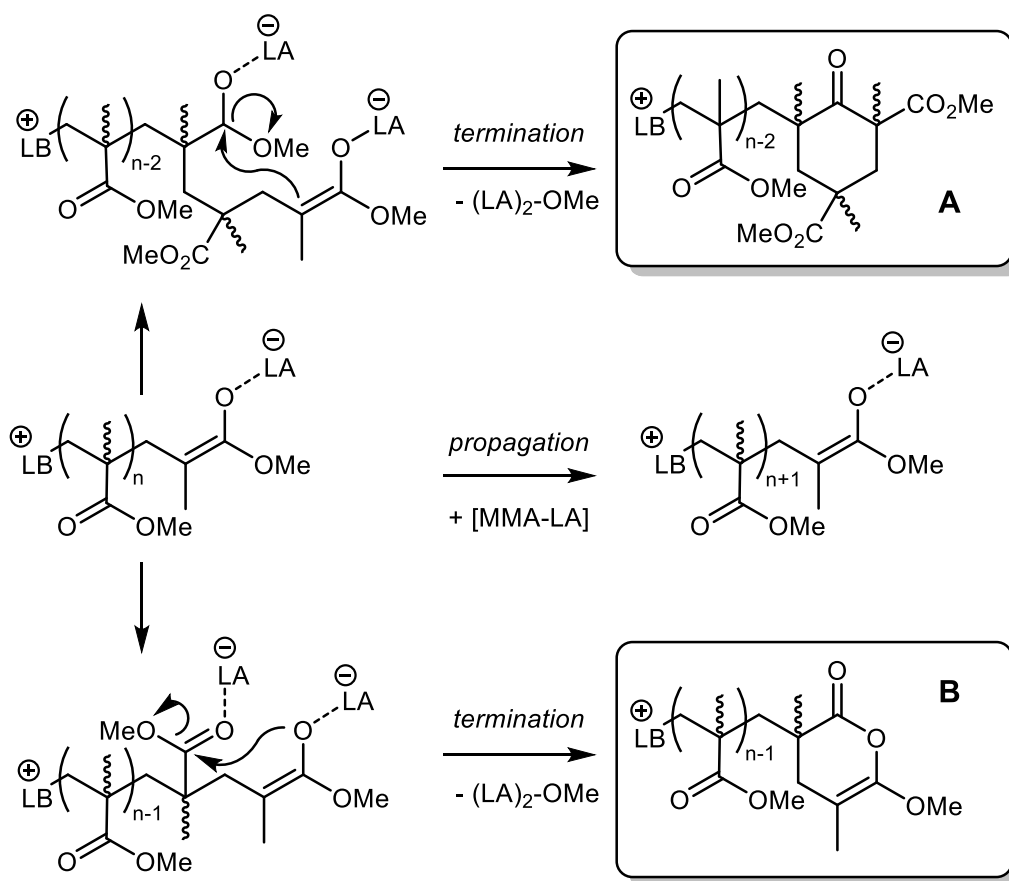


Figure 3: Selected examples of LBs and monomers investigated for LPP by *Chen* and co-workers. MMA = Methyl methacrylate, MBL = α -methylene- γ -butyrolactone, γ -MMBL = γ -methyl- α -methylene- γ -butyrolactone.^{56, 65}



Scheme 27: LPP of substituted acrylates, exemplified with methyl methacrylate (MMA). The mechanism was elucidated by *Chen et al.*^{56, 65} First, a zwitterionic active species is formed *via* sequential addition of LA and LB (A). Propagation then takes place through a bimetallic mechanism, where the active species performs a nucleophilic attack on an activated monomer (B). Hereby, one LA molecule is liberated that can again act as a monomer activator. $M = Al, B$.

(Figure 3) outperformed every other investigated LP and reached a TOF of $96\,000\text{ h}^{-1}$, while generating PMMA with a molar mass of $M_n = 212\text{ kg}\cdot\text{mol}^{-1}$ ($D_M = 1.34$). As evidenced by reported D_M values, despite their remarkable activity, the control of the catalytic systems described above still remains short of living polymerization methods. Hence, the study of chain termination reactions was vital in understanding how this issue could be mitigated, and control over the reaction could be improved. Here, two possible pathways of termination could be identified, with both being induced by back-biting reactions.⁶⁶ For the upper termination pathway leading to product A, the sp^2 -carbon atom of the growing enolate species will perform a nucleophilic attack on the ester carbon of the after next repeating unit, eliminating an $(LA)_2\text{-OMe}$ species and forming a β -ketoester moiety (Scheme 28, top). On the other hand, the lower termination pathway leading to compound B features a nucleophilic attack of the enolate-oxygen to the ester carbon of the adjacent repeating unit, again liberating an $(LA)_2\text{-OMe}$ molecule and forming a δ -valerolactone-derived end group (Scheme 28, bottom). Here, density functional theory (DFT) calculations found, that compound B is kinetically favoured, while compound A is about $20\text{ kcal}\cdot\text{mol}^{-1}$ more stable than compound B and is thus thermodynamically favoured. Yet, clearly these side-reactions pose a major issue if one desires to develop living

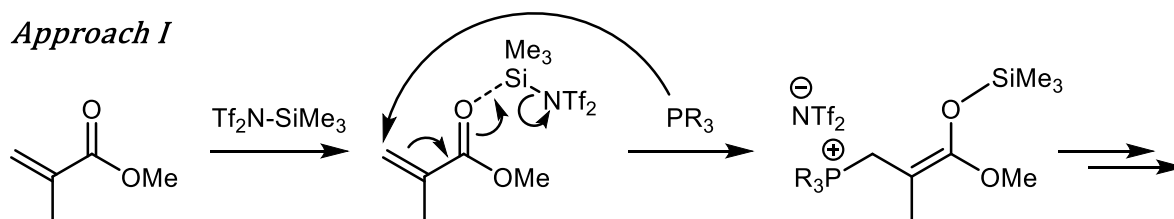


Scheme 28: Back-biting termination reactions present in $M(C_6F_5)_3$ -mediated LPP of acrylates (exemplified using MMA). Compound A is formed *via* a nucleophilic attack of the tertiary carbon atom of the LA-activated end group on the ester carbon of the after next repeating unit, liberating an $(LA)_2\text{-OMe}$ molecule and forming a β -ketoester as end group. The lower pathway depicts formation of compound B *via* nucleophilic attack of the LA-coordinated oxygen-atom on an adjacent ester carbon atom, again cleaving an $(LA)_2\text{-OMe}$ moiety and finally leading to a δ -valerolactone-derived end group. Scheme adapted from literature.⁶⁶

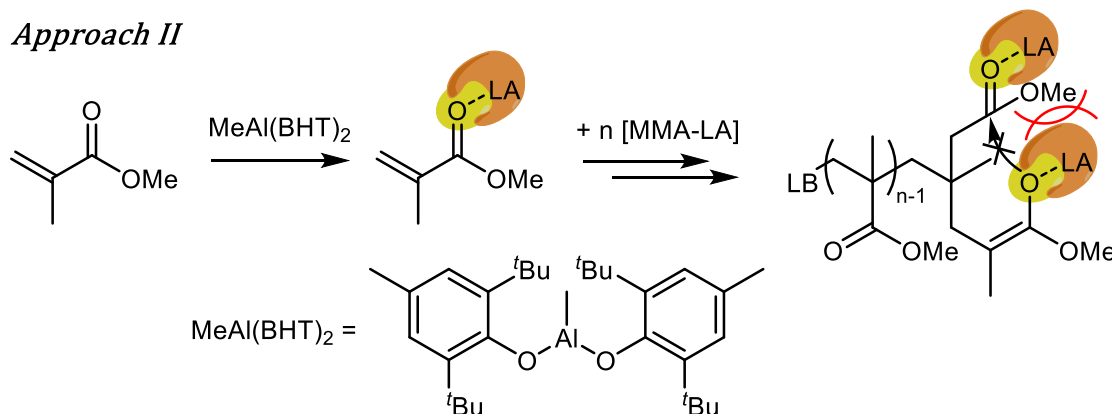
polymerizations employing LPs. Here, multiple methods have been developed to increase control and mitigate intramolecular cyclizations, also pervasive in anionic acrylate polymerizations. As the extent of those back-biting reactions clearly depends on the applied LA, it is a straightforward approach to reduce the Lewis acidity of the applied LA. For example, *Taton* and co-workers succeeded in employing a weak silane-based LA (*N*-(trimethylsilyl)bis(trifluoromethane sulfonyl)imide, $\text{Me}_3\text{SiNTf}_2$) together with common LBs (tri-*n*-butylphosphine, ${}^n\text{Bu}_3\text{P}$ or tri-*tert*-butylphosphine, ${}^t\text{Bu}_3\text{P}$) to form well-defined PMMA polymers of predictable molar mass and low \overline{M}_w values (< 1.08).⁶⁷ The increased control over the reaction was attributed to the less reactive propagating ends, that formed neutral species rather than zwitterionic ones as is the case when applying aluminium-based LAs (cf. Scheme 27, Scheme 29, approach I). Another elegant approach to mitigate back-biting is to introduce steric demand in the LA. Doing so will preclude the nucleophilic attack of the active enolate species on adjacent repeating units, leading to an improved control over molecular

weights and polydispersities. In this context, *Hong* et al. have demonstrated the use of sterically demanding $\text{MeAl}(\text{BHT})_2$ (BHT = 3,5-di-*tert*-butyl-4-hydroxytoluene) together with selected NHCs (Scheme 29, approach II) yielding PMMA of high molar masses and controlled dispersities (M_n up to $130 \text{ kg}\cdot\text{mol}^{-1}$, $D_M = 1.06 - 1.13$).⁶⁸ In 2016, *Rieger* et al. introduced the application of highly interacting LPs or even CLAs for the controlled polymerization of methacrylates and acrylamides.⁶⁹ By judicious choice of the LP components, the authors managed to generate very well-defined polymers from *tert*-butyl methacrylate with a high initiation efficiency of 93 % (LP = $\text{AlMe}_3\cdot\text{PMe}_3$, TOF = 200 h^{-1} , $D_M = 1.01$, $M_n = 61 \text{ kg}\cdot\text{mol}^{-1}$, Scheme 29, approach III). Again, the addition sequence was of utmost importance, as premixing LA and LB will form an inactive adduct, quantitatively quenching polymerization reactivity. On the other hand, the preformed monomer-LA-adduct forms highly active polymerization systems when subjected to a LB. Finally, unifying the aforementioned concepts, *Chen* and co-workers reported the first true living LPP of MMA and benzyl methacrylate.^{21d} Using a LP comprised of two sterically hindered compounds, namely *N*-heterocyclic olefins (NHOs) as LBs and $\text{MeAl}(\text{BHT})_2$ as LA, the authors developed a catalytic system featuring a delicate and fine-tuned balance of the key features necessary for practically perfect control: $\text{MeAl}(\text{BHT})_2$ possesses just enough Lewis acidity to efficiently activate the monomer, while being sufficiently benign to quell irreversible chain termination (back-biting). The applied NHOs were sterically encumbered to minimize interactions with the LA, yet still featured significant Lewis basicity due to their highly polarized exocyclic double bond, ensuring virtually quantitative initiation (Scheme 29, approach IV). Here, the livingness of this LPP has been substantiated by five key features of the polymerization. The molar mass of the generated polymer was fully predictable (M_n up to $351 \text{ kg}\cdot\text{mol}^{-1}$) while possessing narrow molar mass distributions ($D_M = 1.05 - 1.09$), the initiation efficiencies were practically quantitative and both plots of the molar mass vs. conversion and monomer-to-initiator ratio featured linearity. Also, multiple chain extension reactions were realized together with the successful preparation of well-defined di- and triblock copolymers, regardless of the addition sequence of the comonomers. Furthermore, the addition sequence of LA, LB and monomer did not entail any effect on the polymerization outcome, since an FLP is being formed. This marked the first

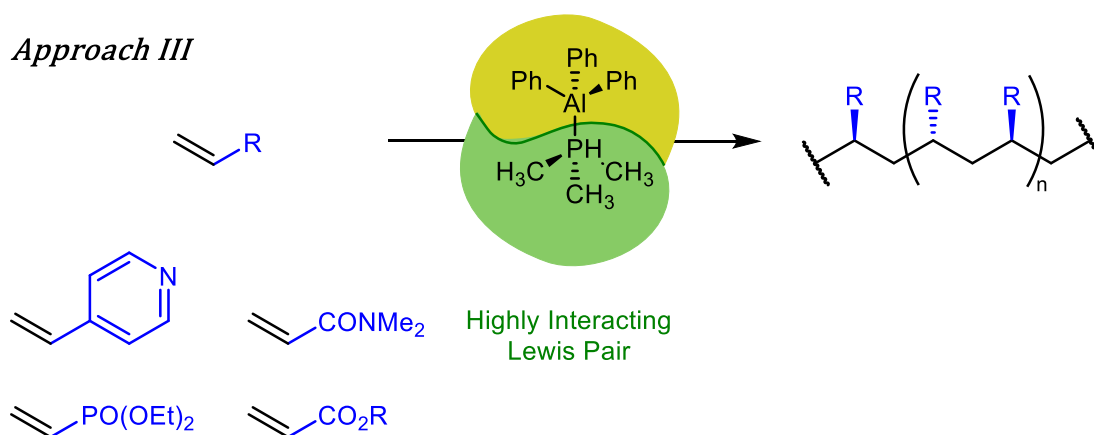
Approach I



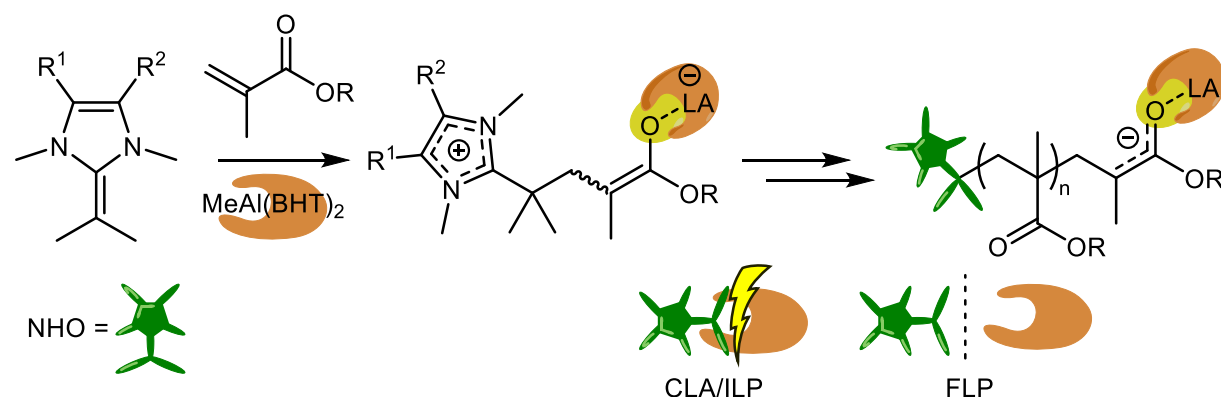
Approach II



Approach III



Approach IV



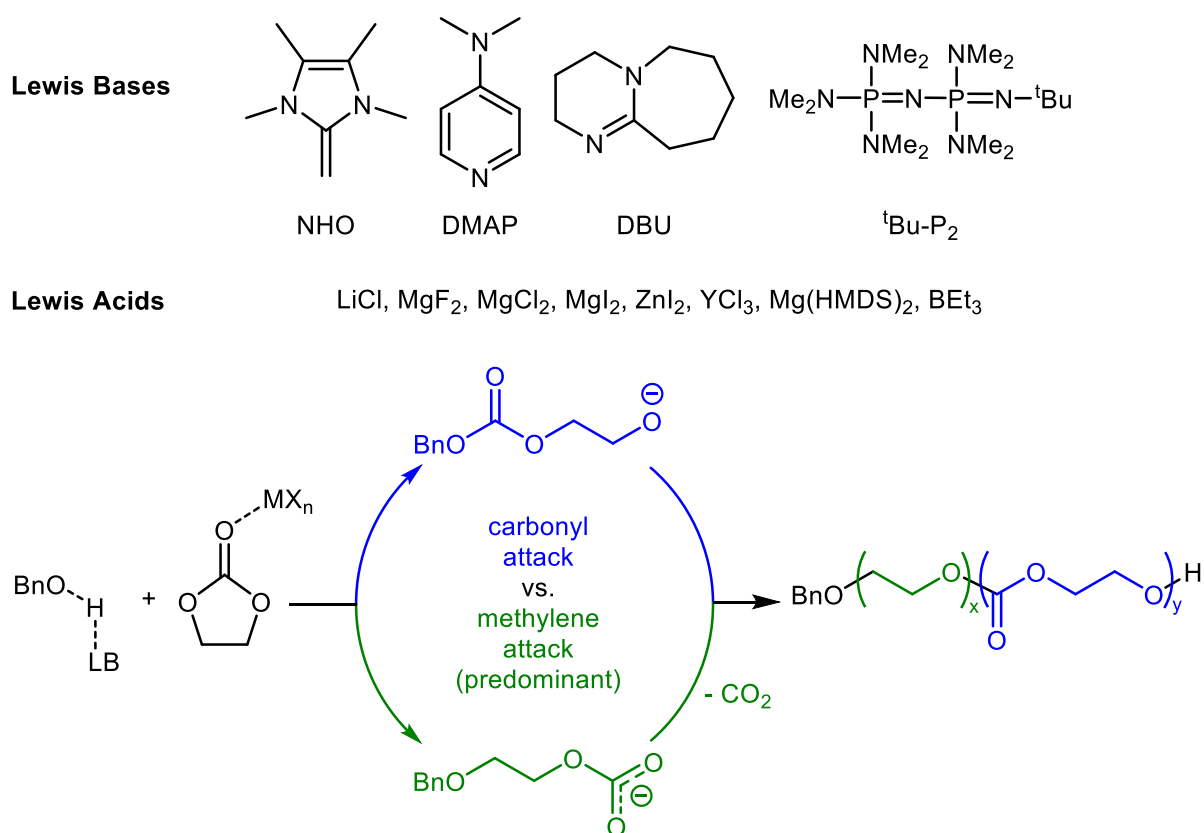
Scheme 29: Different approaches to mitigate back-biting in LP-mediated acrylate polymerizations. Approach I: instead of using highly Lewis acidic $\text{Al}(\text{C}_6\text{F}_5)_3$, a benign silane-based LA was applied, generating neutral propagating end groups instead of a zwitterionic species.⁶⁷ Approach II: the application of sterically encumbered LAs attenuates back-biting.⁶⁸ Approach III: highly interacting LPs were successfully applied in the polymerization of vinylic monomers. Hereby, the assembling sequence is crucial for the activity of the system.⁶⁹ Approach IV: combining the methodologies of using milder, sterically encumbered LAs and sterically protected LBs will form an FLP, that possesses a delicate, fine-tuned balance to achieve the first true living LPP.^{21d} Schemes adapted from cited literature.

true living LP-mediated polymerization of substituted acrylates, and again corroborates the potential of LP catalysis. Moving from linear to cyclic acrylates, the first LPP has been established in 2010 by *Chen* and co-workers.⁵⁶ However, it is important to note that despite their structural kinship with lactones, the cyclic structure during polymerization is not ring-opened, leading to an incorporation of the heterocycle into the polymer backbone and improving material properties of the resulting polymers. Interestingly, for γ -MMBL (Figure 3) *Chen* and *Xu* found an inverted reactivity: the CLA of $\text{Ph}_3\text{P}\cdot\text{B}(\text{C}_6\text{F}_5)_3$ exhibited the highest activity towards the formation of poly(γ -MMBL), while investigated FLPs (inter- and intramolecular) were virtually inactive.⁷⁰ This observation was attributed to the significant steric demand surrounding the otherwise free phosphorous and boron sites, that precluded the coordination to the monomer. Furthermore, $\text{Ph}_3\text{P}\cdot\text{B}(\text{C}_6\text{F}_5)_3$ only forms a CLA in the solid state; in solution, the CLA dissociates into an FLP which then readily coordinates to donor solvents or monomer molecules, priming them for initiation and propagation. However, this effect also possesses a delicate balance between Lewis acidity and basicity of the components that need to be accounted for by the respective sterical demands, since the strongest CLA with the least sterical stress ($\text{Me}_3\text{P}\cdot\text{B}(\text{C}_6\text{F}_5)_3$) could no longer dissociate in solution and was rendered inactive. Other monomer classes accessible *via* LPP are embodied by conjugated, vinyl-bearing monomers like 2-vinylpyridine (2-VP) or 2-isoprenyl-2-oxazoline (2-*POx*), that feature a $\text{C}=\text{C}-\text{C}=\text{N}$ -moiety. Here, the formation of a zwitterionic active species has been proven by *Chen* et al. in 2014, *via* the isolation of FLPs consisting of $\text{NHC}^{[+]}-2\text{-VP}-\text{Al}(\text{C}_6\text{F}_5)_3^{[-]}$ and $\text{NHC}^{[+]}-2\text{-}POx-\text{Al}(\text{C}_6\text{F}_5)_3^{[-]}$ and determination of their corresponding single crystal X-ray structures, that were effective in producing high molar mass polymers from the respective monomers.⁶⁶ Other vinyl-bearing congeners available to LPP are e.g. vinyl phosphonates and divinyl acrylic monomers. Hereby, the polymerization of divinyl acrylic monomers proceeds in a chemoselective manner, where only the conjugated vinyl bond which is part of the Michael-acceptor system will be polymerized, offering the possibility to post-functionalise the resulting polymers.⁷¹

However, not only linear monomers are accessible using LPP, there also exists a wide range of ROPs mediated by Lewis Pairs. As a major part is embodied by the ROP of cyclic esters and epoxides, this will be discussed in detail in chapter 2 and 3, whereby here only non-ester and -epoxide monomers will be mentioned. Besides these two

choosing an electronically and sterically balanced LP. Very recently, the scope of available monomers has been broadened by *Naumann* et al. to encompass the homopolymerization of ethylene carbonate (EC).⁷³ The authors aimed to develop a system capable of influencing the degree of decarboxylation occurring during polymerization (Scheme 31), which would ensue the formation of biodegradable polyethers. Therefore, they applied a combination of various LBs (NHO, DMAP (4-dimethylamino pyridine), DBU (1,8-diazabicyclo[5.4.0]undec-7-ene) and the phosphazene ^tBu-P₂, Scheme 31) together with LAs embodied by simple metal salts (LiCl, MgX₂ (X = F, Cl, I, HMDS), ZnI₂, YCl₃, BEt₃). During initial polymerization reactions it became abundantly clear, that the crucial component of this catalytic setup was the applied LA. Depending on the salt, either no polymer was generated (MgCl₂, MgI₂, ZnI₂, YCl₃, 180 °C, 3 h, microwave), or the polymerizations proceeded smoothly (LiCl, MgF₂, Mg(HMDS)₂, BEt₃). Control reactions again corroborated the pivotal importance of the LA, as no noteworthy influence was observed when employing the different LBs alone (> 90 % conversion, 13-16 % carbonate content, 2200-4300 g·mol⁻¹ in all cases). This picture changed dramatically when an additional LA was added: not only the polymerization rate was affected, but also the carbonate content and resulting molar masses were significantly influenced. While the application of LiCl resulted in a carbonate-content of < 5 % in the resulting polymer and moderate molar masses (< 2100 g·mol⁻¹, $\bar{D}_M = 1.4 - 2.5$, 71 - 91 % conversion), applying Mg(HMDS)₂ entailed a rapid and quantitative monomer consumption and a higher carbonate content of about 20 % in the generated polymers ($M_n = 800 - 2200$ g·mol⁻¹, $\bar{D}_M = 1.6 - 3.1$). Again, switching the LB only had marginal impact on the resulting polymers. Intensifying their research efforts, the authors managed to generate poly(carbonate-*co*-ether) polymers with molar masses of about 10 000 g·mol⁻¹ and varying carbonate contents of 8 - 21 %, while realizing TOFs of up to 5800 h⁻¹ (NHO/BnOH/Li(HMDS), 3 h, 200 °C, 87 % conversion, 6800 g·mol⁻¹). The difference in carbonate content was attributed to the difference in the LA's coordinating ability: while Li⁺ is known to exclusively but weakly coordinate *via* the carbonyl oxygen, the activation achieved by Mg²⁺-ions is likely to be much stronger, favouring the nucleophilic attack on the carbonyl atom rather than on the methylene unit. Furthermore, the ability to complex propagating carboxylate anions is also much more pronounced for Mg²⁺, as is the case for Li⁺. As one would expect, the varying carbonate content was also perceivable in the resulting material properties. DSC

measurements revealed that polymers with a carbonate content of < 10 % transition from amorphous materials into semi-crystalline polymers, exhibiting a melting point that converges with the melting points of polyether materials with decreasing carbonate content. The improved molecular weight most likely resulted from the selective activation of the LA, which is prone to monomer coordination, rather than coordination of the polymer backbone. Yet, MALDI-ToF MS measurements revealed an α,ω -dihydroxy-terminated species as the main population, that is attributable to transcarbonylation side-reactions. This emphasizes the need for improvement of the control over the reaction, which might be realized with other, more suitable LPs. Captivatingly, the utilization of as-received, non-purified EC did not impair the polymerization process – even the commercially available LB DBU was able to generate polymers under these conditions. Furthermore, degradation studies applying 1.4 M alkaline ethanol solutions showed that a high- M_n sample is degraded to < 1000 $\text{g}\cdot\text{mol}^{-1}$ in 3 h at room temperature. This highlights the possibility of a one-pot, one-step procedure to generate biodegradable, PEG-like polymers from abundantly available EC with simple metal salts and commercial organobases.

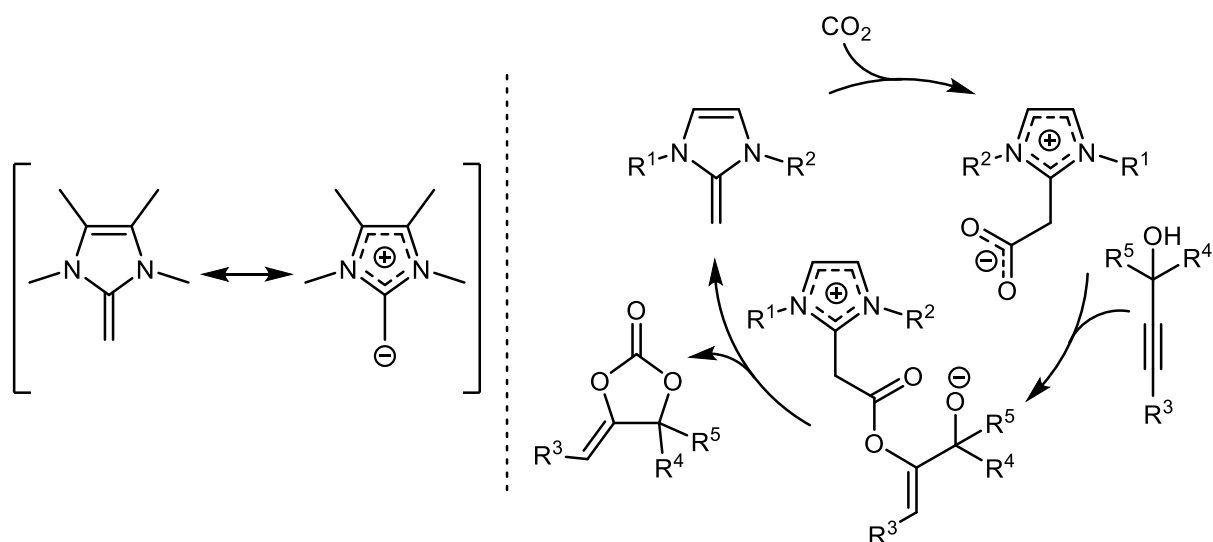


Scheme 31: LP-mediated ROP of ethylene carbonate (EC). The equilibrium between carbonyl and methylene attack was influenced by judicious choice of LA. Selective monomer activation further mitigated side-reactions, enabling the synthesis of high-MW, biodegradable poly(ether carbonate)s.⁷³

1.3. N-Heterocyclic Olefins

1.3.1. Introduction

The first congeners of *N*-heterocyclic olefins (NHOs, or ene-1,1-diamines, ketene aminated) were reported as early as 1967 by Schäfer and co-workers.⁷⁴ Despite being known for several decades, their potential in catalysis has been largely neglected until about ten years ago. The recent publication history finally accommodates this lack of recognition and begins to harness the intriguing and versatile properties of NHOs. One of their unique characteristics is the highly polarized, electron rich, exocyclic double bond, that earned them the title of “most ylidic alkenes”.^{11e} In fact, the exocyclic carbon atom (C_{exo}) is rendered more basic and nucleophilic by mesomeric stabilization, than the nitrogen atoms in the same molecule. Provided the presence of the right structural motives, this mesomeric stabilization will ensue an aromatization of the *N*-heterocycle, essentially locking the negative charge on the exocyclic carbon and corroborating that the reactive center is localized on this atom (Scheme 32, left side). This also is one of the most striking differences compared to NHCs, their *N*-heterocyclic congeners: while NHCs feature an electron sextet on the carbene, NHOs are neutral in their free state and can thus be conceived as latent carbanions. As will be discussed later, this enables an exceptional reactivity that often (out)rivals the most active, established systems or even gives access to wholly novel chemistry. The rekindled research interest burgeoned in 2013 by seminal work from *Lu et al.*, demonstrating the outstanding ability of NHOs to sequester CO_2 and transform propargylic alcohols into cyclic carbonates under mild conditions (Scheme 32, right side).^{11a} The available scope of reactions mediated by NHOs has improved ever since, and is highly likely to keep doing so, as the sheer structural diversity of NHOs has largely been untapped. By now, several conceivable reviews have been published, that offer a comprehensive synopsis of recent advances in NHO chemistry.^{2d, 11c, e, 75} As polymerizations mediated by NHOs have either already been discussed above (cf. chapter 1.2.3), or address monomer classes that will be discussed later (cf. chapter 2 and 3), it will be omitted to cover polymerizations here. Instead a brief overview over the rationale behind the structural design, properties and other chemical transformations mediated by NHOs will be given, that not only encompasses small molecule activation (*vide supra*), but also a variety of other catalytic applications, as well as organometallic chemistry.



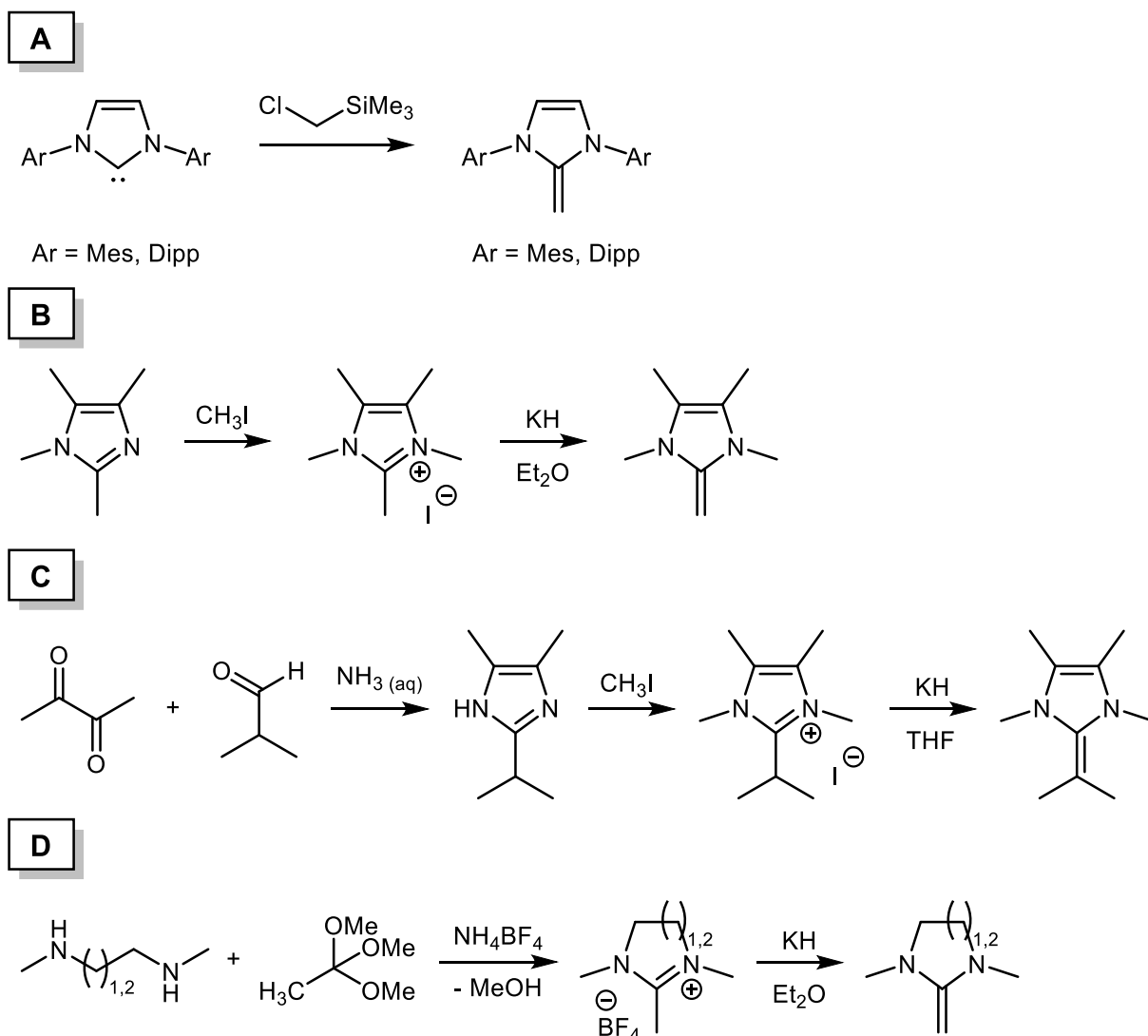
Scheme 32: Left: mesomeric structure of a typical NHO, highlighting the strongly polarized exocyclic double bond and its electron excess. Right: pioneering work of *Lu* et al. in NHO-mediated small molecule activation, marking the resurgence of NHO research. Only the more dominant pathway of cyclization is depicted. Please refer to the original publication to receive a detailed discussion of a possible NHO-mediated deprotonation of propargylic alcohol with subsequent CO₂ sequestration and cyclization.^{11a}

1.3.2. Synthetic Methods, Rationale of Design and Distinctive Features of NHOs

1.3.2.1. Synthesis

The synthesis of NHOs largely benefits from their structural kinship to NHCs and can generally be divided into four approaches. This is best demonstrated by the straightforward access to a multitude of NHOs *via* direct methylation of free NHCs, as published by *Rivard* et al. on a multigram scale (Scheme 33, method A).⁷⁶ Another representative method of synthesizing NHOs is the deprotonation of the corresponding precursor salt, whereby the salt itself is typically accessible in one or two steps (Scheme 33, methods B – D). Hence, one of the most employed NHOs for polymerization catalysis (1,3,4,5-tetramethyl-2-methyleneimidazoline, Scheme 32, left) is synthesized in two steps from 1,2,4,5-tetramethylimidazole *via* methylation with methyl iodide (CH₃I, MeI) and subsequent deprotonation with potassium hydride (KH) in diethyl ether (Et₂O) (Scheme 33, method B). What is more, the highly soluble free NHO can be directly extracted from the deprotonation mixture simply by extraction with *n*-pentane, and upon evaporation of the solvent, the NHO is received as a spectroscopically pure solid or liquid. For imidazole-derived NHOs with distinctive substitution patterns, the *Radziszewski* reaction can be employed.⁷⁷ Here, the *N*-heterocyclic ring is built in one step from aqueous ammonia, a diketone and an aldehyde. Subsequent methylation affords the precursor salt, which can then in turn

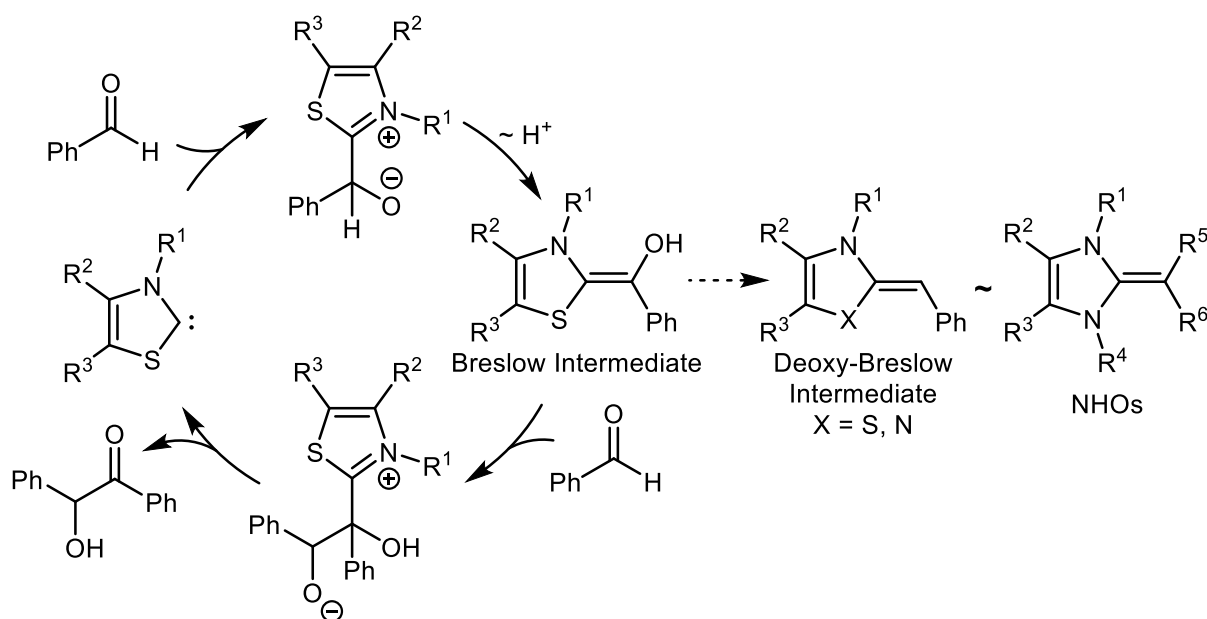
be deprotonated to liberate the free NHO (Scheme 33, method C). Lastly, saturated NHO structures are for example accessible from diamines, that are subjected to orthoesters in the presence of ammonium tetrafluoroborate (NH_4BF_4). The deprotonation of the thus generated precursor salt again yields the desired NHO (Scheme 33, method D). However, there exist far more approaches than the ones described herein, limited only by chemist's ingenuity to design NHO structures (mesoionic NHOs,⁷⁸ bicyclo-derived NHOs,⁷⁹ ...); the brief overview given here is only meant to corroborate the straightforward accessibility of multiple NHO structures. Furthermore, as the NHOs depicted in Scheme 33 represent some of the most intensively applied NHOs, it clearly underlines the hitherto significantly limited scope of structural diversity in NHO chemistry and also clearly elucidates future research prospects.



Scheme 33: Straightforward synthetic approaches to multiple NHO structures. Mes = 2,4,6-trimethylphenyl; Dipp = 1,3-diisopropylphenyl.

1.3.2.2. Rationale of Design and Distinctive Features

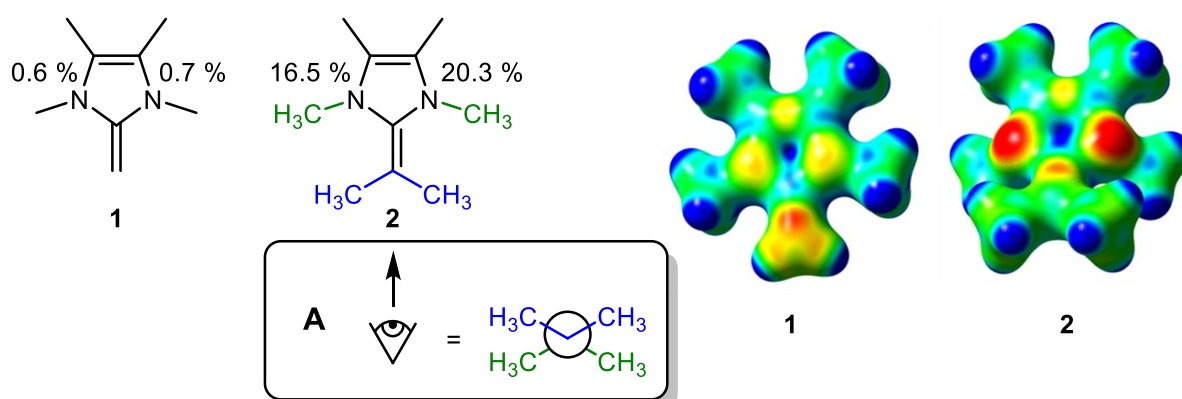
As potent catalysts, it is rather obvious that free NHOs should be stored under inert conditions (e.g. inside a glove box). For some of the most reactive compounds, storage at reduced temperatures is recommended, as decomposition has been observed. Further, it is interesting to note, that the precursor salts can be stored on the shelf under ambient conditions. Hence, a convenient method is to synthesize a large amount of precursor salt, and deprotonate only the needed amounts to generate free NHO in order to guarantee a steady supply of active NHO. Since the available data set for pK_a -values of NHO in literature is unfortunately small, a way to classify and compare the basicity of NHOs to other compounds is presented by proton affinities (PA). These have recently been calculated for a selection of NHOs and revealed PAs in the range of other organic superbases, in some cases even bordering on so-called hyperbasicity (defined as $PA > 300$).^{12, 80} It is abundantly clear that the structural motives present in NHOs directly affect this value. For example, as outlined above, choosing an imidazolium-based cyclic structure will ensue an aromatization upon protonation, acting as driving force and “locking” the negative charge on the active site (cf. Scheme 32, left). This is in stark contrast to saturated congeners of NHOs: the area of conjugation is limited to the *N-C-N*-motive of the heterocycle, significantly reducing the delocalization of the positive charge and resulting in a lower overall basicity. This reasoning is again corroborated by studies from *Mayr* et al. concerning the nucleophilicity of *O*-methylated Breslow-intermediates, an intermediate-class commonly encountered in NHC-mediated catalysis that is structurally similar to NHOs (deoxy-Breslow-intermediates, Scheme 34).⁸¹ There, it was found that imidazole derivatives are the most nucleophilic congeners studied in the publication, and up to $10^3 - 10^4$ times more reactive than thiazole- or triazole-derived compounds. Hence, it is clearly evident that progress in NHO research will also benefit NHC-related chemistry, as key-intermediates of NHC catalysis are closely linked to the structure of NHOs. Furthermore, one of the most distinctive features of NHOs is the ability to directly manipulate the active site of the catalyst. Here, even small changes like the introduction of a dimethyl-substitution on the exocyclic carbon can induce a pivotal influence on chemical behaviour and reactivity. This is best exemplified when considering two of the most frequently employed imidazole-derived NHOs, namely



Scheme 34: Left: Breslow's proposed mechanism for carbene-mediated benzoin condensation, identifying the Breslow intermediate.⁸² Right: deoxy-Breslow intermediates and their structural kinship to NHOs.

1,3,4,5-tetramethyl-2-methyleneimidazoline (Scheme 35, 1) and 1,3,4,5-tetramethyl-2-(propan-2-ylidene)imidazoline (Scheme 35, 2). On the first glance, both NHOs seem to be rather similar: both structures appear planar, the reactivities should be similar and only differ due to the +I-effect of the dimethyl-substitution; due to steric congestion on the active site one can also imagine an attenuated nucleophilicity of **2**. However, theoretical calculations conducted in course of the determination of PAs revealed an intriguing and vastly different situation.¹² In fact, compound **2** is not planar – the methyl groups on the exocyclic carbon atom (Me_{exo}) impose significant sterical pressure on the *N*-methyl groups (Me_{N}), leading to a distortion of the seemingly planar ring structure as both methyl moieties (Me_{exo} , Me_{N}) bend in order to evade steric congestion (Scheme 35, A). However, this worsens the conjugation of the exocyclic double bond, ultimately rendering the exocyclic carbon of compound **2** less nucleophilic than that of compound **1**. Upon protonation, the sp^2 -configuration of the exocyclic double bond is transformed into sp^3 , enabling the rotation of both Me_{exo} out of plane and finally leading to a planarization of the protonated **2**. The extent of this effect was quantified by determining the pyramidalization (*P*) of the nitrogen atoms, which reflects the degree to which the nitrogen atoms have assumed an sp^3 -like conformation (Scheme 35, percentage values next to nitrogen atoms). Furthermore, these effects were visualized by calculating the so-called molecular electrostatic potentials of selected NHOs. This generates a “heat-map” of nucleophilicity by subjecting a proton probe alongside the

surface of a molecule and calculating the corresponding attractive and repulsive forces (Scheme 35, right). The essential point of the above deliberations is, that already a very minor manipulation of the active site ensues a huge impact on the resulting reactivity: compound **1** is planar and the exocyclic double bond is well-conjugated with the *N*-heterocyclic ring, rendering C_{exo} highly *nucleophilic* and increasing the propensity of a direct nucleophilic attack from **1** onto monomers or substrates. Compound **2** on the other hand is not planar; the following distortion of the ring increases its ring-strain and worsens the conjugation of the exocyclic double bond. Furthermore, the dimethyl substitution on C_{exo} impedes a nucleophilic attack. Hence, the only way of **2** to release strain and obtain a planar conformation, is the protonation of C_{exo} , rendering it not nucleophilic, but highly *basic*. Notably, these elaborations fit extremely well with the observed reactivity of these compounds and either of the two reactivities – nucleophilic or basic – can be addressed exclusively.⁶ Another unique feature of NHOs is the electronic situation on the reactive site. As outlined above, NHCs feature an electron sextet on their reactive center, while NHOs can be considered as latent carbanions. This renders both as strong σ -donors in metal complexes; NHOs, however, lack the ability to enter significant back-bonding *via* the p - π -orbital like NHCs, due to their HOMO being located in the π -orbital of the double bond.⁷⁶ On the other hand, this lack of back-bonding results in the ability of NHOs to transfer more electron density onto the metal center than a comparable NHC. Yet, with no significant back-bonding in NHO-metal complexes, the overall bond strength



Scheme 35: Left: valence bond structures of two commonly encountered NHOs. The only difference is the dimethylsubstitution of C_{exo} on compound **2**. Percentage values represent the nitrogen atom's degree of pyramidalization (P), reflecting the degree to which the nitrogen atoms have assumed a sp^3 -like conformation. A: visualization of the distortion due to steric pressure, view alongside the C-C-double bond. Right: molecular electrostatic potentials (MEPs) of compounds **1** and **2**. Note that the site of highest attractive forces is located on C_{exo} for compound **1**, while being the *N-C-N*-moiety in compound **2**. Values for P and MEPs were taken from literature.¹²

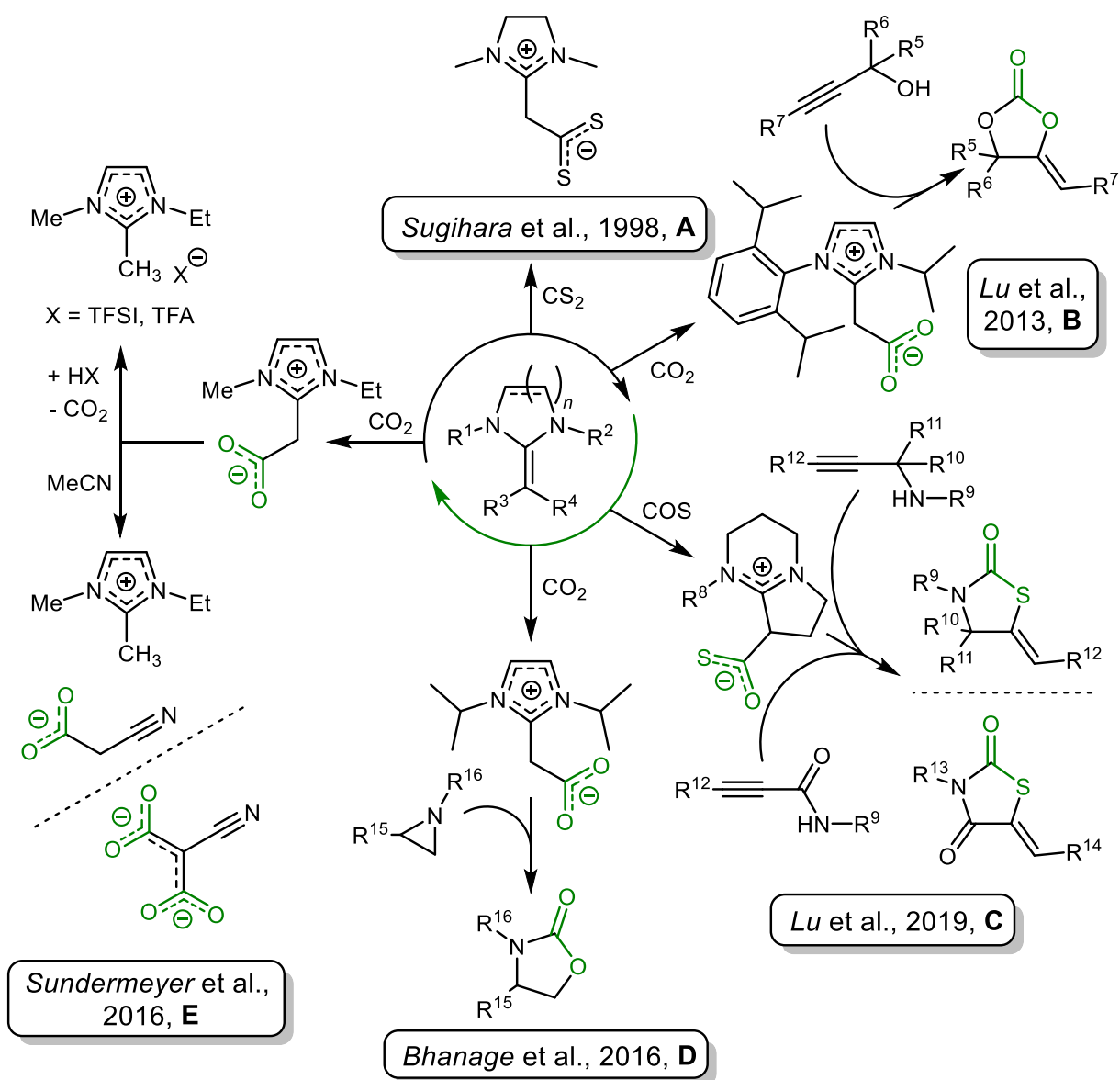
of the NHO-metal bond is weakened and NHOs tendentially are weaker Lewis bases than their corresponding NHCs. Furthermore, NHOs generally carry a positive charge in metal complexes, while the negative charge is formally transferred to the metal center. This enables NHOs as soft, end-on ligands that might even be suitable for the complexation of soft metal centers like Ni or Pd(0).

1.3.3. Catalytic Transformations Mediated by NHOs

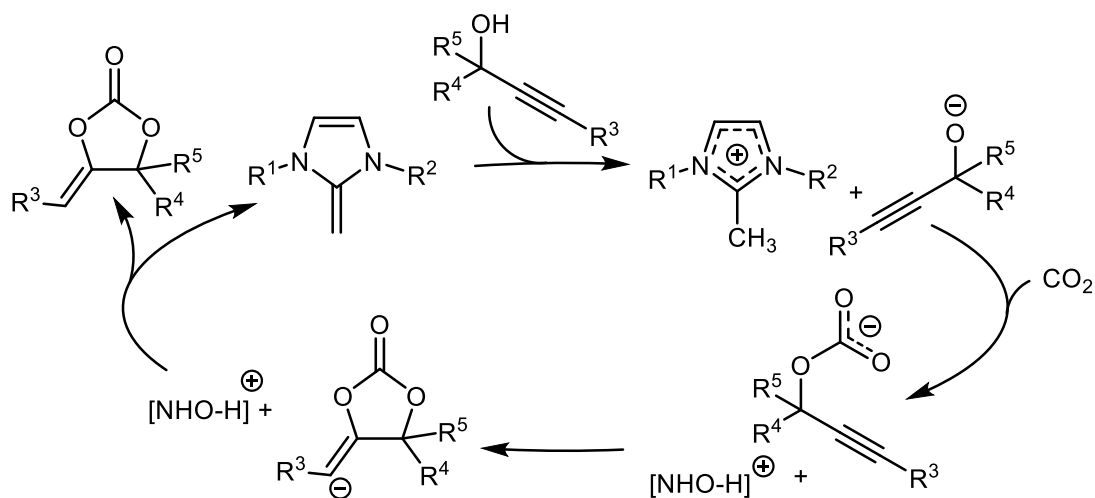
1.3.3.1. Small-Molecule-Activation

Following the first reports that harnessed NHO's significant nucleophilicity to form stable NHO-CS₂-adducts in 1998 (Scheme 36, A),⁸³ 15 years later, with the inspiring work from *Lu* et al. in 2013, NHO research experienced a second wind and re-entered the research focus of small-molecule-activation. The NHO-CO₂-adducts readily formed under mild conditions (1 atm of CO₂) and were subsequently purified by precipitation under inert gas. Intriguingly, these adducts were significantly less stable than their corresponding NHC-CO₂-adducts: thermal degradation at 40 °C in CH₂Cl₂ was quantitative for NHO congeners, while no noteworthy CO₂-liberation was observed for NHC-derived adducts. This is further corroborated by single crystal X-ray measurements, where a bond-elongation is observed for the C_{exo} – C_{carboxylate} bond (155 – 157 pm) compared to C_{carbene} – C_{carboxylate} (152 – 153 pm). The conclusions drawn from these findings pose considerable impact on the applicability of such adducts in catalytic cycles. While the substantial stability of NHC-CO₂-adducts (which enables them as latent catalysts) represents a thermodynamic sink and thus demands for (at least) harsher reaction conditions, NHO-CO₂-adducts readily release CO₂ and ensure a steady supply of catalytically active species. In fact, this has successfully been applied in the carboxylative cyclization of propargyl alcohols (Scheme 36, B), where NHO-adducts were about 10-200 times more active than the corresponding NHC-adducts at the same conditions. Interestingly, in the original publication *Lu* et al. proposed a nucleophilic addition mechanism being at work. However, this has been reevaluated by *Lyu* and co-workers in 2016 using DFT calculations.⁸⁴ Actually, according to natural population and molecular orbital analyses, it is more likely that a “basic ionic pair” mechanism is at play here (Scheme 37). In this case, the NHO will deprotonate the propargylic alcohol which will then in turn attack CO₂ and form the

anionically charged cyclic carbonate. Proton transfer finally regenerates the free NHO and releases the product. This also explains, why NHOs display a pronounced activity in this catalysis compared to NHCs: since the catalytically active species is actually the free NHO, the dissociation of the corresponding adduct is pivotal to its activity. Hence, the more stable the adduct, the less activity will be observed, which nicely coincides with the observations described above. In 2017, *Lu* et al. have extended the scope of investigated NHOs to also encompass C_{exo}-alkylated congeners for CO₂ sequestration and subsequent carboxylative cyclization.⁸⁵ Importantly, the alkylated versions exhibited an improved activity in the cyclization reactions, which again corroborates the proposed basic mechanism, as C_{exo}-alkylated NHOs tendentially feature an increased basicity compared to their non-alkylated versions (*vide supra*). Furthermore, this again demonstrates that the ability to perform subtle changes to the reactive center can lead to the desired adjustment of the NHO's reactivity. Another interesting adjustment of the reactive center is embodied by a bicyclo-derived NHO, where one C_{exo}-substituent is fixed in a cyclic system (Scheme 36, C). Derivatives of this NHO were applied in the cyclization of propargylic amines and amides with COS, leading to the formation of thiazolidin-2-ones and 2,4-thiazolidinones with full *Z*-selectivity.⁸⁶ Interestingly, the proposed mechanism did not envision the NHO as a base, rather the NHO-COS-adduct was proposed to act as Lewis base that activates the amine/amide *via* hydrogen bonding, which entails the formation of a partial negative charge on the amine, leading to nucleophilic attack on another COS molecule. The catalysis was further successfully employed in the total synthesis of rosiglitazone, an anti-diabetic agent. As *Bhanage* and co-workers have demonstrated, the formation of oxazolidinones is also feasible applying NHO-CO₂-adducts and aziridines.^{11h} The NHO-CO₂-adduct hereby performs a nucleophilic attack on the aziridine, which is ring-opened and incorporates CO₂ to form the oxazolidinone (Scheme 36, D). Furthermore, together with a reducing agent, NHO-CO₂-adducts were employed in the formylation of amines which proposedly proceeds *via* a formate intermediate (see SI of cited reference). Another field of application in small-molecule-activation stems from the obvious structural kinship of NHO-CO₂-adducts with ionic liquids (ILs). *Sundermeyer* et al. have demonstrated that ILs are readily accessible from CO₂-adducts of NHOs, by subjecting them to acids with weakly nucleophilic counter ions [X]⁻, ultimately forming ILs after decarboxylation (Scheme 36, E).⁸⁷ Also, subjecting



Scheme 36: Schematic overview of reactions mediated by NHO-activated small molecules. TFSI = bis(trifluoromethanesulfonyl)imide, TFA = trifluoroacetate.



Scheme 37: Revaluated mechanism of the carboxylative cyclization of propargylic alcohols, where the NHO acts as a base rather than the NHO-alcohol adduct performing a nucleophilic attack (cf. Scheme 32, right).⁸⁴

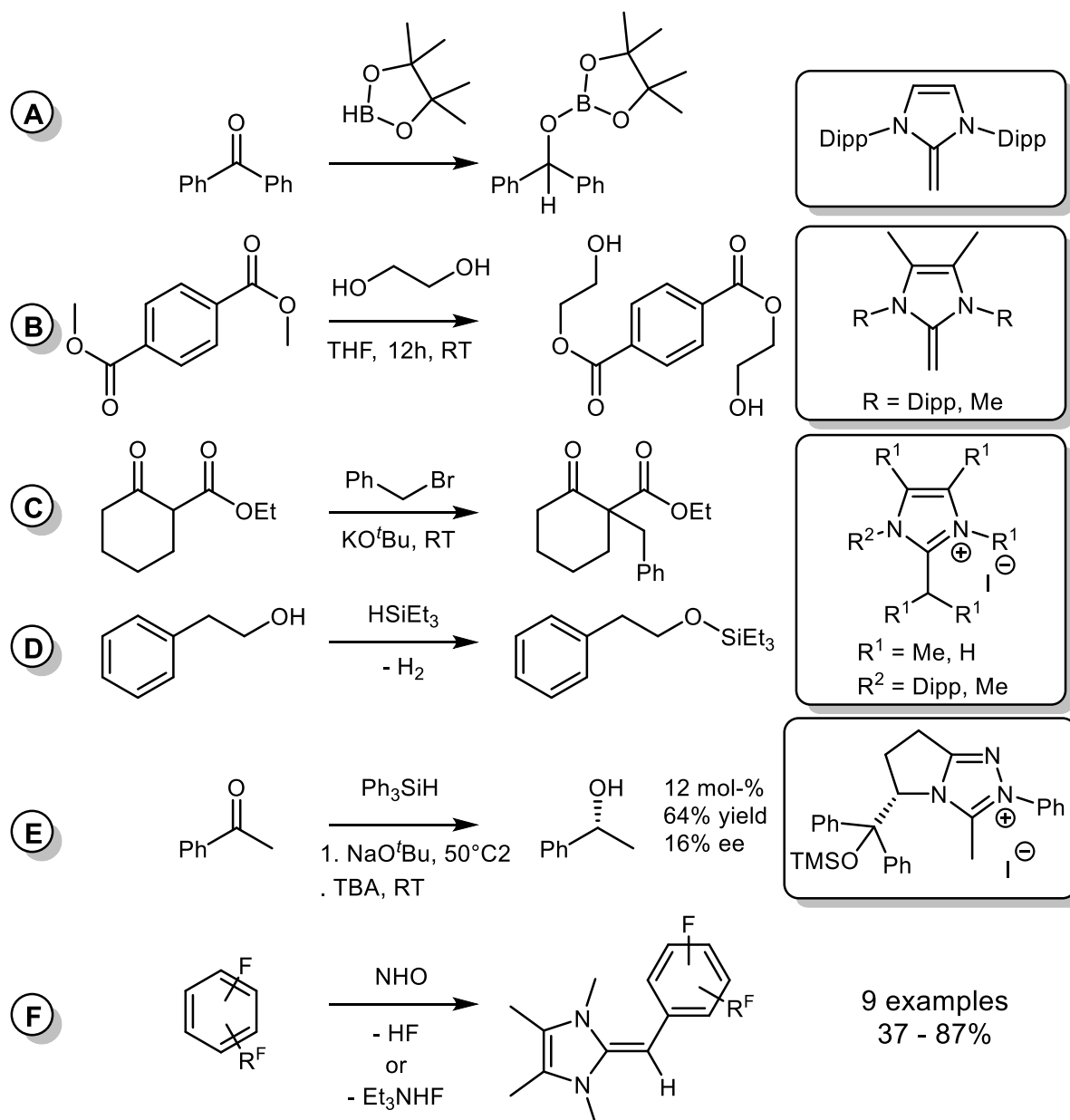
NHO-CO₂-adducts to CH acids like acetonitrile ensues a carboxylation reaction, allowing for the preparation of cyanoacetates and -malonates, representing the first C-C bond-forming carboxylation reaction mediated by NHO-CO₂-adducts.

1.3.3.2. Other Catalytic Transformations

It was only a matter of time, until the accomplishments in small-molecule-activation lead to a proliferation of catalytic applications for NHOs. However, the thus far limited range of examples clearly shows, that NHO-organocatalysis has yet to emerge from its infantile stage, and there is yet much potential to be unravelled. One of the first catalytical transformations mediated by NHOs was actually discovered by serendipity: while investigating the formation of NHO-borane complexes, *Rivard* et al. revealed that NHOs themselves represent potent organocatalysts for the hydroborylation of ketones and aldehydes.⁸⁸ Hitherto, this was only realizable using metal-based complexes, yet 5 mol-% of NHO sufficed to mediate the quantitative hydroborylation of benzophenone using pinacolborane (Scheme 38, A). Furthermore, this catalysis displayed chemoselectivity when applied to acetylbenzaldehyde, leaving the ketone moiety completely intact. Notably, the corresponding NHC demonstrated much lower activity and only a limited scope under identical conditions. Prompted by the distinct features of high basicity and nucleophilicity, *Enders, Nguyen* and co-workers investigated the ability of NHOs to mediate transesterification reactions (Scheme 38, B).^{11d} Here, both free and *in situ* generated NHOs were active, and dimethyl terephthalate was efficiently converted into bis(2-hydroxyethyl) terephthalate in the presence of excess ethyleneglycol. Furthermore, primary alcohols exhibited the best reactivity, while tertiary alcohols only entailed negligible conversion. Importantly, the possibility to degrade poly(ethylene terephthalate) (PET) was demonstrated using this approach. Based on these findings, the authors also extended the scope to the alkylation of β -ketoesters by primary alkyl halides in a solid/organic-phase transfer setup (Scheme 38, C).⁸⁹ Again, free NHOs were generated *in situ* starting from the respective precursor salts and proved to be more efficient than comparable standard phase-transfer catalysts, while being significantly faster than NHCs. So far, however, no selectivity was achieved regarding mono- vs. bisalkylation; yet, mechanistic studies employing isotope labelling experiments determined, that the NHO is indeed the kinetically active base, highlighting that by judicious manipulation of the NHO this

issue might be mitigated. Another indication that structural adjustment of the NHO might improve catalysis is the occurrence of an alkylation side reaction of the NHO, again demonstrating the dual reactivity (basic or nucleophilic) of NHOs. In 2017, the same group developed the dehydrogenative silylation and hydrosilylation of alcohols and carbonyls, respectively (Scheme 38, D).⁹⁰ The NHO was hereby liberated *in situ* from its precursor salt using a base, which then activates the alcohol moiety *via* hydrogen bonding, rendering it susceptible to efficient silylation. Cleavage of H₂ then resulted in the formation of the final product and regeneration of the active species. Interestingly, imidazolium-derivatives performed best, and needed to be protected in the 4,5-position in order to preclude the formation of abnormal NHCs (aNHCs), since otherwise product mixtures and lowered yields were obtained. Furthermore, the reaction precluded the application of tertiary alcohols. In the same study, the hydrosilylation of carbonyl-bearing compounds was also investigated. Here, the first and only example of an asymmetric organocatalysis using a chiral NHO should be highlighted (Scheme 38, E). Despite its moderate enantioselectivity of 16 % ee, acetophenone could be converted to (*R*)-1-phenylethanol in good yields (64 %) using the chiral, triazole-derived NHO precursor salt that was again converted to the free NHO *in situ*. Earlier this year, a novel field of application for NHO catalysis was developed by *Sarkar, Schulzke, Chandrasekhar, Jana* and co-workers. The groups impressively demonstrated, that a large variety of aromatic C–F-bonds are selectively activated by NHOs, leading to an aromatic nucleophilic substitution reaction (S_NAr) and generating fluoroaryl-substituted alkenes without additional catalysts (Scheme 38, F).⁹¹ Two possible pathways were postulated: after the formation of a transition state, either the product is directly formed *via* liberation of HF, or an ionic intermediate [NHO-Ar]⁺[F]⁻ is formed, that is finally converted into the product using NEt₃. This method provides chemists with a tool to directly synthesize fluoroaryl-substituted alkenes starting from readily available compounds, a feat otherwise exclusive to transition-metal complexes.

As can be seen from the examples provided above, NHOs often rival or even outperform established systems. In some cases, NHOs even exploit catalytic transformations that are usually unique to metal-based catalysts; considering the limited scope of structural diversity of the investigated NHOs, the scope of reactions accessible to NHO-mediation is highly likely to keep expanding in the years to come.



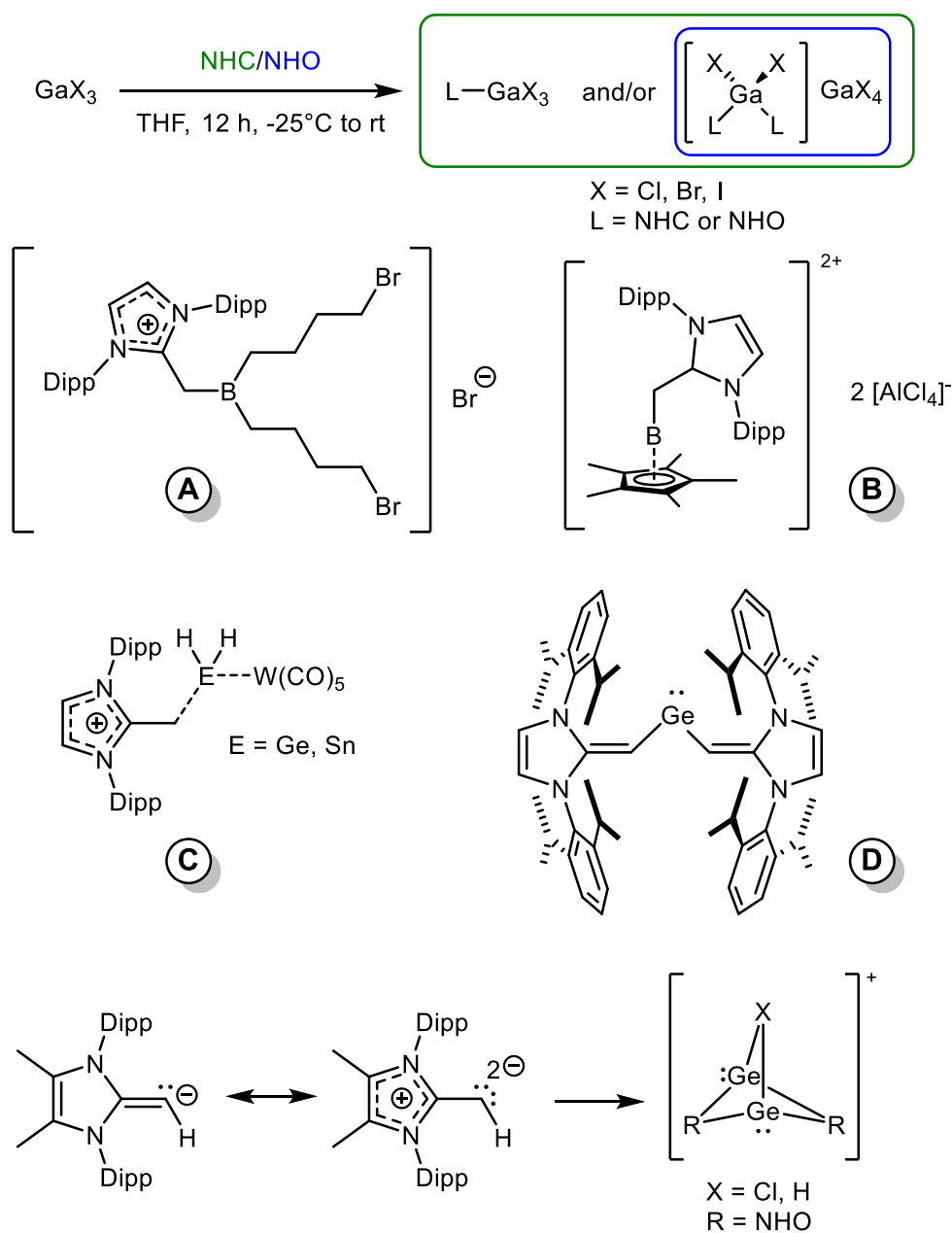
Scheme 38: Organocatalytic transformations mediated by various NHOs, that are highlighted on the right. Note the so far limited structural diversity, hinting to the untapped potential of catalyses that could be mediated by more sophisticated structures. Dipp = 2,6-diisopropylphenyl, TMS = trimethylsilyl, *t*Bu = *tert*-butyl.

1.3.4. N-Heterocyclic Olefins as Ligands in Complexes

1.3.4.1. NHOs as Ligands in Main Group Metal Complexes

Considering the above-described electronic properties of NHOs, they represent promising and versatile ligands for many metal complexes. However, so far, main group metal complexes with NHO ligands are relatively scarce despite repeatedly delivering unexpected results and succeeding in the stabilization of unusual metal species. For example, two NHCs were compared to an NHO in the coordination towards gallium halides by *Gordon* and co-workers.⁹² Here, the NHO exclusively delivered relatively rare ionic adducts, which was attributed to its higher nucleophilicity compared to the NHCs, as determined by their corresponding HOMO energies (Scheme 39, top). *Robinson* et al. developed NHO-stabilized borane complexes with BBr_3 .⁹³ Unexpectedly, these complexes were able to ring-open THF, resulting in borenium cations stabilized by NHOs (Scheme 39, A), while the corresponding NHC analogues with BBr_3 were completely inert towards THF. Other NHO-borane complexes were developed by *Chiu* et al. in 2016.⁹⁴ The $\eta^5\text{-Cp}^*\text{-B-NHO}$ complexes were stabilized with an NHO that featured sterically demanding *N*-substituents alongside non-nucleophilic counter ions (Scheme 39, B). Although the preparation of the respective NHC-complexes was also feasible, the boron-center in the NHO complexes was more Lewis acidic than in NHC complexes. This effect was explained by the increased steric repulsion of the NHO and the Cp^* -ligand due to the NHO's bent geometry, which reduces the electron donation from the Cp^* -ligand to the boron center. In 2011 developed by *Rivard* et al., low-oxidation state main group metal hydrides (metal = Ge, Sn) were stabilized by NHOs. Making use of the amphoteric nature of Ge and Sn, these adducts were coordinated to $\text{W}(\text{CO})_5$ (Scheme 39, C). This was possible due to the metals possessing a lone-pair donor site complimented with an empty *p*-orbital for back-bonding, whereby the latter was partially filled by the coordinating NHO. Generally, the C-Ge/Sn bonds were determined to be rather weak; NHO bonding was thus reasoned to be understood as a "slipped" olefin, hinting to multiple bonding modes being feasible for NHOs depending on its structure and the electronic situation of the metal center. Further harnessing the properties of NHOs, in 2016, *Rivard* et al. developed base-free divinyl germylene that was stabilized by NHOs with sterically demanding *N*-substituents (Scheme 39, D).⁹⁵ The bis(diisopropylphenyl)-ligands hereby formed a protective

cavity around the metal center, while the narrow $C-Ge-C$ angle suggested a significant p -character of the bonds. Finally, this research established NHOs as four-electron donors in 2020;⁹⁶ the deprotonation of C_{exo} enabled NHOs to donate two electrons *via* the σ -orbital and two additional electrons from the π -orbital (Scheme 39, bottom). This led to the formation of bimetallic Ge-complexes with a bridging Cl- or H-atom and two stabilizing NHOs. During preparation, however, the anionically charged NHO showed a tendency towards bridging and 1,2-migration, which potentially facilitates future preparation of bimetallic species.

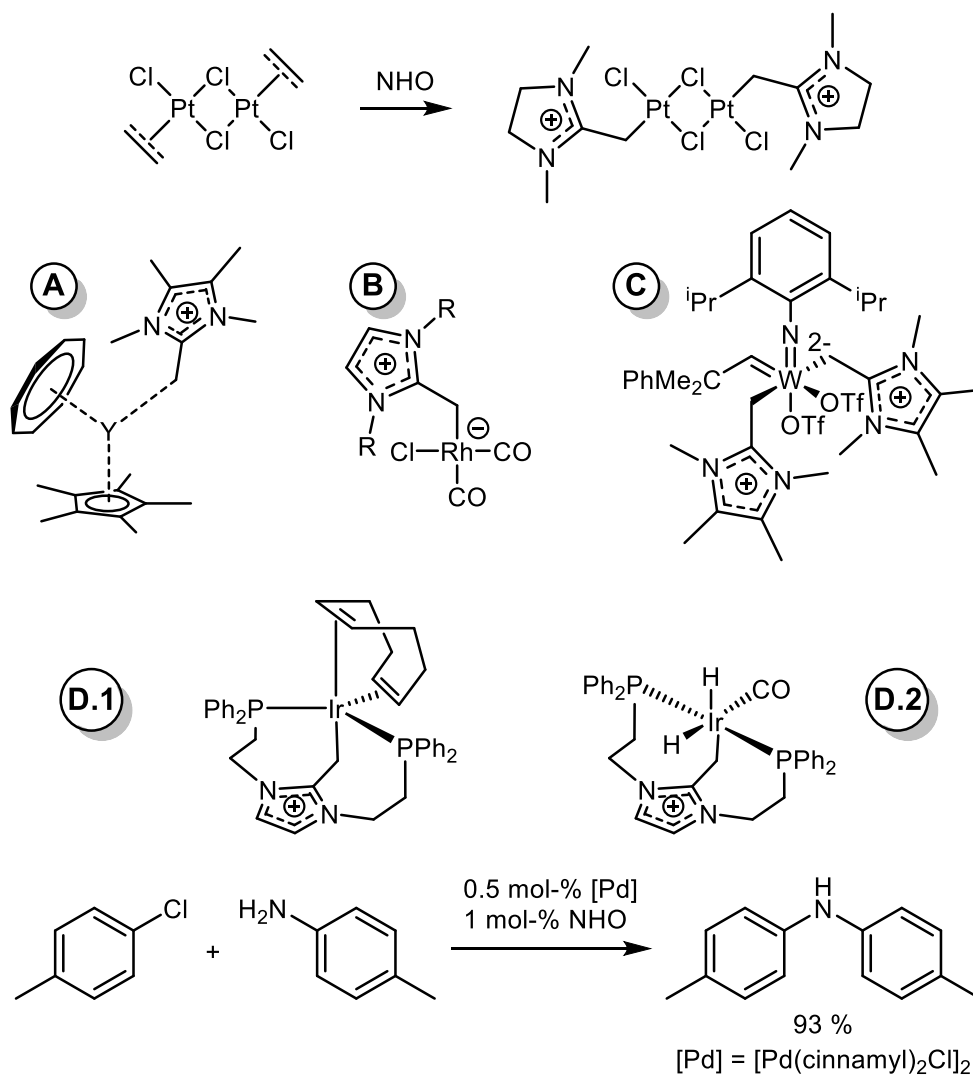


Scheme 39: Main group metal complexes with NHOs as ligands. Dipp = diisopropylphenyl.

1.3.4.2. NHOs as Ligands in Transition Metal Complexes

Compared to main group metal complexes of NHOs, transition metal complexes have been known since 1979, where *Kaska* et al. investigated the reaction of Zeise's dimer with a saturated NHO congener.⁹⁷ This early example readily afforded an NHO platinum complex, and, importantly, already determined several imperative properties of NHOs as ligands: an end-on coordination, a strong σ -donating ability and negligible π -back-bonding (Scheme 40, top). 16 years later, Schumann and Kuhn synthesized well-defined complexes starting from $\text{Ln}(\text{HMDS})_3$ ($\text{Ln} = \text{La}, \text{Nd}$) and $(\eta^5\text{-Cp}^*)\text{Y}(\eta^8\text{-C}_8\text{H}_8)$ (Scheme 40, A).⁹⁸ In the resulting complexes, single crystal X-ray analyses again suggested the NHO coordination to take place in the ylidic state, due to an aromatization of the heterocycle and a bond elongation of $\text{C}_{\text{endo}} - \text{C}_{\text{exo}}$. However, this finding was opposed by the slightly slanted coordination of the NHO ligand, the distribution of the electronegativity between Ln and C and the good solubility of the complexes. In 2008, *Fürstner* et al. clarified this picture: the synthesized Rh(I) complex again revealed an aromatized heterocyclic moiety and end-on coordination, together with an extraordinary electron donating ability (Scheme 40, B). These findings convinced the authors of an ylidic coordination of the NHO, which was later further corroborated by *Tamm* et al.: the investigation of NHOs featuring a C_{exo} -substitution revealed, that these NHOs quickly lost the ability to form Rh(I) complexes;⁹⁹ yet, NHOs with sterically demanding *N*-substituents were still suitable ligands for complex formations.⁷⁶ The first example of a transition-metal-NHO-complex being employed in catalysis was delivered by *Buchmeiser* et al. in 2016, where a tungsten-alkylidene-NHO-complex was applied in ring-closing metathesis (Scheme 40, C).¹⁰⁰ The two NHO ligands coordinated in a *trans*-manner to each other to form a distorted octahedral geometry, while their sp^3 -like configuration suggested a quantitative charge separation. This ensued a formally double negative charge on tungsten, which resulted in a rather attenuated reactivity (TON 140-250). The isolation of a complex with only one NHO ligand did not succeed, as the preparation with 1 equiv. of NHO resulted in 1:1 mixtures of the starting compound and the two-fold NHO-coordinated complex. Impressive studies harnessing the versatility of NHOs as ligands were conducted by *Iglesias, Oro* and co-workers. Through the design of a *P-C-P*-pincer ligand derived from an NHO, they succeeded in the synthesis of iridium complexes that showcased the remarkable properties of NHOs as dynamic ligands

(Scheme 40, D).¹⁰¹ In their initially synthesized trigonal-bipyramidal iridium complex (Scheme 40, D.1), the NHO occupied a facial coordination while C_{exo} was located in the apical position and exerted a notable *trans*-effect on the opposing Ir–olefin-bond. This complex was then transformed with CO and H₂ into complex D.2, which featured an octahedral coordination sphere. Here, the NHO-pincer-ligand now occupied a meridional position; this transformation was only possible due to its dual donor character (olefin/ylide), and in the resulting complex, the C_{endo}-C_{exo}-bond exhibited a more olefinic character than in the starting complex. Of course, the ylidic character still dominates over the olefinic coordination mode and the degree of olefin contribution in a π -bonding manner can be regarded as a “slippage” along the double bond axis. This signifies that NHOs can adapt (to a certain degree) to steric and electronic changes in metal complexes, a situation most often encountered in catalytic cycles, proposing NHOs as electronically flexible ligands that might be able to stabilize important transition states and intermediates likewise. The author’s hypothesis was verified in the transfer hydrogenation of aldehydes, ketones and imines. The Ir-pincer-complex proved to be extremely active, reaching a maximum TOF of 28 500 h⁻¹ for benzaldehyde and rivalling the hitherto most active systems. Furthermore, DFT studies revealed that the pincer ligand is hemilabile during the catalysis: in intermediate states, the ligand is coordinated to the iridium complex, while it de-coordinates during transition states. This ensues a constant and preferential square-planar geometry for the iridium center during catalysis, which lowers the respective activation barriers and enhances overall catalytic activity. Finally, *Rivard* et al. investigated NHOs regarding their ability to stabilize soft Pd(0) centers during Buchwald-Hartwig-aminations (Scheme 40, bottom).¹⁰² The rationale was, that the increased softness and decreased steric bulk compared to NHCs will facilitate halide-amine exchange reactions. Yet, while NHOs readily formed Pd(II) complexes, these were completely inert towards amination reactions. This issue was resolved by generating the catalytic species *in situ* with various Pd species and NHOs. The most active Pd species was hereby [Pd(cinammyl)Cl]₂ which achieved > 90 % conversion after 1 h at 1.0 mol-% NHO loading. Catalyst-poisoning experiments further showed, that NHO-stabilized colloidal Pd was responsible for the catalysis.



Scheme 40: Transition metal complexes with NHOs as ligands.

2. Ring-Opening Polymerization of Lactones

2.1. Introduction

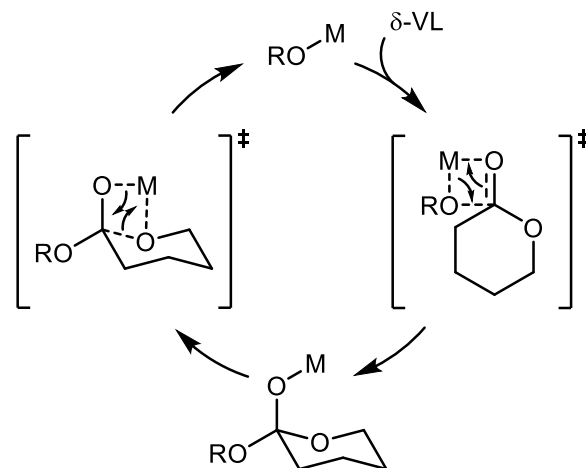
Polyesters are an intriguing class of polymers, that are both biocompatible and biodegradable. Early synthesis routes mostly employed a step-growth polycondensation procedure, based on either monofunctional AA-BB or bifunctional AB-AB systems. However, as known from step-growth polymerizations kinetics, nearly quantitative conversion and minuscule control over monomer ratios (in the case of an AA-BB system) is a necessity to reach high molar masses. Ever since *Carothers* developed the ring-opening polymerization of Lactones in 1932,¹⁰³ this alternative method to produce polyesters has experienced extensive research interest that did not subside even until today. Nowadays, unimodal and narrow molecular weight distributions, high molar masses and tailor-made architectures are readily feasible applying elaborated catalytic systems. However, in order to gain control over side-reactions (transesterification, cf. chapter 1.1.2, Scheme 13), one needs to be aware of the various parameters that influence the polymerization. The ring-size of the monomer, its substituents as well as their position, number and chemical nature, reaction parameters like initiator/catalyst concentration, the chosen solvent, monomer concentration, and the temperature affect the control over the polymerization. Furthermore, attempts to identify general rules that are applicable to all lactones have failed thus far, leading to the issue that highly specialized catalysts are often only applicable to a narrow range of monomers. Still, given the fact that this area of research has been active for almost 90 years now, a myriad of different catalytic systems has been established that encompass basically all relevant lactones. However, describing all of these catalytic systems would absolutely go beyond the scope of this thesis, and encompassing reviews have been published that the gentle reader might refer to.^{1, 3, 104} Hence, only important milestones shall be highlighted in this chapter, intended to give the reader a general grasp of current challenges and limitations of the ring-opening polymerization of lactones.

2.2. Mechanisms

Generally, three different mechanisms are accessible in the ROP of lactones. The first two, anionic and cationic, have already been discussed earlier (cf. chapter 1.1.4) and will only be briefly recapitulated here. Chapter 2.2.1 will then introduce the main mechanism operable in metal-mediated ROP of lactones, the coordination – insertion mechanism. In anionic ROPs of lactones, the catalyst can either act as a nucleophile and directly perform a nucleophilic attack on the monomer, leading to ring-opening and formation of a propagating species. Or, the catalyst acts as a base to deprotonate either the monomer itself or an initiator which subsequently attacks the monomer and causes the ring-opening (cf. Scheme 19). The cationic ROP of lactones proceeds *via* the activated monomer mechanism. Here, the monomer is activated by Brønsted acids, acylating or alkylating agents that will form a positively charged monomer. Subsequently, this activated monomer is attacked by a non-activated monomer, leading to ring-opening and the formation of an active species (cf. Scheme 21). Overall, anionic processes offer a better control over the reaction, which is why cationic polymerization methods are rarely encountered with lactones.

2.2.1. Coordination – Insertion Mechanism

Given the abundance of metal-based initiating systems for lactone ROP, the coordination – insertion mechanism is amongst the most-encountered mechanisms in this field of research. Here, the metal-center coordinates to the carbonyl oxygen, while the alkoxide will attack the sp^2 -ester carbon to form a tetrahedral intermediate. Subsequently, the ring is opened *via* acyl-bond-cleavage which ensues the formation of a new alkoxide (Scheme 41).

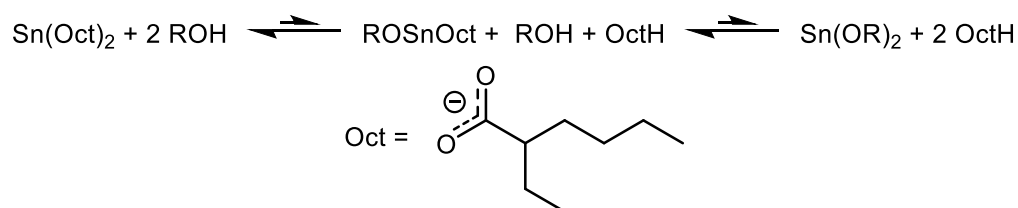


Scheme 41: Coordination - Insertion mechanism using the example of δ -Valerolactone (δ -VL). OR = alkoxide group of the initiator, or propagating chain-end.

2.3. Initiators

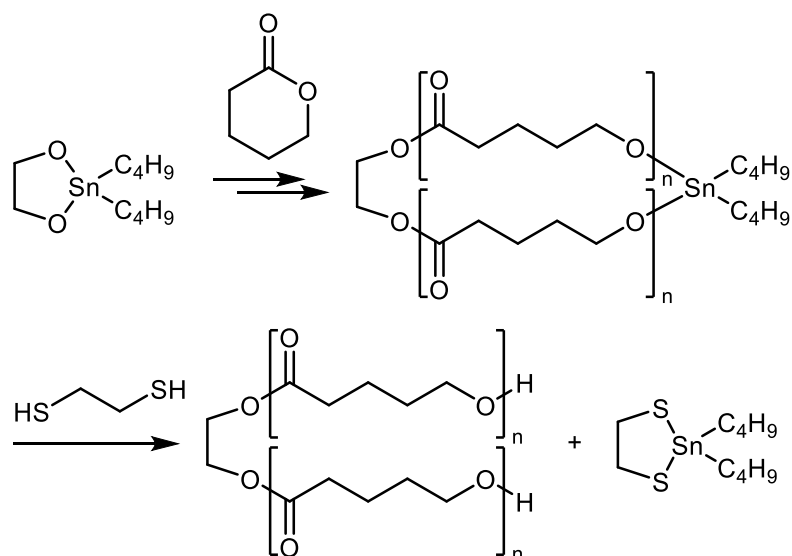
2.3.1. Metal Alkoxides

Over the time, the scope of initiating systems has been broadened and transcends simple metals or metal alkoxides, albeit they still represent a prominent class of lactone polymerization catalysts, as their efficiency and availability still outrival a large portion of other systems. First and foremost, tin(II) 2-ethylhexanoate ($\text{Sn}(\text{Oct})_2$) has to be mentioned in this context. Together with an initiating alcohol, this system can still be referred to as the benchmark system for novel catalysts that want to claim industrial relevance. Indeed, industrial polyester is mainly synthesized *via* ROPs of CL and Lactide, catalysed by $\text{Sn}(\text{Oct})_2$.¹⁰⁵ In 1998, *Penczek* and co-workers reevaluated the until-then accepted underlying mechanism and found, that the actual initiator is not $\text{Sn}(\text{Oct})_2$, but is generated *in situ* by ligand scrambling with ROH (Scheme 42).¹⁰⁶ Furthermore, the authors stated that $\text{Sn}(\text{Oct})_2$ acts as a retarder, temporarily deactivating the propagating chain-end *via* protonation and increasing control, corroborating the living nature of the polymerization. However, despite being recognized as “indirect additives used in food contact substances” by the FDA,² $\text{Sn}(\text{Oct})_2$ has been identified as cytotoxic catalyst.¹⁰⁷ This of course poses a problem for the generated polyesters that are intended to be used in e.g. biomedical applications, as the removal of $\text{Sn}(\text{Oct})_2$ is not a trivial matter. *Albertsson* et al. have developed an elegant approach to reduce the tin-contamination of prepared samples of poly(CL) on a multi-gram scale.¹⁰⁸ Instead of $\text{Sn}(\text{Oct})_2$, the authors used 1-di-*n*-butyl-1-stanna-2,5-dioxacyclopentane to initiate the polymerization, and finally remove it *via* reacting the finished polymer with 1,2-ethanedithiol (Scheme 43). Using this approach, the tin-contamination could be reduced from over 1000 ppm to 23 ppm by precipitating the prepared batch samples that ranged from 5 – 50 g.



Scheme 42: *In Situ* formation of the active species in $\text{Sn}(\text{Oct})_2$ -catalysed polymerizations.¹⁰⁶

² <https://pubchem.ncbi.nlm.nih.gov/compound/Stannous-octoate#section=Food-Additives-and-Ingredients>, accessed on: 26.06.2020



Scheme 43: Method developed by *Albertsson* et al. to remove residual Sn-impurities from polymers on an industrially relevant scale.¹⁰⁸

Another prominent example of metal alkoxides is aluminium(III) isopropanolate ($\text{Al}(\text{O}^i\text{Pr})_3$). However, polymerizations mediated by this catalyst feature an induction period, attributable to the formation of unreactive aggregates and leading to a prolonged reaction time (few hours ($\text{Sn}(\text{Oct})_2$) vs. few days ($\text{Al}(\text{O}^i\text{Pr})_3$)). Actually, it has been shown that only the trimer of $\text{Al}(\text{O}^i\text{Pr})_3$ is responsible for propagation, while the tetramer is unreactive during the course of polymerization. Nevertheless, high molar masses are accessible using $\text{Al}(\text{O}^i\text{Pr})_3$ that range up to $10^5 \text{ g}\cdot\text{mol}^{-1}$.¹⁰⁹ Finally, the last example that shall be highlighted here, is a lanthanide-alkoxide complex developed by *Stevens* and co-workers in 1996.¹¹⁰ Using commercially available $\text{Y}(\text{O}^i\text{Pr})_3$ (which actually forms aggregates and is present in the form of $\text{Y}_5(\mu\text{-O})(\text{O}^i\text{Pr})_{13}$), the authors were able to polymerize Lactide in a few minutes at room temperature (solvent = THF, $D_M = 1.02$, $M_n = 20 \text{ kg}\cdot\text{mol}^{-1}$). Of course, this is only a tiny portion of the available metal alkoxide systems capable of polymerizing lactones; however, the examples given here are suitable to generate a general picture of what novel catalytic systems will be compared to. Furthermore, the success of metal alkoxide spurred the development of well-defined metal complexes for ROPs of lactones to eliminate the possibility of aggregate formation, as will be discussed in the next chapter.

2.3.2. Well-Defined Metal Complexes

The first well-defined metal complexes were developed in 2001, embodied by biphenolate complexes with aluminium, zinc and lithium that were probed for their ability to polymerize Lactide.¹¹¹ Despite their bulky ligands, aluminium- and zinc-derived complexes exhibited a dimeric structure, while lithium complexes formed higher aggregates (Figure 4). Out of the described systems, the lithium-based congeners displayed the highest activity (few h, 0 °C, full conversion, 14 kg·mol⁻¹, $\bar{D}_M \approx 1.1$, CH₂Cl₂). A few years later, *Okuda et al.* developed chalcogen-bridged, rare-earth-based complexes that were highly effective in the heteroselective polymerization of *rac*-Lactide (Scheme 44, left).¹¹² Out of the investigated systems, the yttrium-based complex together with isopropanol performed best; only a few minutes at room temperature sufficed to reach full conversion, with narrowly distributed, high molar masses ($M_n = 20$ kg·mol⁻¹, $\bar{D}_M \approx 1.02$). Another prominent group of ligands is based on β -diketimines, as developed by the groups of *Coates* and *Dove* (Scheme 44, middle).¹¹³ Mg, Ca, Zn, Fe and Sn complexes have been investigated, and their reactivity correlates with the metal's electropositivity (Mg > Zn \approx Fe > Sn). Especially the lone-pair centered on tin was attributed to attenuate the activity, since it induces constraints on the coordination geometry of the tin complexes and causes electronic repulsion between the metal center and the alkoxide or the growing chain-end.^{113b} Despite its powerful performance, the coordination – insertion mechanism is defined by the insertion of a monomer between an alkoxide species or the growing chain-end. Hence, it is not a catalytic process *per se* – the first catalytic ROP of lactones was developed by *Carpentier et al.* in 2006.¹¹⁴ Using an yttrium-based complex with a tetradentate N/O-donor ligand, the authors were able to lower the catalyst loadings

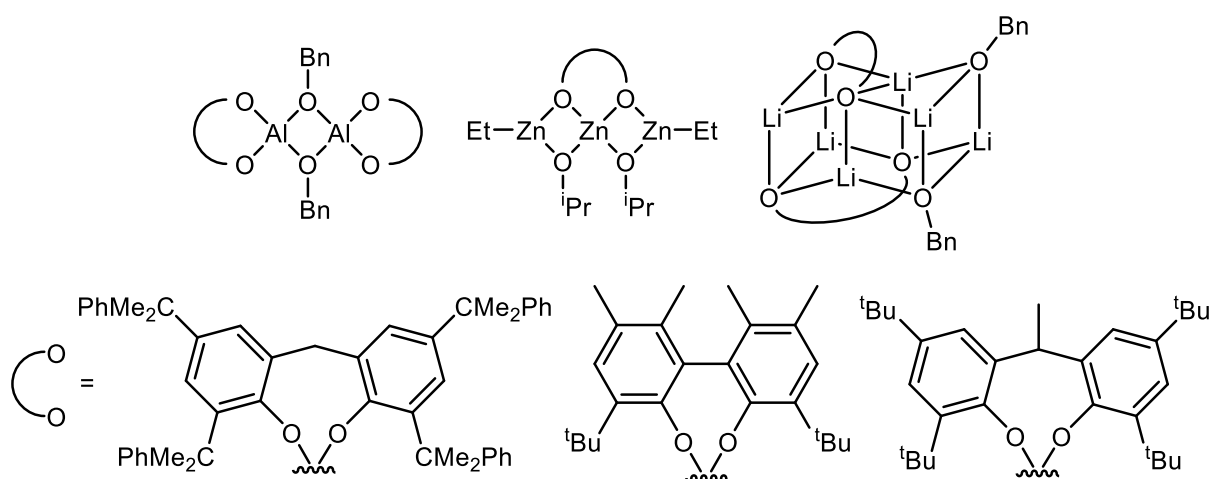
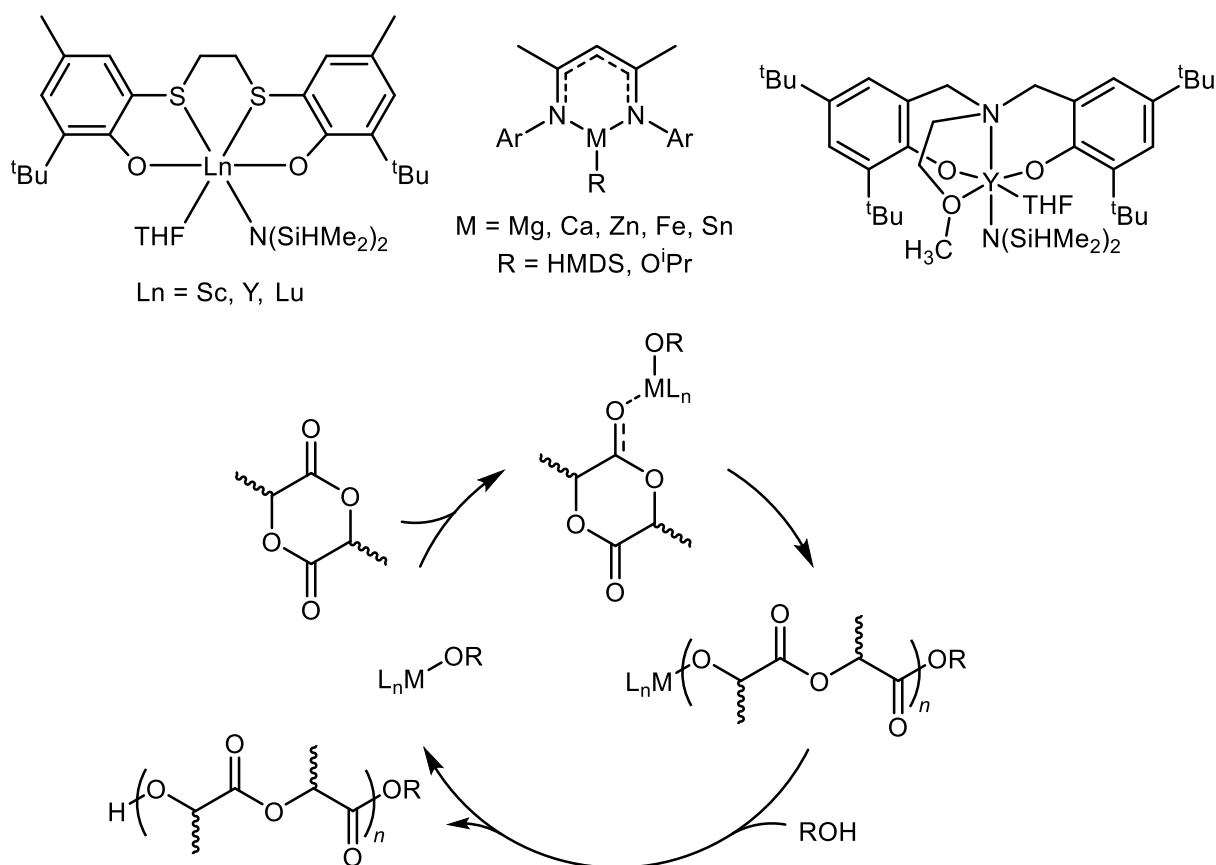
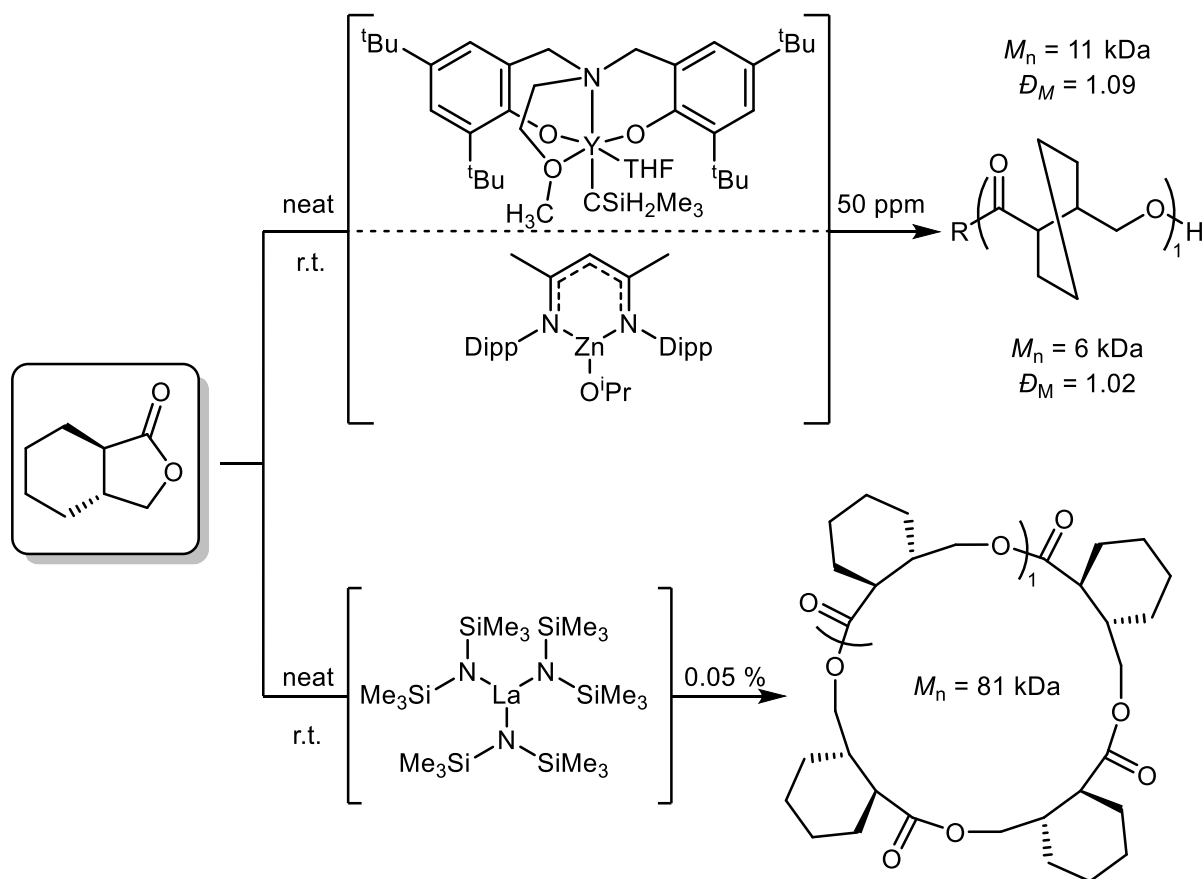


Figure 4: Well-defined aluminium-, zinc- and lithium-based bisphenolate complexes for the ROP of lactones.



Scheme 44: Top: various metal complexes with multidentate ligands. Bottom: First catalytic ROP of *rac*-Lactide using the yttrium-based complex on the top right.

down to 0.02 mol-% in the living and immortal polymerization of *rac*-Lactide (Scheme 44, right and bottom, M_n up to 160 kg·mol⁻¹, $D_M = 1.06 - 1.40$, $t = 5 - 360$ min, $T = 20$ °C).^{114a} The same yttrium-based complex, together with Ln(HMDS)₃ complexes (Ln = La, Y, Sm), was also recently employed to form quantitatively recyclable polymers derived from γ -Butyrolactone ($M_n \approx 8$ kg·mol⁻¹, $D_M \approx 1.7$, $T = -40$ °C).⁵ The same group further developed their method by modifying the monomer into a condensed ring-system, to increase the driving force of the polymerization (release of ring-strain) and thus be able to perform the reaction at r.t.. Also, the catalyst scope was broadened to encompass zinc complexes with a β -diketiminate-ligand (Scheme 45).^{13f} One of the main advantages of well-defined metal complexes compared to traditional metal alkoxides, is the ability to control stereochemistry during polymerization. Lactide, as one of the prime monomers of lactones, features two stereocenters that, if controlled well enough during polymerization, can significantly improve material properties of the resulting (co)polymers. Thus, substantial research efforts have been focused on developing



Scheme 45: Elaborate approach by *Chen* et al. for the synthesis of thermally degradable polymers with quantitative and repeatable chemical recyclability. Scheme adapted from literature.^{13f}

catalytic systems, that are able to induce tacticity during polymerization. Generally, two different mechanisms govern the stereocontrol during polymerization: on the one hand, if the last inserted monomer unit determines the enantiomeric form of the next inserted monomer, a chain – end – control mechanism is operable. On the other hand, enantiomorphic site-control is at hand if the chirality of the catalyst determines the stereochemistry of monomer insertion. The latter was hitherto only evidenced for metal-based catalysts, that are operating *via* a coordination – insertion mechanism, whereby the chain–end–control mechanism can also be employed with organocatalysts. In 2000, *Coates* et al. developed a racemic aluminium-salen-catalyst, that was capable of generating stereoblock poly(lactic acid) from *rac*-Lactide (Figure 5, left).¹¹⁵ The utilization of only one enantiomer of the catalyst resulted in enantiomerically enriched isotactic polymers during initial stages of the polymerization, and formed a gradient polymer during later stages due to primarily consuming only one isomer until its equilibrium concentration is reached. In 2003, *Feijen* and co-workers employed another chiral aluminium-salen-complex to further

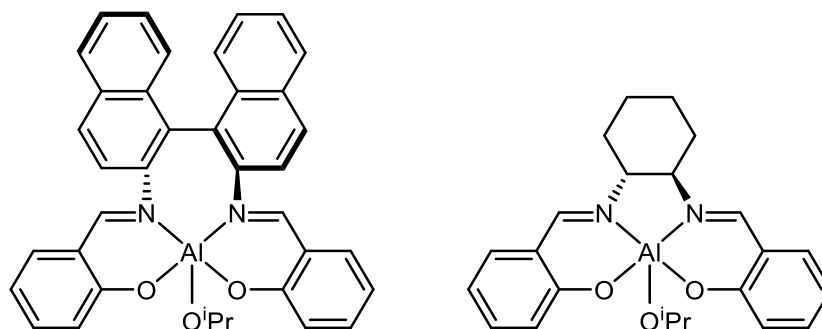
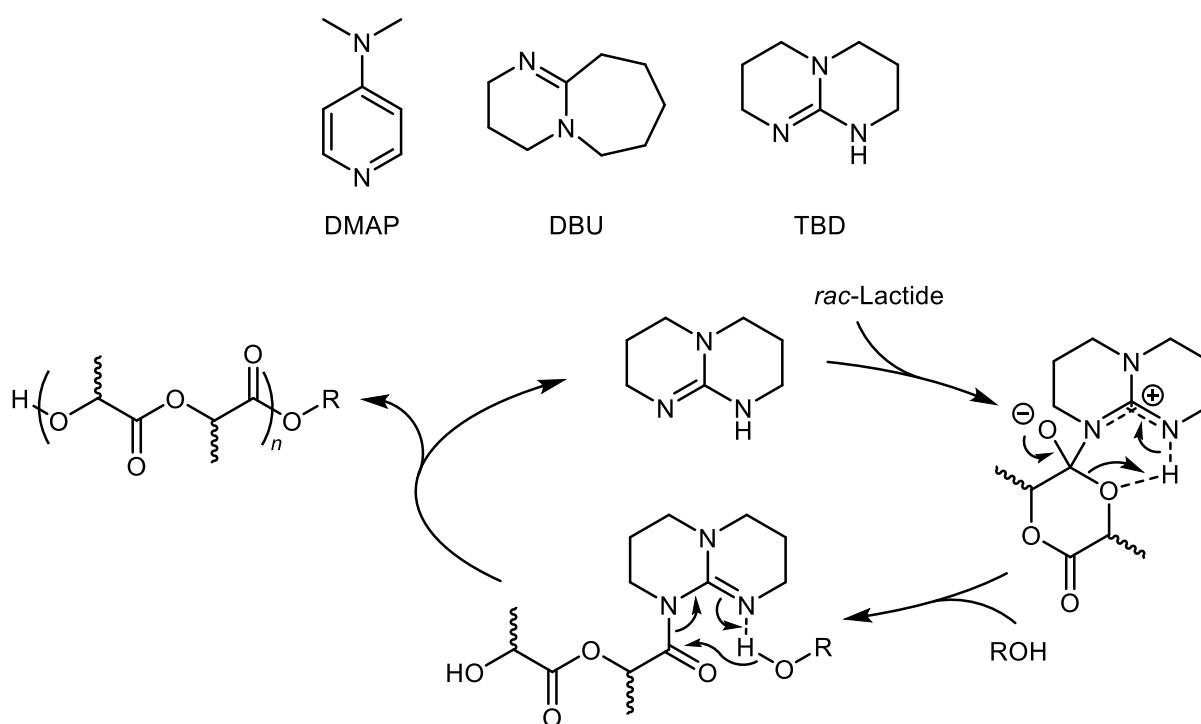


Figure 5: Aluminium-based salen complexes capable of stereoselective polymerization of *rac*-Lactide.

enrich the available catalyst systems for stereoselective polymerization of Lactide, which preferred *L*-Lactide over the *R*-isomer (Figure 5, right).¹¹⁶

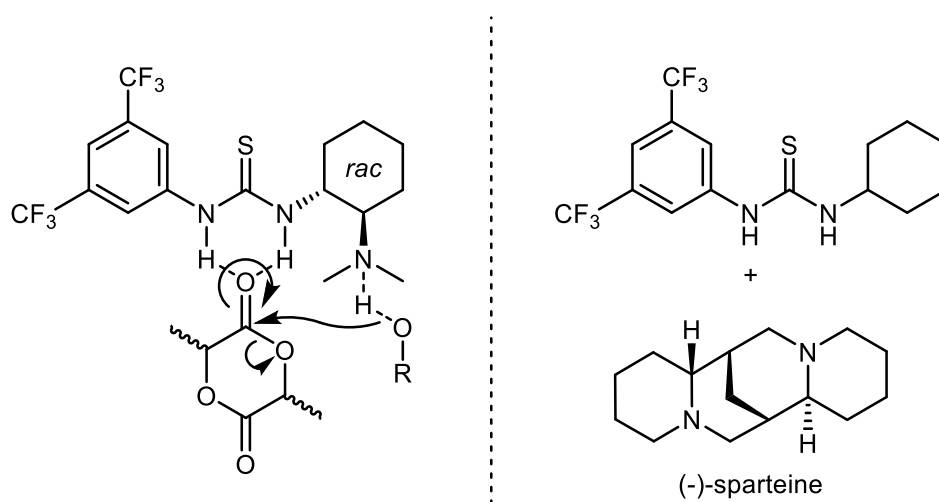
2.3.3. Organocatalysts

As mentioned above, poly(esters) often find application in biomedical areas. Hence, residual metal-contaminations often pose serious issues, as they are often cytotoxic and their separation from the polymer often proves challenging. Thus, many metal-free approaches for the ROP of lactones have been developed, mainly focussing on tertiary amines, pyridines, phosphazenes and NHCs.¹ Generally, two possible modes of operation are accessible using organocatalysts: either the catalyst acts as a



Scheme 46: Top: chemical structures of common organocatalysts employed in ROPs of lactones. Bottom: bifunctionality of TBD that combines monomer and initiator activation.

nucleophile, directly attacking the monomer and initiating polymerization, or the catalyst acts as a base and deprotonates the monomer/initiator. In both cases, as well as in metal-based systems, counter ions, complexing agents, solvent polarity and the chemical nature of the propagating chain end (alkoxides, carboxylates or both) influence the nature of the growing species and can shift the equilibrium between free ions and covalent species either way. Typical and readily available initiators are represented by 4-Dimethylaminopyridine (DMAP), 1,8-Diazabicyclo(5.4.0)undec-7-ene (DBU) or 1,5,7-Triazabicyclo(4.4.0)dec-5-ene (TBD) that are depicted in Scheme 46, top. DMAP and DBU usually work in junction with alcohol initiators;¹¹⁷ TBD additionally features an inherent dual reactivity, that makes it suitable to also be employed alone: the lactone can be ring-opened *via* nucleophilic attack of the imine onto the monomer, while the alkoxide which results from an acyl-bond cleavage is stabilized by H-bonding of the amine (Scheme 46, bottom).¹¹⁸ The bifunctionality of TBD is further corroborated by the fact, that *N*-methylated TBD shows significantly reduced activity, suggesting the involvement of the proton in the manner described above. Another type of bifunctional catalyst system was developed by *Hedrick* and co-workers, using a tertiary amine and a thiourea derivate together with an initiating alcohol (Scheme 47, left).¹¹⁹ Here, the thiourea moiety will act as monomer initiator, while the tertiary amine activates the initiator *via* H-bonding. However, the authors also identified that it is not necessary to incorporate both moieties into one molecule – in fact, not only offer two separate compounds a greater variability, but also an increased activity if a suitable combination is found. This was indeed the case for the



Scheme 47: Left: Bifunctional catalyst developed by *Hedrick* et al. for the polymerization of Lactide.¹¹⁹ Right: improved system, that uses separate compounds to activate monomer/initiator.¹¹⁸

combination of a thiourea-derivative together with (-)-sparteine, which enabled the reduction of the reaction time from a couple of days to only a few hours at r.t., while also being functional group tolerant and having reduced catalyst loadings (Scheme 47, right).¹¹⁸ This success spurred researchers to employ NHCs in the organocatalytic ROP of lactones. The most prominent congeners in this context are 1,3-bis(2,4,6-trimethylphenyl)imidazol-2-ylidene (IMes), its saturated version 1,3-bis(2,4,6-trimethylphenyl)-4,5-dihydroimidazol-2-ylidene (sIMes), and 1,3,4-Triphenyl-4,5-dihydro-1H-1,2,4-triazol-5-ylidene (TPT) as depicted in Figure 6, top. Generally, the synthesis of high-molecular-weight polyesters using NHCs is readily feasible and proceeds in a well-controlled/living manner.^{104a, c, 120} However, there are some peculiarities that deserve to be explicitly mentioned in this context. For example, applying sIMes without an alcohol as initiator in the polymerization of β -butyrolactone (BBL), leads to the formation of spirocycles.¹²¹ These spirocycles are efficient initiators for the ring-expansion polymerization of BBL with linear species being absent during catalysis, leading to the formation of cyclic esters. Furthermore, since NHCs are also potent nucleophiles, they can be readily employed without additional protic initiators. Yet, a direct nucleophilic attack of an NHC onto the acyl-carbon atom ensues the formation of a so-called azylazolium moiety – a highly unstable species, that is susceptible to substitution and will lead to the exclusive formation of cyclic poly(estere)s. NHCs have also been applied in a biphasic setup consisting of an ionic liquid (IL, [EMIM][BF₄]) and THF.^{120a} Using this approach, the NHC catalyst can be generated *in situ*, while the biphasic setup allows for easy

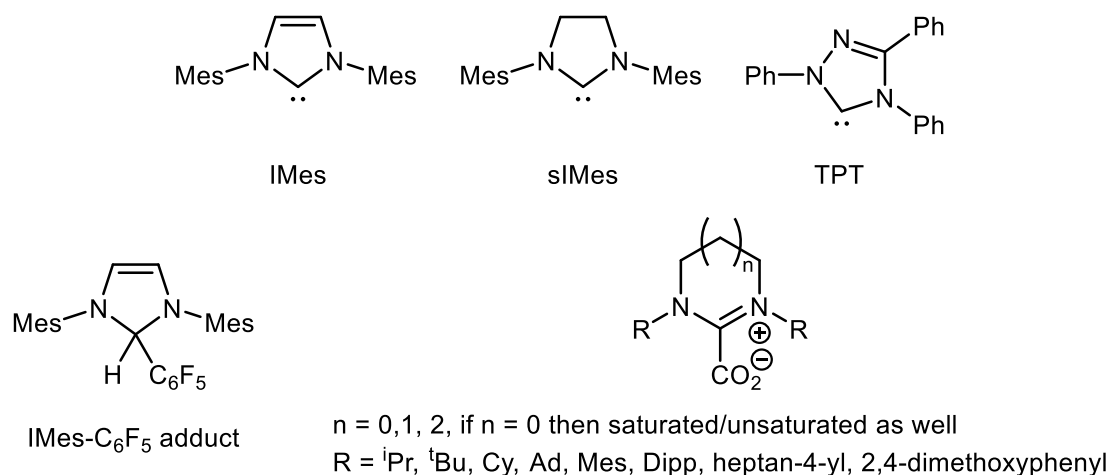


Figure 6: Top: Chemical structures of typical NHCs employed in ROPs of lactones. Mes = 2,4,6-trimethylphenyl. Bottom: NHC-adducts applied in ROPs of lactones. Cy = cyclohexyl, Ad = adamantyl, Dipp = 2,6-diisopropylphenyl.

separation of the resulting polymer from the THF phase. Furthermore, the IL can also be recycled. The *in situ* generation of the active catalyst can also be realized using the IMes – pentafluorophenyl adduct (Figure 6, bottom).¹²² This r.t.-stable adduct, however, only possesses limited applicability, since a racemization of Lactide has been observed. *Buchmeiser* et al. have improved this approach by synthesizing NHC-CO₂ adducts (Figure 6, bottom).^{2a} The adducts achieved full latency at room temperature, combined with high activity at elevated temperatures and were applied in the polymerization of ϵ -Caprolactone. Another prominent class of organocatalysts that has received increased attention in the last couple of years are phosphazenes. Featuring a pK_a -value that places them amongst super- or even hyper-bases, they are efficient, non-nucleophilic bases that are readily employed together with protic initiators in the ROP of lactones. For example, elegant work by *Chen* et al. enabled the polymerization of a lactone, that has been known as “non-polymerizable”: applying the phosphazene ^tBu-P₄, the polymerization of γ -Butyrolactone (GBL) to molecular weights up to 27 kg·mol⁻¹ ($M_n = 1.16 - 2.11$, up to 90 % conversion, -40 °C) was realized in only a few hours (Figure 7, left).^{13c} Intriguingly, the resulting polymers were thermally, and even more important, quantitatively recyclable. Heating the polymers for 1 h at 260 °C led to full depolymerization and fully regenerated the monomer, that could again be converted to polymers. Furthermore, the copolymerization with other lactones was also feasible with this technique.^{13d} This approach was also used by other groups to generate polymers of GBL using a cyclic phosphazene (Figure 7, right).^{13e}

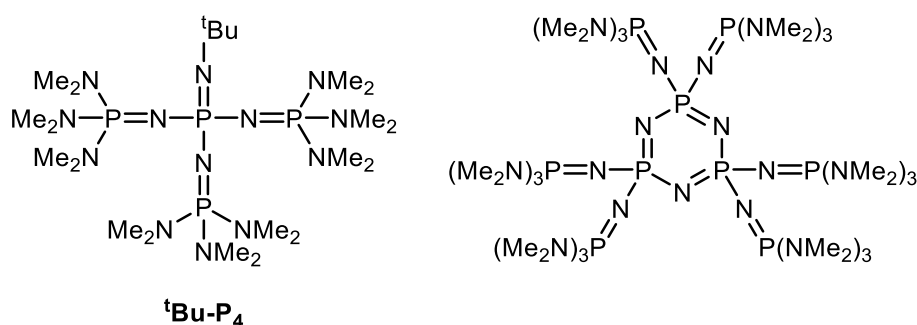
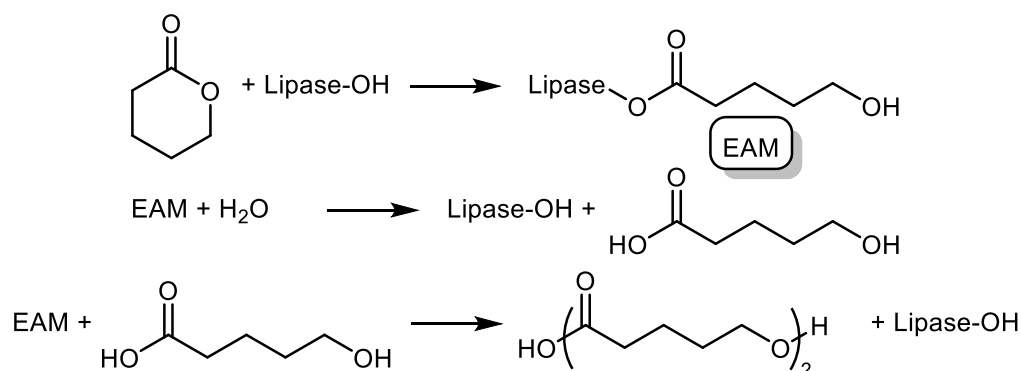


Figure 7: Left: Phosphazene used in the ROP of GBL by *Chen* and co-workers to form fully recyclable polymers. Right: cyclic phosphazene developed by *Zhao* and co-workers.

2.3.4. Enzymes

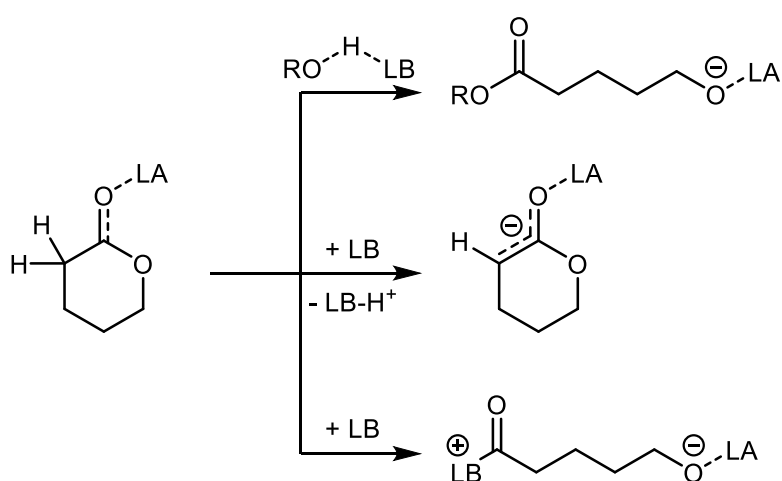
Appearing first in 1993,¹²³ the enzyme-mediated ROP of lactones has been well-researched and -reviewed in literature.^{1, 28a, 104d, 105, 124} Thus, it shall suffice to mention the general advantages and drawbacks, while also briefly discussing the underlying mechanism. As with all reaction that apply enzymes, the ROP of lactones can be performed under mild conditions regarding pH, temperature and pressure. Furthermore, the resulting polymers are easily separated from enzymes, leaving no contamination, and enzymes are generally accepted as “green” catalysts. Also, multiple solvent systems can be realized with enzymes: be it organic solvents, ionic liquids, bulk reactions or immobilized on surfaces, enzymes have shown to be applicable in all of these approaches. Enzymes even tolerate certain amounts of water, while still maintaining their high regio- and stereoselectivity. What is more, macrolactones that are generally more challenging to polymerize, are readily converted into polymers using enzymes, since the active center of enzymes is lipophilic and thus favours monomers with longer aliphatic chains. Yet, they rarely find application in industrial relevant processes, as they are comparably expensive and large amounts are needed in order to reach high conversions. Furthermore, traditional metal- and organocatalytic systems outperform enzymes in terms of molecular weights and polydispersities of the generated polymers. In ROPs of lactones, enzymes applied are typically lipases like *candida antarctica* (Novozyme 435) or *candida rugosa*. The rate-determining step of enzyme-catalysed ROP of lactones has been identified as the formation of an enzyme-activated monomer (EAM). Together with a protic molecule (water, alcohol, growing polymer), the lipase is regenerated and the monomer is ring-opened. Another monomer unit is then added to this ring-opened monomer from an EAM, propagating the polymerization (Scheme 48).



Scheme 48: Mechanism of enzyme-mediated ROPs of lactones, exemplified using δ -Valerolactone.

2.3.5. Other Initiating Systems

Since anionic and coordination – insertion mechanisms largely prevail in ROPs of lactones, only very few other initiating systems exist that exhibit a comparable reactivity, while operating through a different mechanism. Despite being generally feasible, cationic ROPs of lactones usually proceed in an ill-controlled manner and often suffer from significant side-reactions. Investigated systems encompass Lewis acid (LA)-based systems (AlCl_3 , BF_3 , FeCl_3 , ZnCl_2 , ...), alkylating and acylating agents, or protic systems (HCl , RCOOH , RSO_3H).^{1, 125} Yet, trifluoromethanesulfonic acid (HOTf) proved to be surprisingly efficient in polymerizing Lactide: in only a few hours at r.t., full conversion was reached.⁴⁰ Furthermore, the polymerization proceeded in a well-controlled manner, as substantiated by the quantitative incorporation of the protic initiator and linear correlations of M_n vs. conversion and \bar{D}_M , respectively. Also, despite the significant acidity of HOTf, no epimerization of Lactide was observed when polymerizing *L*-Lactide, while the easy removal of HOTf residue, its ready availability, and the higher activity compared to DMAP further corroborate the applicability of this approach. The mechanism hereby follows the activated monomer mechanism depicted in chapter 1.1.4.2, Scheme 21. Another interesting method has been developed by *Liu* et al. in 2004.¹²⁶ Here, the authors applied natural amino acids that act as both initiator and activator, to form polymers from CL in 1 – 2 days at 160 °C with reasonable control (M_n up to 27 kg·mol⁻¹, $\bar{D}_M = 1.50 - 1.89$).



Scheme 49: General mechanisms operable with Lewis Pair mediated ROPs of lactones, exemplified using δ -valerolactone.

2.3.6. Polymerizations mediated by Lewis Pairs

Already in 1997 found *Jérôme* and *Dubois* that additives have a beneficial effect on the $\text{Al}(\text{O}^i\text{Pr})_3$ -mediated polymerization of Lactides. Hereby, triphenylphosphine and 4-picoline were employed as Lewis bases (LBs) to work in junction with the initiator to affect polymerization rates and molar masses of the resulting polymers.¹²⁷ However, the LB was hereby considered to only act as a ligand towards the aluminium center, facilitating monomer insertion by donating electron density onto the metal. Still, by adding 4-picoline, the reaction reached full conversion up to 17-times faster than without additive, while still featuring predictable molar masses (at least up to 150 °C). Generally, Lewis Pairs (LPs) can facilitate polymerization *via* three different mechanisms (Scheme 49). Probably the most common approach is to use the LP to activate monomer and initiator separately, whereby the LA will coordinate to the monomer, while the LB activates the initiator, often acting as a “proton shuttle” that is readily able to stabilize a positive charge (Scheme 49, top). Depending on the basicity of the LB, the activated monomer might be deprotonated to form, in the case of lactones, an enolate which in turn will initiate polymerization (Scheme 49, middle). Finally, now depending on the nucleophilicity of the LB, the LB might directly attack the activated monomer, achieving ring-opening and initiation of the polymerization by itself (Scheme 49, bottom). Hereby, the LP can also be of intramolecular nature, as shown by *Arnold* et al. in 2006.¹²⁸ Applying bifunctional yttrium(III) and titanium(IV) NHC catalysts, the authors achieved remarkable activities in the polymerization of *rac*-Lactide (Figure 8, 1 and 2). Complex 2, for example, achieved a TOF of 34 000 h⁻¹, while being still reasonably controlled ($\mathcal{D}_M = 1.47$, $M_n = 66 \text{ kg}\cdot\text{mol}^{-1}$). The less lewis acidic titanium-complex 1 did not perform as well as the yttrium-based complex (TOF = 2550 h⁻¹, $\mathcal{D}_M = 1.17$, 23 kg·mol⁻¹, \mathcal{D}_M broadens over time due to transesterification). Furthermore, NHC-capped polymer chains were detected, hinting to a nucleophilic side-reaction apparent during polymerization. The same group reported another set of ROP-active, bifunctional NHC catalysts in a follow-up publication, this time employing magnesium and zinc as metal centers (Figure 8, 3 - 6).¹²⁹ It was found, that the initiation with magnesium-complexes proceeded *via* the carbene, while the alkoxide-bond was responsible in zinc complexes. This was explained by the weaker Mg-carbene bond compared to zinc-complexes. Furthermore, this reasoning was corroborated by the fact, that depending on the

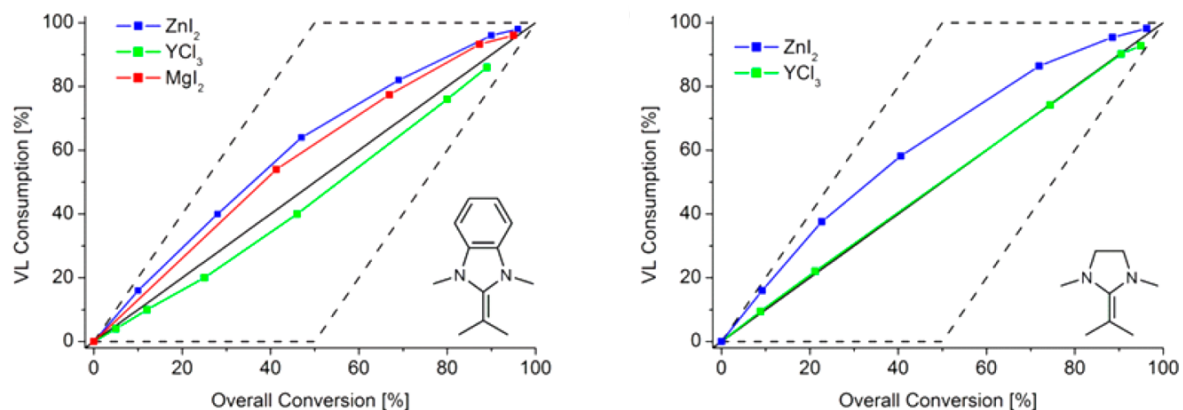
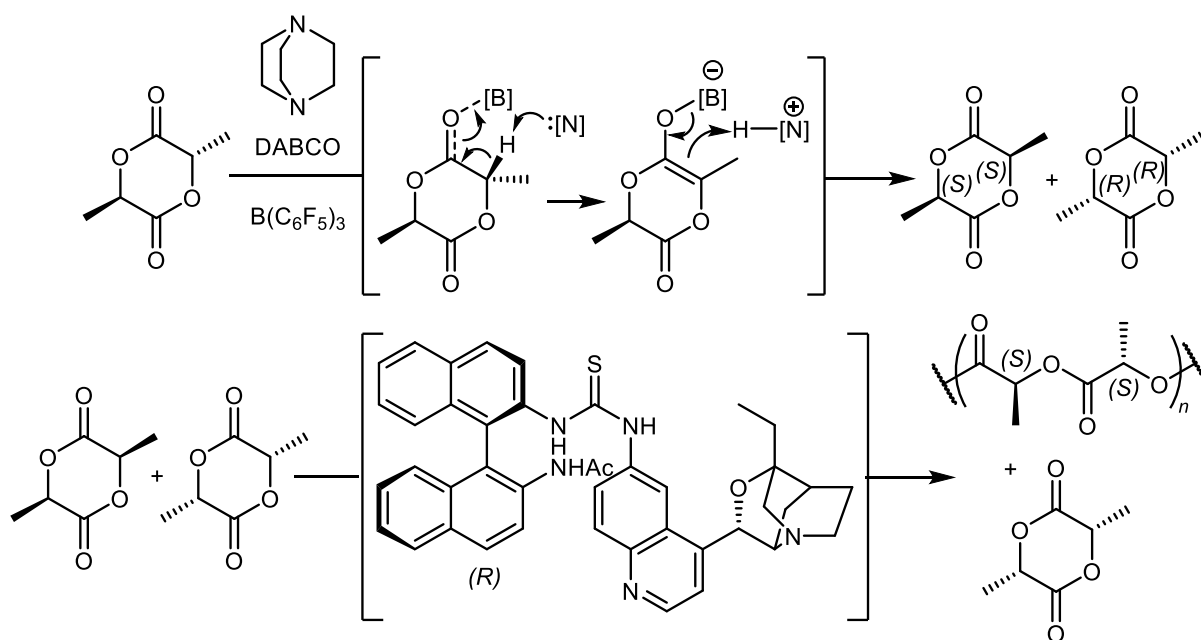


Figure 9: Copolymerization of CL/VL with depicted NHOs and LAs, using BnOH as initiator. Displayed is the respective VL consumption vs. overall conversion denoting different tendencies of incorporation depending on the applied LP. Conditions: NHO/BnOH/LA/VL/CL = 1:2:5:100:100, r.t., THF, $[M]_0 = 1.0 \text{ mol}\cdot\text{L}^{-1}$. Figure taken from cited literature.^{2c}

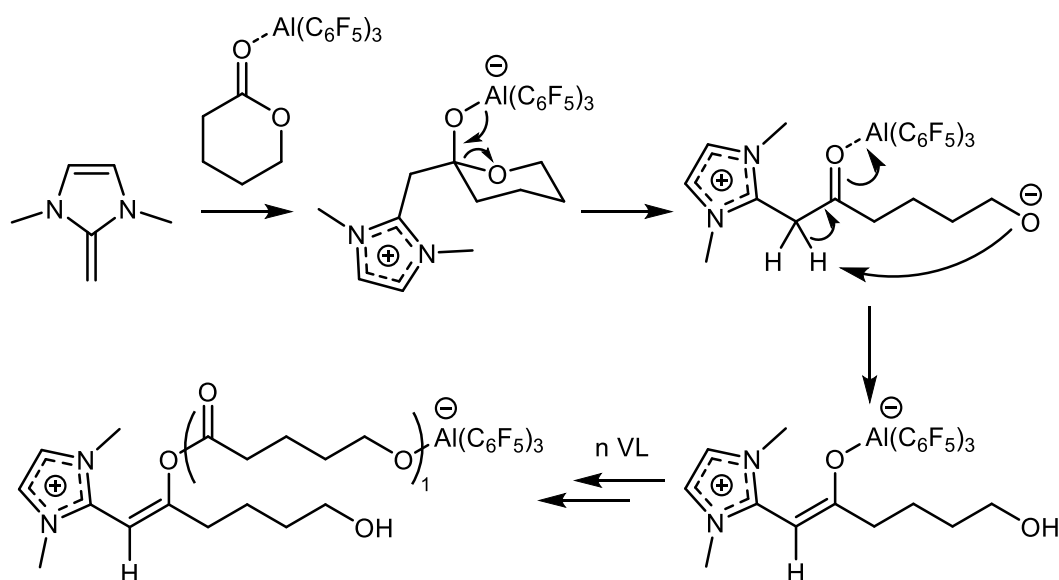
which was attributed to the Li^+ -ions being in close proximity to the growing chain-end, thus precluding cyclization. In 2016, NHOs took the stage of lactone polymerization. *Naumann* et al. employed LPs consisting of various NHOs and readily available LAs in the (co)polymerization of CL and VL.^{2c} While still having pivotal influence over the reactivity of the LP, the authors further elucidated that the LA also influences copolymerization parameters. The (co)polymerizations proceeded smoothly, with linear correlation of M_n vs. conversion ($D_M = 1.05 - 1.37$). Several tasks were identified to be accomplished by the LA: firstly, the LA acts as a monomer activator to facilitate ring-opening; secondly, it will mitigate side-reactions *via* coordination of the growing chain-end and selective monomer activation; thirdly, forming closely interacting LPs will further reduce free NHO from the polymerization mixture, again attenuating side-reactions. Theoretical investigations performed by *Naumann* et al. in 2018 further illuminated the underlying activation mechanism.⁸⁰ NHOs were found to coordinate to LAs *via* the exocyclic carbon atom, as is also the case for other NHO-(transition)metal-complexes (cf. chapter 1.3.4). Also, the adduct-formation tendency was determined to be in the order of $\text{ZnCl}_2 > \text{MgCl}_2 > \text{LiCl}$; calculations for a metal-free setup determined, that no deprotonation of a protic initiator (ROH) takes place, while the process becomes exothermic and exhibits a low activation barrier if a LA is considered. In 2013, *Amgoune* and co-workers employed a LP consisting of $\text{Zn}(\text{C}_6\text{F}_5)_2$ and 1,2,2,6,6-pentamethylpiperidine (PMP) for the polymerization of *rac*-Lactide.¹³¹ The resulting polymers displayed a linear correlation of M_n vs. conversion and exclusively cyclic topologies. The cyclization was suspected to be caused by a back-biting reaction at the very end (or during work-up)

of the polymerization, as also a broadening of the molar mass distribution was observed (\mathcal{D}_M from 1.1 to 1.5). Furthermore, *via* sequential polymerization of *rac*-Lactide and CL, cyclic block copolymers could be obtained using the PMP-Zn(C₆F₅)₂ system. Lewis Pair polymerizations of lactones are also able to induce stereoselectivity, as demonstrated by *Tolman* et al. in 2010.¹³² Here, the authors employed InCl₃ as LA with BnOH as initiator and NEt₃ as LB to achieve a heterotacticity of $P_r \leq 0.97$ (P_r denotes the probability of racemic enchainment of monomer stereoisomers). They further elucidated, that all three components are necessary in order to promote polymerization (TOF ≤ 40 h⁻¹), which proceeded *via* a coordination – insertion mechanism with [InCl_(3-n)(OBn)_n]_m and NEt₃-H⁺ as counterion. Another elaborate approach to achieve kinetic resolution was developed in 2015 by *Chen* and co-workers. Here, starting from *meso*-Lactide which is often seen as waste, a rapid and quantitative epimerization using B(C₆F₅)₃ and 1,4-diazabicyclo[2.2.2]octane (DABCO) formed *rac*-Lactide, which was subsequently converted into isotactic PLA by a bifunctional catalyst that only consumed one stereoisomer (Scheme 50). The chiral thiourea hereby acts as monomer activator, while the chiral amine coordinates the propagating hydroxyl species, achieving 91 % ee at 50.6 % conversion under optimized conditions. Using this approach, a one-pot setup was developed to transform *meso*-Lactide into isotactic poly(*L*-Lactide) and *D*-Lactide.



Scheme 50: One-pot approach developed by *Chen* et al. to transform *meso*-Lactide into isotactic poly(*L*-Lactide). In a first step, *meso*-Lactide is epimerized using DABCO and B(C₆F₅)₃. Subsequently, *L*-Lactide is polymerized using a bifunctional, chiral thiourea-based catalyst.

Finally, in 2017, the same group also developed a living LP-based polymerization system for CL and VL, applying an NHO and $\text{Al}(\text{C}_6\text{F}_5)_3$ (Scheme 51).^{21a} This system reached molecular weights up to $855 \text{ kg}\cdot\text{mol}^{-1}$ ($D_M = 1.02$), while exhibiting a linear correlation of M_n vs. conversion and $\frac{[M]}{[I]}$, respectively. Furthermore, chain extension experiments were successfully conducted, synthesizing PCL-*b*-PVL diblock and PCL-*b*-PVL-*b*-PCL triblock copolymers ($D_M < 1.15$). The polymerization hereby proceeded *via* the formation of a zwitterionic species, that is generated by a nucleophilic attack of the NHO on the LA-activated monomer, which is then ring-opened and relocates the proton to the chain end.



Scheme 51: Proposed polymerization mechanism of the living ROP of CL and VL, exemplified using VL. Scheme adapted from literature.^{21a}

2.4. Publications

As can be seen from the examples provided above, the field of ring-opening lactone polymerization is both industrially and scientifically relevant to this day, and has been since the early 20th century. There exist a multitude of catalysts that display outstanding activity and/or selectivity towards specific lactones. Yet, a catalytic system applicable to a broad range of structurally diverse lactones, while maintaining its activity, remains elusive. Hence, the publications presented in this chapter aimed to alleviate this issue. On the basis of previously built knowledge in our group,^{2c} readily and benign LAs like MgX₂ (X = Cl, I), ZnI₂ or YCl₃ were applied together with NHOs to form a dual catalytic setup for the polymerization of PDL, GBL, CL and VL. This polymerization setup specifically targeted lactones of largely differing ring-size (5-, 6-, 7- and 16-membered), aiming to demonstrate the versatility and broad applicability of this approach. Successful (co)polymerization of PDL (16-membered) with its other congeners validated this rationale. Notably, even PDL-GBL copolymers with up to 20 % GBL incorporation were formed, despite the fact that PDL-polymerization is an entropy-driven process requiring elevated temperatures (~ 100 °C), while GBL homopolymerization is thermodynamically handicapped (almost no ring-tension) and typically performed at very low temperatures (-40 °C). These results then enticed us to further map out the limits of this catalytic setup, employing it for the homopolymerization of GBL. This is a tremendously difficult task, which is exclusively accomplished by most active systems, since GBL was notorious for being “non-polymerizable” until recently.^{5, 13c, d, f} While clearly featuring room for improvement, the dual catalysis was still successful in generating high-oligomers/low-polymers of GBL with moderate activity. Intriguingly, depending on the NHO's structure, the topology of the resulting macromolecules could be influenced. These results burgeoned in the second publication presented in this chapter. Taken together, both publications corroborate the relevance of dual catalysis in developing highly and readily adaptable catalytic systems, that might one day become industrially relevant processes.

1st Publication:

P. Walther, S. Naumann*, *Macromolecules* **2017**, *50*, 8406-8416.


2nd Publication:

P. Walther, W. Frey, S. Naumann*, *Polym. Chem.* **2018**, *9*, 3674-3683.

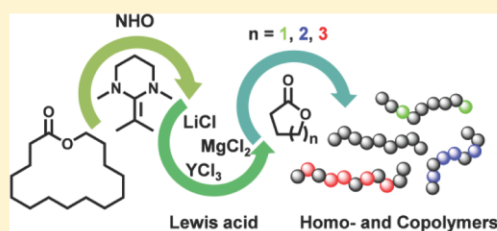
N-Heterocyclic Olefin-Based (Co)polymerization of a Challenging Monomer: Homopolymerization of ω -Pentadecalactone and Its Copolymers with γ -Butyrolactone, δ -Valerolactone, and ϵ -Caprolactone

Patrick Walther and Stefan Naumann*

Institute of Polymer Chemistry, University of Stuttgart, Pfaffenwaldring 55, D-70569 Stuttgart, Germany

 Supporting Information

ABSTRACT: A setup consisting of *N*-heterocyclic olefins (NHOs) and several simple Lewis acids (such as MgCl_2 or LiCl) was employed to homopolymerize ω -pentadecalactone (PDL) and to copolymerize it with five-, six-, and seven-membered lactones (γ -butyrolactone (GBL), δ -valerolactone (VL), and ϵ -caprolactone (CL)). Also, the copolymerization of GBL with VL and CL was investigated separately. This dual catalytic approach succeeded for the entropically driven high-temperature polymerization of PDL in course of fast, operationally simple polymerization procedures. PPDL could be generated in short reaction times to reach high conversion (85–97%), whereby the polymerization rates are significantly modulated by the metal halide cocatalyst (ranging from virtually 0 to >80% conversion after 15 min, 1% NHO loading). Application of mildly activating Lewis acids ensured that the frequently encountered excessive transesterification was reduced to yield relatively well-controlled polyester (M_n up to 40 kg/mol, $D_M = 1.5$ –1.8). The 1:1 copolymerization of PDL and GBL—unifying two lactones with thermodynamically opposite polymerization preferences—was observed to be strongly dependent on the applied Lewis pair, with yield (15–50%) and GBL content (5–22%, by ^{13}C NMR) determined by the Lewis acid. Likewise, GBL/CL and GBL/VL copolymers displayed varying, catalyst-dependent compositions and were obtained as well-defined polyester ($D_M = 1.1$ –1.2) with intermediate molecular weight (2–8 kg/mol) if a suitable cocatalyst pair was chosen. One-pot 1:1 PDL/VL copolymerizations resulted in high or low PDL content, as well as virtually exclusive VL consumption, if Lewis pairs containing YCl_3 , ZnI_2 , or MgI_2 were employed, with the reaction temperature a convenient tool to further manipulate the polymer structure. Finally, PDL/CL copolymers were readily formed, reaching high or quantitative conversion ($M_n = 10$ –30 kg/mol) whereby 50% PDL content and perfectly random polymer structures were accessible. For selected copolymers the thermal properties were elucidated by DSC measurements.



INTRODUCTION

The formation of aliphatic polyester from lactones via ring-opening polymerization (ROP) is nowadays an established, intensively researched field of polymer chemistry.^{1–3} The intrinsic properties of the materials combined with the convenient characteristics of ROP render them attractive for a number of applications, broadly ranging from drug delivery to tissue engineering and beyond.^{4–7} Part of this allure is the considerable scope of readily available lactone monomers which can be used as building blocks. This flexibility is further accentuated by the ability to copolymerize various lactones, enabling a manipulation of almost all mechanical, thermal, and chemical properties, including degradation times, and a tailoring of the polymer composition (block copolymers, random copolymers).^{8–11} However, to exploit this potential to its full extent, powerful catalysts are needed; the ability to (co)polymerize lactones at will is presently still elusive. This is essentially down to two interlocked issues. For one, some lactones are reluctant to polymerize because of thermodynamic constraints. This is especially true for macrocyclic lactones and

five-membered species.¹ Consequently, the copolymerization of such lactones with other, readily polymerizable cyclic esters commonly results in a low content of the more problematic monomers. Second, albeit numerous high-performing catalysts for lactone polymerization have been reported,^{12–19} there is currently no example—of a single catalyst or a catalyst family—we are aware of that is compatible with the whole range of lactones, from the small, highly strained four-membered cycles to large and strain-free macrocycles like PDL. This is true both for organometallic polymerization catalysts,^{12–14} which tend to be specifically adapted to a certain monomer by a skillfully designed ligand sphere, and for organocatalysts.^{15–19} Even *N*-heterocyclic carbenes (NHCs), perhaps the most potent and versatile class of organopolymerization catalyst, face similar problems.^{20–22}

Received: August 3, 2017

Revised: September 20, 2017

Published: October 19, 2017

Even if a suitable catalyst is applicable to a range of lactones, it remains a challenge to alter the copolymerization parameters in a rational manner. Polymerization propensities for a given catalyst and two lactones will mirror the underlying thermodynamics. To shift such parameters, for example from a gradient copolymer toward a more random structure, a redesign of the catalyst would be necessary. Albeit not impossible, it is not instantly obvious how a complex ligand sphere or the chemical structure of an NHC should be changed in order to favor one lactone over the other.

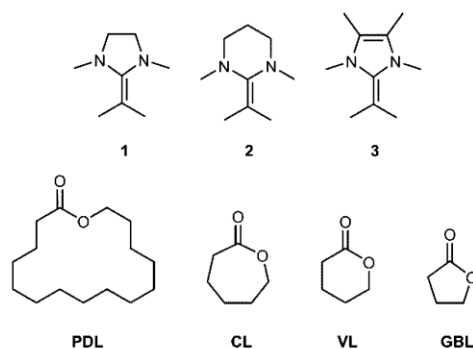


Figure 1. Scope of NHOs and lactone monomers.

In view of these issues, our group turned to dual catalysis as a potential means to overcome or alleviate these difficulties, in the form of Lewis pairs (LPs) consisting of *N*-heterocyclic olefins (NHOs) and metal halides as Lewis acids. In such a setup the Lewis acid will activate the lactone monomer to facilitate ring-opening, while the organic Lewis base activates or deprotonates the alcohol-based initiator. In spite of its simplicity and successful precedents for application in polymerization chemistry,^{23–31} this type of catalysis has not been studied in a systematic manner, nor are the underlying mechanisms fully clear. Several aspects were envisioned to be beneficial for lactone (co)polymerization. (i) Inherently, dual catalysis is modular and readily adaptable, since both components can be varied independently; potentially, this is an advantage when the range of monomers is as diverse as cyclic esters. (ii) Selectivity and activity are not necessarily coupled. Commonly, more active organocatalysts are achieved by rendering them more basic or nucleophilic to drive the ring-opening. This also favors transesterification and thus limits polymerization control, a frontier of current research.^{32,33} Rather than tuning the activity of the organocatalyst component, the dual catalytic approach employs activation of the monomer. If this activation can differentiate between the monomer and the ester groups in the polymer chain, as might be assumed for Lewis acid coordination, transesterification is reduced while polymerization rates are increased in parallel. (iii) The copolymerization parameters can be influenced. The series of lactones displays different bond angles and electron densities, in addition to varying steric demands. This can be exploited, since it can be assumed that different metal salts will activate the different cyclic esters with a degree of selectivity.

The general feasibility of this concept was recently demonstrated for the copolymerization of VL and CL, where NHO/metal salt combinations delivered well-defined polyester, crucially with the monomer consumption markedly influenced by the cocatalysts, including inverted polymerization prefer-

ences when using YCl_3 instead of $MgCl_2$, for example.³⁴ While the application of benign and simple salts such as $MgCl_2$ has obvious benefits, NHOs are distinguished by their strong polarization, structural flexibility, convenient preparation, and tunable electronic properties.^{35–47}

Hence, it is of interest to extend this method to other, less readily polymerizable lactones. To map out the true potential of this dual catalytic, Lewis pair-based approach, two of the more notorious lactone monomers were chosen for the present study. PDL, a 16-membered macrolactone, is essentially strain-free.¹ Polymerization can still be achieved on account of a small gain in entropy upon polymerization, when the reaction temperature is sufficiently high. Typically, PPDL synthesis suffers from a broad molecular weight distribution and a still somewhat limited set of suitable catalysts, which includes enzymes and some metal-based catalysts.^{29,48–54} Organopolymerization of PDL has been reported using TBD²² and phosphazenes.⁵⁵ NHOs can also slowly polymerize this monomer under certain conditions.⁵⁶ Probably for the same reasons, copolymers of PDL with other lactones have rarely been reported. Generally, rapid transesterification generates randomized polymer structures. This has been shown to be the case for CL and VL,^{22,57,58} so far, only sterically shielded ϵ -substituted ϵ -lactones resist interblock scrambling.^{59–61} Block copolymers have also been prepared from PDL and lactide in two-step processes.^{62,63}

GBL, in contrast to PDL, has long since been considered not polymerizable at all under practicable conditions, with only oligomers resulting from high-pressure experiments.⁶⁴ Recently, Chen and co-workers detailed how to synthesize poly(GBL), an intriguing material for its recycling properties and its biosourced feedstock.^{65,66} Key to success is the employment of very low reaction temperatures ($-40\text{ }^\circ\text{C}$) and high monomer concentration (10 M). Commonly, the copolymerization of GBL with other lactones has resulted in rather low GBL contents, with the polymerization stopping after the corresponding comonomer had been used up. For 1:1 polymerizations, the limited set of reports discloses GBL contents of about 5–15%^{67–73} and rarely higher.^{74,75} The degree of GBL incorporation can be influenced by tuning of the monomer feed; a large excess of GBL somewhat increases its mole fraction in the resulting polymer, but obviously this makes not very efficient use of the monomer. Although different catalysts tend to incorporate different amounts of GBL, a systematic modulation of this property via the adaption of the catalyst system is notably absent from the literature, recommending a readily adaptable catalytic system as described in the following.

RESULTS AND DISCUSSION

Homopolymerization of PDL Using Different LPs.

NHOs 1–3 were synthesized according to convenient two-step procedures (Supporting Information Figure S1). The resulting compounds were obtained as pale yellow liquids (1, 2) or orange solid (3) and stored at $-36\text{ }^\circ\text{C}$ inside the glovebox. Structurally, these compounds represent three distinctive types of NHO. The three different backbones—saturated five- and six-membered rings as well as the nonsaturated imidazole derivative—have a major influence on reactivity, which is qualitatively in the order of $3 \gg 2 > 1$. While literature suggests that 2 has a somewhat more pronounced propensity to donate electron density than 1,⁷⁶ the more relevant difference between the saturated and nonsaturated NHOs is related to the ability of the latter to stabilize a positive charge more efficiently.⁷⁷ The strong polarization found in the double bond of NHOs,

sufficient to bind to CO₂^{39,78–80} or to complex metals end-on rather than side-on,^{38,41,44} can be represented as charge separation, resulting in a zwitterion. If an aromatic imidazolium moiety can form, as for compound 3, this will consequently increase the nucleophilicity and basicity of the NHO. Hence, the polymerization activity of 3 was observed to be markedly different from its saturated analogues in some instances.^{43,56,77}

Also, all organic cocatalysts 1–3 bear a dimethyl substitution on their exocyclic carbon. This feature will further increase the electron density; more importantly, however, the introduction of the methyl groups also suppresses the occurrence of potential side reactions. Sterically “naked”, =CH₂-bearing NHOs are prone to directly ring-open lactone monomers. The resulting structure features a methylene unit placed between a carbonyl moiety and a positively charged imidazolium group and is thus sufficiently acidified to be easily deprotonated.^{31,56} This side reaction will quench the polymerization activity, but it can obviously be circumvented when =CH₂ is replaced by =C(CH₃)₂ (see Figure S2 for further details).

All three NHOs were then applied in combination with a number of simple, inorganic salts for the polymerization of PDL, using different temperatures and investigating both toluene and THF as solvents (initiator = BnOH). The most relevant results are given in Table 1, while the full data set is

Table 1. Polymerization of PDL Using Various NHO/Lewis Acid Combinations^a

no.	NHO	Lewis acid	time [min]	conv ^b [%]	M_n^c [g mol ⁻¹]	D_M^c
1	1	MgI ₂	15	77	19200	1.62
2	1	MgI ₂	60	95	22900	1.64
3	1	MgI ₂	240	96	17100	1.73
4	1	MgCl ₂	15	26	7400	1.45
5	1	MgCl ₂	60	84	26200	1.58
6	1	MgCl ₂	240	94	30000	1.49
7	3	MgI ₂	240	95	20900	1.58
8	3	MgCl ₂	240	75	26500	1.49
9	3	YCl ₃	240	74	18200	1.61
10	3	ZnI ₂	240	14	3700	1.61
11	3	LiCl	240	86	26600	1.52
12 ^d	2	MgI ₂	240	97	33600	1.54
13 ^e	2	MgI ₂	19h	87	40800	1.57
14 ^d	3	LiCl	240	39	18900	1.46
15 ^f	3	LiCl	240	85	27700	1.57
16 ^g	3	LiCl	240	30	8800	1.79
17 ^h	3	LiCl	240	2		

^aConditions: molar ratio of NHO/BnOH/ M_x /PDL = 1:2:5:100, $[M]_0$ = 1.0 M in toluene, 110 °C. ^bMonomer conversion determined via ¹H NMR spectroscopy. ^cDetermined via SEC analyses (CHCl₃). ^dNHO/BnOH/ M_x /PDL = 1:2:5:200. ^eNHO/BnOH/ M_x /PDL = 1:2:5:400. ^f80 °C. ^g50 °C. ^hRoom temperature.

provided in Tables S1–S3. Initial findings immediately revealed a strong polymerization activity, regulated by the employed Lewis pair, and significant differences to the homopolymerization of VL and CL by the same system.³⁴ In toluene at 110 °C with an initial monomer concentration of 1.0 mol/L (NHO/BnOH/ M_x /PDL = 1:2:5:100), all three NHOs were able to deliver fast monomer consumption coupled with a relatively good control over the molecular weight distribution. In many cases, polydispersity reliably stayed around 1.5, while molecular weights of M_n = 10–40 kg/mol were readily delivered. Notably,

under suitable conditions such conversion could be obtained very rapidly, for example 2/MgI₂ effected a monomer consumption of 80% after only 15 min (Figure 2 and Table S3). Prolonged polymerization times in the presence of MgI₂ routinely entailed a degradation of molecular weight by transesterification; in contrast, activation by MgCl₂ resulted only in a minor slowdown of the polymerization while high molecular weights were retained over the observed time span of 4 h (see Table 1, entries 1–3 and 4–6 for 1/MgI₂ and 1/MgCl₂, respectively). Since under the given conditions both setups reach high conversion early on, the reduced transesterification in the case of MgCl₂ is down to not only a weaker activation or slower polymerization but also a higher selectivity of ring-opening over transesterification.

As a result of the generally not excessive transesterification, a correlation of M_n with conversion is possible (Figure 3 and Figure S3; see also Table S4 for a correlation of GPC results with molecular weights derived from ¹H NMR end-group analysis). In line with previous results, the chemical nature of the NHO seems less important than a suitable choice of the Lewis acid, which determined the success of the polymerization to a high degree. Coherently, for all cases the polymerization rates decreased in the order of MgI₂ > MgCl₂ > YCl₃ > ZnI₂. The striking exception to this rule is found for LiCl. With this cocatalyst, polymerizations employing 1 and 2 more or less failed, yielding only low conversion. In contrast, in conjunction with imidazole derivative 3 an efficient conversion of PDL is observed. While an increase of monomer loading to 200 and 400 equiv accompanied by longer reaction times still achieved high conversion (entries 12–14), a lowering of the reaction temperature below 80 °C significantly slowed down the polymerization (entries 15–17). While at 80 and 50 °C after 4 h a conversion of 85% and 30% was found, the identical setup at room temperature is virtually inactive. Still, these results indicated that there is some room for copolymerizations under milder conditions. Notably, control reactions (Table S1) in the absence of any metal salt showed no polymerization for 1 and 2, while application of 3 entailed a conversion which plateaued at about 40%, corroborating earlier reports⁵⁶ and underlining the synergy won by the addition of Lewis acids.

Copolymerization of PDL with CL, VL, and GBL

Copolymerizations of PDL and CL were conducted in THF (100 °C, pressure tube). The more polar solvent provided improved solubility compared to toluene for which the formation of precipitate was observed during the reaction. In contrast, the homopolymerization of PDL in toluene reported above had resulted in clear reaction mixtures. Monomer consumption was monitored individually for each lactone by ¹H NMR over a time of 4–8 h. While conversion was achieved in every case, the polymerization rates proved again to be susceptible to the chemical nature of the LP. Compared to PDL homopolymerization, the reactions proceeded slower and to somewhat broader molecular weight distributions. Under identical conditions (NHO/BnOH/ M_x /PDL/CL = 1:2:5:100:100, $[M]_{0,\text{total}}$ = 2.0 M; Table 2), the highest conversion and highest PDL incorporation were found for the application of MgI₂, which resulted in practically quantitative conversion, to deliver copolyester with M_n > 20 kg/mol. Uniformly, in all cases, ¹H NMR monitoring revealed that CL was consumed rapidly in the beginning, followed by a much slower conversion of PDL. This did not, however, result in block copolymer structures. ¹³C NMR analysis highlighted the prominent presence of heterodyads. Further, at high

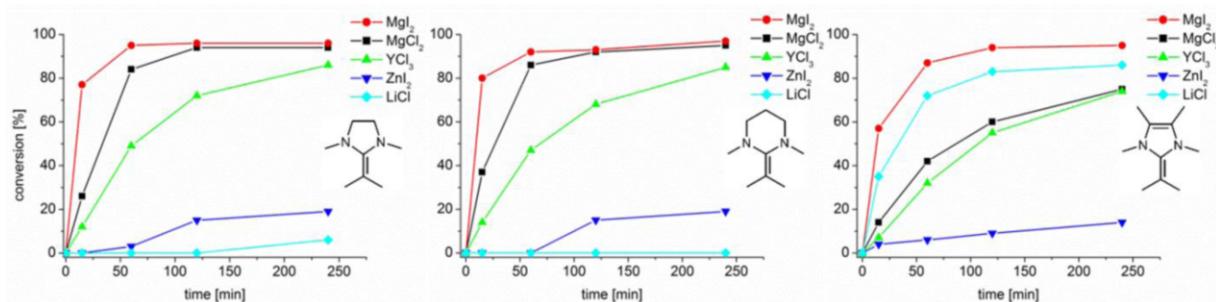


Figure 2. Conversion over time for various combinations of 1–3 with metal halides regarding the homopolymerization of PDL (NHO/BnOH/ M_x /PDL = 1:2:5:100, $[M]_0 = 1.0$ M in toluene, 110 °C).

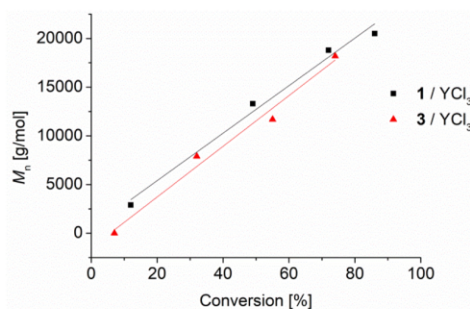


Figure 3. Correlation of M_n vs conversion for PDL homopolymerization. NHO/BnOH/ M_x /PDL = 1:2:5:100, $[M]_0 = 1.0$ mol/L, toluene, $T = 110$ °C.

conversion hetero- and homodyads displayed practically the same intensity for both lactones (**2**/MgI₂, Figure 4), while DSC measurements showed only a single melting point at $T_m = 74$ °C for this polymer. Together, these findings confirm that a perfectly randomized polymer was formed.^{22,57,58} The same trend was observed for all other combinations of NHO **2** and metal halides (Table 2; see Figures S8–S13 for exemplary ¹³C NMR data). Surprisingly, LiCl performed well in spite of its virtual inactivity when **2**/LiCl was employed for PDL homopolymerization. In fact, the material recovered from reactions with this Lewis pair had the highest molecular weight (28 kg/mol, entry 1) and the relatively best controlled molecular weight distribution ($\bar{D}_M = 1.71$). In contrast to LiCl, but in line with above reasoning, ZnI₂ was even more reluctant to incorporate PDL than when applied for homopolymerization. After 4 h at 100 °C, clearly less than 10% of the resulting polymer is made of PDL repeating units using this combination of cocatalysts (Table 2, entry 4). Hence, in this case again a randomized polyester is received, but with a

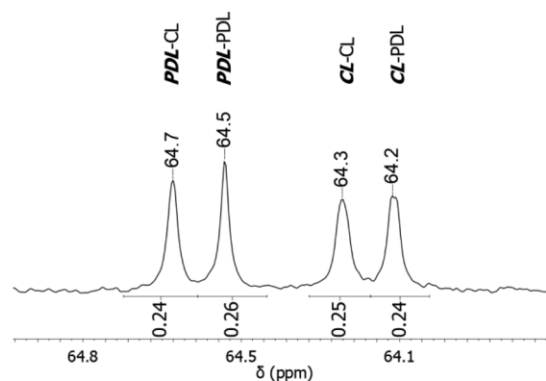


Figure 4. ¹³C NMR spectroscopy (CDCl₃, 300 K, O–CH₂ region) with dyad sequence analysis of a PDL/CL copolymer resulting from application of **2**/MgI₂.

low degree of PDL content, which also shows in the thermal properties ($T_m = 53$ °C, Figure 5).

Moving to VL, a quick screening revealed that at 110 °C (toluene) and reaction times of 4 h a relatively sluggish conversion occurs (see Table S5). With the notable exception of YCl₃ (78% conversion, 41% PDL content), monomer consumption remained well below 50%, whereby almost exclusively VL was consumed. The high polymerization temperature was probably responsible for the nonquantitative VL conversion as a consequence of an increased equilibrium concentration for this lactone at 110 °C.¹ To improve this situation, a temperature step was introduced and the polymerization times were extended. To promote conversion of VL, the reaction was first held at 50 °C for 8 h; then the temperature was increased to 110 °C to support PDL incorporation, focusing on the more promising Lewis acid cocatalysts.

Table 2. Copolymerization of PDL/CL Using Various NHO/Lewis Acid Combinations^a

no.	NHO	Lewis acid	time [min]	conv ^b [%]	M_n ^c [g mol ⁻¹]	\bar{D}_M ^c	dyad sequence distribution [%] ^d			
							PDL–CL	PDL–PDL	CL–CL	CL–PDL
1	2	LiCl	240	88	28100	1.72	26	19	29	26
2	2	MgCl ₂	240	77	18600	2.1	21	17	41	21
3	2	MgI ₂	240	97	23300	1.83	24	26	25	24
4	2	ZnI ₂	240	54	10900	1.84	5	2	85	8
5	2	YCl ₃	480	84	20700	1.78	24	18	33	25

^aConditions: molar ratio of NHO/BnOH/ M_x /PDL/CL = 1:2:5:100:100, $[M]_{0,\text{total}} = 2.0$ M in THF, 100 °C. ^bMonomer conversion determined via NMR spectroscopy. ^cDetermined via GPC analysis (CHCl₃). ^dDetermined from ¹³C NMR.

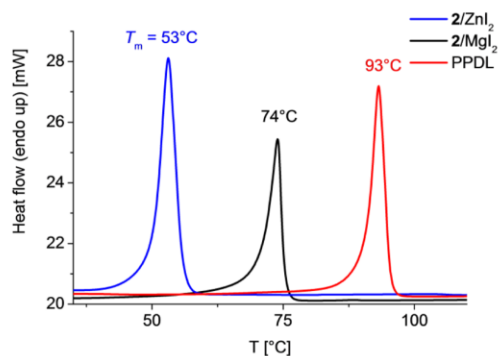


Figure 5. Detail of DSC scans (5 K/min) showing melting points for two PDL/CL copolymers with different PDL content in comparison to PDL homopolymer.

Surprisingly clear results were obtained from this approach (see Table 3). At 50 °C, virtually pure PVL is formed when 2/ZnI₂ was applied (Figure S10). Even MgI₂, itself a potent cocatalyst for PDL homopolymerization, incorporated only minimal amounts of PDL. In view of the considerable transesterification occurring (see \bar{D}_M values, Table 3) and the low amounts of VL remaining free in solution, this is remarkable. YCl₃, as implied by the initial screenings, was most prone to consume PDL, but contents remained low (<10%). The subsequent increase in polymerization temperature changed this picture, albeit in a different manner for the individual LPs. PDL consumption rose markedly for 2/YCl₃, where after 24 h a perfectly random copolymer was delivered (50% PDL content, entry 6). The received polyester was relatively well-defined with an expectedly higher molecular weight ($M_n = 23$ kg/mol, $\bar{D}_M = 1.53$) compared to the polymer before temperature increase. The prolonged polymerization at elevated temperature also enabled a higher PDL incorporation with 2/ZnI₂, yet conversion, molecular weight, and PDL content remained significantly below the ones found for 2/YCl₃. Remarkably, the LP consisting of 2 and MgI₂ resisted even those rather harsh conditions; PDL was not consumed to any relevant degree even after 24 h, and coherently no increase in molecular weight was found. Regarding the pronounced propensity of this LP for PDL homopolymerization (80% conversion in 15 min, see above), this selectivity for VL is striking. Potentially, the Lewis acid is preferentially complexed by VL to a degree that excludes any coordination to the large PDL monomer, or it is engaged in nonproductive polymerization–depolymerization equilibria of the formed PVL. Nonetheless, as described for CL, randomized PDL/VL copolymers can be formed in one-pot reactions by

NHO-mediated LP catalysis, whereby the PDL content is regulated from almost 0 to 50% by the cocatalyzing metal halide. The differences in copolymer composition are also mirrored by the respective melting points of the prepared polyester. The low-PDL content polymer prepared by 2/MgI₂ (entries 1 and 2) displayed almost identical thermograms after 480 min and 24 h, corroborating the NMR results. In this case, two distinct features are found: a well-defined melting point at 29 °C and a broader melting area peaking at 35–41 °C (Figure S14). Both are below the melting point of PVL homopolymer (56 °C) and can be interpreted to represent the melting point of the copolymer and additionally crystallized PVL domains, which can still imperfectly form because the PDL content is so low. Contrasting this, the polymer received after 24 h from 2/ZnI₂ and 2/YCl₃ displayed only a single, sharp melting peak at 59 and 72 °C (Figures S15 and S16), respectively, mirroring the increased PDL incorporation.

Finally, PDL was also copolymerized with GBL in a 1:1 manner, using a one-pot, one-step procedure (2/BnOH/ M_x /PDL/GBL = 1:2:5:100:100, $[M]_{0,\text{total}} = 2.0$ M in THF, 100 °C, Table 4). This type of copolymerization is of interest because any polymerization involving GBL which is not conducted at very low temperatures or high monomer concentration was expected not to deliver meaningful incorporation of GBL–GBL dyads let alone GBL homopolymerization.^{65,66} At the same time, going from higher to lower reaction temperatures, PDL polymerization is getting less favored. It was thus hoped to achieve higher than usual GBL contents in such a setup, ideally moving toward more alternating polymer structures. To the best of our knowledge, GBL/PDL copolyester has not been described before.

All polymerizations were monitored over extended times and stopped once conversion seemed to plateau or became impractically slow (reaction times in Table 4 represent the end point of observation; for time-dependent conversion and comparability see Table S6). The properties of the final polymers are listed in Table 4. A first range of reactions (entries 1–4) was conducted at 100 °C (pressure tube). Expectedly, the chemical nature of the LP prominently influenced the polymerization results. YCl₃ delivered a copolymer with $M_n = 21$ kg/mol ($\bar{D}_M = 1.8$) after an extended period of stirring. Dyad analysis showed that 15% GBL content were obtained this way. 2/ZnI₂ leveled off at around 35% total conversion; correspondingly, the molecular weight of the resulting polymer was lower ($M_n = 15$ kg/mol), and overall less GBL was incorporated with notably no GBL–GBL dyads at all detectable in ¹³C NMR analysis. In contrast, MgCl₂ yielded lower molecular weight material, albeit with a comparatively strong GBL-derived content (22%). Interestingly, in this case a clear

Table 3. Copolymerization of PDL/VL Applying a Temperature Step^a

no.	NHO	Lewis acid	time	conv. ^b [%]	M_n^c [g mol ⁻¹]	\bar{D}_M^c	dyad sequence distribution [%]			
							PDL–VL	PDL–PDL	VL–VL	VL–PDL
1	2	MgI ₂	480 min	41	8500	1.77	2		96	2
2 ^d			24 h	33	6800	1.70	4		92	4
3	2	ZnI ₂	480 min	39	7400	1.29			100	
4 ^d			24 h	52	10800	1.50	24	12	40	24
5	2	YCl ₃	480 min	44	8000	1.63	7		86	7
6 ^d			24 h	68	23000	1.53	26	24	24	26

^aConditions: molar ratio of NHO/BnOH/ M_x /PDL/VL = 1:2:5:100:100, $[M]_0 = 1.0$ M in toluene, 50 °C. ^bMonomer conversion determined via NMR spectroscopy. ^cDetermined via GPC analysis (CHCl₃). ^dAfter 8 h, the reaction mixtures were heated to 110 °C.

Table 4. Copolymerization of PDL/GBL Using 2/ M_x Lewis Pairs^a

no.	NHO	Lewis acid	time [h]	conv ^b [%]	M_n^c [g mol ⁻¹]	D_M^c	dyad sequence distribution [%]			
							PDL-GBL	PDL-PDL	GBL-GBL	GBL-PDL
1	2	LiCl	24	19	7600	1.43	12	65	11	12
2	2	MgCl ₂	27	21	5000	1.31	12	67	10	12
3	2	ZnI ₂	48	35	14600	1.80	6	88		6
4	2	YCl ₃	86	58	20900	1.79	10	74	5	10
5 ^d	2	LiCl	63	43	27600	1.54	14	65	7	14
6 ^e	2	LiCl	24	20	6200	1.97	19	65		16

^aConditions: molar ratio of NHO/BnOH/ M_x /PDL/GBL = 1:2:5:100:100, $[M]_{0,\text{total}} = 2.0$ M in THF, 100 °C. ^bMonomer conversion determined via NMR spectroscopy. ^cDetermined via SEC analyses (CHCl₃). ^d $T = \text{rt}$. ^e $T = -36$ °C.

Table 5. Copolymerization of GBL with CL or VL Using 2/ M_x Lewis Pairs^a

no.	comonomer (Co)	Lewis acid	time	conv ^b [%]	M_n^c [g mol ⁻¹]	D_M^c	dyad sequence distribution [%]			
							Co-GBL	Co-Co	GBL-GBL	GBL-Co
1	CL	LiCl	120 min	52	6900	1.49	11	74	4	11
2	CL	MgCl ₂	120 min	36	4100	1.09	16	68		16
3	CL	YCl ₃	120 min	61	4600	1.18	15	70		15
4	VL	LiCl	120 min	24	2200	2.2	9	82		9
5	VL	MgCl ₂	120 min	16	2700	1.13	8	84		8
6	VL	YCl ₃	120 min	37	3900	1.24	12	76		12
7 ^d	CL	LiCl	24 h	66	6600	2.4	22	56		22
8 ^d	CL	ZnI ₂	24 h	39	4800	1.06	10	73	7	10
9 ^d	VL	LiCl	24 h	46	5400	1.45	9	82		9
10 ^d	VL	MgCl ₂	24 h	24	2000	1.11	8	84		8
11 ^d	VL	ZnI ₂	24 h	49	5200	1.09	5	90		5

^aConditions: molar ratio of NHO/BnOH/ M_x /GBL/Co = 1:2:5:100:100 $[M]_{0,\text{total}} = 2.0$ M in THF, rt. ^bMonomer conversion determined via NMR spectroscopy. ^cDetermined via SEC analyses (CHCl₃). ^d $T = -36$ °C.

peak assigned to GBL homodyads was observed with an overall share of 10% in relation to the dyad sequence distribution. Experiments employing LiCl as cocatalyst yielded promising results with a GBL content >20% (entry 1). Consequently, this LP was applied for a polymerization setup at room temperature (entry 5). The polymer generated this way proved to have the highest molecular weight in this series ($M_n = 28$ kg/mol) while displaying a relatively controlled molecular weight distribution ($D_M = 1.5$). Crucially, again a considerable GBL incorporation exceeding 20% was found, yet no increase relative to experiments at 100 °C. This prompted us to lower the reaction temperature again, to -36 °C, with the intention of further increasing both molecular weights and GBL incorporation (entry 6). However, under these conditions a slow conversion resulting in low molecular weights and only a moderate GBL content were delivered. This behavior was tentatively related to the competing complexation of free NHO by the Lewis acid, which will be favored by lower polymerization temperatures. DSC thermograms of the PDL/GBL copolymers all showed single, well-defined melting points (Figure S17) ranging between $T_m = 79$ –91 °C, where by tendency higher GBL contents entailed lower values.

Copolymerization of GBL with VL and CL. Finally, GBL was copolymerized with its direct ring-expanded homologues, VL and CL. Two sets of experiments were conducted (NHO/BnOH/ M_x /GBL/Co = 1:2:5:100:100, $[M]_{0,\text{total}} = 2.0$ M in THF): one at room temperature and one at -36 °C.

Reactions stopped after 2 h at room temperature displayed differences depending on LP and comonomer. For CL, conversions of 42–61% were found with GBL contents varying between 10 and 20% (Table 5; see Table S7 for full data set). With VL the overall conversion dropped to 17–37%, and GBL

contents were also markedly depressed (6–12%). With few exceptions, the molecular weight distribution was found to be relatively controlled ($D_M = 1.12$ –1.24), while the molecular weights did not exceed 10 kg/mol as a consequence of nonquantitative conversion. As the readily polymerizable lactone is increasingly depleted, conversion as a whole will level off because no homopolymerization of GBL can occur under these conditions. The copolymerization of VL with CL proceeds swiftly and nicely controlled;³⁴ hence, it is clear that the presence of GBL retards the polymerization to a considerable degree—even if there are still residual amounts of CL or VL left in solution. Polymerizations at -36 °C entailed a somewhat different picture (Table 5, entries 7–11). With the exception of LiCl-cocatalyzed polymerizations, polydispersity further improved to $D_M = 1.1$ and below (see Figures S6 and S7 for exemplary chromatograms). GBL contents improved to a degree for GBL/CL but were virtually unchanged for GBL/VL. Microstructure analysis by ¹³C NMR (Figures S12 and S13) and the DSC results again clearly underline that no block copolymer is formed, as expected. GBL-derived signals appear almost exclusively in the form of heterodyads, although it is interesting to note that for some polymers small GBL-GBL homodyads can be observed (Table 5, entries 1 and 8). In contrast, 2/LiCl (entry 10) delivered a relatively high GBL content of 22% without any observable GBL homodyads. GBL is thus only placed between PDL-derived repeating units, giving the polymer a structure that is neither fully random nor fully alternating; the considerable transesterification ($D_M = 2.4$) is possibly favoring this dyad structure as over time initially formed GBL homodyads will be broken down to heterodyads under conditions that are adverse to GBL homopolymerization. The chemical nature of the LP

thus regulates not only the amount of GBL incorporated in the polymer but also, to a limited degree, the dyad structure of the resulting polyester. Observation of the individual lactone consumption (GBL/CL) via ^1H NMR further suggests that GBL is consumed right from the beginning; the formation of a relevant gradient can thus be excluded. Within a set of polymerizations (GBL/CL or GBL/VL) the degree of GBL incorporation can vary by a factor of 2 depending on the cocatalyzing metal halide (Table 5). The melting peaks for the copolymers as observed by DSC were well-defined (with shoulders in some cases) and ranged from $T_m = 31$ to 45 °C, below the melting point of the homopolymers and mirroring the bandwidth of GBL content. Coherently, the sample with the lowest GBL incorporation displayed the highest melting point (Table 5, entry 11; see also Table S8 for a list of all melting points and Figure S18 for a representative thermogram).

Mechanistic Considerations. Narrowed down to its core principles, the employed type of dual catalysis seems simple enough. The increased polymerization rates are the consequence of a facilitated ring-opening step; this effect is caused by coordination of the Lewis acid to the lactone monomer, which increases the electron deficiency on the carbonyl carbon, the attacking spot of nucleophiles. The nucleophile in the present case is the BnOH initiator or correspondingly the growing polymer chain. These species are activated by the NHO through deprotonation (or partial H-abstraction), likewise favoring ring-opening. Hence, organic Lewis base and inorganic Lewis acid support each other in a cooperative manner.

However, this crude picture does not satisfactorily explain all the peculiarities observed for this system so far; also, a closer inspection reveals the individual steps in this mechanism to be not trivial at all. For example, it is not clear how the Lewis acid will actually coordinate to the monomer (and how many lactone equivalents will do so). Three distinct coordination modes can be envisioned, namely via the carbonyl oxygen or via the endocyclic oxygen and additionally a chelating interaction by both. It is important to understand these details, as the observed polymerization preferences of some metal halides for specific lactones might be connected to the mode of activation. Literature yields only circumstantial evidence so far. YCl_3 has been shown to form *mer*-octahedral $\text{YCl}_3(\text{CL})_3$ complexes when crystallized from a solution in bulk CL, having three lactones ligated via the carbonyl oxygen (Figure 6a).⁸¹ Zhao has recently described a NHO/ $\text{Al}(\text{C}_6\text{F}_5)_3$ LP and isolated it in interaction with a lactone monomer (no initiator present, Figure 6b).³¹ Both examples suggest monodentate, carbonyl-coordinated complexes to be favored, yet it is unclear whether this situation is the same in solution and in the presence of initiator. In this regard, we were able to elucidate the interaction of alcohol and NHO. To check whether an actual anionic mechanism occurs by direct deprotonation, ^1H NMR experiments were conducted ($2/\text{BnOH} = 1:1$, $\text{THF-}d_8$). Surprisingly, no protonation of the NHO was detected. Only a relatively weak interaction was found, resulting in the doublet and triplet of $-\text{CH}_2-\text{OH}$ to appear as two singlets instead, without a change in chemical shift, after NHO had been added to BnOH (Figure S19). This situation was markedly different in the presence of metal halides ($2/\text{BnOH}/\text{M}_x = 1:1:1$, $\text{THF-}d_8$, see Figure S19 for a sample spectrum). Here, a clear protonation was found, as evident for example by the appearance of a distinctive doublet and septet from the newly generated isopropyl group. Interestingly, the position of the

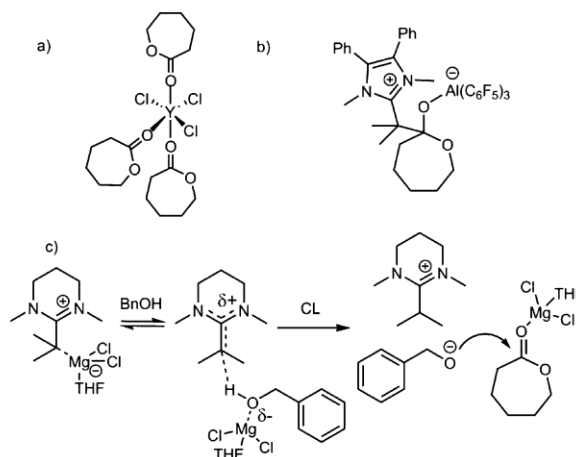


Figure 6. (a) *mer*-octahedral $\text{YCl}_3(\text{CL})_3$ complex.⁸¹ (b) NHO/ $\text{Al}(\text{C}_6\text{F}_5)_3$ in interaction with CL (isolated).³¹ (c) Proposed, simplified initiation mechanism for NHO LPs and lactones.

equilibrium between free and protonated form is considerably influenced by the chemical nature of the Lewis acid (Figure 7).

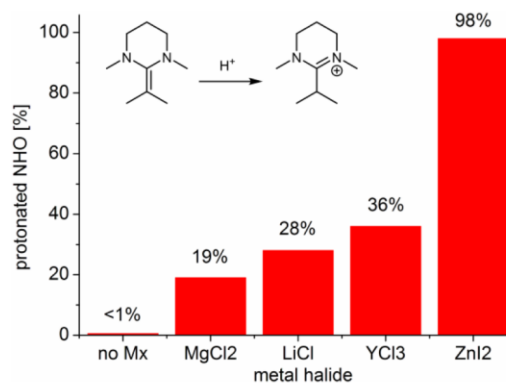


Figure 7. Percentage of protonated NHO in the presence of BnOH and different Lewis acids (all equimolar, determined by ^1H NMR analysis, $\text{THF-}d_8$, 300 K).

While in the presence of MgCl_2 most of the NHO remains nonprotonated, ZnI_2 entails an almost quantitative conversion. The improved ability of the NHO to abstract the proton from BnOH when interacting with these simple Lewis acids can be attributed to acidification of the alcohol. The electron deficiency of the metal halides stabilizes the negative (partial) charges on the alcohol oxygen, rendering the initiator more prone to give up its proton. Importantly, these findings underline that it is reasonable to assume the existence of anionic species in the polymerization setup, enabled by a cooperative interaction of NHO and Lewis acids. However, it is equally clear that this is only one layer of the cooperativity in the polymerization process as a whole: there is no obvious correlation of the ability to support the deprotonation and the polymerization activity of the individual cocatalyzing metal halides. ZnI_2 , entailing the most effective proton transfer, is only marginally active when PDL (co)polymerization is concerned, but much better suited for (co)polymerization of GBL, VL, and CL (compare Tables 1 and 5).³⁴

MgI₂ is absent from the list of investigated Lewis acids, as we were unable to prepare a fully homogeneous sample under identical conditions, which again underlines the importance of lactones for solubilizing the metal halides.

These, still limited, findings support a polymerization mechanism (Figure 6c) where NHO and metal halide exist as a Lewis pair, whereby the associated and dissociated forms are in a temperature- and monomer-dependent equilibrium. A cooperative deprotonation occurs when BnOH is encountered; the proton is transferred to the NHO, forming the positively charged counterion. The alcoholate will then attack the lactone monomer, which itself is activated by coordination to a Lewis acid, most probably via the carbonyl oxygen. The energy barrier for ring-opening is thus lowered, and the polymerization can proceed rapidly. It should be noted that control reactions using either NHO or Lewis acids alone have brought about no activity, or in the case of 3/PDL only a sluggish conversion (Table S1), strongly supporting the cooperative manner of the proposed mechanism.

The role of the Lewis acid is clearly dominant in this reaction scheme, and tellingly the order of activity of different metal halides for PDL homopolymerization is always found to be MgX₂ > YCl₃ > ZnX₂, irrespective of whether DMAP, DBU, different NHCs, or different NHOs are applied as the organic cocatalyst.²⁹ Overall control and speed of polymerization, however, also depend on the Lewis base, with NHOs performing best in this regard. This may be connected to the ability of the organic component to act as a proton reservoir and also on its size and interaction with the growing (anionic) chain end. Supposedly, the competition between the formation of an associated NHO/metal halide LP (Figure 6c) and its catalytically active, dissociated species might explain why the application of strongly polarized NHOs does not make a big difference in polymerization activity. High polarization of the NHO (as found in 3) potentially also increases the stability of the corresponding metal complexes, thus counteracting any benefits from increased charge separation by limiting the amount of free NHO in solution. Similarly, very strong Lewis acids might be hindered by the same effect: AlCl₃ has been described to be much less adept at lactone polymerization in comparable conditions.^{29,34}

The copolymer compositions and polymerization results observed in this study can be explained by interplay of the underlying thermodynamics and monomer specific activation by the catalyst pairs. As briefly mentioned in the Introduction, the macrolactone PDL lacks relevant ring tension. Its polymerization is driven by entropy, and consequently elevated polymerization temperatures have to be applied, while it is relatively rare to achieve efficient PDL conversion near room temperature.⁵⁵ Similarly, as detailed in Table 1, for NHO-based LPs the homopolymerization of PDL slows down and finally comes to a halt as the reaction temperature is lowered (entries 15–17). The practically nonexistent ring tension and elevated reaction temperatures aggravate the occurrence of transesterification and typically a polydispersity in the range of $\bar{D}_M = 1.5$ –2.5 can be observed for PPDL. Potentially, this situation could be improved when the cyclic monomer is selectively activated while the polyester chain is not; in the context of the described dual catalytic approach such a phenomenon might account for the fact that the mild activation by MgCl₂ results in molecular weight distributions on the better end of the scale ($\bar{D}_M = 1.45$ –1.60). Even with prolonged reaction times (4 h) this relative good control is retained (Table 1, entries 4–6).

Still, transesterification occurs much more readily than for medium sized lactones with the same system.³⁴ As another consequence of this side reaction, copolymerizations with other lactones typically result in randomized structures, even though more readily polymerizable monomers (CL and VL) are consumed first.^{22,57,58} This effect is also observed for NHO LPs as detailed in this study (Tables 2 and 3). Hence, the randomized copolymers of CL and PDL with different PDL content starting from the same 1:1 mixtures are the result of transesterification (causing randomization) and monomer selective activation (responsible for varying PDL content). In principle, the same is true for the more unusual observations in PDL/VL copolymerization, but in this case PDL incorporation is massively disfavored (Table 3). At 50 °C, practically pure PVL is formed in the presence of ZnI₂ or MgI₂; VL conversion is not quantitative, potentially because equilibrium conditions are reached. Even at 100 °C, MgI₂ does not entail the polymerization of relevant amounts of the macrolactone, while other Lewis acids lead to the expected random copolymer structure, as evidenced by ¹³C NMR and the observed melting points.

For GBL homopolymerization, Chen has recently determined the equilibrium temperature to be $T_{eq} = -30$ °C and $T_{eq} = -15$ °C for 8.00 and 9.45 M solutions in CD₂Cl₂, respectively.⁶⁵ Very low reaction temperatures and high monomer concentration are thus necessary for successful homopolymerization, again as a result of negligible ring strain, but in this case the reaction is enthalpy driven. For copolymerizations, this means that under common reaction conditions no long GBL-derived blocks can form, and once the comonomer is used up, the polymerization will not proceed to incorporate the remaining GBL, which sets a limit to conversion. GBL–GBL repeating units can only survive if they are “locked” in a polymer chain by other lactones; excessive transesterification will over time break up such motifs and disperse single GBL repeating units along randomized polyester chains. These characteristics are mirrored by above results but modulated to their extent by the Lewis pair employed. For all copolymerizations with other lactones (PDL, CL, VL), GBL is the minority component in the resulting material. Correspondingly, conversion cannot be quantitative and never exceeds 70% in equimolar polymerization setups. However, the extent to which GBL is consumed is determined by the Lewis acid; under identical conditions the consumption may vary by a factor of 3 (Table 4) to yield polyester where slightly more than 20% of the repeating units are made up from GBL. A relatively high GBL incorporation accompanied by a broadening of the molecular weight distribution and the absence of GBL–GBL dyad placement is indicative of the described change in microstructure due to transesterification (Table 5, entry 7).

CONCLUSIONS

It was successfully demonstrated that NHO/metal halide Lewis pair polymerization can be extended to the macrolactone PDL. The cooperative interaction renders a NHO like **2**, which is completely polymerization-inactive on its own, a powerful cocatalyst when combined with readily available, simple salts like MgCl₂, LiCl, or YCl₃. In such a constellation, PDL can be homopolymerized rapidly without excessive transesterification occurring. The high speed, which is on par with the most effective catalysts reported to date, its convenient modulation by the cocatalyzing Lewis acid, and also the good control

recommend this operationally simple polymerization technique as an alternative to more established methods. Notably, the inherently adaptive dual catalysis could also be employed to copolymerize PDL with CL, VL, and GBL. From the same equimolar mixtures, very different copolyester can be generated. Fully randomized polymer with 50% PDL content was realized by application of 2/MgI₂ and 2/YCl₃ for CL and VL, respectively. Highlighting the monomer specific activity of these LPs, an inverse setup resulted in almost pure PVL (96–98%) when 2/MgI₂ is used for PDL/VL copolymerization and in less incorporation of PDL when 2/YCl₃ was employed for PDL/CL systems. Crucially, it was even possible to copolymerize PDL and GBL, with the latter “non-(homo)-polymerizable” under the applied reaction conditions. GBL content varied by a factor of more than 3 for the LP least and most inclined to incorporate GBL in the copolymer. Molecular weights of 5–28 kg/mol ($D_M = 1.3–2.0$) were realized with GBL contents of 6–23%. Finally, it was also demonstrated that NHO-based LPs can copolymerize GBL with VL and CL. Depending on cocatalysts and comonomer, GBL contents of 5–22% were achieved with good molecular weight control (polydispersity down to <1.1) and intermediate molecular weights (2–8 kg/mol). While the polymerization mechanism is still unclear in several details, it was demonstrated that the existence of anionic species is very probable on account of cooperative deprotonation of the initiator.

Apart from the simplicity of the described polymerizations, the relevance of these findings lies in the fact that the various copolymer compositions are all based on one-pot reactions where the monomer feed was not manipulated. Instead, the copolymerization propensity was directly influenced, presumably by monomer specific activation of the lactone monomers. Our group currently aims to further extend the applicability of this concept. Further experimental and theoretical approaches shall elucidate the underlying mechanisms and move the field from an exploratory phase toward rational catalyst design.

■ ASSOCIATED CONTENT

Supporting Information

The Supporting Information is available free of charge on the ACS Publications website at DOI: 10.1021/acs.macromol.7b01678.

Experimental procedures, DSC and GPC results, NMR analysis, further tabular data (PDF)

■ AUTHOR INFORMATION

Corresponding Author

*E-mail: Stefan.naumann@ipoc.uni-stuttgart.de (S.N.).

ORCID

Stefan Naumann: 0000-0003-2014-4434

Notes

The authors declare no competing financial interest.

■ ACKNOWLEDGMENTS

S.N. gratefully acknowledges funding by the German Research Foundation (Deutsche Forschungsgemeinschaft, DFG, NA-1206/2). The Leni Schöninger Foundation is acknowledged for providing instrumentation. The authors also thank M. Sc. Jan Meisner and Johannes Karwounopoulos (University of Stuttgart) for helpful discussions.

■ REFERENCES

- (1) *Handbook of Ring-Opening Polymerization*; Raquez, J.-M., Coulembier, O., Dubois, P., Eds.; Wiley-VCH: Weinheim, 2009.
- (2) Jérôme, C.; Lecomte, P. Recent advances in the synthesis of aliphatic polyesters by ring-opening polymerization. *Adv. Drug Delivery Rev.* **2008**, *60*, 1056–1076.
- (3) Lecomte, P.; Jérôme, C. Recent Developments in Ring-Opening Polymerization of Lactones. In *Synthetic Biodegradable Polymers*; Rieger, B., Künkel, A., Coates, G. W., Reichardt, R., Dinjus, E., Zevaco, T. A., Eds.; Advances in Polymer Science; Springer: Berlin, 2012; pp 173–217.
- (4) Albertsson, A.-C.; Varma, I. K. Recent developments in ring opening polymerization of lactones for biomedical applications. *Biomacromolecules* **2003**, *4*, 1466–1486.
- (5) Woodruff, M. A.; Hutmacher, D. W. The return of a forgotten polymer—Polycaprolactone in the 21st century. *Prog. Polym. Sci.* **2010**, *35*, 1217–1256.
- (6) Ulery, B. D.; Nair, L. S.; Laurencin, C. T. Biomedical Applications of Biodegradable Polymers. *J. Polym. Sci., Part B: Polym. Phys.* **2011**, *49*, 832–864.
- (7) Seyednejad, H.; Ghassemi, A. H.; van Nostrum, C. F.; Vermonden, T.; Hennink, W. E. Functional aliphatic polyesters for biomedical and pharmaceutical applications. *J. Controlled Release* **2011**, *152*, 168–176.
- (8) Cameron, D. J. A.; Shaver, M. P. Aliphatic polyester polymer stars: synthesis, properties and applications in biomedicine and nanotechnology. *Chem. Soc. Rev.* **2011**, *40*, 1761–1776.
- (9) Arias, V.; Olsén, P.; Odelius, K.; Höglund, A.; Albertsson, A.-C. Forecasting linear aliphatic copolyester degradation through modular block design. *Polym. Degrad. Stab.* **2016**, *130*, 58–67.
- (10) *Biodegradable Polyesters*; Fakirov, S., Ed.; Wiley-VCH Verlag GmbH & Co. KGaA: Weinheim, Germany, 2015.
- (11) Hillmyer, M. A.; Tolman, W. B. Aliphatic polyester block polymers: renewable, degradable, and sustainable. *Acc. Chem. Res.* **2014**, *47*, 2390–2396.
- (12) Agarwal, S.; Mast, C.; Dehnicke, K.; Greiner, A. Rare earth metal initiated ring-opening polymerization of lactones. *Macromol. Rapid Commun.* **2000**, *21*, 195–212.
- (13) Labet, M.; Thielemans, W. Synthesis of polycaprolactone: a review. *Chem. Soc. Rev.* **2009**, *38*, 3484–3504.
- (14) Ajellal, N.; Carpentier, J.-F.; Guillaume, C.; Guillaume, S. M.; Helou, M.; Poirier, V.; Sarazin, Y.; Trifonov, A. Metal-catalyzed immortal ring-opening polymerization of lactones, lactides and cyclic carbonates. *Dalton Trans.* **2010**, *39*, 8363–8376.
- (15) Lohmeijer, B. G. G.; Pratt, R. C.; Leibfarth, F.; Logan, J. W.; Long, D. A.; Dove, A. P.; Nederberg, F.; Choi, J.; Wade, C.; Waymouth, R. M.; et al. Guanidine and Amidine Organocatalysts for Ring-Opening Polymerization of Cyclic Esters. *Macromolecules* **2006**, *39*, 8574–8583.
- (16) Kamber, N. E.; Jeong, W.; Waymouth, R. M.; Pratt, R. C.; Lohmeijer, B. G. G.; Hedrick, J. L. Organocatalytic Ring-Opening Polymerization. *Chem. Rev.* **2007**, *107*, 5813–5840.
- (17) Thomas, C.; Peruch, F.; Bibal, B. Ring-opening polymerization of lactones using supramolecular organocatalysts under simple conditions. *RSC Adv.* **2012**, *2*, 12851–12856.
- (18) Kiesewetter, M. K.; Shin, E. J.; Hedrick, J. L.; Waymouth, R. M. Organocatalysis: Opportunities and Challenges for Polymer Synthesis. *Macromolecules* **2010**, *43*, 2093–2107.
- (19) Dove, A. P. Organic Catalysis for Ring-Opening Polymerization. *ACS Macro Lett.* **2012**, *1*, 1409–1412.
- (20) Fèvre, M.; Pinaud, J.; Gnanou, Y.; Vignolle, J.; Taton, D. N-Heterocyclic carbenes (NHCs) as organocatalysts and structural components in metal-free polymer synthesis. *Chem. Soc. Rev.* **2013**, *42*, 2142–2172.
- (21) Naumann, S.; Dove, A. P. N-Heterocyclic carbenes as organocatalysts for polymerizations: trends and frontiers. *Polym. Chem.* **2015**, *6*, 3185–3200.
- (22) Bouyahyi, M.; Pepels, M. P. F.; Heise, A.; Duchateau, R. ω -Pentadecalactone Polymerization and ω -Pentadecalactone/ ϵ -Capro-

lactone Copolymerization Reactions Using Organic Catalysts. *Macromolecules* **2012**, *45*, 3356–3366.

(23) Zhang, Y.; Miyake, G. M.; John, M. G.; Falivene, L.; Caporaso, L.; Cavallo, L.; Chen, E. Y.-X. Lewis pair polymerization by classical and frustrated Lewis pairs: acid, base and monomer scope and polymerization mechanism. *Dalton Trans.* **2012**, *41*, 9119–9134.

(24) Piedra-Arroñi, E.; Amgoune, A.; Bourissou, D. Dual catalysis: new approaches for the polymerization of lactones and polar olefins. *Dalton Trans.* **2013**, *42*, 9024–9029.

(25) Piedra-Arroñi, E.; Ladavière, C.; Amgoune, A.; Bourissou, D. Ring-Opening Polymerization with $Zn(C_6F_5)_2$ -Based Lewis Pairs: Original and Efficient Approach to Cyclic Polyesters. *J. Am. Chem. Soc.* **2013**, *135*, 13306–13309.

(26) Naumann, S.; Schmidt, F. G.; Frey, W.; Buchmeiser, M. R. Protected N-heterocyclic carbenes as latent pre-catalysts for the polymerization of ϵ -caprolactone. *Polym. Chem.* **2013**, *4*, 4172–4181.

(27) Jia, Y.-B.; Wang, Y.-B.; Ren, W.-M.; Xu, T.; Wang, J.; Lu, X.-B. Mechanistic Aspects of Initiation and Deactivation in N-Heterocyclic Olefin Mediated Polymerization of Acrylates with Alane as Activator. *Macromolecules* **2014**, *47*, 1966–1972.

(28) Jia, Y.-B.; Ren, W.-M.; Liu, S.-J.; Xu, T.; Wang, Y.-B.; Lu, X.-B. Controlled Divinyl Monomer Polymerization Mediated by Lewis Pairs: A Powerful Synthetic Strategy for Functional Polymers. *ACS Macro Lett.* **2014**, *3*, 896–899.

(29) Naumann, S.; Scholten, P. B. V.; Wilson, J. A.; Dove, A. P. Dual Catalysis for Selective Ring-Opening Polymerization of Lactones: Evolution toward Simplicity. *J. Am. Chem. Soc.* **2015**, *137*, 14439–14445.

(30) Knaus, M. G. M.; Giuman, M. M.; Pothig, A.; Rieger, B. End of Frustration: Catalytic Precision Polymerization with Highly Interacting Lewis Pairs. *J. Am. Chem. Soc.* **2016**, *138*, 7776–7781.

(31) Wang, Q.; Zhao, W.; He, J.; Zhang, Y.; Chen, E. Y.-X. Living Ring-Opening Polymerization of Lactones by N-Heterocyclic Olefin/ $Al(C_6F_5)_3$ Lewis Pairs: Structures of Intermediates, Kinetics, and Mechanism. *Macromolecules* **2017**, *50*, 123–136.

(32) Zhang, X.; Jones, G. O.; Hedrick, J. L.; Waymouth, R. M. Fast and selective ring-opening polymerizations by alkoxides and thioureas. *Nat. Chem.* **2016**, *8*, 1047–1053.

(33) Fastnacht, K. V.; Spink, S. S.; Dharmaratne, N. U.; Pothupitiya, J. U.; Datta, P. P.; Kiesewetter, E. T.; Kiesewetter, M. K. Bis- and Tris-Urea H-Bond Donors for Ring-Opening Polymerization: Unprecedented Activity and Control from an Organocatalyst. *ACS Macro Lett.* **2016**, *5*, 982–986.

(34) Naumann, S.; Wang, D. Dual Catalysis Based on N-Heterocyclic Olefins for the Copolymerization of Lactones: High Performance and Tunable Selectivity. *Macromolecules* **2016**, *49*, 8869–8878.

(35) Gruseck, U.; Heuschmann, M. 2-Alkylidenimidazolidine - Synthese, Basizität, 1H- und 13C-NMR-Spektren. *Chem. Ber.* **1987**, *120*, 2053–2064.

(36) Kuhn, N.; Bohnen, H.; Kreutzberg, J.; Bläser, D.; Boese, R. 1,3,4,5-Tetramethyl-2-methyleneimidazoline-an Ylidic Olefin. *J. Chem. Soc., Chem. Commun.* **1993**, 1136–1137.

(37) Quast, H.; Ach, M.; Kindermann, M. K.; Rademacher, P.; Schindler, M. Synthese, NMR-Spektren und Photoelektronen-Spektren von cyclischen Keten-N,XI-acetalen (2-Alkyliden-N-heterocyclen). *Chem. Ber.* **1993**, *126*, 503–516.

(38) Fürstner, A.; Alcarazo, M.; Goddard, R.; Lehmann, C. W. Coordination chemistry of ene-1,1-diamines and a prototype “carbodicarbene”. *Angew. Chem., Int. Ed.* **2008**, *47*, 3210–3214.

(39) Wang, Y.-B.; Wang, Y.-M.; Zhang, W.-Z.; Lu, X.-B. Fast CO_2 sequestration, activation, and catalytic transformation using N-heterocyclic olefins. *J. Am. Chem. Soc.* **2013**, *135*, 11996–12003.

(40) Ghadwal, R. S.; Reichmann, S. O.; Engelhardt, F.; Andrada, D. M.; Frenking, G. Facile access to silyl-functionalized N-heterocyclic olefins with $HSiCl_3$. *Chem. Commun.* **2013**, *49*, 9440–9442.

(41) Kronig, S.; Jones, P. G.; Tamm, M. Preparation of 2-Alkylidene-Substituted 1,3,4,5-Tetramethylimidazolines and Their Reactivity Towards Rh (I) Complexes and $B(C_6F_5)_3$. *Eur. J. Inorg. Chem.* **2013**, *2013*, 2301–2314.

(42) Iglesias, M.; Iturmendi, A.; Sanz Miguel, P. J.; Polo, V.; Perez-Torrente, J. J.; Oro, L. A. Tuning PCP-Ir complexes: the impact of an N-heterocyclic olefin. *Chem. Commun.* **2015**, *51*, 12431–12434.

(43) Naumann, S.; Thomas, A. W.; Dove, A. P. N-Heterocyclic Olefins as Organocatalysts for Polymerization: Preparation of Well-Defined Poly(propylene oxide). *Angew. Chem., Int. Ed.* **2015**, *54*, 9550–9554.

(44) Imbrich, D. A.; Frey, W.; Naumann, S.; Buchmeiser, M. R. Application of imidazolium salts and N-heterocyclic olefins for the synthesis of anionic and neutral tungsten imido alkylidene complexes. *Chem. Commun.* **2016**, *52*, 6099–6102.

(45) Powers, K.; Hering-Junghans, C.; McDonald, R.; Ferguson, M. J.; Rivard, E. Improved synthesis of N-heterocyclic olefins and evaluation of their donor strengths. *Polyhedron* **2016**, *108*, 8–14.

(46) Crocker, R. D.; Nguyen, T. V. The Resurgence of the Highly Ylidic N-Heterocyclic Olefins as a New Class of Organocatalysts. *Chem. - Eur. J.* **2016**, *22*, 2208–2213.

(47) Blümel, M.; Noy, J.-M.; Enders, D.; Stenzel, M. H.; Nguyen, T. V. Development and Applications of Transesterification Reactions Catalyzed by N-Heterocyclic Olefins. *Org. Lett.* **2016**, *18*, 2208–2211.

(48) van der Meulen, I.; de Geus, M.; Antheunis, H.; Deumens, R.; Joosten, E. A. J.; Koning, C. E.; Heise, A. Polymers from Functional Macrolactones as Potential Biomaterials: Enzymatic Ring Opening Polymerization, Biodegradation, and Biocompatibility. *Biomacromolecules* **2008**, *9*, 3404–3410.

(49) van der Meulen, I.; Gubbels, E.; Huijser, S.; Sablong, R.; Koning, C. E.; Heise, A.; Duchateau, R. Catalytic Ring-Opening Polymerization of Renewable Macrolactones to High Molecular Weight Polyethylene-like Polymers. *Macromolecules* **2011**, *44*, 4301–4305.

(50) Nakayama, Y.; Watanabe, N.; Kusaba, K.; Sasaki, K.; Cai, Z.; Shiono, T.; Tsutsumi, C. High activity of rare earth tetrahydroborates for ring-opening polymerization of ω -pentadecalactone. *J. Appl. Polym. Sci.* **2011**, *121*, 2098–2103.

(51) Wilson, J. A.; Hopkins, S. A.; Wright, P. M.; Dove, A. P. ‘Immortal’ ring-opening polymerization of ω -pentadecalactone by $Mg(BHT)_2(THF)_2$. *Polym. Chem.* **2014**, *5*, 2691–2694.

(52) Bouyahyi, M.; Duchateau, R. Metal-Based Catalysts for Controlled Ring-Opening Polymerization of Macrolactones: High Molecular Weight and Well-Defined Copolymer Architectures. *Macromolecules* **2014**, *47*, 517–524.

(53) Jasinska-Walc, L.; Bouyahyi, M.; Rozanski, A.; Graf, R.; Hansen, M. R.; Duchateau, R. Synthetic Principles Determining Local Organization of Copolyesters Prepared from Lactones and Macrolactones. *Macromolecules* **2015**, *48*, 502–510.

(54) Myers, D.; Witt, T.; Cyriac, A.; Bown, M.; Mecking, S.; Williams, C. K. Ring opening polymerization of macrolactones: High conversions and activities using an yttrium catalyst. *Polym. Chem.* **2017**, *8*, 5780.

(55) Ladelta, V.; Bilalis, P.; Gnanou, Y.; Hadjichristidis, N. Ring-opening polymerization of ω -pentadecalactone catalyzed by phosphazene superbases. *Polym. Chem.* **2017**, *8*, 511–515.

(56) Naumann, S.; Thomas, A. W.; Dove, A. P. Highly Polarized Alkenes as Organocatalysts for the Polymerization of Lactones and Trimethylene Carbonate. *ACS Macro Lett.* **2016**, *5*, 134–138.

(57) Wilson, J. A.; Hopkins, S. A.; Wright, P. M.; Dove, A. P. Synthesis of ω -Pentadecalactone Copolymers with Independently Tunable Thermal and Degradation Behavior. *Macromolecules* **2015**, *48*, 950–958.

(58) Ceccorulli, G.; Scandola, M.; Kumar, A.; Kalra, B.; Gross, R. A. Cocrystallization of random copolymers of ω -pentadecalactone and ϵ -caprolactone synthesized by lipase catalysis. *Biomacromolecules* **2005**, *6*, 902–907.

(59) Jasinska-Walc, L.; Hansen, M. R.; Dudenko, D.; Rozanski, A.; Bouyahyi, M.; Wagner, M.; Graf, R.; Duchateau, R. Topological behavior mimicking ethylene-hexene copolymers using branched lactones and macrolactones. *Polym. Chem.* **2014**, *5*, 3306–3310.

(60) Jasinska-Walc, L.; Bouyahyi, M.; Rozanski, A.; Graf, R.; Hansen, M. R.; Duchateau, R. Synthetic Principles Determining Local

Organization of Copolyesters Prepared from Lactones and Macrolactones. *Macromolecules* **2015**, *48*, 502–510.

(61) Wilson, J. A.; Hopkins, S. A.; Wright, P. M.; Dove, A. P. Synthesis and Postpolymerization Modification of One-Pot ω -Pentadecalactone Block-like Copolymers. *Biomacromolecules* **2015**, *16*, 3191–3200.

(62) Todd, R.; Tempelaar, S.; Lo Re, G.; Spinella, S.; McCallum, S. A.; Gross, R. A.; Raquez, J.-M.; Dubois, P. Poly(ω -pentadecalactone)-*b*-poly(l-lactide) Block Copolymers via Organic-Catalyzed Ring Opening Polymerization and Potential Applications. *ACS Macro Lett.* **2015**, *4*, 408–411.

(63) Pepels, M. P. F.; Hofman, W. P.; Kleijnen, R.; Spoelstra, A. B.; Koning, C. E.; Goossens, H.; Duchateau, R. Block Copolymers of “PE-Like” Poly(pentadecalactone) and Poly(l-lactide): Synthesis, Properties, and Compatibilization of Polyethylene/Poly(l-lactide) Blends. *Macromolecules* **2015**, *48*, 6909–6921.

(64) Korte, F.; Glet, W. Hochdruckreaktionen. II. Die Polymerisation von γ -Butyrolacton und δ -Valerolactam bei hohen Drücken. *J. Polym. Sci., Part B: Polym. Lett.* **1966**, *4*, 685–689.

(65) Hong, M.; Chen, E. Y.-X. Completely recyclable biopolymers with linear and cyclic topologies via ring-opening polymerization of γ -butyrolactone. *Nat. Chem.* **2015**, *8*, 42–49.

(66) Hong, M.; Chen, E. Y.-X. Towards Truly Sustainable Polymers: A Metal-Free Recyclable Polyester from Biorenewable Non-Strained γ -Butyrolactone. *Angew. Chem., Int. Ed.* **2016**, *55*, 4188–4193.

(67) Tada, K.; Numata, Y.; Saegusa, T.; Furukawa, J. Copolymerization of γ -butyrolactone and β -propiolactone. *Makromol. Chem.* **1964**, *77*, 220–228.

(68) Kricheldorf, H. R.; Mang, T.; Jonté, M. Copolymerization of glycolide with beta-propiolactone, γ -butyrolactone or δ -valerolactone. *Makromol. Chem.* **1985**, *186*, 955–976.

(69) Duda, A.; Biela, T.; Libiszowski, J.; Penczek, S.; Dubois, P.; Mecerreyes, D.; Jérôme, R. Block and random copolymers of ϵ -caprolactone. *Polym. Degrad. Stab.* **1998**, *59*, 215–222.

(70) Nakayama, A.; Kawasaki, N.; Aiba, S.; Maeda, Y.; Arvanitoyannis, I.; Yamamoto, N. Synthesis and biodegradability of novel copolyesters containing γ -butyrolactone units. *Polymer* **1998**, *39*, 1213–1222.

(71) Nishiura, M.; Hou, Z.; Koizumi, T.-A.; Imamoto, T.; Wakatsuki, Y. Ring-Opening Polymerization and Copolymerization of Lactones by Samarium(II) Aryloxide Complexes. *Macromolecules* **1999**, *32*, 8245–8251.

(72) Duda, A.; Libiszowski, J.; Mosnáček, J.; Penczek, S. Copolymerization of Cyclic Esters at the Living Polymer-Monomer Equilibrium. *Macromol. Symp.* **2005**, *226*, 109–120.

(73) Du, G.; Wei, Y.; Zhang, W.; Dong, Y.; Lin, Z.; He, H.; Zhang, S.; Li, X. Bis(imino)diphenylamido rare-earth metal dialkyl complexes: synthesis, structure, and catalytic activity in living ring-opening ϵ -caprolactone polymerization and copolymerization with γ -butyrolactone. *Dalton Trans.* **2013**, *42*, 1278–1286.

(74) Lee, C. W.; Urakawa, R.; Kimura, Y. Copolymerization of γ -butyrolactone and β -butyrolactone. *Macromol. Chem. Phys.* **1997**, *198*, 1109–1120.

(75) Bhaw-Luximon, A.; Jhurry, D.; Motala-Timol, S.; Lochee, Y. Polymerization of ϵ -Caprolactone and its Copolymerization with γ -Butyrolactone using Metal Complexes. *Macromol. Symp.* **2005**, *231*, 60–68.

(76) Ye, G.; Chatterjee, S.; Li, M.; Zhou, A.; Song, Y.; Barker, B. L.; Chen, C.; Beard, D. J.; Henry, W. P.; Pittman, C. U. Push–pull alkenes from cyclic ketene- N,N' -acetals: A wide span of double bond lengths and twist angles. *Tetrahedron* **2010**, *66*, 2919–2927.

(77) Naumann, S.; Mundsinger, K.; Cavallo, L.; Falivene, L. N-Heterocyclic olefins as initiators for the polymerization of (meth)acrylic monomers: A combined experimental and theoretical approach. *Polym. Chem.* **2017**, *8*, 5803–5812.

(78) Saptal, V. B.; Bhanage, B. M. N-Heterocyclic Olefins as Robust Organocatalyst for the Chemical Conversion of Carbon Dioxide to Value-Added Chemicals. *ChemSusChem* **2016**, *9*, 1980–1985.

(79) Finger, L. H.; Guschlbauer, J.; Harms, K.; Sundermeyer, J. N-Heterocyclic Olefin-Carbon Dioxide and -Sulfur Dioxide Adducts: Structures and Interesting Reactivity Patterns. *Chem. - Eur. J.* **2016**, *22*, 16292–16303.

(80) de Lima Batista, A. P.; de Oliveira-Filho, A. G. S.; Galembeck, S. E. Computationally Designed 1,2,4-Triazolylidene-Derived N-Heterocyclic Olefins for CO₂ Capture, Activation, and Storage. *ACS Omega* **2017**, *2*, 299–307.

(81) Evans, W. J.; Shreeve, J. L.; Doedens, R. J. Isolation and Crystal Structure of a Six Coordinate Yttrium Trichloride Complex of ϵ -Caprolactone, YCl₃(C₆H₁₀O₂)₃. *Inorg. Chem.* **1993**, *32*, 245–246.

Supporting Information

Experimental

Materials and Synthesis

ϵ -Caprolactone (CL), δ -Valerolactone (VL) and γ -Butyrolactone (GBL) were stirred over CaH_2 overnight, distilled under nitrogen, degassed twice and subsequently stored under inert conditions (glove box, LabMaster, *MBraun*, Germany). ω -Pentadecalactone was dissolved in toluene and stirred over molecular sieves (3 Å) overnight. After exchanging the molecular sieves and additional stirring overnight, toluene was removed under reduced pressure. THF and toluene used in polymerizations were taken from a solvent purification system (*MBraun*, Germany) and stored inside the glove box over molecular sieves (3 Å). LiCl (*Sigma Aldrich*, powder, $\geq 99.99\%$ trace metals basis), MgCl_2 (*Alfa Aesar*, "ultra dry", 99.9%), MgI_2 (*ABCR*, "ultra dry", 99.996%, beads, ampouled under argon), YCl_3 (*Alfa Aesar*, "ultra dry", 99.99%, ampouled under argon) and ZnI_2 (*Acros*, "extra pure", 99.999%) were used as received and stored inside the glove box under exclusion of light.

For characterization of NHOs **1** – **3**, see published literature.^{2c, 10, 133} The thus received NHOs were stored inside the glove box under nitrogen at $-36\text{ }^\circ\text{C}$.

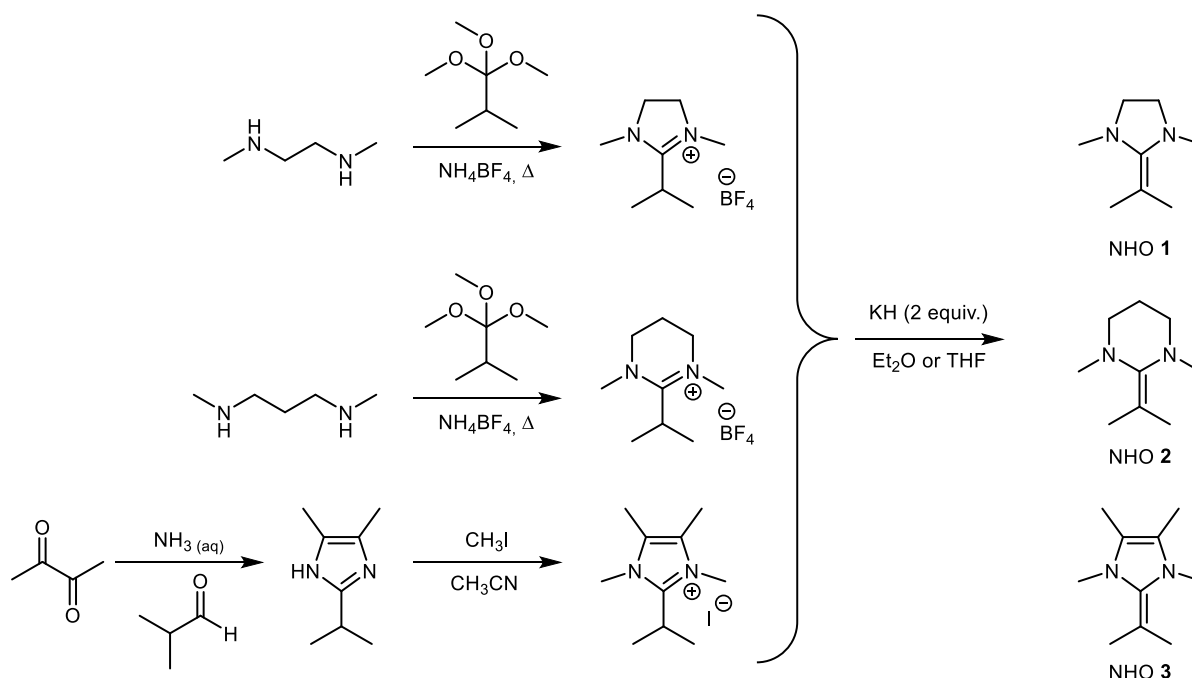


Figure S1. General procedure for the preparation of NHOs **1** – **3** used in this work.

General Polymerization Procedures

Prior to setting up the individual polymerization reactions, a 1.0 M stock solution of the corresponding monomer (ω -Pentadecalactone) in the respective solvent (THF or toluene) was prepared. Reactions at room temperature were conducted inside the glove box, whereas reactions at elevated temperatures were performed under inert atmosphere (N_2) using standard Schlenk techniques. The polymerizations were stopped by precipitation from high-boiling petroleum ether, affording a colorless precipitate, except for reactions where Lewis Acids containing iodide (MgI_2 , ZnI_2) were employed. In these cases, the precipitate exhibited off-white to yellow discoloration. Proton NMR spectroscopy was used to determine the conversion, by monitoring the $-CH_2-O-$ signal of the applied monomers (PDL: $\delta = 4.13$ ppm, CL: $\delta = 4.22$ ppm, VL: $\delta = 4.34$ ppm, GBL: $\delta = 4.31$ ppm) and resulting polymers (PPDL: $\delta = 4.08$ ppm, PGBL: $\delta = 4.07$ ppm). Heat-dried glass pipettes ($110\text{ }^\circ\text{C}$, overnight) were used to draw aliquots from reactions outside the box, while applying N_2 - flow. For determination of M_n via NMR end group analysis, the CH_2 -unit of the initiator (BnOH) was used ($\delta = 5.05$ ppm, $CDCl_3$).

Homopolymerization of PDL

After providing the respective Lewis Acid (0.125 mmol) inside a suited reaction vessel, 2.5 mL of the stock solution was added with an Eppendorf syringe and stirred vigorously to afford a clear solution. Subsequently, the initiator BnOH (0.05 mmol) and the corresponding *N*-Heterocyclic Olefin (0.025 mmol) were added to result in a total molar ratio of $NHO/BnOH/M_x/PDL = 1:2:5:100$ in the reaction solution.

General Procedure for the Copolymerization Reactions

Copolymerization reactions were assembled analogously to the procedure mentioned above, to give a resulting molar ratio of $NHO/BnOH/LA/Co(1)/Co(2)$ of $1:2:5:100:100$ and an initial monomer concentration (total of both lactones) of 2 mol/L. Prior to setting up the reaction, the accuracy of the stock solution was controlled using proton NMR spectroscopy. Analyzing the above mentioned triplets of both respective comonomers and resulting copolymers (PPDL-PCL: $\delta = 3.97 - 4.11$ ppm, PPDL-PVL: $\delta = 3.95 - 4.05$ ppm, PGBL-PCL: $\delta = 4.00 - 4.13$ ppm, PGBL-PVL: $\delta = 3.99 - 4.10$ ppm), the conversion was followed by 1H NMR spectroscopy. Isolation of the copolymers was realized by precipitation from high-boiling petroleum ether to yield colorless to yellowish (MgI_2 and ZnI_2) solids for

copolymers incorporating PPDL, or colorless, oily liquids when the copolymers contained GBL-derived repeating units. The molecular weight of the isolated and dried copolymers was investigated using GPC (CHCl₃).

Characterization and Analysis

¹H/¹³C NMR spectra were recorded on a *Bruker* Avance III 400 spectrometer, with the chemical shifts being reported relative to reference peaks of the applied deuterated solvents (CDCl₃: $\delta = 7.26/77.16$ ppm for proton and carbon spectra, respectively). GPC (CHCl₃, 40 °C) was used to determine the molecular weight of synthesized (co)polymers, calibrated with a polystyrene standard. A chromatographic assembly comprising a *PSS*SDV 5 μm 8*50mm guard column, three *PSS*SDV 100 000 Å 5 μm 8*50mm columns and an *Agilent* 1200 Series G1362A detector (RI) was used. The concentration of the prepared samples amounted to 2.5 mg/mL, and a flow-rate of 1 mL/min was applied during the analyses. For Differential Scanning Calorimetry (DSC), a Perkin Elmer DSC 4000 was used (scanning rate 5 K/min, 20 mL/min nitrogen flow, temperature range 0°C to 100°C and 30°C to 130°C, respectively). Thermograms were analyzed using the second heating/cooling cycle.

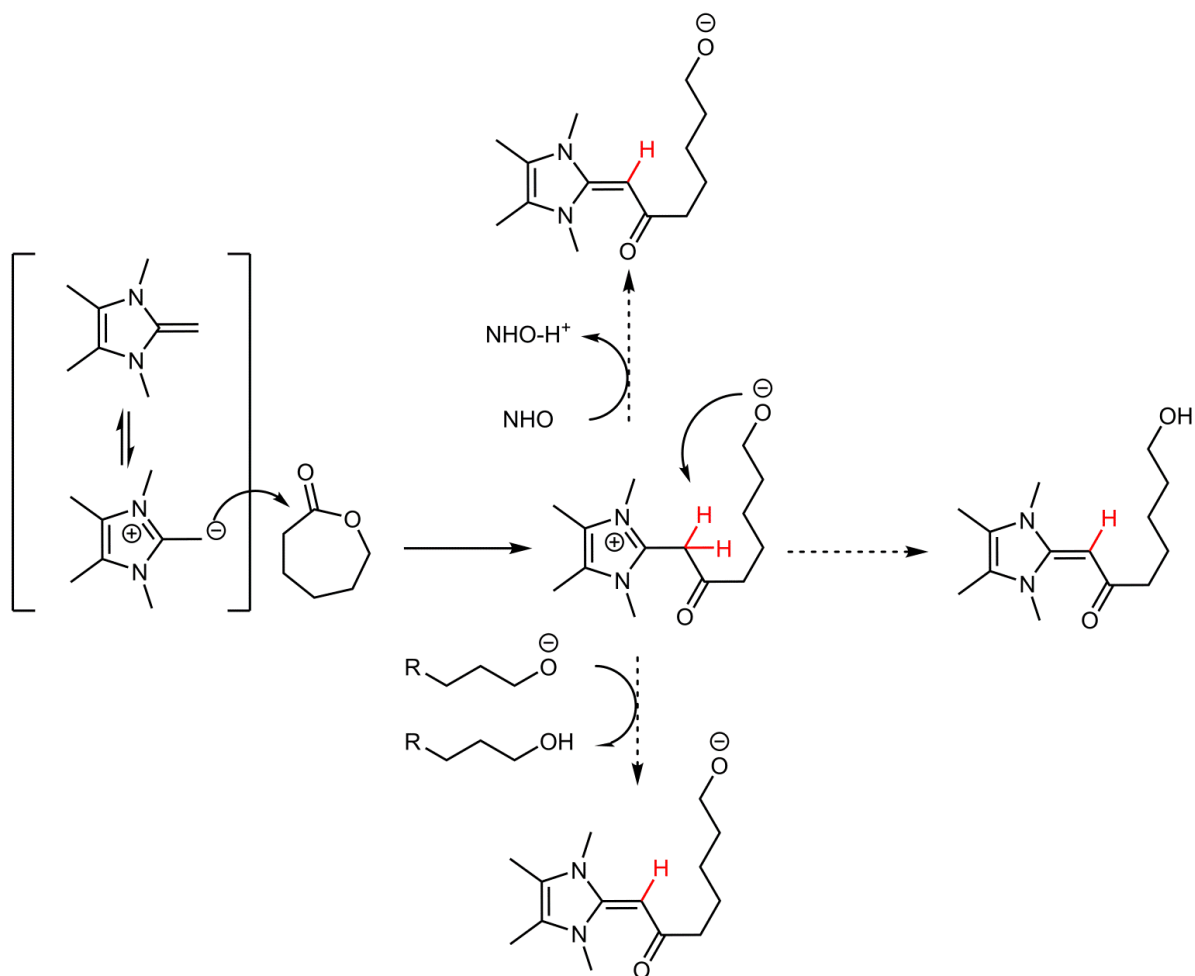


Figure S2. Schematic representation of enamine formation (= deoxy Breslow intermediate) in lactone polymerization using $=CH_2$ -bearing NHOs. These compounds can directly ring-open the monomer, forming a zwitterionic intermediate. This structure displays acidified protons (red). Supposedly, a proton transfer can occur with several basic species present in the polymerization setup, including deprotonation by growing anionic chain ends (intra- and intermolecular) or by free NHOs. In either case, one equivalent of catalyst is deactivated. This side reaction cannot occur with substituted NHOs ($=CR_2$).

Control Reactions (no dual catalysis)

Table S1. Control reactions for PDL polymerization in the absence of Lewis acid.

NHO	Lewis Acid (MX _n)	NHO/BnOH/MX _n /PDL	Time [min]	Conversion ^a [%]
1	-	1:2:0:100	240	0
1	-	1:0:0:100	240	0
2	-	1:2:0:100	240	0
2	-	1:0:0:100	240	0
3	-	1:2:0:100	240	40 ^b
3	-	1:0:0:100	240	0

Polymerization conditions: 110 °C in toluene, [M]₀ = 1.0 M. ^aMonomer conversion determined via ¹H-NMR spectroscopy. ^bmolecular weight of the polymer determined via GPC (CHCl₃) to be 15000 g/mol, with $\bar{M}_w = 1.52$.

Homopolymerization of PDL

Table S2. Homopolymerization of PDL using NHO/metal halide LPs (THF).

NHO	Lewis Acid	Time [min]	Conversion ^a [%]	M_n^b [g·mol ⁻¹]	\bar{M}_w^b
2	MgI ₂	60	89	34200	1.35
		120	94	31000	1.61
		240	96	24000	2.0
2	ZnI ₂	60	10	1800	1.52
		120	17	2200	1.95
		240	28	8200	1.43
2	YCl ₃	60	13	2500	1.26
		120	19	4900	1.23
		240	33	8700	2.2

Polymerization conditions: 100 °C in THF, [M]₀ = 1.0 M. ^aMonomer conversion determined via ¹H-NMR spectroscopy. ^bmolecular weight determined via GPC (CHCl₃).

Table S3. Homopolymerization of PDL using NHO/metal halide LPs (toluene).

NHO	Lewis Acid	Time [min]	Conversion ^a [%]	M_n^b [g·mol ⁻¹]	\bar{D}_M^b	
1	LiCl	240	6	-	-	
		15	26	7400	1.45	
	MgCl ₂	60	84	26200	1.58	
		120	94	25200	1.76	
		240	94	30000	1.49	
		15	77	19200	1.62	
	MgI ₂	60	95	22900	1.64	
		120	96	20700	1.64	
		240	96	17100	1.73	
		15	2	-	-	
	ZnI ₂	60	13	2300	1.27	
		120	20	4000	1.56	
		240	35	4500	2.4	
		15	12	2900	1.36	
	YCl ₃	60	49	13300	1.51	
		120	72	18800	1.61	
		240	86	20500	2.2	
		240	2	-	-	
	2	MgCl ₂	15	37	6600	1.49
			60	86	12400	2.0
120			92	13800	2.0	
240			95	14200	2.1	
MgI ₂		15	80	11600	1.73	
		60	92	10700	2.0	
		120	93	12600	1.60	
		240	97	9600	1.91	
ZnI ₂		120	15	3600	1.05	
		240	19	4600	1.26	
		15	14	3000	(1.22)	

2	YCl ₃	60	47	6700	(1.66)
		120	68	10000	1.69
		240	85	12200	1.78
3	LiCl	15	35	10500	1.51
		60	72	20600	1.51
		120	83	24300	1.54
		240	86	26600	1.52
	MgCl ₂	15	14	5600	1.46
		60	42	14500	1.57
		120	60	22100	1.48
		240	75	26500	1.49
	MgI ₂	15	57	17000	1.47
		60	87	21500	1.60
		120	94	22100	1.65
		240	95	20900	1.58
ZnI ₂	240	14	3700	1.61	
	60	32	7900	1.68	
	120	55	11700	1.95	
	240	74	18200	1.61	

Polymerization conditions: 110 °C in toluene, [M]₀ = 1.0 M. ^aMonomer conversion determined via ¹H-NMR spectroscopy. ^bmolecular weight determined via GPC (CHCl₃).

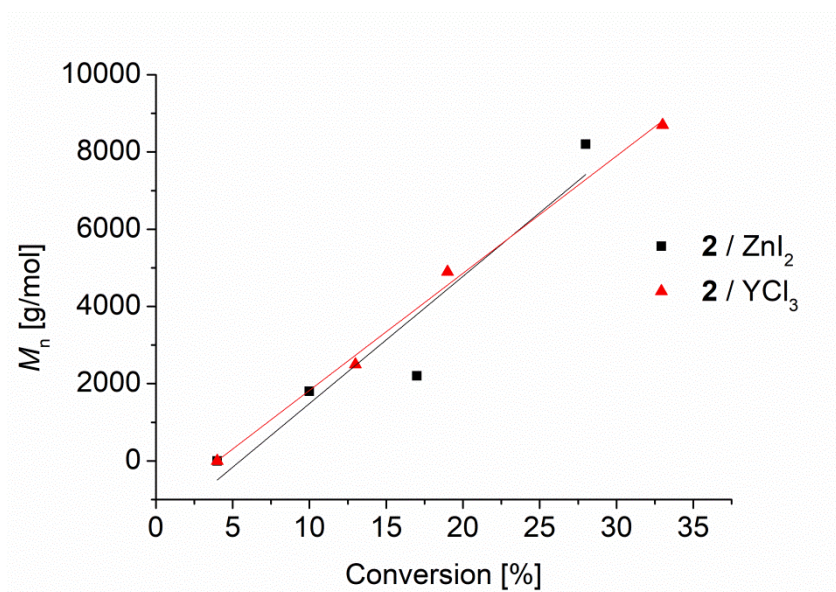
Correlation of M_n and conversion

Figure S3. Correlation of molecular weight (determined by GPC ($CHCl_3$)) vs. conversion for PDL homopolymerization using **2** with ZnI_2 and YCl_3 . Conditions: **2**/ $BnOH/MX_n/PDL = 1:2:5:100$, $[M]_0 = 1.0$ mol/L, toluene, $T = 110$ °C.

Correlation of M_n (GPC) and M_n (NMR) in PDL homopolymerizationTable S4. Comparison of molecular weights determined via GPC (CHCl₃, PS, data from Table S2) and end group analysis (¹H NMR spectroscopy).

NHO	MX _n	time [min]	Conversion ^{a)} [%]	$M_{n,GPC}^{b)}$ [g/mol]	$M_{n,NMR}^{c)}$ [g/mol]
1	LiCl	240	6	2900	1575
		15	26	7400	6300
1	MgCl ₂	60	84	26200	21150
		120	94	25200	24525
		240	94	30000	24975
		15	77	19200	18675
1	MgI ₂	60	95	22900	21150
		120	96	20700	24300
		240	96	17100	31725
		60	13	2300	2700
1	ZnI ₂	120	20	4000	4950
		15	12	2900	3150
1	YCl ₃	60	49	13300	12150
		120	72	18800	17775
		240	86	20500	23175
		15	37	6600	7650
2	MgCl ₂	60	86	12400	17550
		120	92	13800	17550
		60	92	10700	9900
2	ZnI ₂	60	5	2200	1575
		120	15	3600	2250
		240	22	4600	5400
2	YCl ₃	15	14	3000	3600
		60	47	6700	10350
3	LiCl	15	35	10500	9900
		60	72	20600	19800
		120	83	24300	21600
		240	86	26600	24300

3	MgCl ₂	15	14	5600	4050
		60	42	14500	10125
3	MgI ₂	15	57	17000	13725
		60	87	21500	23175
		120	94	22100	30375
		240	95	20900	25425
3	ZnI ₂	240	14	3700	4050
		60	32	7900	8550
3	YCl ₃	120	55	11700	13275
		240	74	18200	18675

^{a)} conversion determined via ¹H NMR analysis (CDCl₃); ^{b)} molecular weight determined via GPC (CHCl₃, PS); ^{c)} molecular weight determined via ¹H NMR endgroup analysis (multiplied by a correctional factor of 2.25).

Copolymerization reactions

Copolymerization of PDL/VL

Table S5. Copolymerization of PDL/VL using various NHO/Lewis Acid combinations.^a

no.	NHO	Lewis Acid	time [min]	conv. ^b [%]	M_n^c [g·mol ⁻¹]	\bar{D}_M^c
1	2	LiCl	240	41	3800	1.99
2	2	MgI ₂	240	38	6100	1.79
3	2	ZnI ₂	240	36	10000	1.35
4	2	YCl ₃	240	78	15900	1.87

^aConditions: molar ratio of NHO/BnOH/M_x/PDL/VL = 1:2:5:100:100, [M]_{0,total} = 2.0 M in toluene, 110 °C. ^bMonomer conversion determined via NMR spectroscopy. ^cDetermined via GPC analysis (CHCl₃).

Copolymerization of PDL/GBL

Table S6. Copolymerization of PDL with GBL using **2** and various Lewis Acids.^a

no.	Lewis Acid	time [min]	conv. ^b [%]	M_n^c [g·mol ⁻¹]	D_M^c
1	LiCl	240	18	6900	1.43
		20 h	19	7600	1.43
		24 h	19	7900	1.45
2	MgCl ₂	240	10	2700	1.12
		24 h	11	4100	1.28
		27 h	21	5000	1.31
3	ZnI ₂	240	11	4800	1.27
		20 h	25	13900	1.52
		24 h	27	14500	1.68
		48 h	35	14600	1.80
4	YCl ₃	15	5	-	-
		60	10	2000	1.45
		120	11	3600	1.55
		240	17	7100	1.59
		86 h	58	20900	1.79

^aConditions: molar ratio of NHO/BnOH/M_x/PDL/VL = 1:2:5:100:100, [M]_{0,total} = 2.0 M in toluene, 110 °C. ^bMonomer conversion determined *via* NMR spectroscopy. ^cDetermined *via* GPC analysis (CHCl₃).

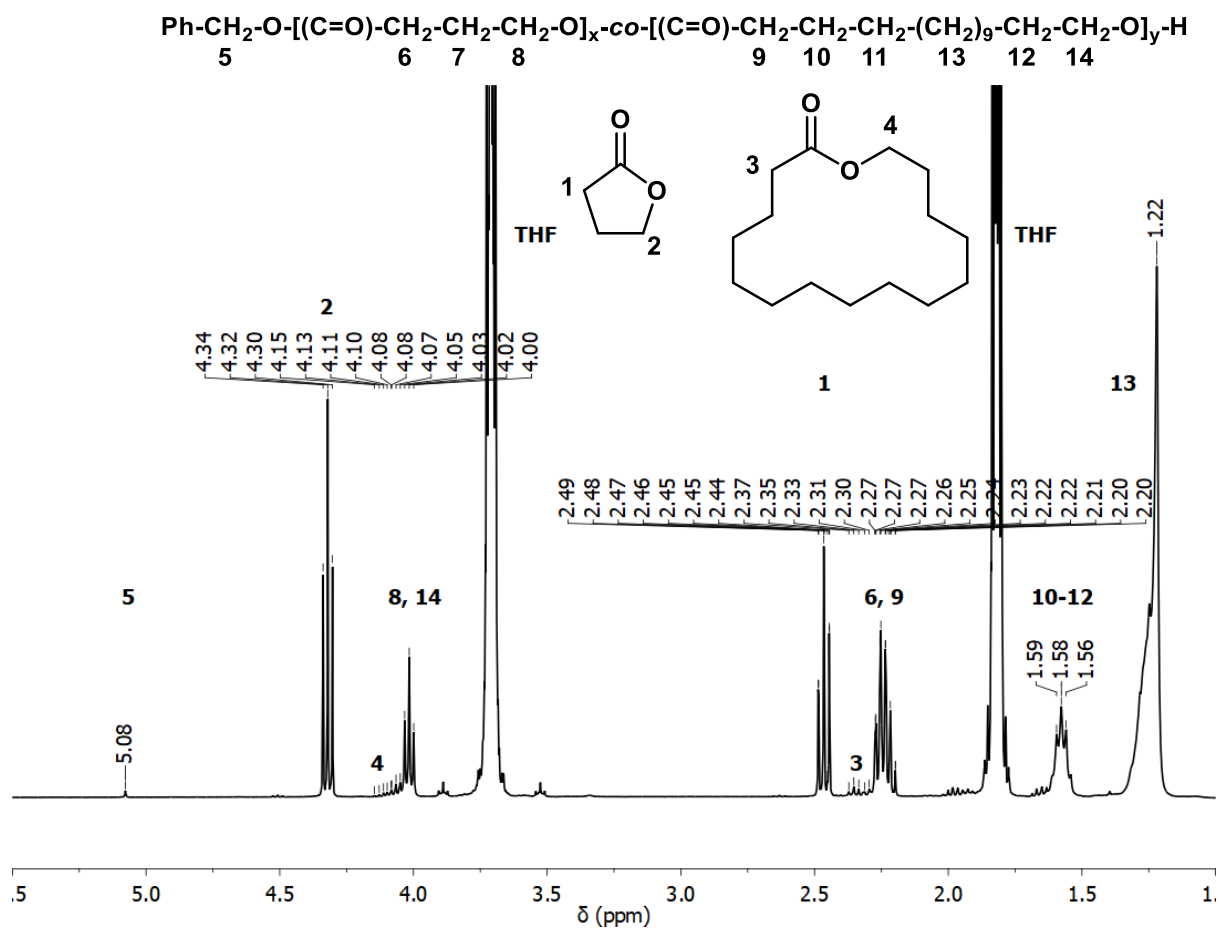


Figure S5. $^1\text{H-NMR}$ spectrum (CDCl_3 , 400 MHz) of an aliquot drawn from a copolymerization using $\mathbf{2}/\text{YCl}_3$. Conditions: $\mathbf{2}/\text{BnOH}/\text{YCl}_3/\text{PDL}/\text{GBL} = 1:2:5:100:100$, toluene, $[\text{M}]_{\text{o, total}} = 2.0 \text{ mol/L}$, 58 % conversion, after 8 h at 50 °C and 16h at 110 °C. In order to fully preclude evaporation of GBL, the sample was not dried *in vacuo* prior to $^1\text{H NMR}$ analysis. $^1\text{H-NMR}$ (400 MHz, CDCl_3) $\delta = 5.08$ (Ph- $\text{CH}_2\text{-O-}$), 4.32 (t, $J = 7.1 \text{ Hz}$, GBL- $\text{CH}_2\text{-O-(C=O)-}$), 4.15 – 4.00 (m, Poly- $\text{CH}_2\text{-O-}$), 2.47 (t, $J = 8.2 \text{ Hz}$, GBL- $\text{CH}_2\text{-(C=O)-}$), 2.38 – 2.16 (m, Poly- $\text{CH}_2\text{-(C=O)-}$), 1.59 – 1.56 (m), 1.22 (m).ppm.

Copolymerization of GBL with CL and VL

Table S7. Full data set of GBL copolymerization with CL and VL, using **2** in combination with various Lewis acids.

no.	Comonomer (Co)	Lewis Acid	time [min]	conv. ^b [%]	M_n^c [g·mol ⁻¹]	\mathcal{D}_M^c	Dyad sequence distribution [%]			
							Co-GBL	Co-Co	GBL-Co	GBL-GBL
1	CL	LiCl	120	52	6900	1.49	11	74	11	4
2	CL	MgCl ₂	120	36	4100	1.09	16	68	16	-
3	CL	MgI ₂	120	42	5900	1.12	11	78	11	-
4	CL	ZnI ₂	120	55	8000	1.13	10	80	10	-
5	CL	YCl ₃	120	61	4600	1.18	15	70	15	-
6	VL	LiCl	120	24	2200	2.2	9	82	9	-
7	VL	MgCl ₂	120	16	2700	1.13	8	84	8	-
8	VL	MgI ₂	120	37	5300	1.14	6	88	6	-
9	VL	ZnI ₂	120	9	4900	1.22	4	91	4	1
10	VL	YCl ₃	120	37	3900	1.24	12	76	12	-
11 ^d	CL	LiCl	24 h	66	6600	2.4	22	56	22	-
12 ^d	CL	MgCl ₂	24 h	33	600	1.34	-	-	-	-
13 ^d	CL	ZnI ₂	24 h	39	4800	1.06	10	73	10	7
14 ^d	CL	YCl ₃	24 h	57	1200	2.0	15	70	15	-
15 ^d	CL	-	24 h	3	-	-	-	-	-	-
16 ^d	VL	LiCl	24 h	46	5400	1.45	9	82	9	-
17 ^d	VL	MgCl ₂	24 h	24	2000	1.11	8	84	8	-
18 ^d	VL	ZnI ₂	24 h	49	5200	1.09	5	90	5	-
19 ^d	VL	YCl ₃	24 h	42	800	1.68	-	-	-	-
20 ^d	VL	-	24 h	6	-	-	-	-	-	-

^aConditions: molar ratio of NHO/BnOH/M_x/GBL/Co = 1:2:5:100:100 [M]_{o,total} = 2.0 M in THF, r.t. ^bMonomer conversion determined via NMR spectroscopy. ^cDetermined via GPC analysis (CHCl₃). ^dT = -36°C.

Representative GPC traces resulting from GBL-CL/VL copolymers

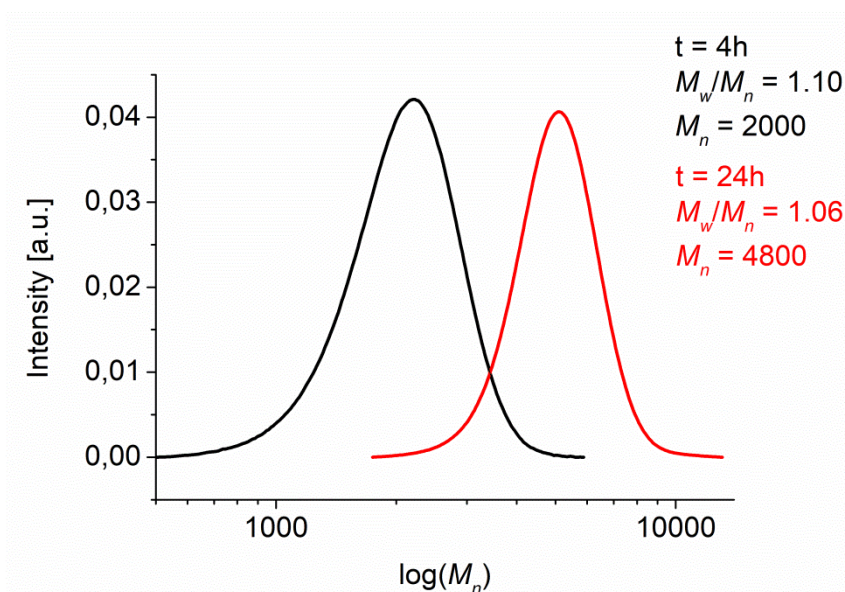


Figure S6. GPC trace received from a GBL/CL copolymer, synthesized *via* application of **2**/ZnI₂ after 4 h and 24 h. NHO/BnOH/MX_n/GBL/CL = 1:2:5:100:100, [M]_{0,total} = 2.0 mol/L, THF, T = -36 °C.

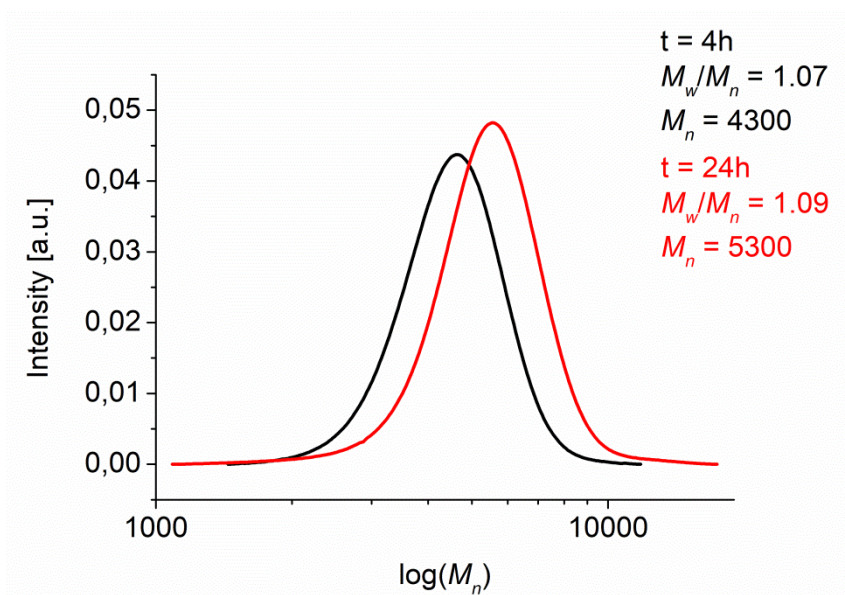


Figure S7. GPC trace received from a GBL/VL copolymer, synthesized *via* application of **2**/ZnI₂ after 4 h and 24 h. NHO/BnOH/MX_n/GBL/VL = 1:2:5:100:100, [M]_{0,total} = 2.0 mol/L, THF, T = -36 °C.

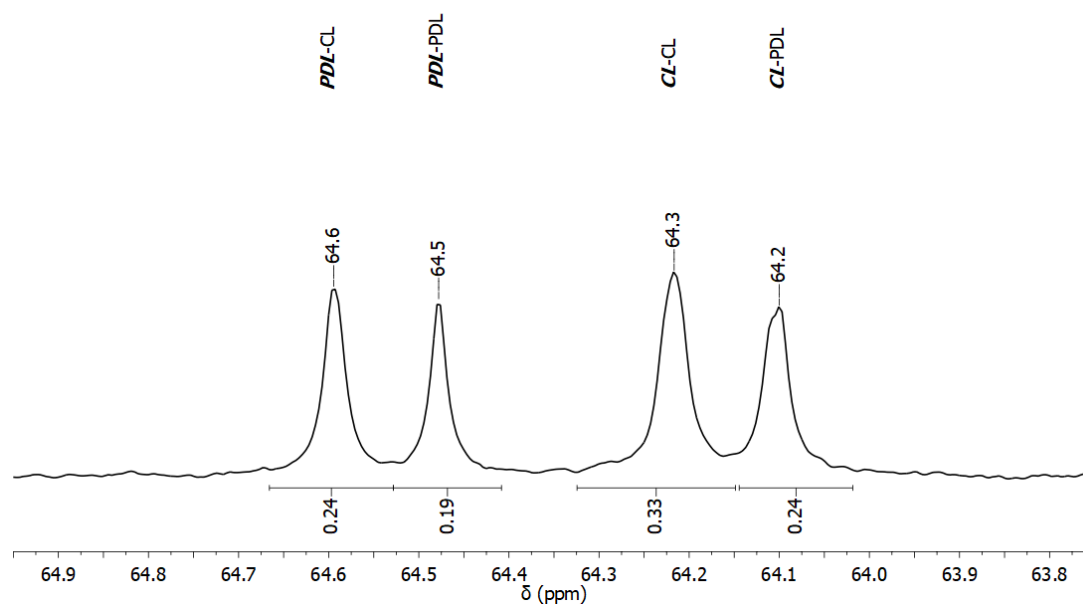
^{13}C NMR analysis

Figure S8. ^{13}C NMR spectroscopy (CDCl_3 , 300 K, $\text{O}-\underline{\text{C}}\text{H}_2$ region) with dyad sequence analysis of a PDL/CL copolymer resulting from application **2**/LiCl after 2 h at 100 °C.

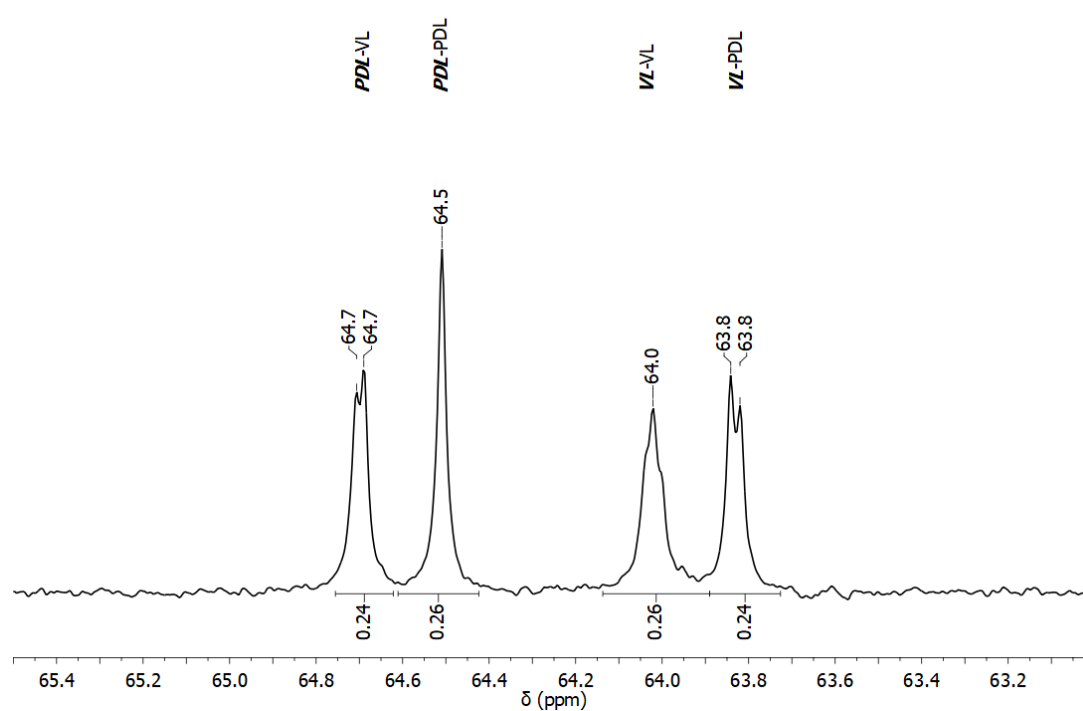


Figure S9. ^{13}C NMR spectroscopy (CDCl_3 , 300 K, $\text{O}-\underline{\text{C}}\text{H}_2$ region) with dyad sequence analysis of a PDL/VL copolymer resulting from application **2**/ YCl_3 after 24 h at 150 °C.

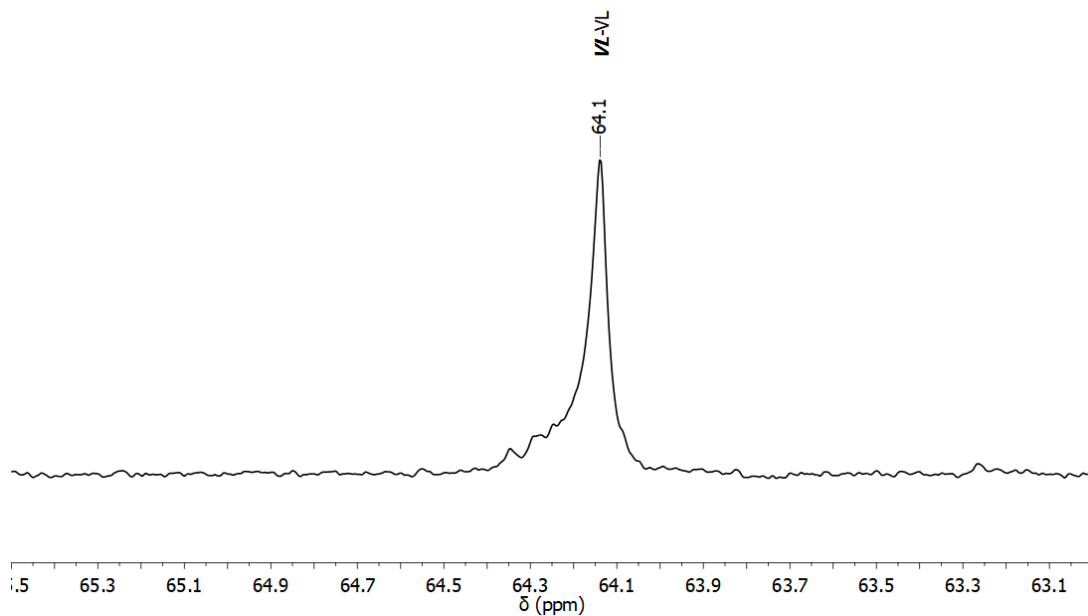


Figure S10. ^{13}C NMR spectroscopy (CDCl_3 , 300 K, $\text{O}-\underline{\text{C}}\text{H}_2$ region) with dyad sequence analysis of a PDL/VL copolymer resulting from application $\mathbf{2}/\text{ZnI}_2$ after 8 h at 50 °C.

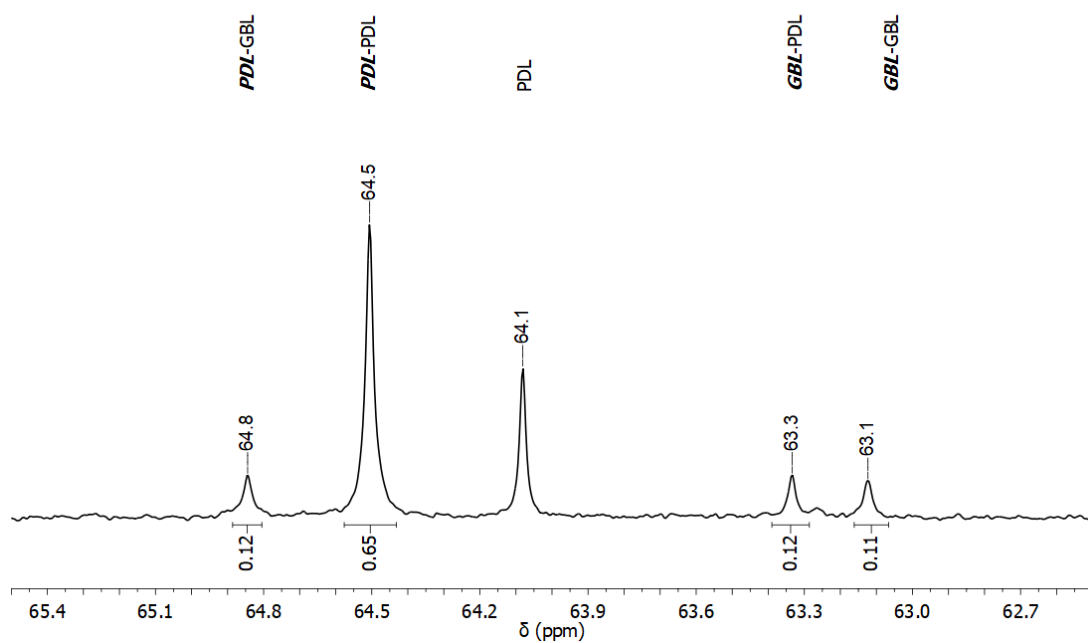


Figure S11. ^{13}C NMR spectroscopy (CDCl_3 , 300 K, $\text{O}-\underline{\text{C}}\text{H}_2$ region) with dyad sequence analysis of a PDL/GBL copolymer resulting from application $\mathbf{2}/\text{YCl}_3$ after 24 h at 100 °C.

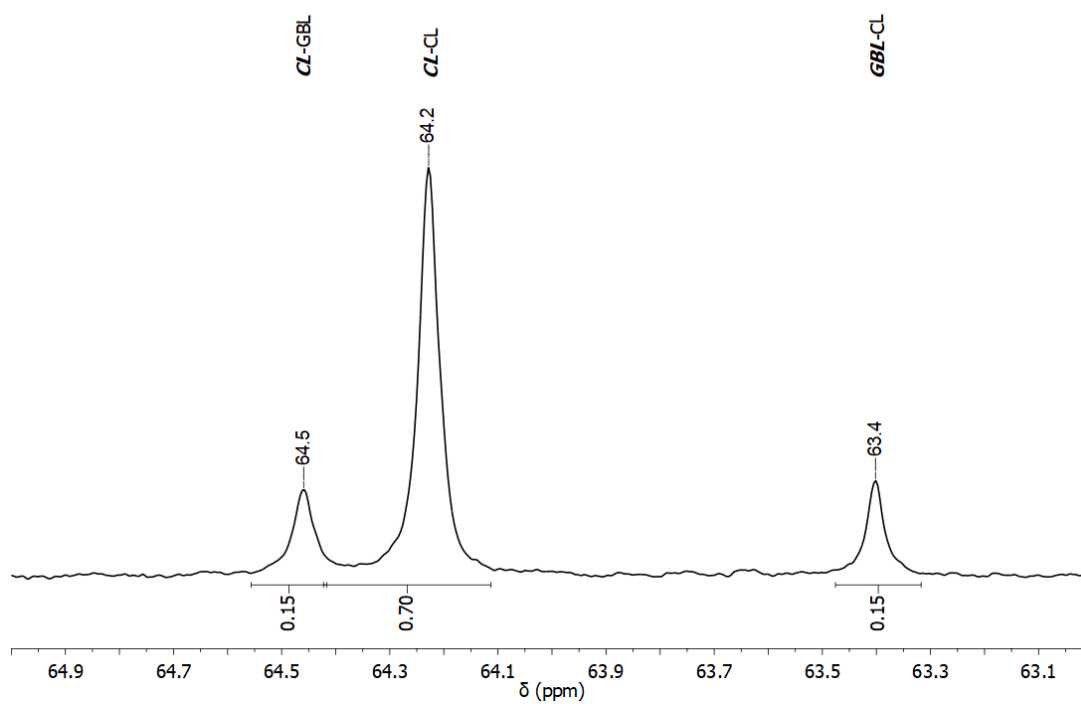


Figure S12. ^{13}C NMR spectroscopy (CDCl_3 , 300 K, O- CH_2 region) with dyad sequence analysis of a GBL/CL copolymer resulting from application 2/ YCl_3 after 2 h at room temperature.

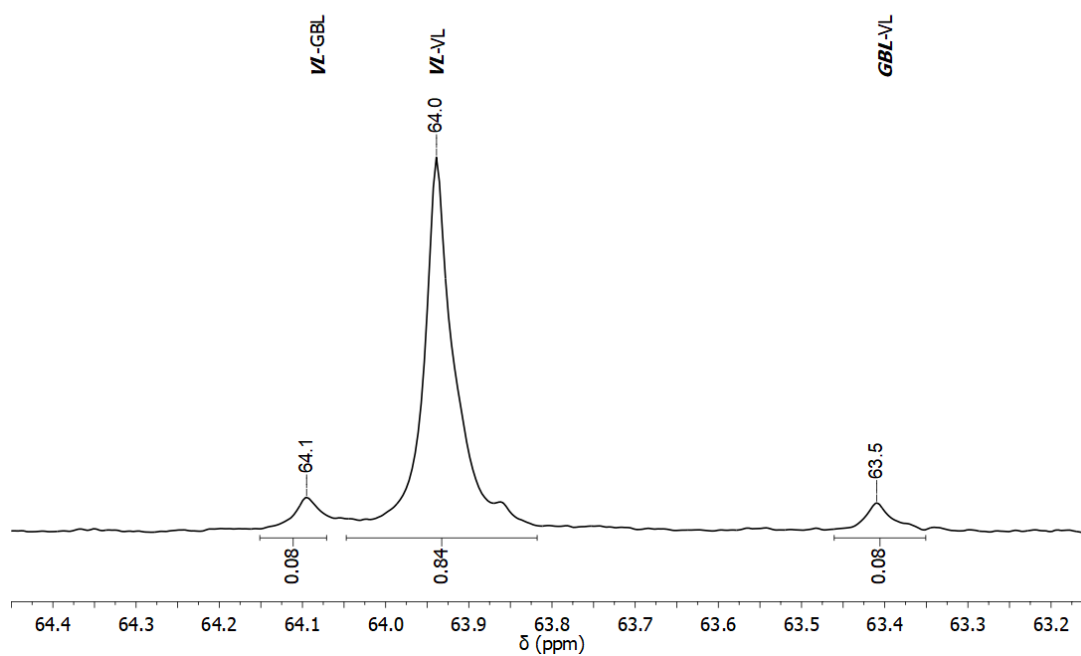


Figure S13. ^{13}C NMR spectroscopy (CDCl_3 , 300 K, O- CH_2 region) with dyad sequence analysis of a GBL/VL copolymer resulting from application 2/ LiCl after 2 h at room temperature.

DSC analysis of synthesized copolymers

Table S8. Melting points of copolymers determined via DSC analyses (heat rate = 5 K/min, purge gas flow (N₂) = 20 mL/min). For more details, see correlated tables.

Table in paper	Entry	NHO/M _x	Polymerization time		(Co)monomers	T _m [°C]
				[min]		
1	6	1/MgCl ₂		240	PDL -	93
2	1	2/LiCl		240	PDL CL	72
2	2	2/MgCl ₂		240	PDL CL	70
2	3	2/MgI ₂		240	PDL CL	74
2	4	2/ZnI ₂		240	PDL CL	53
2	5	2/YCl ₃		480	PDL CL	80
3	1	2/MgI ₂		240	PDL VL	39
3	2	2/MgI ₂	24 h		PDL VL	59
3	3	2/ZnI ₂		240	PDL VL	29/41
3	4	2/ZnI ₂	24 h		PDL VL	30
3	5	2/YCl ₃		240	PDL VL	38
3	6	2/YCl ₃	24 h		PDL VL	72
4	1	2/LiCl	24 h		PDL GBL	79
4	2	2/MgCl ₂	27 h		PDL GBL	84
4	3	2/ZnI ₂	48 h		PDL GBL	85
4	4	2/YCl ₃	86 h		PDL GBL	91
4	5	2/LiCl	63		PDL GBL	86
4	6	2/LiCl	24		PDL GBL	79
5	4	2/ZnI ₂		120	GBL CL	42
5	5	2/YCl ₃		120	GBL CL	35
5	8	2/MgI ₂		120	GBL VL	39
5	9	2/YCl ₃		120	GBL VL	31
5	10	2/LiCl	24 h		GBL CL	34
5	11	2/ZnI ₂	24 h		GBL CL	39
5	13	2/LiCl	24 h		GBL VL	40
5	15	2/ZnI ₂	24 h		GBL VL	45

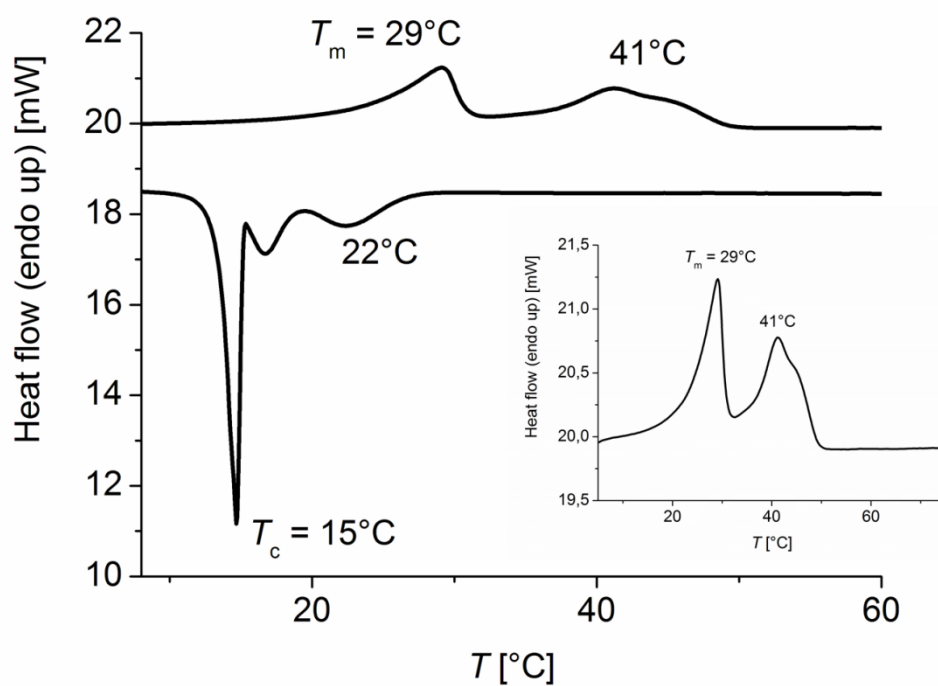


Figure S14. DSC investigation (5 K/min, second cycle) of copolymer derived from PDL and VL using **2**/ MgI_2 ($\text{NHO}/\text{BnOH}/\text{M}_x/\text{PDL}/\text{VL} = 1:2:5:100:100$, 480 min, 50°C , toluene).

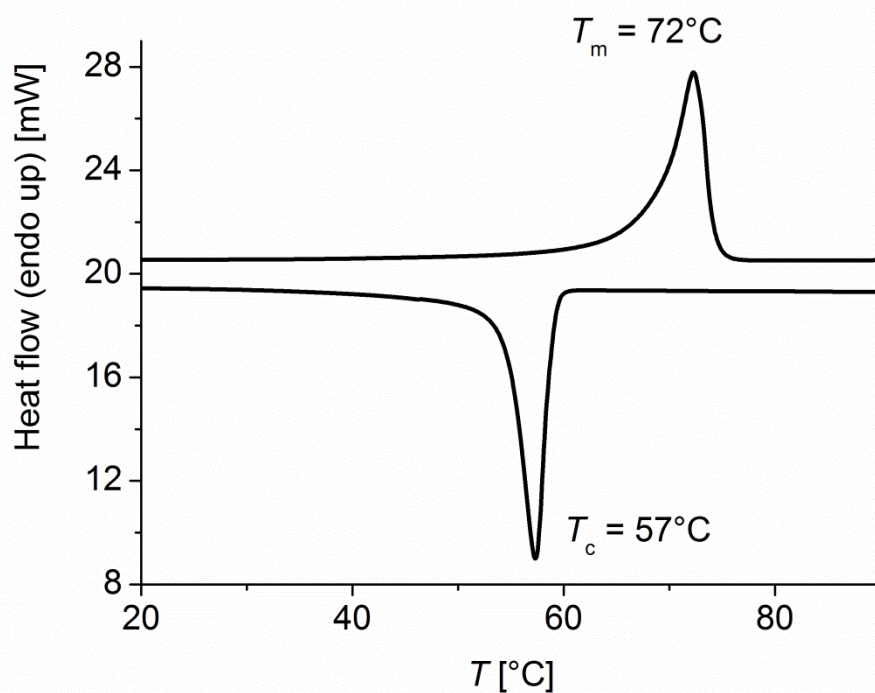


Figure S15. DSC investigation (5 K/min, second cycle) of copolymer derived from PDL and VL using **2**/ YCl_3 ($\text{NHO}/\text{BnOH}/\text{M}_x/\text{PDL}/\text{VL} = 1:2:5:100:100$, 24 h, 110°C , toluene).

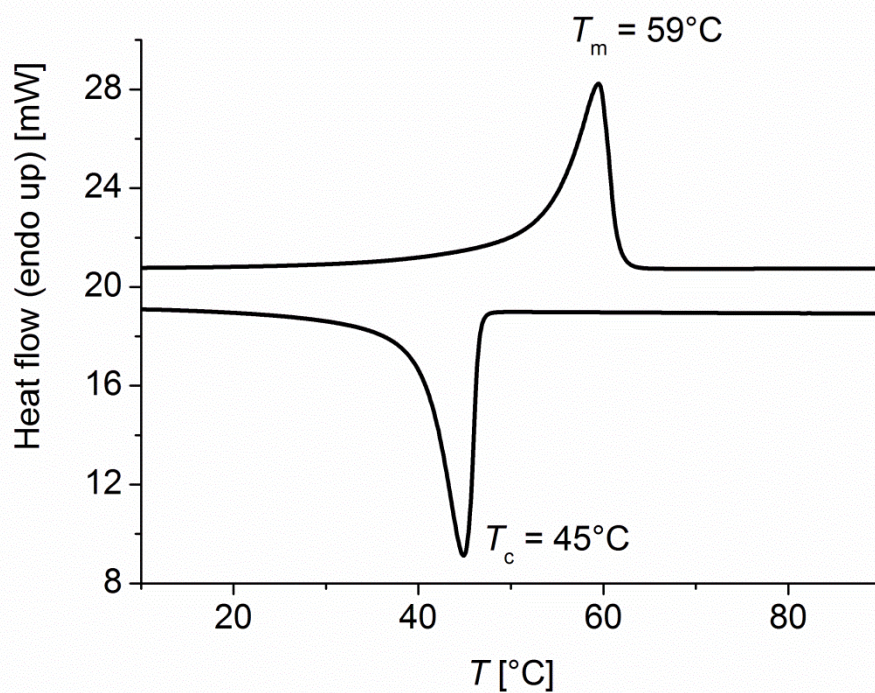


Figure S16. DSC investigation (5 K/min, second cycle) of copolymer derived from PDL and VL using **2**/ ZnI_2 (NHO/BnOH/ M_x /PDL/VL = 1:2:5:100:100, 24 h, 110°C , toluene).

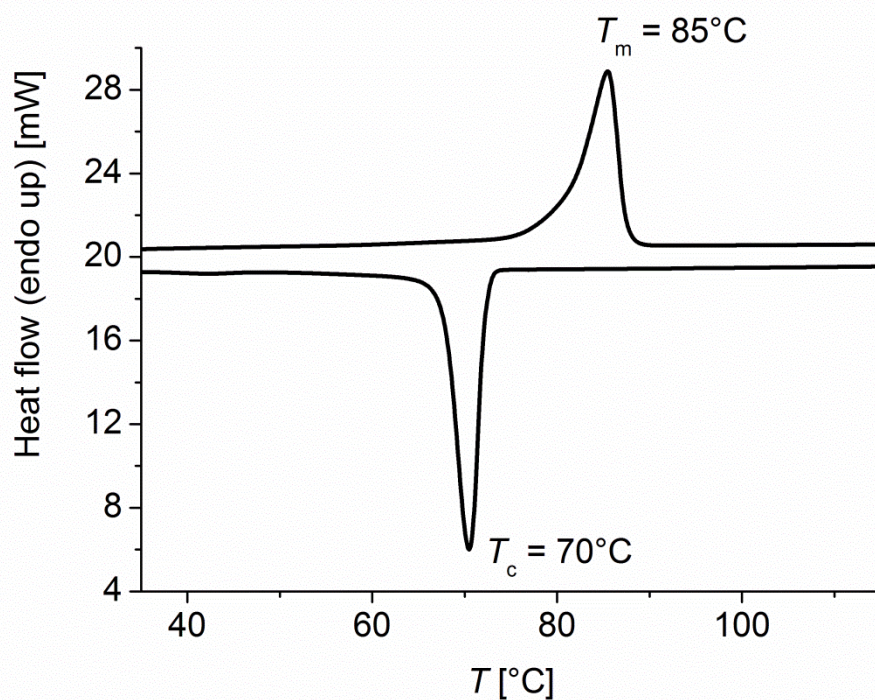


Figure S17. DSC investigation (5 K/min, second cycle) of copolymer derived from PDL and GBL using **2**/ ZnI_2 (NHO/BnOH/ M_x /PDL/GBL = 1:2:5:100:100, 48 h, 100°C , THF).

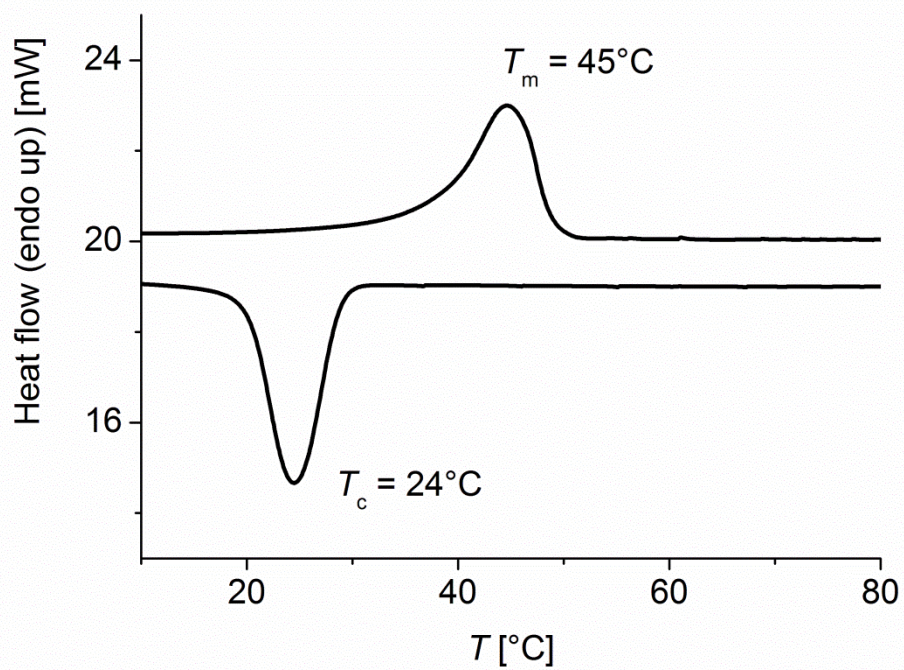


Figure S18. DSC investigation (5 K/min, second cycle) of copolymer derived from GBL and VL using **2**/ ZnI_2 (NHO/BnOH/ M_x /GBL/VL = 1:2:5:100:100, 24 h, -36°C , THF).

Complexation experiments analyzed via $^1\text{H-NMR}$ spectroscopy

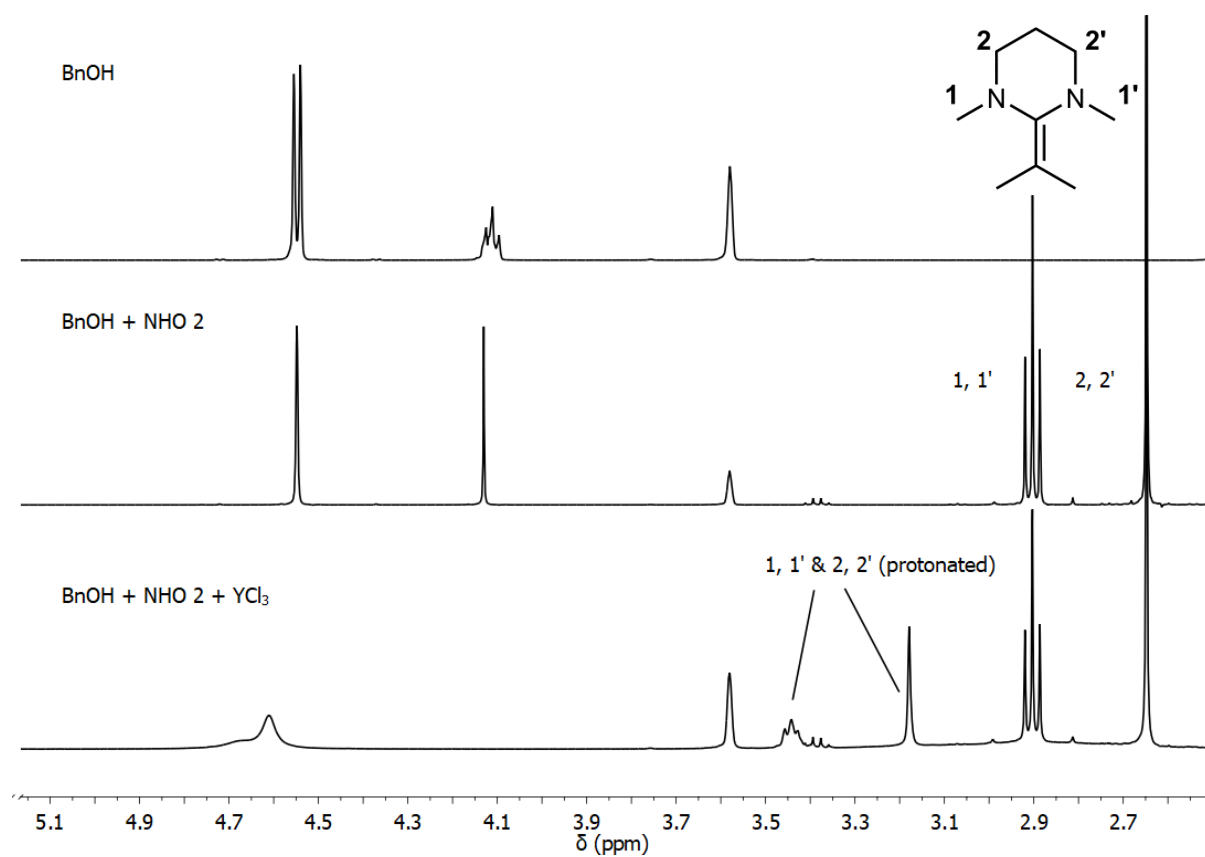


Figure S19. Complexation experiments with **2** and various Lewis Acids, as well as the $^1\text{H-NMR}$ spectrum of the initiator BnOH.



Cite this: DOI: 10.1039/c8py00784e

Polarized olefins as enabling (co)catalysts for the polymerization of γ -butyrolactone†

Patrick Walther,^a Wolfgang Frey^b and Stefan Naumann *^a

Suitable methods to polymerize γ -butyrolactone (GBL) by ring-opening polymerization (ROP) have emerged only recently. In view of the exciting properties of the corresponding aliphatic polyester, organocatalytic or simple metal-based catalyst systems are called for. To extend the currently limited set of suitable catalysts and to explore mechanisms beyond the “superbasic”, anionic pathway based on phosphazenes, so-called *N*-heterocyclic olefins (NHOs) have been employed for GBL homopolymerization. It was found that they can be applied in an organocatalytic setup but also in combination with lithium salts as cooperative Lewis pairs under bulk conditions (−36 °C). Metal-free setups succeed only in the presence of initiator (BnOH), whereby TONs of 140–230 have been realized by using the six-membered NHO 1,3-dimethyl-2-(1-methylethylidene)tetrahydropyrimidine (**3**, 70% conversion, 0.5 mol% NHO loading). MALDI-ToF MS analysis revealed that a mixture of cyclic and linear species is generated, whereby the proportion of cyclic material increases in the later stages of the polymerization. Conversely, when several NHOs were employed with lithium salts as Lewis pairs (NHO, LiX (X = Cl, I, OTf) and BnOH), the formation of macrocycles was found to be retarded. In the absence of protic initiator (BnOH) but presence of lithium salt, the polymerization mechanism can change from an anionic one to a zwitterionic ROP. As underlined by MALDI-ToF investigations, three different situations can occur, depending on the chemical structure of the NHO. Firstly, highly nucleophilic NHOs (**7**) will form stable zwitterionic species: the NHO is directly attached to the chain and cationizing it. As a bad leaving group, the NHO moiety cannot be substituted and exclusively linear poly(GBL) is generated. Less nucleophilic, sterically hindered NHOs (**6**) will still form zwitterions under these conditions, but substitution can occur, favouring a macrocyclic poly(GBL) topology. Finally, sterically encumbered but strongly basic NHOs (**4**) prefer enolization of the lactone over nucleophilic ring-opening, thus operating on an anionic polymerization pathway, comparable to phosphazene catalysis. Overall, the prepared poly(GBL) was found to be in the range of low polymeric/high oligomeric molecular weights (1000–9000 g mol^{−1}, GPC) with the organocatalytic approaches delivering significantly higher conversion than reactions in the presence of lithium salts.

Received 24th May 2018,
Accepted 18th June 2018
DOI: 10.1039/c8py00784e
rsc.li/polymers

Introduction

γ -Butyrolactone (GBL), a five-membered cyclic ester, has traditionally been largely ignored for application as monomer on account of adverse thermodynamics.¹ Unlike its smaller- and larger-ring size analogues, GBL is almost strain-free and consequently the most common driving force for ring-opening polymerization does not apply for this lactone; high-pressure approaches have been met with limited success.^{2,3}

Pioneering work by Chen and co-workers resulted in a major advancement of the field when it was understood that indeed a miniscule but existing ring-tension can be exploited for polymerization.⁴ Two main strategies were employed. For one, it was recognized that a (very low) ceiling temperature for the polymerization–depolymerization equilibrium must exist. Reactions were therefore conducted at −40 °C with [GBL]₀ = 10 mol L^{−1}. Secondly, polymerizations were led in a manner as to precipitate or crystallize the polyester out of the solution, thereby removing the poly(GBL) from the depolymerization equilibrium.

It was also demonstrated that there is compelling reason for finding suitable polymerization procedures for GBL. The monomer itself can be obtained from succinic acid, one of the most successful renewable platform compounds.^{5,6} The lactone in turn serves as a precursor for several value-added derivatives such as pyrrolidones, 1,4-butanediol or THF.⁷ Thus,

^aUniversity of Stuttgart, Institute of Polymer Chemistry, 70569 Stuttgart, Germany. E-mail: stefan.naumann@ipoc.uni-stuttgart.de, stefan.naumann@itcf-denkendorf.de

^bUniversity of Stuttgart, Institute of Organic Chemistry, 70569 Stuttgart, Germany
† Electronic supplementary information (ESI) available. CCDC 1842215. For ESI and crystallographic data in CIF or other electronic format see DOI: 10.1039/c8py00784e

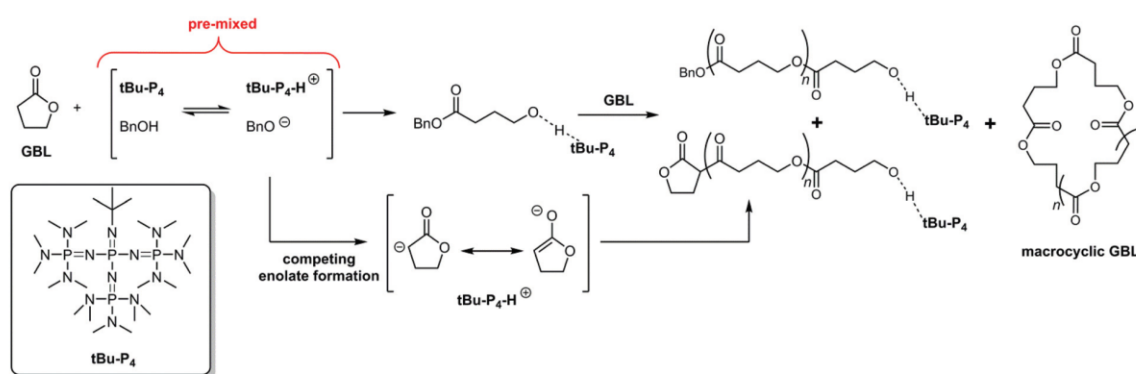
it can be anticipated that biosourced GBL will remain a cheap and rather abundant material. This is especially fortunate as its homopolymer, poly(GBL), has been shown to possess attractive properties, including full thermal recyclability into the monomer, ready degradability and interesting mechanical properties depending on the polymer topology (linear or macrocyclic architecture).⁴ Poly(GBL) is also structurally identical to poly(4-hydroxybutyrate) (P4HB), a material used for soft tissue ligation prepared by a bacterial fermentation process; a chemical route seems here rewarding and potentially more competitive from an economic perspective.⁸

These beneficial properties are obviously best realized with a catalytic setup that is itself benign and succeeds without problematic components (metals, solvents), recommending organocatalytic approaches. In a recent study a range of organocatalytically active compounds was investigated for their ability to deliver poly(GBL) with the result that “superbasic” phosphazenes (*t*Bu-P₄) were identified as superior compared to 1,8-diazabicyclo[5.4.0]undec-7-en (DBU), 1,5,7-triazabicyclo[4.4.0]dec-5-ene (TBD) or even *N*-heterocyclic carbenes.⁹ With *t*Bu-P₄, conversions of 90% (4 h, 1 mol% catalyst loading, -40 °C, 10 M, benzyl alcohol as initiator) could be obtained with relatively high molecular weights (25 kDa) and limited control over polydispersity ($D_M = 2.0$ – 2.4). While these are exciting results, a number of issues remain. GBL homopolymerization proceeds in a non-living manner under these conditions. While solidification of the highly concentrated polymerization mixture may aggravate matters, especially competing enolate formation has been revealed as an important side reaction (Scheme 1).⁹ Thus, the poly(GBL) obtained from phosphazene catalysis displays different end groups and also a mixture of macrocyclic and linear polymer architecture, irrespective of reaction conditions and sequence of addition. Interestingly, however, the composition can be shifted from predominantly linear to predominantly cyclic by adaption of the polymerization reactions. Liu and Li have recently demonstrated the decisive influence of the chemical structure of the phosphazene on polymer topology; lactide/GBL diblockcopolyesters were also reported.^{10,11}

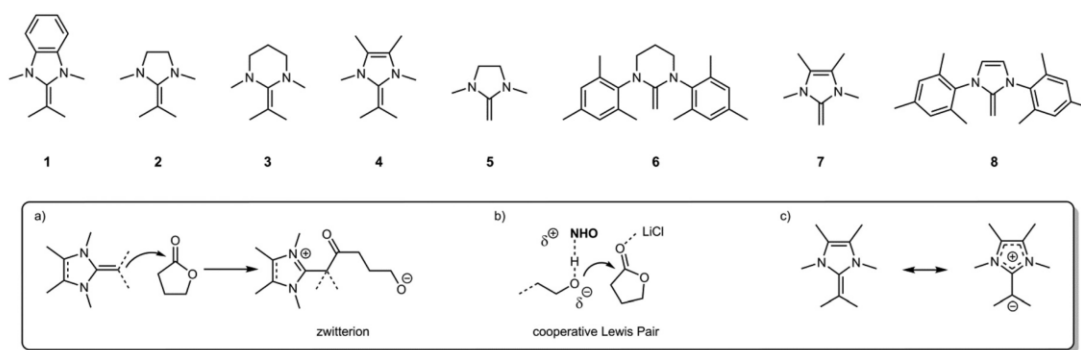
These promising insights clearly suggest that the catalytic setup is a major factor not only influencing conversion and general efficiency of the polymerization, but also central to the properties of the polyester. In fact, from above considerations it can be inferred that perhaps a milder, less “superbasic” type of catalysis could reveal new facets of the challenging GBL homopolymerization. These requirements are met by *N*-heterocyclic olefins (NHOs, Scheme 2),^{12–20} a relatively novel type of (organo)polymerization catalyst.^{21–26} Specifically, NHOs can be used in conjunction with alcohol initiators and have been shown to be powerful (co)catalysts for lactone polymerization, that way mirroring the applicability of phosphazenes to a degree.^{27–29} However, for NHOs the ability to enolize lactones effectively seems to be limited to the most basic ones; competing enolate-initiation can thus be circumvented by judicious choice of the NHO structure.²⁷ NHOs contain a polarized double bond; this locates a certain excess electron density on the exocyclic carbon, the extent of which can be tuned in a number of ways.^{13,15,18,20,22} Still, even for the most basic NHO the pK_a will be considerably lower – by many orders of magnitude – than found for *t*Bu-P₄ ($pK_a(\text{MeCN}) = 43$).^{14,23,30} Also, two further polymerization modes may be added to the existing approaches for GBL polymerization *via* NHOs: a “nucleophilic pathway” under formation of zwitterionic species (Scheme 2a), and a “cooperative mechanism” mediated by NHO/Lewis acid pairs (Scheme 2b), whereby the monomer is activated by simple, benign and commercially available metal halides. This in turn enables the application of mildly reactive NHOs, likewise envisioned to suppress side reactions. Recently we showed that this principle can be applied for copolymerizations of GBL with other lactones.²⁹ In the present study the results for the corresponding GBL homopolymerization will be detailed, with a special emphasis on MALDI-ToF MS analysis focusing on end groups and polymer topology.

Results and discussion

To identify the key properties of NHOs relevant for GBL conversion and poly(GBL) topology, a number of structurally



Scheme 1 Phosphazene-catalyzed polymerization of GBL with concomitant enolate formation.



Scheme 2 NHOs employed in this work. (a) Envisioned zwitterion formation from NHOs and GBL; (b) Lewis acid-supported GBL polymerization; (c) mesomeric structures.

different NHOs have been prepared (1–8, Scheme 2). All compounds were synthesized following established procedures (see ESI† for details).

Novel compound **6**, with a saturated, six-membered backbone (see Fig. 1 for X-ray crystal structure analysis), was prepared *via* carbene formation followed by reaction with methyl iodide, as described analogously by Rivard and co-workers for imidazole-derivative **8**.³¹ All NHOs were selected to represent the range of reactivities currently available for this type of organocatalyst. Imidazole-based compounds (**4**, **7**–**8**) belong to the more reactive end of the scale; the polarization of the double bond is favoured by the propensity of the backbone to accommodate a positive charge, forming an aromatic moiety (Scheme 2c). The corresponding charge separation is further accentuated by the substituents: *N*-alkyl groups stabilize the cationic moiety (**7**), whereas *C*-alkyl substituents (exocyclic carbon) confer additional electron excess on the negatively charged carbon, increasing reactivity further (**4**). Contrasting that, *N*-mesityl substitution (**8**) increases steric demand but decreases the overall electron-richness of the NHO compared to compound **7**. The more electron-rich imidazole-based organocatalysts (**4**, **7**) are additionally outfitted with methyl groups on their C4/C5 positions to prohibit the formation of abnormal carbenes, a side-reaction that seems to be common for this type of NHO.³²

Saturated NHOs are much less reactive, upon formal charge separation the positive (partial) charge is delocalized only on the *N*–*C*–*N* moiety. Consequently, their polymerization behaviour has been found to be clearly distinct from the imidazole derivatives: saturated compounds such as **2**, **3** or **5** are not able to organopolymerize propylene oxide²² or act as organoinitiators for acrylic monomers,²⁴ features that can be achieved by compounds **4** or **7**, for example. For **5** basicity was determined as $pK_a(\text{MeCN}) = 26.6$, giving a lower limit for NHO basicity;¹⁴ the massive difference to *t*Bu-P₄ should be noted (see above). Among the saturated NHOs, the six-membered species can potentially be seen as slightly more reactive.³³ Steric hindrance by the *N*-substituents is exerted more effectively for the six-membered tetrahydropyrimidine-2-alkylidenes since the larger *N*–*C*–*N* angle pushes the substituents in the direction of the exocyclic olefinic carbon. With the exception of **2**, **3** and **5**, all compounds were received as solids. Storage under protective atmosphere at $-36\text{ }^\circ\text{C}$ (glove box freezer) did not lead to any signs of decomposition over extended periods of time (24 months).

With this range of organocatalysts at hand, polymerization experiments were conducted. Four different approaches were investigated: organocatalytic polymerization (NHO) and polymerization *via* cooperative Lewis pairs (NHO and LiCl), both in the absence and presence of additional initiator (benzyl alcohol, BnOH).

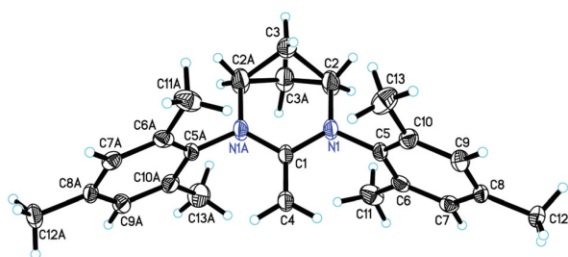


Fig. 1 Single crystal X-ray structure of NHO **6**. Orthorhombic space group *Pbcn*, C1–C4 distance = 134.2 pm. For complete data set see ESI. CCDC number = 1842215.†

Organopolymerization

For a first set of experiments, NHOs **1**–**4** were employed, all of which have different heterocyclic backbones but a uniform *N*-methyl substitution pattern and a dimethyl-bearing exocyclic carbon. Reactions were conducted in bulk GBL at $-36\text{ }^\circ\text{C}$ (box freezer) under stirring, with the addition of BnOH as initiator. Homogeneous mixtures resulted in all cases. Gratifyingly, GBL consumption was observed; the chemical nature of the NHO was found to have a clear impact on performance (Table 1). While benzannellated NHO **1** and imidazole-derivative **4** achieved only 10% and 29% conversion respectively after 72 h reaction time, the saturated organocatalysts entailed much

Table 1 Polymerization of GBL in the presence of BnOH as initiator using NHOs 1–8. NHO/BnOH/GBL = 1 : 2 : 200, bulk, –36 °C

#	NHO	<i>t</i> [h]	Conv. ^a [%]	$M_n^{\text{theo}c}$ [g mol ⁻¹]	$M_n^{\text{exp}b}$ [g mol ⁻¹]	D_M^b
1	1	72	10	—	—	—
2	2	24	44	3800	4800	1.7
3	2	72	68	5800	5300	1.8
4	3	24	68	5800	4900	2.1
5	3	48	70	6000	7200	1.8
6	4	72	29	2500	3300	1.5
7	5	24	27	2300	3500	1.5
8	6	72	49	4200	6600	1.6
9	7	72	45	3900	3200	1.7
10	8	72	74	6300	4300	1.6

^a Determined *via* ¹H NMR. ^b According to GPC (CHCl₃). ^c Calculated from conversion.

higher GBL consumption; five-membered **2** provided 68% conversion after the same time and **3** reached 70% after 48 h already, rendering this NHO the most active in this subset. At a catalyst loading of 0.5 mol% this corresponds to a TON of 140. Longer reaction times did not result in quantitative conversion, most probably a consequence of solidification of the polymerization mixture, which can already be observed at conversions <50%.

Efforts for increasing the degree of polymerization (DP) and molecular weights by using a higher monomer loading (3/BnOH/GBL = 1 : 2 : 800) were frustrated by a relatively low conversion after 48 h (29%, M_n = 6400 g mol⁻¹, D_M = 2.3, TON = 230). Dilution of the polymerization mixtures, by creating 10 M GBL solutions, was also investigated for different solvents (Table S7†). While more polar THF and dichloromethane reduced polymerization activity to <5% conversion, reactions in toluene and diethylether performed better, but not superior to bulk processes. All subsequent reactions were therefore conducted in a solvent-free manner.

Clearly, GBL polymerization is non-living under the conditions described above, as evident by the molecular weight distributions. This is also substantiated by the way molecular weights evolve with conversion. While for a representative polymerization (3/BnOH/GBL = 1 : 2 : 200, bulk, –36 °C, analysis after 1, 2, 5, 10 and 20 h, independent reactions) monomer consumption increases almost linearly with time (up to 70% conversion), the corresponding correlation of conversion and molecular weights (M_n) displays a clear deviation from linear behaviour with increasing conversion/reaction time (Fig. S6†). Molar mass is lower than expected, indicating side reactions such as chain transfer. MALDI-ToF MS analysis was conducted to elucidate these observations. Interestingly, there is a distinct shift in the polymer populations from the early stages of the reaction compared to the later phases. While after 1 h the linear BnO/H terminated poly(GBL) is clearly the dominant species with only minor amounts of macrocycles detectable, this gradually changes so that after 20 h the proportion of macrocyclic species is significantly enlarged, which is also mirrored by GPC results (Fig. S7†). Potentially this explains why molecular weights do not grow while conversion is still increasing: as the reaction mixture

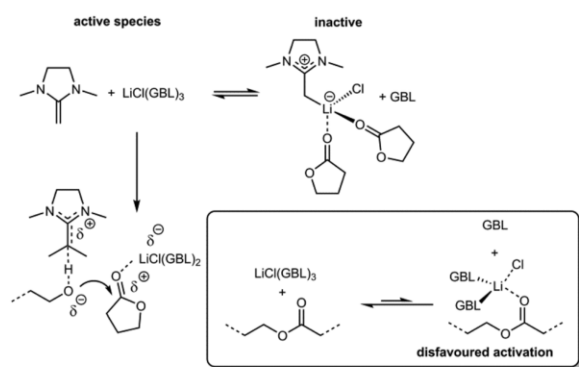
gets depleted of GBL, the probability of backbiting grows, forming macrocyclic species and shorter oligomeric chains which can still add monomer; the kinetic chain is kept intact. Perhaps significantly, the molar mass of the macrocyclic species is invariable at about 1500 Da (distribution maximum) for the whole observation time. This corresponds to oligomers of 17–18 repeat units. The invariable mass indicates that the cycles are not reactivated in this reaction setup and most probably precipitate or crystallize out of the reaction solution. Further analyses of reactions mediated by NHO/BnOH delivered a similar picture, with a distribution peaking at around 1500 Da comprised of the macrocyclic polymer population and a second distribution attributable to linear, BnO/H-terminated poly(GBL) (Fig. S8†).

To broaden the base of catalysts, a second subset of NHOs with a “naked” =CH₂ methylenide moiety was introduced (5–8, Scheme 2). Polymerizations generally resulted in molecular masses and mass distributions similar to those obtained by 1–4 (Table 1, 3000–7000 g mol⁻¹, D_M = 1.5–2.0). NHO 5, presumably less basic and also with less steric demand than **2**, achieved lower conversion, not exceeding 27–30% even after prolonged reaction times. Conversely, imidazole **8** performed well, delivering 74% conversion after 72 h polymerization time. This outperforms NHO 7 (45%) and underlines the observation that strong polarization and electron-richness seem detrimental under these conditions. Conversion grows in the sequence **4** < **7** < **8**, while electron-richness and presumably basicity decrease in the same order.

Crucially, reactions in the absence of BnOH initiator resulted in the complete suppression of polymerization for all NHOs 1–8 (Table S8†), highlighting that metal-free, zwitterionic polymerization of GBL is not possible without further activation of the lactone. Consequently, in a subsequent series of experiments simple metal halides were employed as cocatalysts, envisioning a facilitated GBL ring-opening by Lewis acid-activation of the monomer.

Lewis pair polymerization

Initially, four different simple and commercially available metal halides were screened for reactivity (MgI₂, ZnI₂, YCl₃, LiCl), Lewis acids which had already been successfully



Scheme 3 Stable metal halide – NHO adducts suppress polymerization activity. Insert: Coordination to GBL (= activation) is favoured over interaction with the poly(GBL) chain on account of sterics and *anti*-conformation of the lactone ester moiety.

employed with NHOs for the controlled polymerization of other lactones.^{28,29} Interestingly, reaction conditions as noted earlier (3/BnOH/metal halide/GBL = 1 : 2 : 5 : 200, bulk, $-36\text{ }^{\circ}\text{C}$) did not lead to any monomer conversion (96 h) at all for MgI_2 , ZnI_2 and YCl_3 . The fact that the addition of metal halides actually *quenches* any polymerization activity in a system that works otherwise under metal-free conditions indicates that NHO-metal complex formation might be the issue (Scheme 3), the more so at the rather low reaction temperatures, which will disfavour dissociation of the Lewis pair. Without free NHO, polymerization cannot occur. Application of LiCl, in contrast, succeeds in delivering poly(GBL). A recent study suggests that the association propensity for the formation of NHO–LiCl complexes is much less pronounced than for corresponding $\text{Mg}(\text{II})$ and $\text{Zn}(\text{II})$ chlorides,³⁴ potentially explaining why the NHO/LiCl Lewis pairs remain active for GBL homopolymerization at low temperatures (Table 2). Overall, conversion is somewhat muted compared to the organocatalytic approach; the more polarized NHOs (4, 7) are even more disfavoured in this case, achieving only negligible conversion. All other NHO/LiCl combinations deliver broadly similar conversion (25–44%, 0.5 mol% catalyst loading). Molar masses of the poly(GBL) seem slightly higher

Table 2 Polymerization of GBL in the presence of BnOH and LiCl using NHOs 1–8. NHO/BnOH/LiCl/GBL = 1 : 2 : 5 : 200, bulk, $-36\text{ }^{\circ}\text{C}$

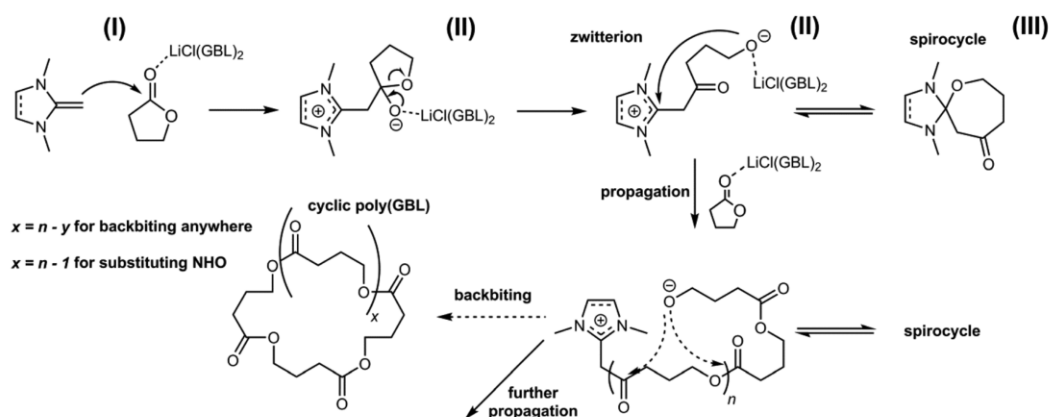
#	NHO	<i>t</i> [h]	Conv. ^a [%]	M_n^b [g mol ⁻¹]	D_M^b
1	1	48	25	6100	1.5
2	1	72	39	6700	1.7
3	2	48	29	5700	1.7
4	2	72	42	7300	1.7
5	3	72	44	4700	1.8
6	4	32	<5	—	—
7	5	48	38	6800	1.6
8	6	48	38	6400	1.4
9	7	48	<5	—	—
10	8	48	32	7800	1.7

^a Determined *via* ^1H NMR. ^b According to GPC (CHCl_3).

than for comparable conversion in the metal-free approach; indeed, observation of the development of M_n with conversion and MALDI-ToF MS analysis of the samples (3/BnOH/metal halide/GBL = 1 : 2 : 5 : 200, bulk, $-36\text{ }^{\circ}\text{C}$) shows that the appearance of macrocyclic species is retarded. Analogously to the metal-free setup their proportion seems to grow over time, but to a smaller degree and slower (Fig. S9†). Fittingly, the molar mass evolves with conversion in a more linear manner (see Fig. S10†) for the observed time span (96 h). Interestingly, application of δ -valerolactone has been described to similarly impact polymer topologies, with a decrease in cyclization propensity.³⁵

Given the superiority of LiCl over other metal halides, polymerizations were also conducted with lithium iodide (LiI) and lithium trifluoromethanesulfonate (LiOTf). Both cocatalysts afforded very similar results with the same tendencies as found for LiCl but generally lower turnover (see Tables S9 and S10†). More importantly, MALDI ToF MS results were quite similar: even for extended reaction times (72 h) the proportion of macrocyclic species was very small, with the linear species being by far the dominant topology (see Fig. S11†). Cyclic polymer is formed by backbiting, and the obvious conclusion is that the presence of hard, Lewis-acidic Li^+ disfavors this intramolecular process relative to monomer addition. Tentatively, this behaviour can be attributed to selective activation (*via* coordination of lithium) of the lactone monomer relative to the activation of the polyester chain (Scheme 3). It is known that the *anti*-conformation of the ester-moiety, as present in GBL, is more basic than the *cis*-conformation prevailing in the polymer chain.³⁶ This and steric factors will facilitate selective monomer activation and therefore a suppression of transesterification reactions such as backbiting will result. An increase of selectivity in dual catalytic lactone polymerization systems has been described for both metal-free and metal-containing setups.^{28,29,37–40}

Much in contrast to metal-free setups, where NHO/GBL alone did not result in polymer formation (alcohol initiator required, see above), application of the NHO/LiCl Lewis pair also allows for direct polymerization of GBL without additional BnOH being present (Table S11,† employing NHOs 4–8). Yields reduced further when compared to reactions with initiator, and molecular weights increased or were found to be higher than expected for the low conversion (NHO/LiCl/GBL = 1 : 5 : 200, 6–23% conversion, 48–72 h, bulk, $-36\text{ }^{\circ}\text{C}$, $M_n = 3000\text{--}9000\text{ g mol}^{-1}$). Mechanistically, this indicates polymerization *via* zwitterionic species,⁴¹ formed by the direct ring-opening of GBL *via* nucleophilic attack of the NHO (Scheme 4). LiCl clearly enables this process, arguably by coordination to the lactone, most probably exclusively *via* the carbonyl oxygen (I).³⁴ This increases the electron deficiency on the carbonyl carbon, the attacking site of nucleophiles, and thus facilitates ring-opening. Additionally, it is also conceivable that the metal species stabilizes the generated oxyanion by coordination, likewise supporting charge separation (II). In such a scenario, propagation is controlled by interaction of the negatively charged chain end with LiCl but especially so with



Scheme 4 Proposed polymerization of GBL via a Lewis acid-supported zwitterionic mechanism initiated by NHOs with competing spirocyclic resting states.

the counter ion, which is the NHO-derived imidazolium- or tetrahydropyrimidinium-moiety. Here, the formation of spirocyclic (resting-)states (III) and their relative stabilities compared to the active, charge-separated species will control how effective polymerization occurs.^{24,42–44} The overall low conversion and relatively higher molecular weights might be explained by a lower initiation efficiency of NHO/LiCl (zwitterionic) relative to NHO/BnOH and NHO/BnOH/LiCl (both anionic, discussed above) and the formation of relatively stable spirocycles.

MALDI-ToF MS analysis supports the proposed zwitterionic reaction mechanism and the crucial influence of the chemical structure of the NHO. Investigations were conducted with and without additional Na⁺-cationizing reagents being present.

Using NHO 7, it was found that the MALDI profiles were identical in both cases, showing the same mass populations in the absence and presence of ionizing reagents (Fig. 2,

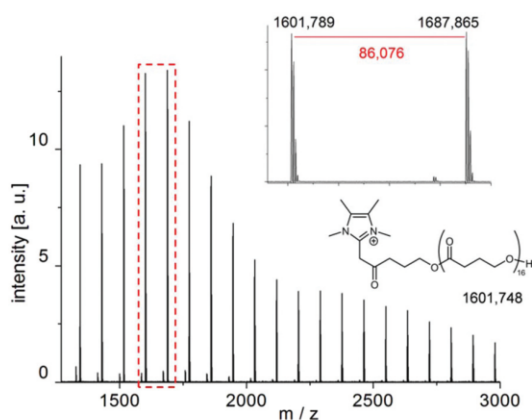


Fig. 2 MALDI-ToF MS analysis of poly(GBL) prepared by the cooperative action of 7 and LiCl (7/LiCl/GBL = 1 : 5 : 200, -36 °C, bulk). No external cationizing agent added.

Fig. S12†). End group calculation shows a perfect fit with an NHO-terminated poly(GBL) structure. The molecule is inherently cationized by the positively charged imidazolium moiety and can therefore be detected without the usually required Na⁺. It should be noted that not even traces of macrocyclic polyester are observable under these conditions. Also the very small second population visible (Fig. 2) can be attributed to linear, NHO-cationized poly(GBL) with the mass difference to the main population resulting in this case from the deoxygenation of the ketone functionality under formation of a double bond in conjugation with the imidazolium-moiety (Fig. S13†).

These data strongly suggest that the resulting polymer is exclusively linear as a direct consequence of introducing a zwitterionic polymerization mechanism, the first of its kind described for GBL polymerization.

Very differently, in the identical reaction setup employing sterically encumbered and less polarized NHO 6 again only one polymer population is observed – but in this case, the masses coincide with macrocyclic polymer, Li⁺-cationized when no external sodium salts were added during matrix preparation (Fig. 3) and Na⁺-ionized with conventional MALDI-ToF preparation (Fig. S14†). Only very low yields were received after 48 h (6%), but ¹H NMR analysis showed the complete absence of signals attributable to enolate-derived initiation (which would display the same masses as macrocyclic poly(GBL)), strongly suggesting that indeed only cyclic species have been formed (Fig. S14†). To increase conversion, reaction times were extended (72 h); monomer consumption consequently rose to 13%. Unfortunately, MALDI-ToF MS analysis and NMR experiments showed that the longer reaction times were accompanied by a degree of enolate-formation, rendering the resulting material a mixture of cyclic and linear topologies (Fig. S15†). It is proposed that this behaviour can be explained by the interplay of nucleophilicity and nucleofugality (see discussion below).

Finally, the material resulting from 4/LiCl was also investigated. Again, a very different mass profile was discovered. Two

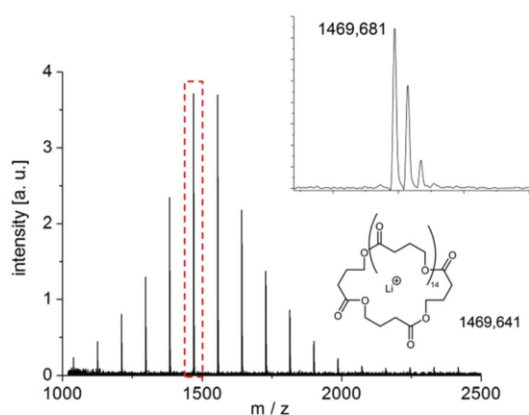


Fig. 3 MALDI-ToF MS analysis of poly(GBL) prepared by the cooperative action of **6** and LiCl (**6**/LiCl/GBL = 1:5:200, $-36\text{ }^{\circ}\text{C}$, bulk, 48 h). No external cationizing agent added.

polymer populations with closely matching intensity distributions were found (Fig. 4). Calculations show that one population fits the mass of either macrocyclic or enolate-derived poly(GBL), while the other would correspond to OH/H-termination (deriving from hydrolysed ester moieties). The latter one could theoretically derive from water initiation or substitution of the NHO imidazolium moiety during work-up and matrix preparation; however, given the reaction conditions (dry, glove box) and the near identical shape of both distributions, hydrolytic cleavage of an ester bond seems the most likely explanation. **4**, unlike other NHOs, shows a clear reaction with GBL when subjected to ^1H NMR experiments (Fig. S16 \dagger). Furthermore, this NHO has been shown to polymerize δ -valerolactone in the absence of any other activators *via* enolate formation and is generally described to have much higher basicity than saturated NHOs.^{22,27} Also, ^1H NMR analysis of the polymer displays signals attributable to a GBL-

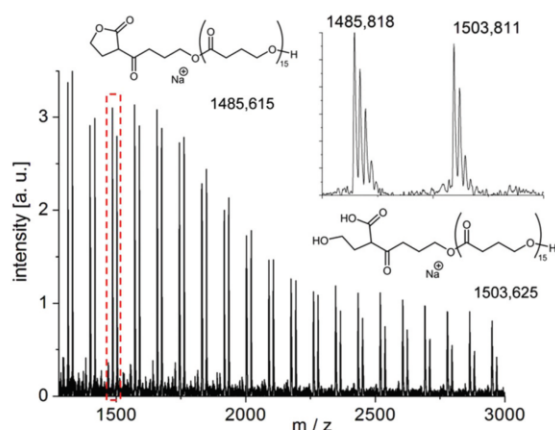


Fig. 4 Mass spectrum of polymer prepared by **4**/LiCl (**4**/LiCl/GBL = 1:5:200, $-36\text{ }^{\circ}\text{C}$, bulk), cationized by sodium. The minor distributions belong to Li^+ -cationized species.

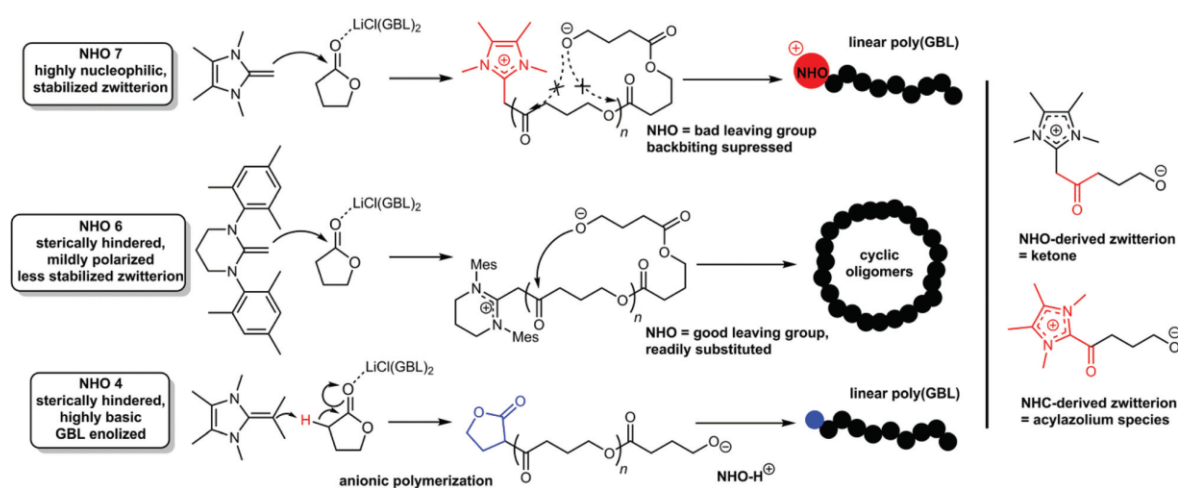
moiety terminating the chain, as identified by Chen for phosphazene-mediated polymerizations (Fig. S17 \dagger).⁹ We therefore propose that the MALDI profile (Fig. 4) represents enolate-derived poly(GBL), one population with intact end group while the other results from polymer with hydrolysed GBL-moiety, most probably a consequence of the acidic MALDI-ToF matrix. This suggests that the polymer prepared this way is predominantly linear, but the occurrence of macrocyclic "impurities" can currently not be fully excluded for this specific Lewis pair.

These results reveal that the chemical structure of the NHO is a critical parameter and might even be used as a tool to pre-determine the resulting poly(GBL) architecture (Scheme 5). Using otherwise identical conditions, application of NHOs **4**, **6** and **7** together with LiCl generates poly(GBL) with different end groups and topologies. While **7** engenders exclusively linear polymer with a cationic, NHO-derived terminus, employment of **4** delivers enolate-derived end groups; this also means that the polymerization mechanism is fundamentally different, with a *zwitterionic* process in the first case and an *anionic* one in the latter. Distinct from both, application of **6** results in the low-yield preparation of exclusively oligocyclic material which displays increasing amounts of enolate-terminated poly(GBL) as reaction time and conversion grow. This suggests that **6** can, to a limited degree, access both zwitterionic (cycles) and anionic (enolate-terminated) polymerization pathways. It is however sterically hindered, aggravating zwitterion formation, and also less electron-rich, minimizing its enolizing ability, most probably explaining for the low conversions observed.

These differences might be explained by considering the nucleophilic/basic dualism observed for NHOs²² (in analogy to the behaviour of NHCs),^{45–47} and the respective propensity of the NHO to act as a leaving group as discussed in the following.

The differences between **4** and **7** have been documented for propylene oxide and other lactones.^{22,27} **4**, with its additional methyl groups on the exocyclic carbon, is sterically too hindered to be able to directly ring-open the monomer in a zwitterionic manner. Instead, its considerable basicity is pronounced enough to enolize lactones (as shown for δ -valerolactone).²⁷ Conversely, NHO **7** is highly nucleophilic; it is very electron-rich but sterically unencumbered. This is sufficient to add to propylene oxide in a zwitterionic manner, for example.²² Given this precedence, the behaviour shown towards GBL is fully in line with earlier findings: while **4** acts as base, **7** behaves as nucleophile.

The striking differences between **6** and **7** regarding the resulting poly(GBL) topology might be best understood when considering that (1) highly nucleophilic **7** aromatizes upon addition to GBL and ring-opening of the lactone, leading to a stabilized zwitterion, (2) for **6**, zwitterion formation – and thus charge separation – will be less attractive, aggravated even more so by the steric pressure exerted by the mesityl groups, (3) once zwitterions are formed, spirocyclic resting states are in competition with the open-chain, propagating species and (4) initiation by the NHOs results in a *ketone functionality*, hence the NHO is much harder to substitute by a nucleophilic attack on the carbonyl carbon than found for other organocatalysts



Scheme 5 Summary of polymerization results using different NHOs in combination with LiCl. Right: NHO- and NHC-derived zwitterions from direct ring-opening of GBL. The acylazolium species is much more susceptible to nucleophilic substitution than the ketone.

(such as NHCs, see Scheme 5). Spirocycles have the potential to retard or even completely quench polymerization activity, depending on their relative stability compared to the charge-separated species, which might be one explanation for the generally low yields. Equally important, they localize the oxyanion in the vicinity of the NHO-derived cation and suppress side reactions by decreasing the concentration of free anions. The fact that, at least initially, for **6**/LiCl no linear, NHO-terminated species could be observed at all suggests that cyclization is taking place by substituting the NHO.⁴⁸ For **6** this seems to be readily possible, while for **7** this option is clearly disadvantaged; it would require the abolishment of the stabilization gained by aromatization upon zwitterion formation. The NHO-terminus derived from **7** is therefore a much worse leaving group than the one deriving from **6** and cannot be dislodged easily by nucleophilic substitution. Complementary, the finding that for **7**/LiCl no cyclic species could be identified at all suggests that backbiting also on ester moieties within the polymer chain is disfavoured, probably by the close interaction of the oppositely charged polymer chain termini.

Overall this suggests that the balance between nucleophilicity and nucleofugality of the NHO is decisive for the generation of specific poly(GBL) topologies and might be used to tailor the polymer architecture. The inherent ability of NHOs to form the relatively stable ketone-type zwitterions is certainly crucial: the generation of considerable molecular weight is only possible if propagation is faster than cyclization.⁴⁰ This only succeeds if the initiator in question is a relatively poor leaving group, a condition that seems to be fulfilled for zwitterions derived from NHOs and lactones. As was demonstrated, this property can also be taken to extremes so that nucleophilic substitution of the NHO-moiety is impossible, leading to linear poly(GBL) (NHO **7**). This is in stark contrast to the behaviour of NHCs, for a reaction in the absence of initiator will always lead to macrocyclic polymer in their case,⁴⁰ and

consequently an NHC-terminated poly(lactone) has never been isolated. However, while this kind of selectivity is certainly of high interest, optimization of the NHO structure (and also the metal-based cocatalysts) is still required; regarding overall conversion and molecular weights, the NHO-mediated polymerization of GBL is still inferior to phosphazene-catalyzed reactions. Using *t*Bu-P₄ and the same base catalyst to GBL ratio (1 : 200, BnOH present), the phosphazene converts more than 50% of the monomer in 12 h reaction time. More pronounced is the difference of the molecular weight of the thus prepared poly(GBL) (M_n up to 25 000 g mol⁻¹).⁹ A recently developed cyclic phosphazene achieves >90% GBL conversion with the same organobase loading within 4 h ($M_n = 16 000$ g mol⁻¹).¹⁰ On the other hand, NHOs are clearly more effective than DBU, TBD, 1,3-dimesityl-imidazole-2-ylidene (IMes) or combinations of thiourea and tertiary amine.⁹

Conclusions

The so far very limited set of catalysts suitable for GBL polymerization has been extended to now also include NHOs. They can be employed alone (organocatalytic) or in combination with LiCl as cooperative Lewis pairs. The resulting poly(GBL) was found to be in the range of low polymeric/high oligomeric molecular weights.

The metal-free setups profit from the application of NHOs with a moderate double-bond polarization. The presence of an alcohol-based initiator is required for successful polymerization. TONs of 140–230 have been achieved by using 1,3-dimethyl-2-(1-methylethylidene)tetrahydropyrimidine (**3**). MALDI-ToF MS analysis has shown that a mixture of cyclic and linear species results, whereby the proportion of cyclic material increases in the later stages of the polymerization. Conversely, when several NHOs were employed with lithium

salts as Lewis pairs, reactions succeeded both in the absence and presence of alcohol initiators. Setups involving **3**, LiX (X = Cl, I, OTf) and BnOH were found to contain considerably less macrocycles. The occurrence of a zwitterionic polymerization mechanism in the absence of protic initiator was proven by MALDI-ToF investigations. For highly nucleophilic 1,3,4,5-tetramethyl-2-methyleneimidazoline (**7**) MALDI-ToF MS analysis found exclusively linear poly(GBL) with a cationic NHO-derived terminus. This is in stark contrast to NHC-mediated lactone polymerization, where in the absence of initiator macrocyclic polyester would be generated and a direct consequence of the stable, ketone-type zwitterions formed by NHOs.

Using a less nucleophilic, strongly basic NHO (2-isopropylidene-1,3,4,5-tetramethylimidazoline, **4**) switched the polymerization mechanism from zwitterionic to anionic, involving enolized GBL as initiator.

The interesting potential features of NHO-mediated zwitterionic polymerization were also outlined by describing a novel, six-membered compound (1,3-dimesityl-2-methylidene-tetrahydropyrimidine, **6**) which indicated that with the right interplay of nucleophilicity and nucleofugality also the preparation of exclusively macrocyclic poly(GBL) could be possible. A mechanism supported by Lewis acid-activation and spirocyclic intermediates was proposed to explain these differences, whereby NHOs with good leaving properties favour cyclization, while linear polymer is generated by strongly nucleophilic NHOs. Research on this topic is progressing in our group with the express aim to increase conversion and molecular weights by optimizing catalyst structures.

Conflicts of interest

There are no conflicts to declare.

Acknowledgements

Dr Dongren Wang (University of Stuttgart) is acknowledged for support with MALDI-ToF MS analysis. SN gratefully acknowledges support by the German Research Foundation (Deutsche Forschungsgemeinschaft, DFG, NA 1206/2).

Notes and references

- 1 *Handbook of ring-opening polymerization*, ed. J.-M. Raquez, O. Coulembier and P. Dubois, Wiley-VCH, Weinheim, 2009.
- 2 F. Korte and W. Glet, *J. Polym. Sci., Part C: Polym. Lett.*, 1966, **4**, 685–689.
- 3 K. Yamashita, K. Yamamoto and J.-i. Kadokawa, *Chem. Lett.*, 2014, **43**, 213–215.
- 4 M. Hong and E. Y.-X. Chen, *Nat. Chem.*, 2016, **8**, 42–49.
- 5 I. Bechthold, K. Bretz, S. Kabasci, R. Kopitzky and A. Springer, *Chem. Eng. Technol.*, 2008, **31**, 647–654.
- 6 C. Delhomme, D. Weuster-Botz and F. E. Kühn, *Green Chem.*, 2009, **11**, 13–26.
- 7 A. Cukalovic and C. V. Stevens, *Biofuels, Bioprod. Biorefin.*, 2008, **2**, 505–529.
- 8 S. F. Williams, S. Rizk and D. P. Martin, *Biomed. Technol.*, 2013, **58**, 439–452.
- 9 M. Hong and E. Y.-X. Chen, *Angew. Chem., Int. Ed.*, 2016, **55**, 4188–4193.
- 10 N. Zhao, C. Ren, H. Li, Y. Li, S. Liu and Z. Li, *Angew. Chem., Int. Ed.*, 2017, **56**, 12987–12990.
- 11 Y. Shen, J. Zhang, N. Zhao, F. Liu and Z. Li, *Polym. Chem.*, 2018, **9**, 2936–2941.
- 12 R. D. Crocker and T. V. Nguyen, *Chem. – Eur. J.*, 2016, **22**, 2208–2213.
- 13 M. M. D. Roy and E. Rivard, *Acc. Chem. Res.*, 2017, **50**, 2017–2025.
- 14 U. Gruseck and M. Heuschmann, *Chem. Ber.*, 1987, **120**, 2053–2064.
- 15 H. Quast, M. Ach, M. K. Kindermann, P. Rademacher and M. Schindler, *Chem. Ber.*, 1993, **126**, 503–516.
- 16 N. Kuhn, H. Bohnen and R. Boese, *Chem. Ber.*, 1994, **127**, 1405–1407.
- 17 A. Fürstner, M. Alcarazo, R. Goddard and C. W. Lehmann, *Angew. Chem., Int. Ed.*, 2008, **47**, 3210–3214.
- 18 S. Kronig, P. G. Jones and M. Tamm, *Eur. J. Inorg. Chem.*, 2013, **2013**, 2301–2314.
- 19 Y.-B. Wang, Y.-M. Wang, W.-Z. Zhang and X.-B. Lu, *J. Am. Chem. Soc.*, 2013, **135**, 11996–12003.
- 20 A. P. de Lima Batista, A. G. S. de Oliveira-Filho and S. E. Galembeck, *ACS Omega*, 2017, **2**, 299–307.
- 21 Y.-B. Jia, Y.-B. Wang, W.-M. Ren, T. Xu, J. Wang and X.-B. Lu, *Macromolecules*, 2014, **47**, 1966–1972.
- 22 S. Naumann, A. W. Thomas and A. P. Dove, *Angew. Chem., Int. Ed.*, 2015, **54**, 9550–9554.
- 23 M. Blümel, J.-M. Noy, D. Enders, M. H. Stenzel and T. V. Nguyen, *Org. Lett.*, 2016, **18**, 2208–2211.
- 24 S. Naumann, K. Mundsinger, L. Cavallo and L. Falivene, *Polym. Chem.*, 2017, **8**, 5803–5812.
- 25 A. Balint, M. Papendick, M. Clauss, C. Müller, F. Giesselmann and S. Naumann, *Chem. Commun.*, 2018, **54**, 2220–2223.
- 26 Q. Wang, W. Zhao, S. Zhang, J. He, Y. Zhang and E. Y.-X. Chen, *ACS Catal.*, 2018, 3571–3578.
- 27 S. Naumann, A. W. Thomas and A. P. Dove, *ACS Macro Lett.*, 2016, **5**, 134–138.
- 28 S. Naumann and D. Wang, *Macromolecules*, 2016, **49**, 8869–8878.
- 29 P. Walther and S. Naumann, *Macromolecules*, 2017, **50**, 8406–8416.
- 30 R. Schwesinger, C. Hasenfratz, H. Schlemper, L. Walz, E.-M. Peters, K. Peters and H. G. von Schnering, *Angew. Chem., Int. Ed. Engl.*, 1993, **32**, 1361–1363.
- 31 K. Powers, C. Hering-Junghans, R. McDonald, M. J. Ferguson and E. Rivard, *Polyhedron*, 2016, **108**, 8–14.
- 32 A. Schumann and C. Hering-Junghans, *Eur. J. Inorg. Chem.*, 2018, **2018**, 2584–2588.
- 33 G. Ye, S. Chatterjee, M. Li, A. Zhou, Y. Song, B. L. Barker, C. Chen, D. J. Beard, W. P. Henry and C. U. Pittman, *Tetrahedron*, 2010, **66**, 2919–2927.

- 34 J. Meisner, J. Karwounopoulos, P. Walther, J. Kästner and S. Naumann, *Molecules*, 2018, **23**, 432.
- 35 Y. A. Chang and R. M. Waymouth, *Polym. Chem.*, 2015, **6**, 5212–5218.
- 36 G. Bouchoux, D. Drancourt, D. Leblanc, M. Yanez and O. Mo, *New J. Chem.*, 1995, **19**, 1243.
- 37 S. Naumann, P. B. V. Scholten, J. A. Wilson and A. P. Dove, *J. Am. Chem. Soc.*, 2015, **137**, 14439–14445.
- 38 J. Liu, C. Chen, Z. Li, W. Wu, X. Zhi, Q. Zhang, H. Wu, X. Wang, S. Cui and K. Guo, *Polym. Chem.*, 2015, **6**, 3754–3757.
- 39 X. Zhang, G. O. Jones, J. L. Hedrick and R. M. Waymouth, *Nat. Chem.*, 2016, **8**, 1047–1053.
- 40 K. V. Fastnacht, S. S. Spink, N. U. Dharmaratne, J. U. Pothupitiya, P. P. Datta, E. T. Kiesewetter and M. K. Kiesewetter, *ACS Macro Lett.*, 2016, **5**, 982–986.
- 41 H. A. Brown and R. M. Waymouth, *Acc. Chem. Res.*, 2013, **46**, 2585–2596.
- 42 L. Falivene and L. Cavallo, *Macromolecules*, 2017, **50**, 1394–1401.
- 43 W. Jeong, J. L. Hedrick and R. M. Waymouth, *J. Am. Chem. Soc.*, 2007, **129**, 8414–8415.
- 44 J. Raynaud, C. Absalon, Y. Gnanou and D. Taton, *Macromolecules*, 2010, **43**, 2814–2823.
- 45 C.-L. Lai, H. M. Lee and C.-H. Hu, *Tetrahedron Lett.*, 2005, **46**, 6265–6270.
- 46 M. Fèvre, J. Pinaud, Y. Gnanou, J. Vignolle and D. Taton, *Chem. Soc. Rev.*, 2013, **42**, 2142–2172.
- 47 S. Naumann and A. P. Dove, *Polym. Int.*, 2016, **65**, 16–27.
- 48 Cyclization only during MALDI preparation, as described for *N*-carboxyanhydrides, cannot be fully ruled out, see: L. Guo and D. Zhang, *J. Am. Chem. Soc.*, 2009, **131**, 18072–18074.

Supporting Information

Experimental

Starting materials and catalyst synthesis

γ -Butyrolactone (GBL, TCI Chemicals, > 99.0 % (GC)) was dried over CaH_2 , and subsequently distilled under static vacuum ($1 \cdot 10^{-3}$ mbar). After degassing the clear liquid with two cycles of freeze-pump-thaw, GBL was stored under protective conditions inside the glove box (LabMaster, MBraun, Germany, freezer, -36 °C). LiCl (Sigma Aldrich, powder, ≥ 99.99 % trace metals basis), MgCl_2 (Alfa Aesar, "ultra dry", 99.9 %), YCl_3 (Alfa Aesar, "ultra dry", 99.99 %, ampouled under argon) and ZnI_2 (Acros, "extra pure", 99.999 %) were used as received and stored inside the glove box under exclusion of light. The solvents used in polymerization reactions were taken from a solvent purification system (MBraun, Germany), and stored under protective conditions (glove box) over molecular sieves (3 Å).

If not stated otherwise, the depicted *N*-Heterocyclic Olefins (NHOs, Figure S10) have been synthesized according to literature-known procedures, where also their characterization is documented.^{2c, 10, 76, 99, 134} An overview regarding the synthetic routes is provided below (Figure S11).

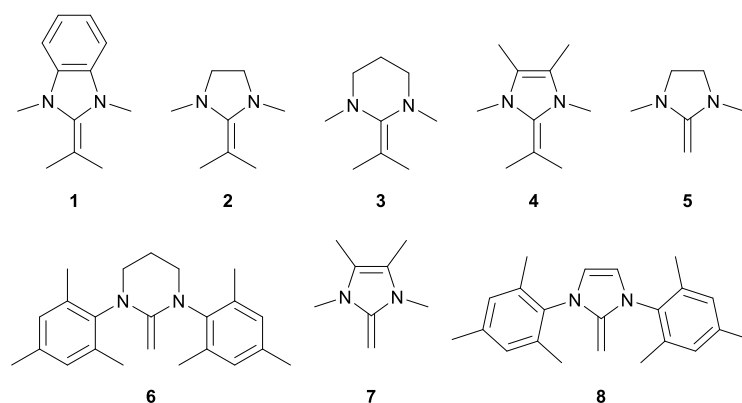


Figure S10. NHOs employed in this study.

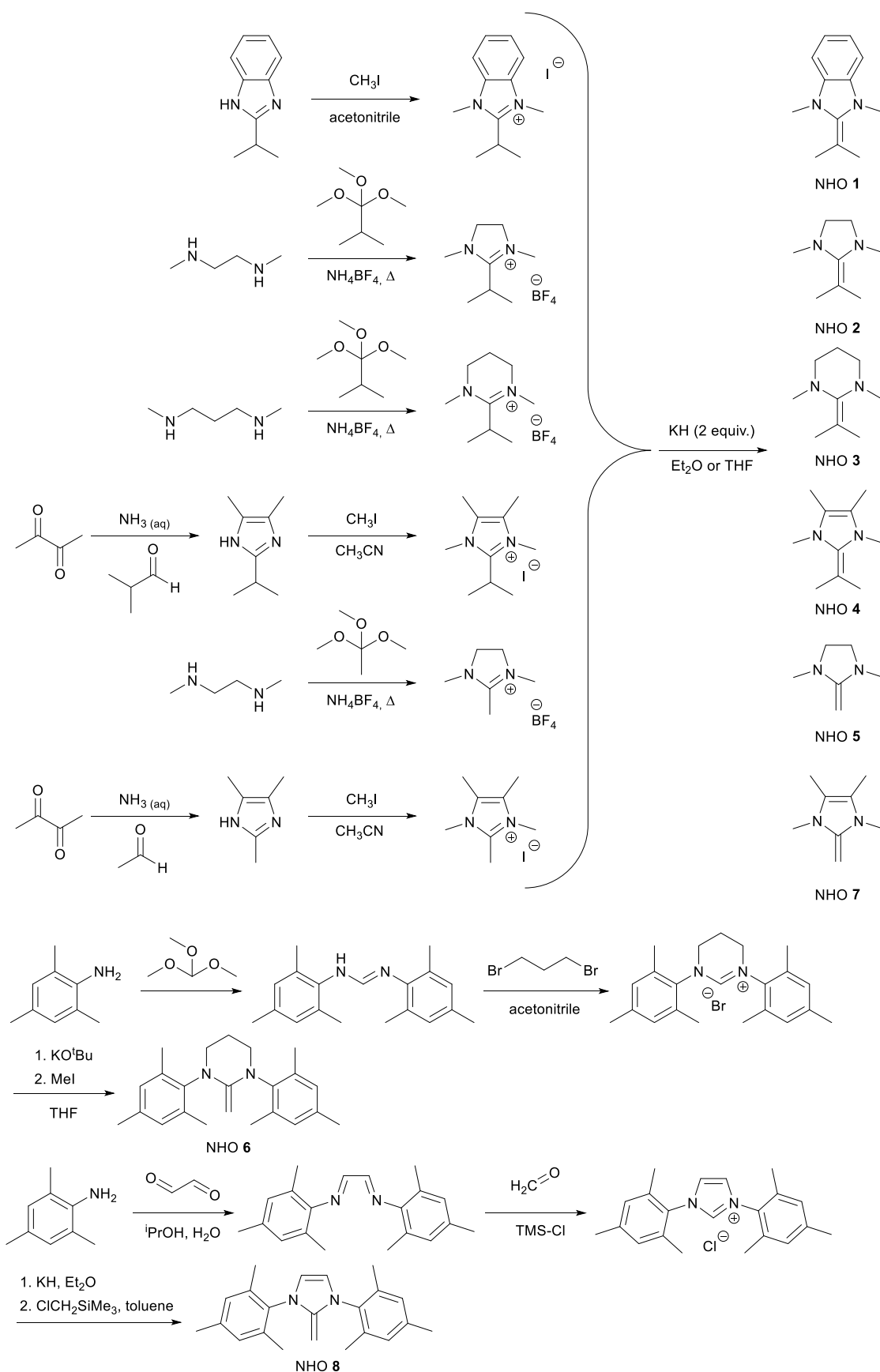


Figure S11. Synthetic routes for the NHOs employed in this study. For detailed preparation procedures, see cited references.^{2c, 10, 76, 99, 134-135}

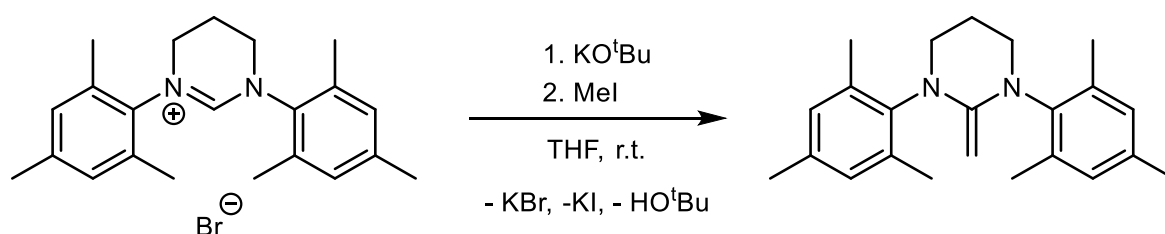
General polymerization procedures

All reactions were carried out inside the box freezer (-36°C). The polymerizations were quenched by adding acidified methylene chloride. Subsequently, the polymer was immediately precipitated in diethyl ether to afford a colourless precipitate. Prior to precipitation, conversion was determined by means of proton NMR spectroscopy, monitoring the $-CH_2-O-$ signal of GBL ($\delta = 4.31$ ppm) and the resulting polymer ($\delta = 4.07$ ppm). To obtain clear reaction solutions, the Lewis acid (0.125 mmol) was dissolved in the solvent (for neat reactions, solvent = GBL) by stirring it for approx. 15 min at room temperature before adding the other component(s) (NHO (0.025 mmol), benzyl alcohol (BnOH, 0.050 mmol) and GBL (5.0 mmol)), resulting in a total molar ratio of NHO/BnOH/MX_n/GBL = 1:2:5:200.

Characterization and analysis

$^1H/^{13}C$ NMR spectra were recorded on a *Bruker Avance III 400* spectrometer, with the chemical shifts being reported relative to reference peaks of the applied deuterated solvents ($CDCl_3$: $\delta = 7.26/77.16$ ppm for proton and carbon spectra, respectively). GPC ($CHCl_3$, 40 °C) was used to determine the molecular weight of the synthesized poly(GBL), against a polystyrene calibration. A chromatographic assembly comprising a *PSS SDV 5 μ m 8*50mm* guard column, three *PSS SDV 100 000 Å 5 μ m 8*50mm* columns and an *Agilent 1200 Series G1362A* detector (RI) was used. The concentration of the prepared samples amounted to 2.5 mg/mL, and a flow-rate of 1 mL/min was applied during the analyses. MALDI-ToF MS measurements were conducted with a *Bruker Autoflex III* (337 nm, reflector mode). The samples were prepared by mixing matrix solution (2,5-dihydroxybenzoic acid, 5 mg/mL in THF), polymer solution (10 mg/ml in THF), and, where required, a solution of sodium trifluoromethanesulfonate (0.1 M in 90% acetone, 10% water) with a ratio of 2:1:2. Polystyrene standards were employed for calibration. Polymerization kinetics were observed by setting up independent reactions which were then stopped after the appropriate polymerization times.

Characterization of 1,3-dimesityl-2-methylene-tetrahydropyrimidine (NHO 6)



Following the procedure of Powers et al. for a related compound,⁷⁶ 1,3-dimesityl-tetrahydropyrimidinium bromide (500 mg, 1.25 mmol) and KO^tBu (559 mg, 4.98 mmol, 4 eq) were combined in THF (15 mL) and stirred at room temperature for 15 min. Subsequently, methyl iodide (354 mg, 2.49 mmol, 2 eq) in THF (5 mL) was added and the resulting yellow reaction mixture was stirred over night at room temperature. After filtering the suspension, volatiles were removed *in vacuo* and the crude precipitates were extracted with *n*-pentane (2x 20 mL). Concentrating the solution upon incipient crystallisation and further storage at -36°C for 72 h resulted in colourless to greenish crystals of **6** (283 mg, 0.80 mmol, 68 %). **1H NMR (400 MHz, C₆D₆):** δ = 6.84 (d, J = 0.6 Hz, 4H, ArCH), 3.14 – 3.08 (t, J = 6 Hz, 4H, (RN-CH₂)₂-CH₂), 2.45 (s, 2H, H₂C=C-(NR)₂), 2.38 (s, 12H, Ar(CH₃)₄), 2.15 (s, 6H, Ar(CH₃)₂), 1.78 – 1.69 (quint, J = 6 Hz, 2H, RN-CH₂-CH₂-NR). **^{13}C NMR (101 MHz, C₆D₆):** δ = 148.3 (RN-C-NR), 141.7 (Ar-C), 137.1 (Ar-C), 136.1 (Ar-C), 129.9 (Ar-C), 54.3 (H₂C=C-(NR)₂), 46.9 ((RN-CH₂)₂-CH₂), 25.1 (RN-CH₂-CH₂-NR), 21.1 (Ar-(CH₃)₂), 18.3 (Ar-CH₃). **GC-MS (rel. intensity):** m/z calc. for C₂₃H₃₀N₂ = 334.24; found: 334.2.

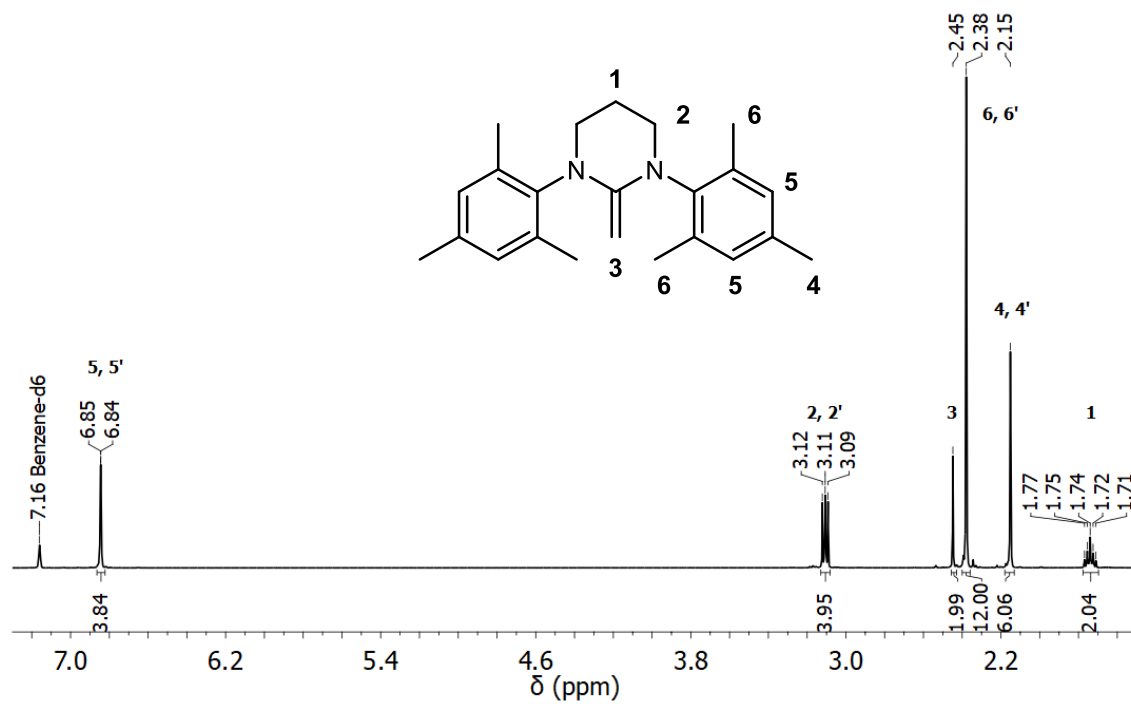


Figure S12. ^1H NMR (400 MHz, 300 K, C_6D_6) of compound 6.

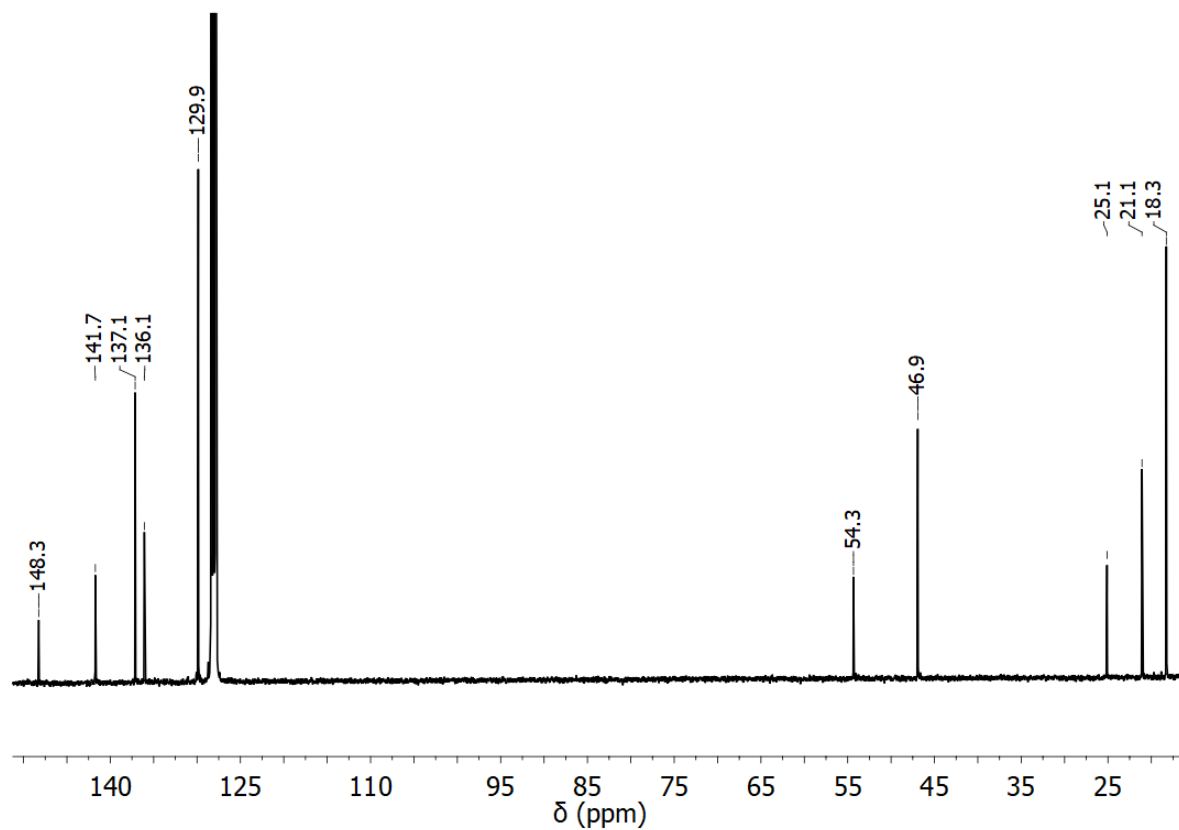


Figure S13. ^{13}C NMR (101 MHz, 300 K, C_6D_6) of compound 6.

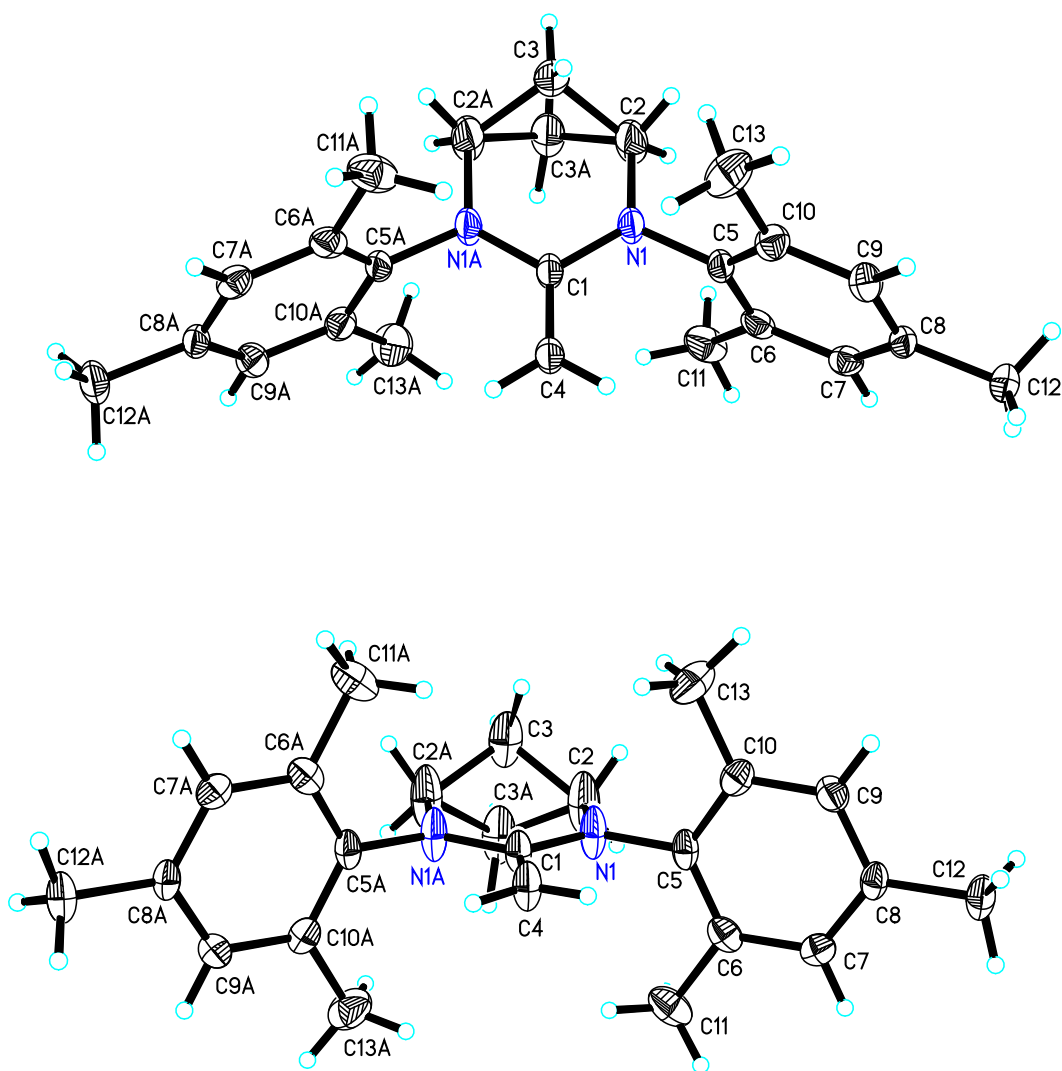


Figure S14. Single crystal x-ray structure of NHO 6.

Table S1. Crystal data and structure refinement for NHO 6.

Identification code	buch210a
Empirical Formula	C ₂₃ H ₃₀ N ₂
Formula weight	334,49
Temperature	130(2) K
Wavelength	0,71073 Å
Crystal system, space group	Orthorhombic, P b c n
Unit cell dimensions	a = 15.5646(19) Å, alpha = 90 deg. b = 7.8895(9) Å, beta = 90 deg. c = 15.9608(17) Å, gamma = 90 deg.
Volume	1959.9(4) Å ³
Z, Calculated density	4, 1.134 Mg/m ³
Absorption coefficient	0.066 mm ⁻¹
F(000)	728
Crystal size	0.57 x 0.56 x 0.09 mm
Theta range for data collection	2.55 to 28.39 deg.
Limiting indices	=-20<=h<=19 -10<=k<=9 -21<=l<=19
Reflections collected / unique	16113 / 2448 [R(int) = 0.0331]
Completeness to theta = 28.39	99.2 %
Absorption correction	Semi-empirical from equivalents
Max. and min. transmission	0.7457 and 0.7197
Refinement method	Full-matrix least-squares on F ²
Data / restraints / parameters	2448 / 3 / 132
Goodness-of-fit on F ²	1.044
Final R indices [I>2sigma(I)]	R1 = 0.0551, wR2 = 0.1529
R indices (all data)	R1 = 0.0830, wR2 = 0.1664
Largest diff. peak and hole	0.478 and -0.193 e.Å ⁻³

Table S2. Atomic coordinates (x 10⁴) and equivalent isotropic displacement parameters (Å² x 10³) for NHO 6. U(eq) is defined as one third of the trace of the orthogonalized Uij tensor.

	x	y	z	U(eq)
N(1)	406(1)	3666(2)	6881(1)	35(1)
C(1)	0	2717(3)	7500	26(1)
C(2)	383(2)	5507(2)	6843(1)	52(1)
C(3)	438(3)	6242(5)	7744(2)	45(1)
C(4)	0	1016(3)	7500	31(1)
C(5)	827(1)	2825(2)	6201(1)	23(1)
C(6)	371(1)	2446(2)	5474(1)	25(1)
C(7)	803(1)	1670(2)	4812(1)	24(1)
C(8)	1673(1)	1288(2)	4859(1)	23(1)
C(9)	2110(1)	1675(2)	5593(1)	26(1)
C(10)	1702(1)	2445(2)	6268(1)	26(1)
C(11)	-572(1)	2865(2)	5407(1)	37(1)
C(12)	2137(1)	477(2)	4130(1)	33(1)
C(13)	2189(1)	2852(3)	7061(1)	42(1)

Table S3. Bond lengths [Å] and angles [deg] for NHO 6.

N(1)-C(1)	1.3910(18)
N(1)-C(5)	1.4312(18)
N(1)-C(2)	1.454(2)
C(1)-C(4)	1.342(3)
C(1)-N(1)#1	1.3910(18)
C(2)-C(3)#1	1.550(4)
C(2)-C(3)	1.553(4)
C(2)-H(2A)	0.967(16)
C(2)-H(2B)	0.992(16)
C(3)-C(2)#1	1.550(4)
C(3)-C(3)#1	1.571(10)
C(3)-H(3A)	1,0188
C(3)-H(3B)	1,1078
C(4)-H(4A)	0.93(2)
C(5)-C(6)	1.393(2)
C(5)-C(10)	1.398(2)
C(6)-C(7)	1.394(2)
C(6)-C(11)	1.508(2)
C(7)-C(8)	1.389(2)
C(7)-H(7)	0,95
C(8)-C(9)	1.389(2)
C(8)-C(12)	1.511(2)
C(9)-C(10)	1.391(2)
C(9)-H(9)	0,95
C(10)-C(13)	1.509(2)
C(11)-H(11A)	0,98
C(11)-H(11B)	0,98
C(11)-H(11C)	0,98
C(12)-H(12A)	0,98
C(12)-H(12B)	0,98
C(12)-H(12C)	0,98
C(13)-H(13A)	0,98
C(13)-H(13B)	0,98
C(13)-H(13C)	0,98
C(1)-N(1)-C(5)	119.81(14)
C(1)-N(1)-C(2)	123.77(14)
C(5)-N(1)-C(2)	116.27(13)
C(4)-C(1)-N(1)#1	122.55(10)
C(4)-C(1)-N(1)	122.55(10)
N(1)#1-C(1)-N(1)	114.89(19)
N(1)-C(2)-C(3)#1	112.1(2)
N(1)-C(2)-C(3)	109.5(2)
C(3)#1-C(2)-C(3)	60.8(3)

N(1)-C(2)-H(2A)	110.1(15)
C(3)#1-C(2)-H(2A)	132.4(15)
C(3)-C(2)-H(2A)	85.2(14)
N(1)-C(2)-H(2B)	106.4(15)
C(3)#1-C(2)-H(2B)	89.9(14)
C(3)-C(2)-H(2B)	140.1(15)
H(2A)-C(2)-H(2B)	98.5(18)
C(2)#1-C(3)-C(2)	102.0(3)
C(2)#1-C(3)-C(3)#1	59.7(3)
C(2)-C(3)-C(3)#1	59.5(3)
C(2)#1-C(3)-H(3A)	108,7
C(2)-C(3)-H(3A)	112
C(3)#1-C(3)-H(3A)	87,1
C(2)#1-C(3)-H(3B)	112,3
C(2)-C(3)-H(3B)	101,6
C(3)#1-C(3)-H(3B)	153,3
H(3A)-C(3)-H(3B)	118,9
C(1)-C(4)-H(4A)	122.5(13)
C(6)-C(5)-C(10)	120.95(13)
C(6)-C(5)-N(1)	119.88(14)
C(10)-C(5)-N(1)	119.13(14)
C(5)-C(6)-C(7)	118.64(14)
C(5)-C(6)-C(11)	120.53(14)
C(7)-C(6)-C(11)	120.82(15)
C(8)-C(7)-C(6)	121.71(14)
C(8)-C(7)-H(7)	119,1
C(6)-C(7)-H(7)	119,1
C(7)-C(8)-C(9)	118.34(13)
C(7)-C(8)-C(12)	121.12(14)
C(9)-C(8)-C(12)	120.54(14)
C(8)-C(9)-C(10)	121.72(14)
C(8)-C(9)-H(9)	119,1
C(10)-C(9)-H(9)	119,1
C(9)-C(10)-C(5)	118.63(14)
C(9)-C(10)-C(13)	120.85(15)
C(5)-C(10)-C(13)	120.51(14)
C(6)-C(11)-H(11A)	109,5
C(6)-C(11)-H(11B)	109,5
H(11A)-C(11)-H(11B)	109,5
C(6)-C(11)-H(11C)	109,5
H(11A)-C(11)-H(11C)	109,5
H(11B)-C(11)-H(11C)	109,5
C(8)-C(12)-H(12A)	109,5
C(8)-C(12)-H(12B)	109,5
H(12A)-C(12)-H(12B)	109,5
C(8)-C(12)-H(12C)	109,5
H(12A)-C(12)-H(12C)	109,5

H(12B)-C(12)-H(12C)	109,5
C(10)-C(13)-H(13A)	109,5
C(10)-C(13)-H(13B)	109,5
H(13A)-C(13)-H(13B)	109,5
C(10)-C(13)-H(13C)	109,5
H(13A)-C(13)-H(13C)	109,5
H(13B)-C(13)-H(13C)	109,5

Table S4. Anisotropic displacement parameters ($\text{Å}^2 \times 10^3$) for NHO 6. The anisotropic displacement factor exponent takes the form: $-2 \pi^2 [h^2 a^{*2} U_{11} + \dots + 2 h k a^* b^* U_{12}]$

U11	U22	U33	U23	U13
N(1)	54(1)	17(1)	33(1)	0(1)
C(1)	34(1)	22(1)	23(1)	0
C(2)	83(2)	20(1)	52(1)	2(1)
C(3)	73(3)	18(2)	44(2)	-6(2)
C(4)	44(1)	20(1)	29(1)	0
C(5)	30(1)	17(1)	23(1)	2(1)
C(6)	23(1)	17(1)	34(1)	4(1)
C(7)	28(1)	20(1)	23(1)	2(1)
C(8)	29(1)	19(1)	19(1)	0(1)
C(9)	22(1)	29(1)	27(1)	1(1)
C(10)	32(1)	25(1)	20(1)	1(1)
C(11)	24(1)	29(1)	59(1)	3(1)
C(12)	40(1)	31(1)	27(1)	-6(1)
C(13)	54(1)	46(1)	26(1)	-6(1)

Table S5. Hydrogen coordinates ($\times 10^4$) and isotropic displacement parameters ($\text{Å}^2 \times 10^3$) for NHO 6.

	x	y	z	U(eq)
H(2A)	958(11)	5950(30)	6777(15)	62
H(2B)	155(14)	5810(30)	6282(12)	62
H(3A)	398	7531	7748	54
H(3B)	1031	5632	7982	54
H(4A)	294(13)	380(30)	7100(13)	45(6)
H(7)	495	1394	4317	28
H(9)	2704	1407	5635	31
H(11A)	-862	2555	5930	56
H(11B)	-826	2229	4941	56
H(11C)	-641	4082	5306	56
H(12A)	1718	133	3704	49
H(12B)	2452	-522	4327	49
H(12C)	2541	1292	3887	49
H(13A)	1974	2143	7519	63
H(13B)	2106	4050	7203	63
H(13C)	2802	2628	6975	63

Table S6. Torsion angles [deg] for NHO 6.

C(5)-N(1)-C(1)-C(4)	1.52(18)
C(2)-N(1)-C(1)-C(4)	177.05(17)
C(5)-N(1)-C(1)-N(1)#1	-178.47(18)
C(2)-N(1)-C(1)-N(1)#1	-2.95(17)
C(1)-N(1)-C(2)-C(3)#1	-27.4(3)
C(5)-N(1)-C(2)-C(3)#1	148.2(2)
C(1)-N(1)-C(2)-C(3)	38.1(3)
C(5)-N(1)-C(2)-C(3)	-146.3(2)
N(1)-C(2)-C(3)-C(2)#1	-61.5(3)
C(3)#1-C(2)-C(3)-C(2)#1	43.6(3)
N(1)-C(2)-C(3)-C(3)#1	-105.0(2)
C(1)-N(1)-C(5)-C(6)	89.75(18)
C(2)-N(1)-C(5)-C(6)	-86.1(2)
C(1)-N(1)-C(5)-C(10)	-92.30(18)
C(2)-N(1)-C(5)-C(10)	91.9(2)
C(10)-C(5)-C(6)-C(7)	0.3(2)
N(1)-C(5)-C(6)-C(7)	178.20(13)
C(10)-C(5)-C(6)-C(11)	-179.84(15)
N(1)-C(5)-C(6)-C(11)	-1.9(2)
C(5)-C(6)-C(7)-C(8)	-0.7(2)
C(11)-C(6)-C(7)-C(8)	179.38(15)
C(6)-C(7)-C(8)-C(9)	1.0(2)
C(6)-C(7)-C(8)-C(12)	-178.84(14)
C(7)-C(8)-C(9)-C(10)	-0.8(2)
C(12)-C(8)-C(9)-C(10)	179.04(15)
C(8)-C(9)-C(10)-C(5)	0.4(2)
C(8)-C(9)-C(10)-C(13)	179.88(16)
C(6)-C(5)-C(10)-C(9)	-0.1(2)
N(1)-C(5)-C(10)-C(9)	-178.02(14)
C(6)-C(5)-C(10)-C(13)	-179.62(15)
N(1)-C(5)-C(10)-C(13)	2.4(2)

Organopolymerization of γ -butyrolactone**Table S7.** Variations of the organocatalyzed polymerization of γ -butyrolactone.

Entry	NHO	Time [h]	Conversion ^{a)} [%]	\overline{M}_n ^{b)}	\mathcal{D} ^{b)}	Variation
1	2	48	15	6100	1.8	NHO:BnOH:GBL = 1:2:800, bulk
2	3	48	29	6400	2.3	NHO:BnOH:GBL = 1:2:800, bulk
3	3	24	4	-	-	THF, $[M]_0 = 10$ M
4	3	24	25	4700	1.6	toluene, $[M]_0 = 10$ M
5	3	24	3	-	-	methylene chloride, $[M]_0 = 10$ M
6	3	24	60	4100	2.2	diethyl ether, $[M]_0 = 10$ M

Conditions: -36°C , NHO:BnOH:GBL = 1:2:200 if not stated otherwise; ^{a)}determined via ^1H NMR spectroscopy; ^{b)}determined via GPC (CHCl_3).

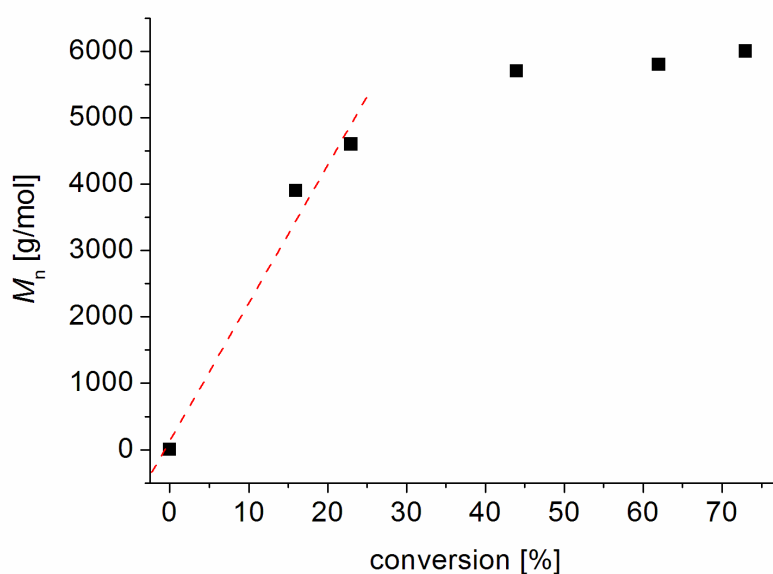


Figure S6. Correlation of M_n vs. conversion for GBL polymerization using NHO 3 with BnOH. 3/BnOH/GBL = 1:2:200, -36°C , bulk. At higher conversion a strong deviation from linear projection occurs, probably attributable to increased backbiting and macrocycle formation (Figure S7).

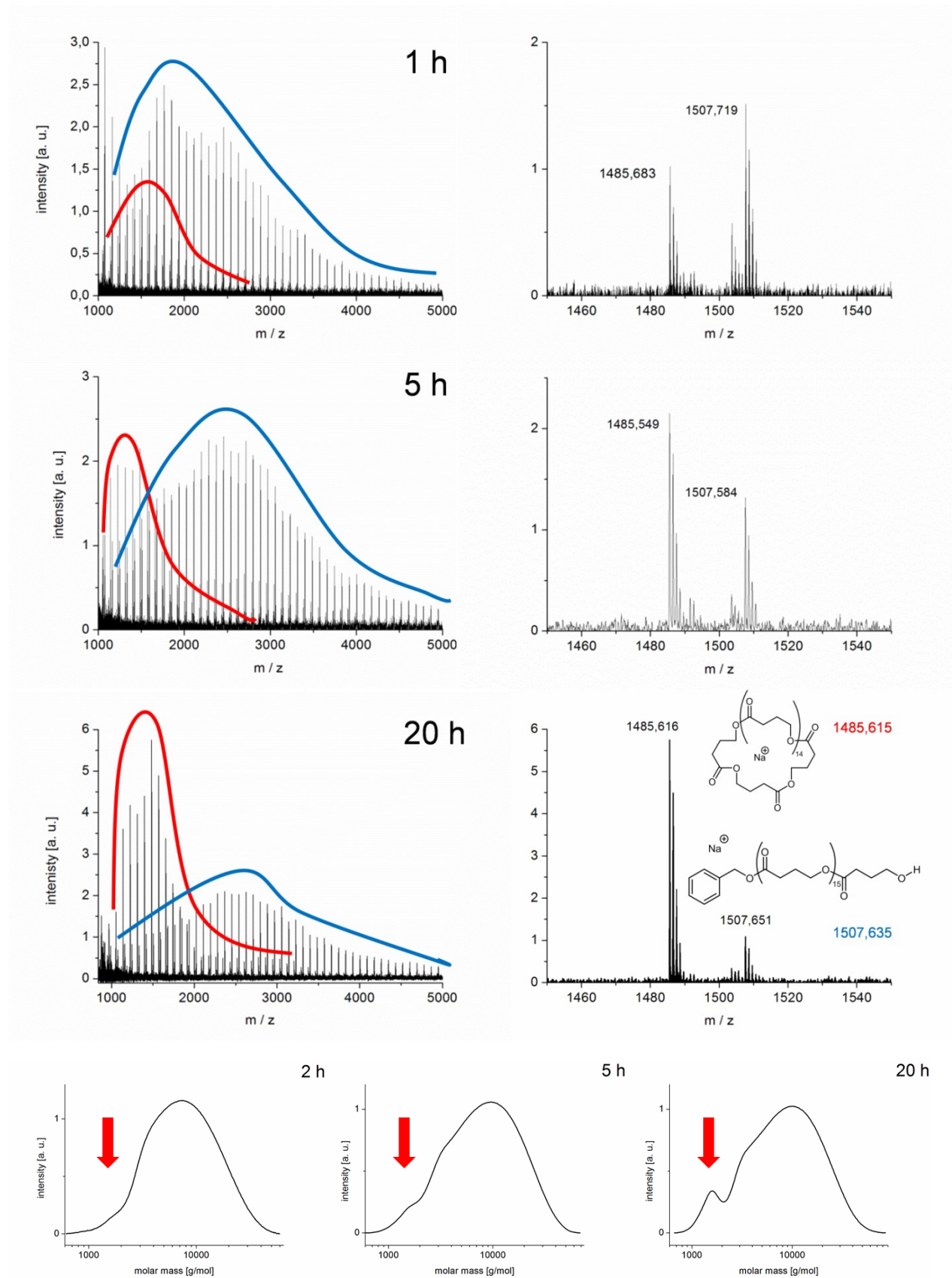


Figure S7. Organopolymerization using 3/BnOH/GBL = 1:2:200, bulk, -36°C. Correlation of polymerization time and MALDI-ToF profiles. As the reaction proceeds, the proportion of cyclic species increases. Bottom: Corresponding chromatograms. Over time, a low-molecular weight peak is gaining intensity. In analogy to MALDI-TOF MS analysis, this mirrors the increasing proportion of macrocyclic poly(GBL) as the polymerization proceeds.

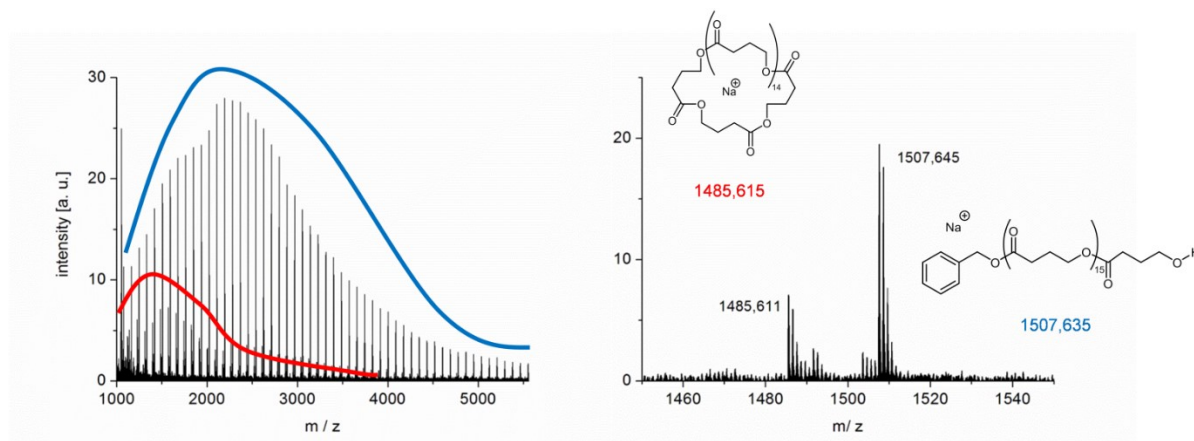


Figure S8. MALDI-ToF MS analysis of reaction 6/BnOH/GBL = 1:2:200, bulk, -36°C, 48 h. A mixture of linear and cyclic species is received.

Table S8. Control reactions conducted without initiator (BnOH).

Entry	NHO	Time [h]	Conversion ^{a)} [%]
1	1	72	-
2	2	72	-
3	3	96	-
4	4	96	-
5	5	72	-
6	6	72	-
7	7	72	-
8	8	72	-

Conditions: -36°C, bulk, NHO/GBL = 1:200; ^{a)}determined via ¹H NMR spectroscopy.

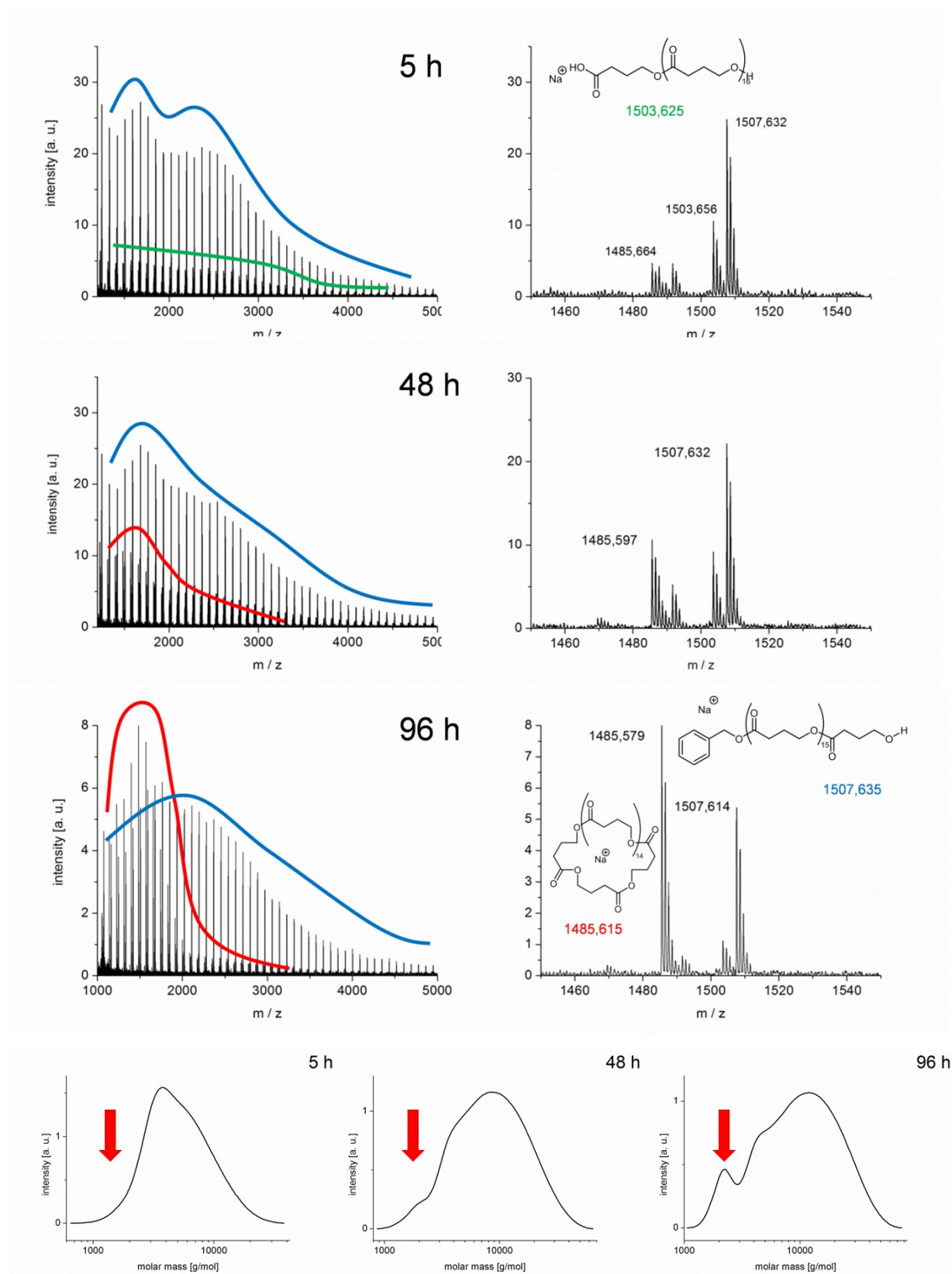
Dual catalytic polymerization of γ -butyrolactone

Figure S9. MALDI-ToF MS analysis of **3**/BnOH/LiCl/GBL = 1:2:5:200, bulk, -36°C . The proportion of the cyclic polymer population increases over time, yet much slower than in the analogous reaction without LiCl (compare **Figure S7**). The population marked green is OH/H terminated, most probably a result of hydrolysis in the acidic MALDI-ToF matrix. Bottom: Corresponding GPC traces, also displaying a low-molecular weight peak increasing over time.

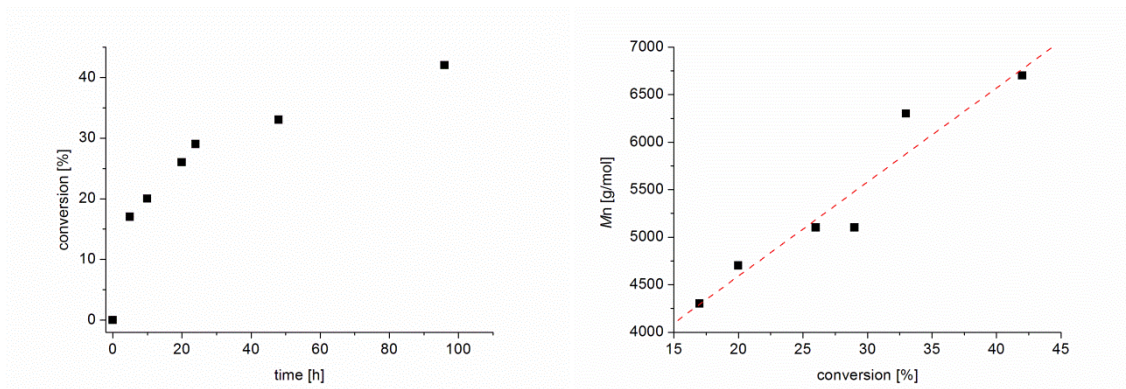


Figure S10. Correlation of conversion vs. time and M_n vs. conversion for **3**/BnOH/LiCl/GBL = 1:2:5:200, bulk, -36°C.

Table S9. Polymerization of GBL using lithium iodide (LiI) as cocatalyst. NHO/BnOH/LiI/GBL = 1:2:5:200, -36°C, bulk.

Entry	NHO	Time [h]	Conversion ^{a)} [%]	\overline{M}_n ^{b)}	\mathcal{D} ^{b)}
1	1	48	9	1400	1.76
2	2	48	27	4200	1.45
3	3	48	24	4500	1.46
4	4	48	-	-	-
5	5	48	-	-	-
6	6	48	16	3700	1.45
7	6	72	20	4500	1.33
8	7	48	15	2300	1.40
9	8	48	16	3800	1.38

^{a)}determined via ¹H NMR spectroscopy; ^{b)}determined via GPC (CHCl₃).

Table S10. Polymerization of GBL using lithium triflate (LiOTf) as cocatalyst. NHO/BnOH/LiOTf/GBL = 1:2:5:200, -36°C, bulk.

Entry	NHO	Time [h]	Conversion ^{a)} [%]	\overline{M}_n ^{b)}	\mathcal{D} ^{b)}
1	1	48	29	5200	1.42
2	2	48	27	4700	1.40
3	3	48	19	4500	1.40
4	4	48	9	3100	1.30
5	5	48	28	4300	1.47
6	6	48	19	4800	1.38
7	6	72	28	5800	1.43
8	7	48	18	4400	1.39
9	8	48	11	4400	1.34

^{a)}determined via ¹H NMR spectroscopy; ^{b)}determined via GPC (CHCl₃).

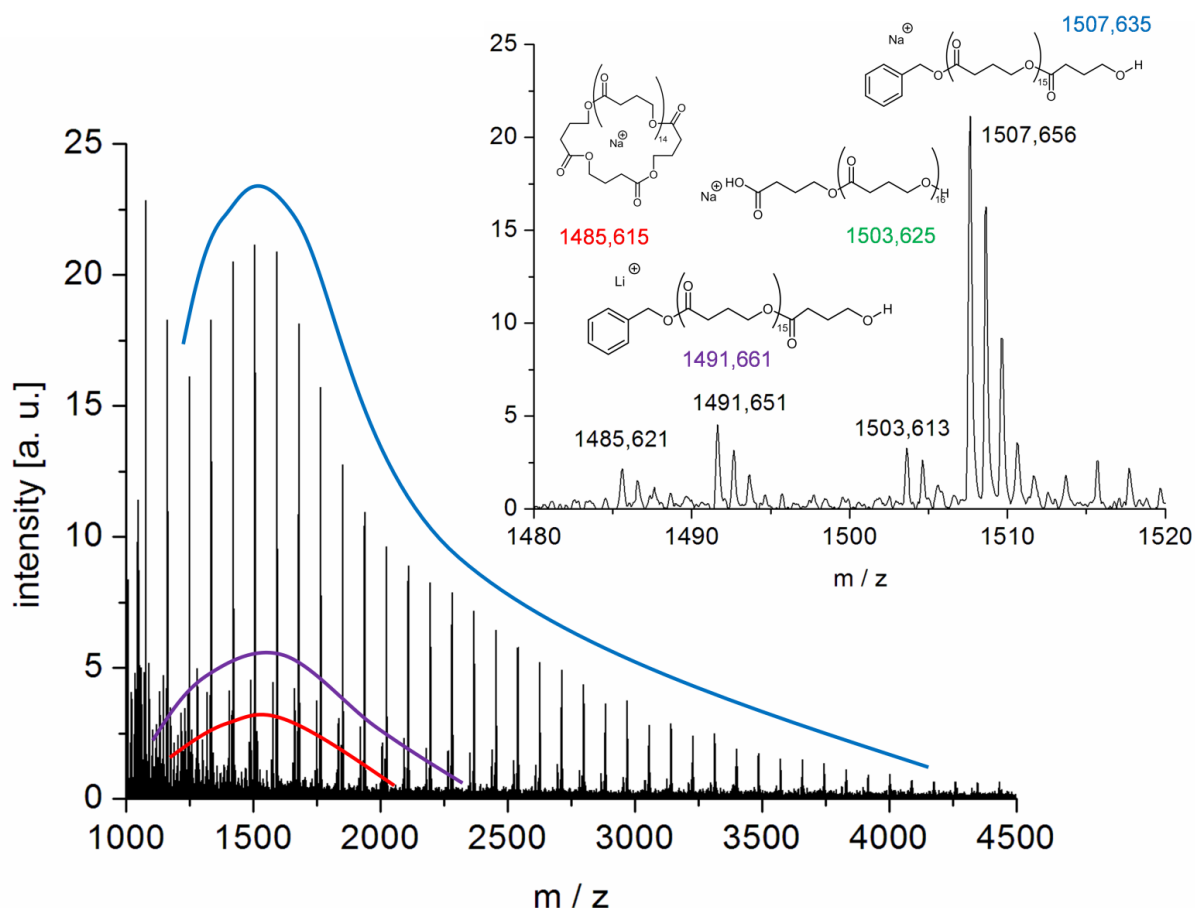


Figure S11. MALDI-ToF profile as received by the action of 6/BnOH/LiI/GBL = 1:2:5:200, bulk, -36°C, 72 h. Even after prolonged reaction time, the linear species terminated by the initiating BnOH stays the dominating population (cationized either by sodium or by residual lithium). The OH/H-terminated fraction (green) can result from hydrolysis of either macrocyclic or linear polyester chains, most probably during matrix preparation.

Table S11. Polymerization of GBL in the presence of lithium salt but absence of BnOH, using different NHOs. NHO/LiX/GBL = 1:5:200, bulk, -36°C.

LiX	NHO	Time [h]	Conversion ^{a)} [%]	\overline{M}_n ^{b)}	\mathcal{D} ^{b)}
LiCl	4	72	16	5800	1.6
LiCl	5	48	23	4500	3.9
LiCl	6	48	6	-	-
LiCl	6	72	13	9000	2.4
LiCl	7	72	15	3000	1.9
LiCl	8	48	17	7500	1.6
LiI	6	48	3	1600	1.7
LiI	6	72	6	2400	2.2
LiOTf	6	48	2	5300	1.4
LiOTf	6	72	4	6000	1.5

^{a)}determined via ¹H NMR spectroscopy; ^{b)}determined via GPC (CHCl₃).

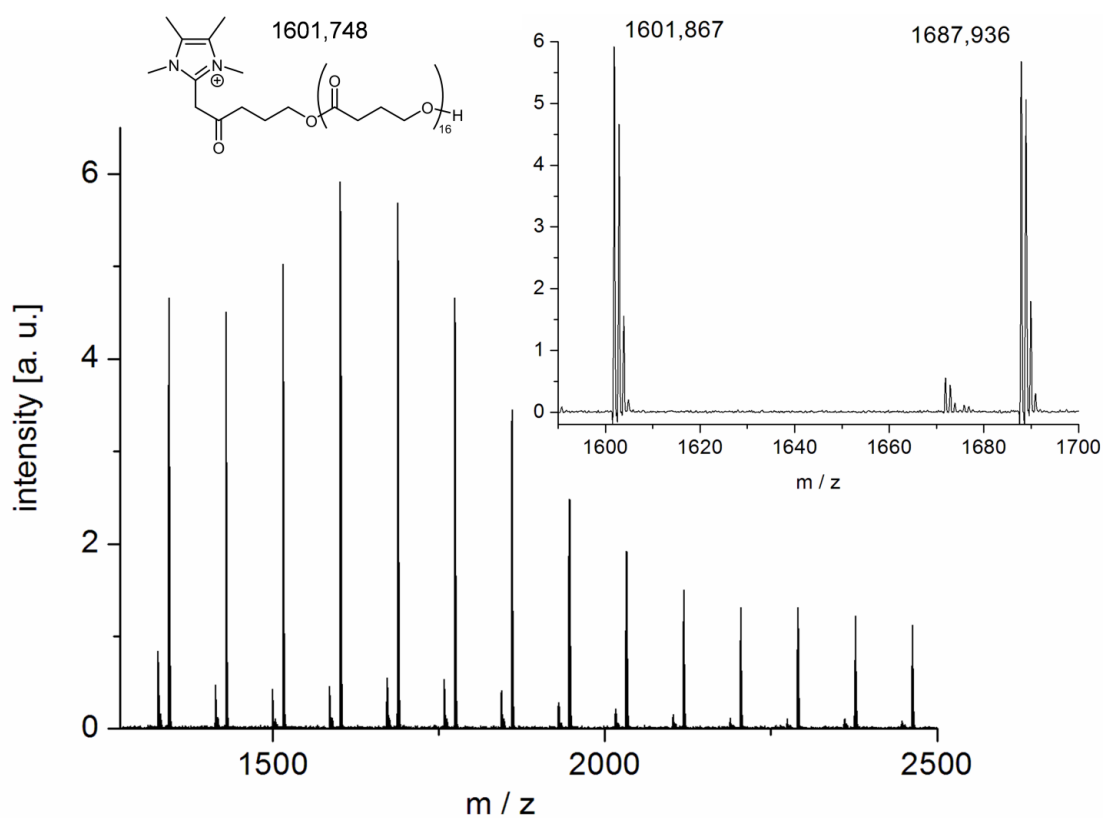


Figure S12. MALDI-ToF MS analysis of poly(GBL) prepared by the cooperative action of 7 and LiCl (7/LiCl/GBL = 1:5:200, bulk, -36°C). External Na⁺-cationizing agent added during matrix preparation.

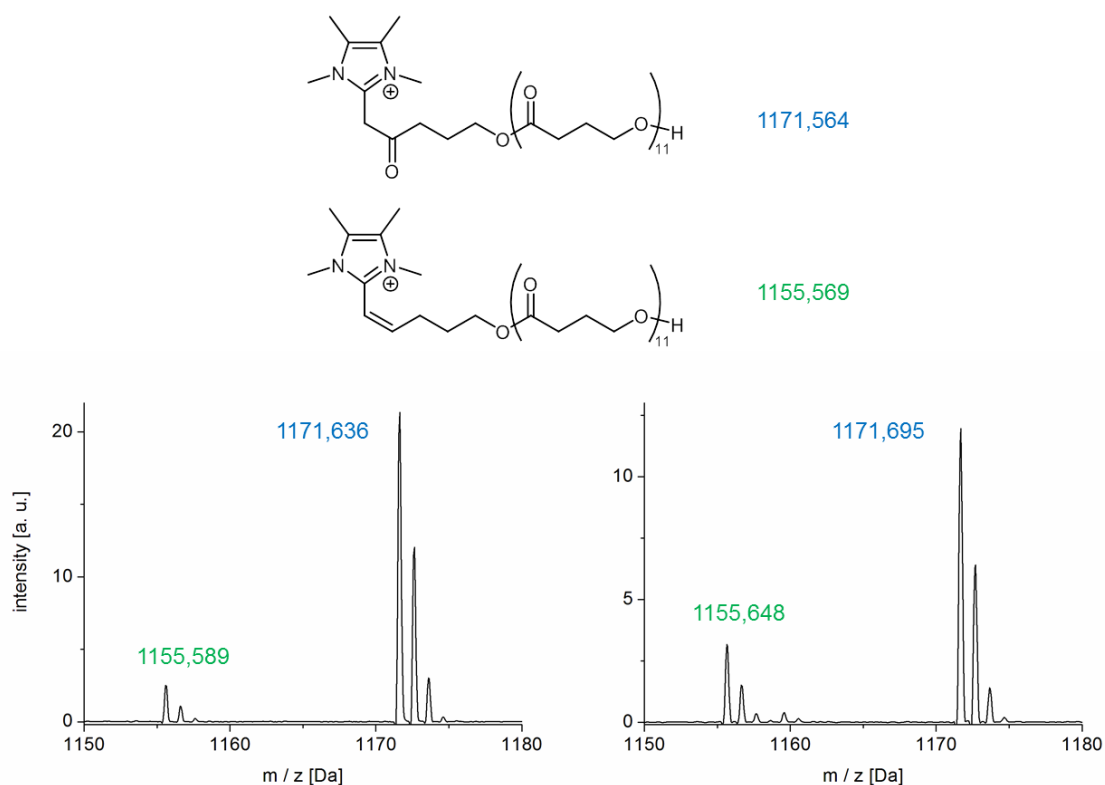


Figure S13. Detail from MALDI-TOF MS analysis regarding the poly(GBL) derived by the action of NHO 7 and LiCl (7/LiCl/GBL = 1:5:200, bulk, -36°C, compare also *Figure 2* and *Figure S12*), without (left) and with (right) Na⁺-cationizing agent added. From the data it can be concluded that also the minor population is NHO-cationized (not by Li⁺ or Na⁺). Deoxygenation, likely acid-catalyzed during matrix preparation, is proposed to account for this behaviour, generating an enlarged conjugated system.

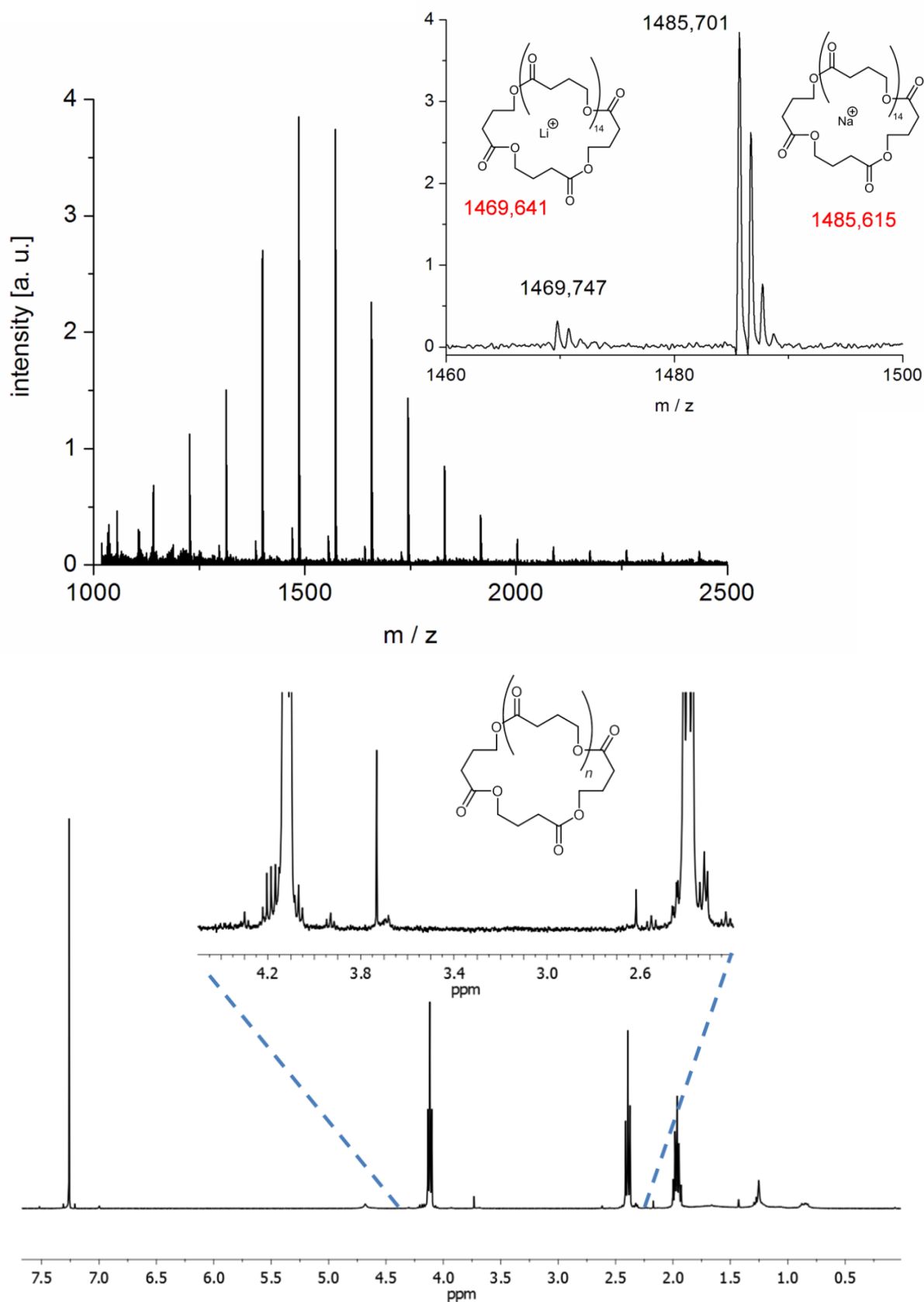


Figure S14. Top: MALDI-ToF MS analysis of poly(GBL) prepared by the cooperative action of **6** and LiCl (**6**/LiCl/BnOH = 1:5:200, bulk, -36°C, 48 h). External Na⁺-cationizing agent added during matrix preparation. Only oligocyclic species observed. Bottom: Corresponding ¹H NMR analysis (CDCl₃, 400 MHz, 300K). Compare *Figure S15*.

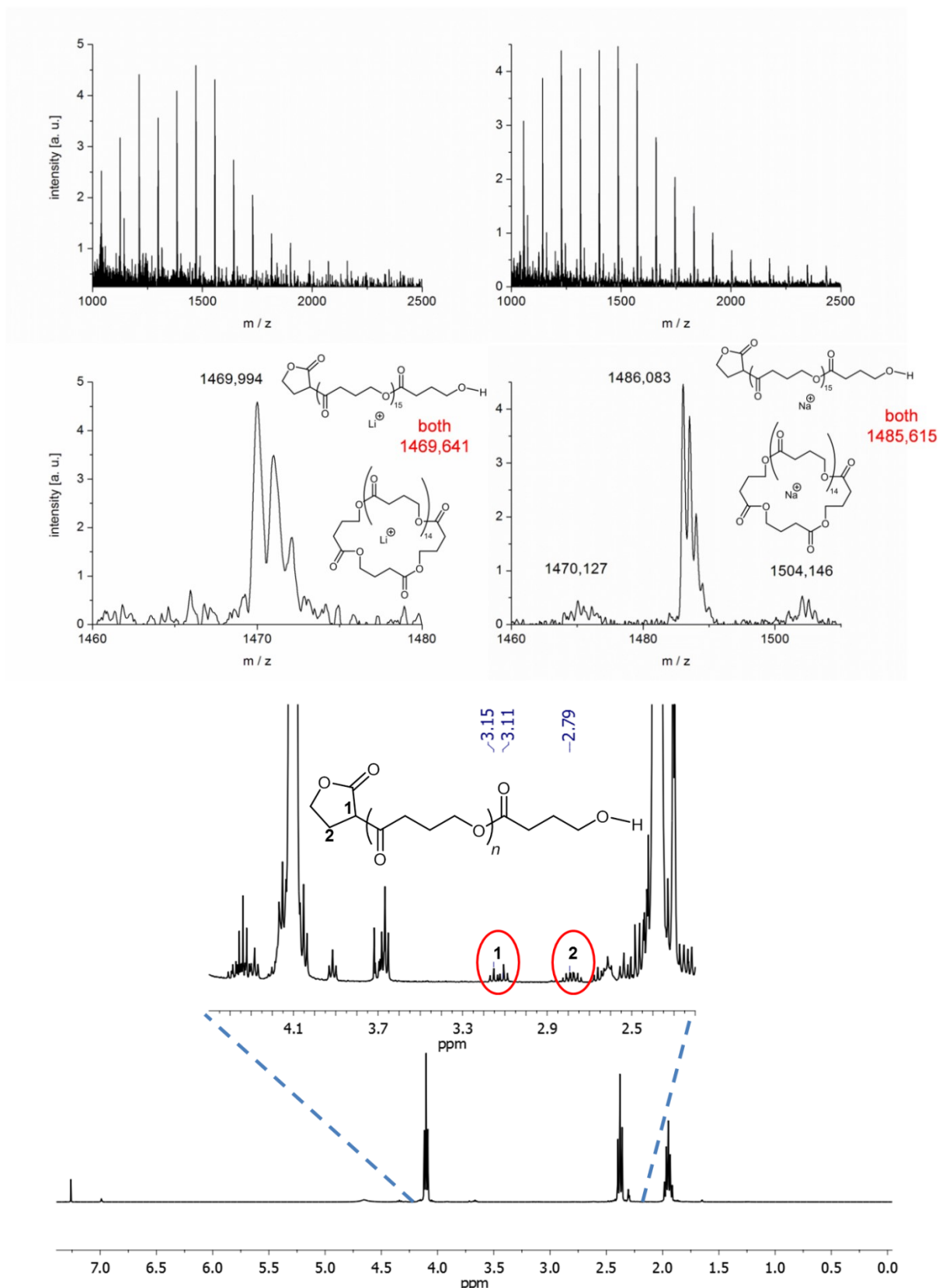


Figure S15. Top: MALDI-ToF MS analysis of polymer prepared by 6/LiCl/GBL = 1:5:200, bulk, -36°C, 72 h. Measurements were conducted with (left) and without (right) specifically added Na⁺-cationizing reagent for matrix preparation. The right profile also contains a small fraction of Li⁺-cationized cyclic species and OH/H-terminated polymer (resulting from hydrolytic cleavage of ester moieties). ¹H NMR analysis (CDCl₃, 400 MHz, 300K) and the distorted MALDI profile indicate that this is a mixture of oligocyclic and linear, enolate-derived poly(GBL). Compare *Figure S14*.

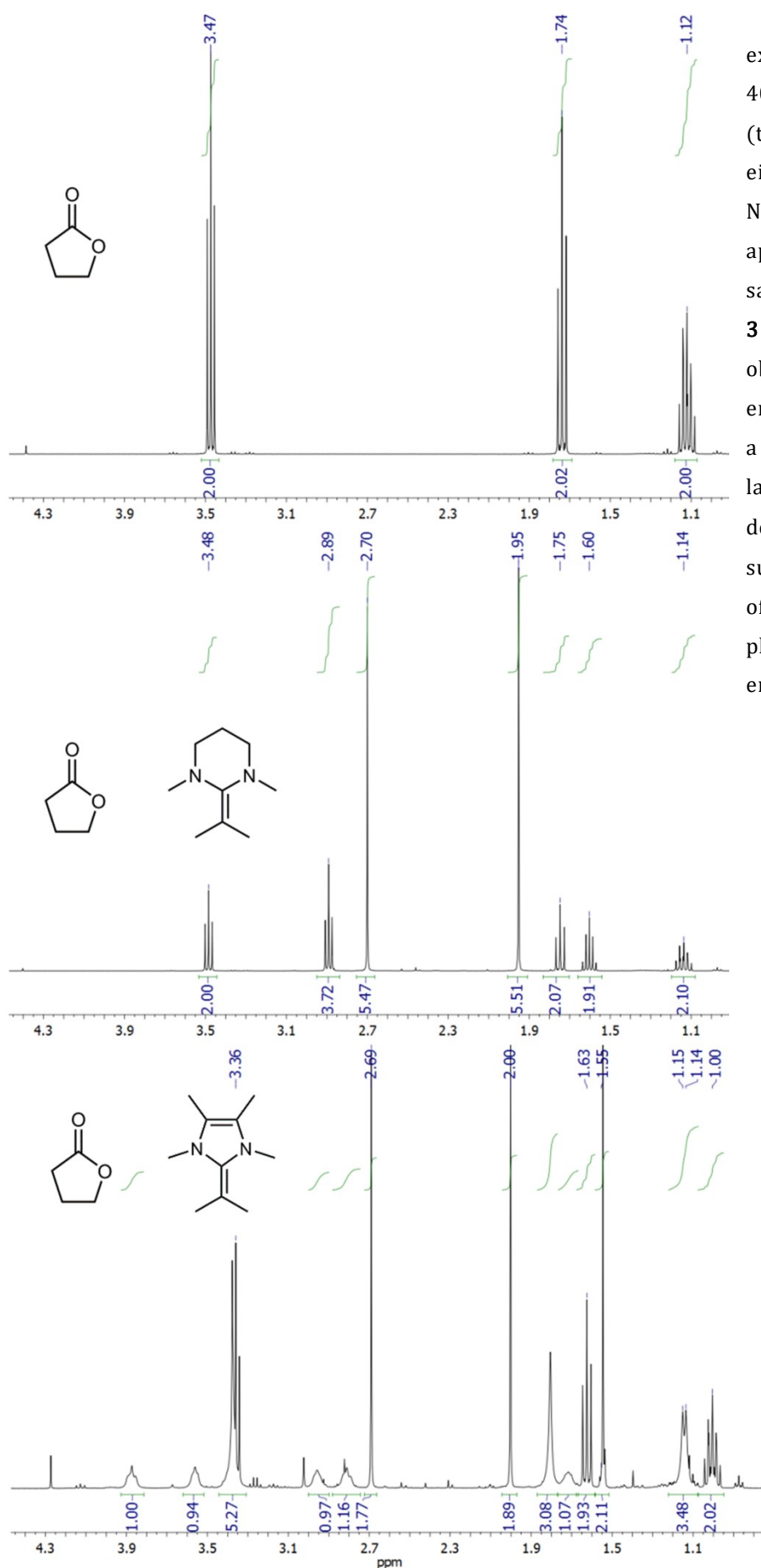


Figure S16. ^1H NMR experiments (C_6D_6 , 300 K, 400 MHz) using GBL alone (top) or in a 1:1 ratio with either NHO **3** (middle) or NHO **4** (bottom). While application of the saturated, six-membered **3** does not entail any observable changes, employment of **4** leads to a reaction. Isolation of the latter failed, but the broad doublet at $\delta = 1.14$ ppm suggests that protonation of the NHO has taken place, in turn indicating enolate formation.

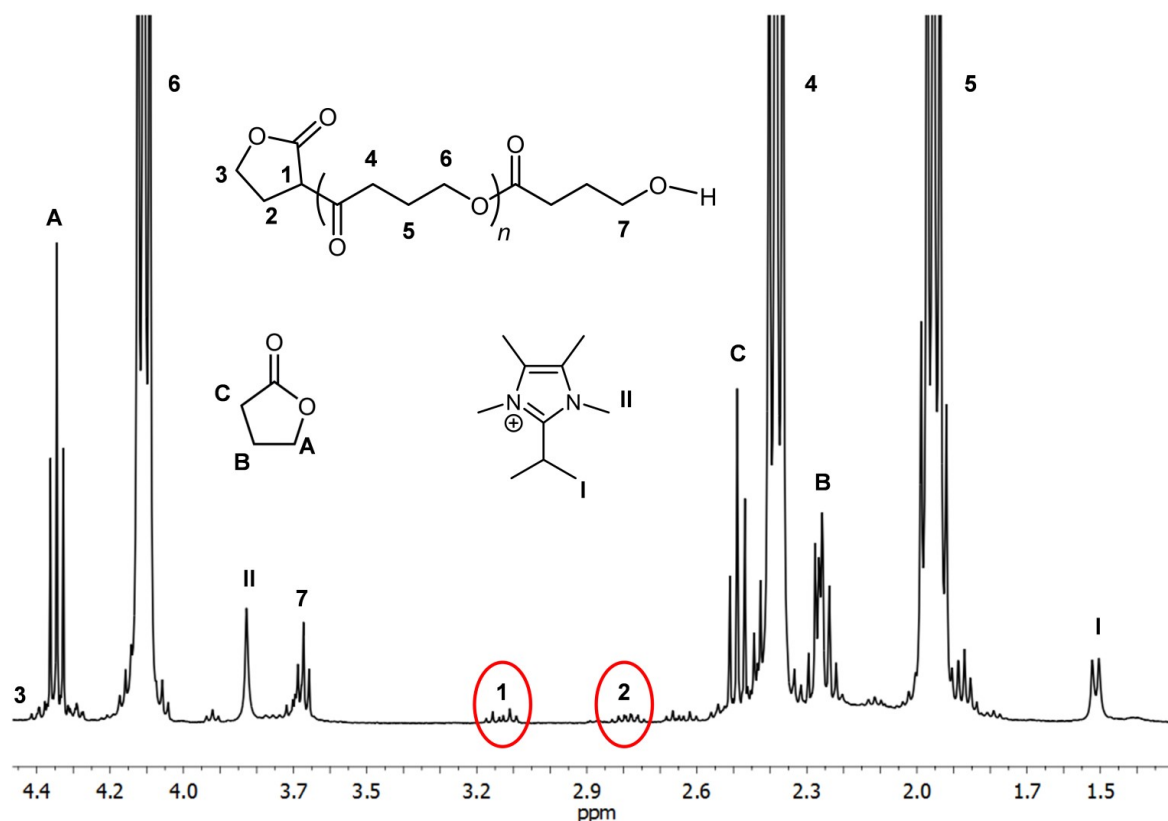


Figure S17. ^1H NMR (CDCl_3 , 300 K, 400 MHz) taken from a polymerization using 4/LiCl/GBL = 1:5:200, bulk, -36°C . Residual amounts of non-converted GBL and protonated NHO can be observed. The signals marked 1 and 2 can be attributed to enolate-derived end groups.

References

1. U. Gruseck and M. Heuschmann, *Chem. Ber.*, 1987, **120**, 2053-2064.
2. S. Kronig, P. G. Jones and M. Tamm, *Eur. J. Inorg. Chem.*, 2013, **2013**, 2301-2314.
3. S. Naumann and D. Wang, *Macromolecules*, 2016, **49**, 8869-8878.
4. K. Powers, C. Hering-Junghans, R. McDonald, M. J. Ferguson and E. Rivard, *Polyhedron*, 2016, **108**, 8-14.
5. H. Quast, M. Ach, M. K. Kindermann, P. Rademacher and M. Schindler, *Chem. Ber.*, 1993, **126**, 503-516.
6. M. Hans, J. Lorkowski, A. Demonceau and L. Delaude, *Beilstein J. Org. Chem.*, 2015, **11**, 2318-2325.
7. C. E. Knappke, J. M. Neudorfl and A. J. von Wangelin, *Org. Biomol. Chem.*, 2010, **8**, 1695-1705.
8. K. Hirano, S. Urban, C. Wang and F. Glorius, *Org. Lett.*, 2008, **11**, 1019-1022.
9. M. Iglesias, D. J. Beetstra, J. C. Knight, L.-L. Ooi, A. Stasch, S. Coles, L. Male, M. B. Hursthouse, K. J. Cavell, A. Dervisi and I. A. Fallis, *Organometallics*, 2008, **27**, 3279-3289.

3. Ring-Opening Polymerization of Epoxides

3.1. Introduction

Polyether materials are nowadays wide-spread amongst commercial applications in everyday life. This success stems from their extraordinary properties: due to the high flexibility of their polymer backbone, these materials possess a glass-transition temperature (T_g) of below $-60\text{ }^\circ\text{C}$, and the incorporated oxygen atoms along the backbone increase their hydrophilicity (e.g. poly(ethylene oxide) (PEO) is fully water-soluble). In order to generate polyether materials, the ROP of epoxides is the most straight-forward and well-established process to do so. Epoxides hereby feature a broad structural versatility, and their high ring-strain ($110 - 115\text{ kJ}\cdot\text{mol}^{-1}$ for ethylene oxide (EO))¹³⁶ represents a strong driving-force of polymerization, essentially turning propagation irreversible.¹ Furthermore, the two most commonly encountered monomers, namely ethylene oxide (EO) and propylene oxide (PO), are abundantly available in industry and readily prepared *via* the oxidation of their respective alkenes. Over the time, multiple approaches for the ROP of epoxides have been developed, and three mechanisms have been established; the first two being base- or acid-initiated, while the third mechanism is based on a coordination polymerization. Out of the three, the oxyanionic process is the most industrially relevant process, and is applied for EO, PO and butylene oxide (BO), annually producing about 33 million tons of polyether materials.⁷ Other epoxides like epichlorohydrine (ECH), longer alkylene epoxides or glycidyl ethers and amines experience an increase in academic research interest, but to date lack commercial importance. This is, on the one hand, justified by their increased synthetic effort, but on the other hand, also due to a lack of synthetic tools to form their respective polymers: especially for longer alkylene epoxides, a significant drop in reaction rates can be noted, up to a point where no polymer formation can be observed.^{9b}

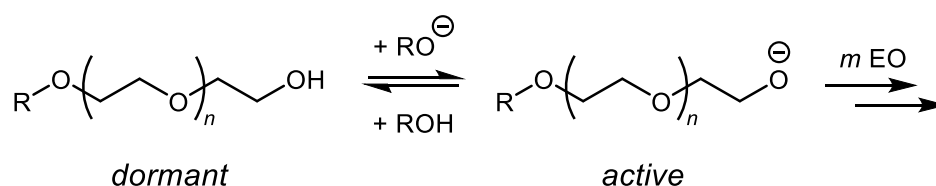
First reported as early as 1863, the ROP of EO has been established by *Wurtz* et al. applying alkali metal hydroxide or zinc chloride to form oligomeric PEO (poly(ethylene glycol), PEG, if MW is below $30\,000\text{ g}\cdot\text{mol}^{-1}$).¹³⁷ In the 1930s, after seminal work by *Staudinger* and *Schweitzer*, PEG was commercialized for applications in pharmaceuticals, lubricants, cosmetics and detergents; the polymerization was initiated by ethylene glycol under basic conditions. *Flory* first established the base-initiated mechanism of EO polymerization in 1940, and predicted a Poisson-type molecular weight distribution for the living chain-growth

process for the first time;^{35a} later that decade, PPO finally found application as liquid polyols for hydraulic fluids and lubricants. In the 1950s, PEO emerged as the most important class of non-ionic surfactants, contributing as polar and water-soluble block, and is nowadays produced on a million-ton scale. Today, both PEO and PPO have established themselves in a broad range of industrial, pharmaceutical, cosmetic and medical applications, owed to their unique material properties. PEO for example is a crystalline, thermoplastic polymer with high water solubility, very low immunogenicity, antigenicity and toxicity.⁷ Intriguingly, this water-solubility is limited to PEO, and stems from the oxygen's distance in the polymer backbone resembling the hydrogen's distance in the water molecule. Depending on the molecular weight, PEOs can either exist as liquids or low-melting solids (65 °C for high-MW PEO), further broadening the versatility of applications. Also, "PEGylated" therapeutic peptides, proteins and liposomes feature greatly enhanced blood circulation times. PPO on the other hand is a material, that possesses a T_g of -70 °C and no melting point, owed to the fact that the usually atactic topology (resulting from the racemic monomer) precludes crystallization. The additional methyl group further impedes the dissolution of PPO in water at r.t., although elevated temperatures somewhat increase the solubility, given that the molecular weight remains in the oligomeric range. The industrial preparation of PPO is realized by using potassium hydroxide together with alcohols as initiators, a low-cost and straight-forward process that, however, suffers from several limitations (*vide infra*). Furthermore, PO is often used for the synthesis of star-polymers (for example as rheology modifiers), whereby multifunctional initiators are employed. PPO applications range from lubricants, to antifoaming agents, softeners, rheology modifiers, flexible poly(urethane)-foams and, in combination with PEG, non-ionic surfactants.

3.2. Catalytic Systems

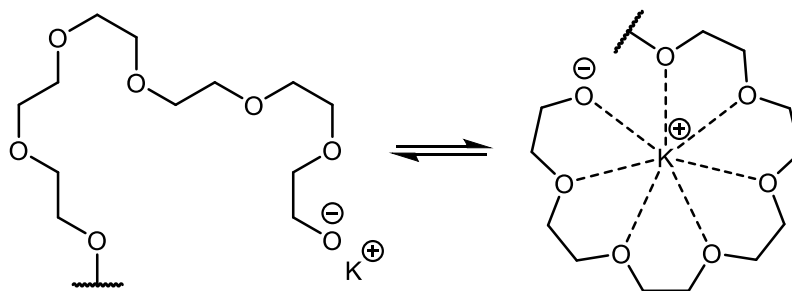
3.2.1. Oxyanionic ROP

Ever since the 1930s, the base-initiated anionic ROP of epoxides represents the key technique to synthesize polyether materials. To date, it is still employed for the majority of PEO/PPO production, despite severe drawbacks regarding molar masses and side-reactions. Hereby, a nucleophile is used as an initiator (e.g. H₂O or alcohols), and the monomer is slowly added to the reaction mixture in presence of alkaline catalysts that feature high nucleophilicity. If higher molar masses are targeted, alkali metal hydrides, alkyls, aryls, hydroxides, alkoxides or amides can be employed in a living anionic ROP of EO, together with an inert solvent. This process is well-understood since 1977,¹³⁸ and several key features have been identified: in this regard, the counterion should possess a low Lewis acidity, to ensure little to no interaction with the propagating chain-end. Furthermore, a polar and aprotic solvent has to be used, typically chosen amongst the range of THF, DMSO, or, historically, HMPA. The process can further be carried out in bulk; however, molar masses will be lower and a broader molecular weight distribution ensues. Representative systems are usually based on sodium, potassium or caesium compounds using THF as a solvent. Furthermore, crown-ethers have been identified as supplements to significantly accelerate epoxide polymerization, as they are able to form complexes with the employed counterions and hamper aggregation.¹³⁹ As the polymerization of EO can be performed in a living manner, a facile and quantitative end-functionalization is feasible. Furthermore, the active chain-end is rather stable, attributable to an equilibrium between the oxyanionic species (active chain-end) and a dormant species (hydroxy-terminated), realized by a rapid proton exchange with an initiator (Scheme 52); this extremely fast proton exchange has been exploited in employing an alkoxide plus its respective alcohol as initiator. The importance of the counter-ion manifests when regarding lithium-based initiating systems. Here,



Scheme 52: Equilibrium between dormant and active species during EO polymerization, interconverted *via* an extremely fast proton exchange.

no polymer formation can be observed; instead only one ring-opening step is realised, leading to the formation of an alkoxide-lithium-bond with noticeable covalent character. This can be justified when considering the “hard and soft acids and bases” (HSAB) concept:¹⁴⁰ the strong interaction between the similarly “hard” oxygen and lithium ions lead to the formation of closely interacting ion-pairs and thus quenching reactivity. Generally, for EO, several factors limit the molar mass of the polymer to about 50 000 g·mol⁻¹, using the oxyanionic approach.¹⁴¹ In accordance with kinetic considerations discussed above (cf. chapter 1.1.3), the nature of the ionic species present during polymerization is pivotal to the respective rate constants of propagation. Hence, it is readily conceivable that close ion pairs with low dissociation constants in THF, as well as ion triplets and higher associates also dictate epoxide polymerization. However, as the PEO-backbone is highly flexible, it can also entangle to self-coordinate the cation by forming crown-ether-like structures, and generating a so-called “penultimate effect” (Scheme 53). Due to this effect, a dependence of the chain-end’s reactivity on the number of monomer units already added is observed. This effect does not occur during PO polymerizations; yet, the molar mass of PPO polymers derived from the oxyanionic approach are even more severely limited to about 6000 g·mol⁻¹. This is caused by the increased basicity of the propagating chain-end. In contrast to EO, the active species during PO polymerization is a secondary alkoxide, that features sufficient basicity to deprotonate a monomer molecule, leading to ill-defined polydispersities and allylic end-groups (Scheme 9). The nature of the counter-ion influences this transfer-to-monomer side-reaction, and is most pronounced for sodium cations, followed by potassium- and caesium-based systems, according to the strength of their interactions with the alkoxide.¹⁴² There exist improved conditions to somewhat mitigate this issue and maintain a living character of oxyanionic PO polymerization, enhancing the achievable molecular weights to 13 000 g·mol⁻¹ by applying crown-ethers as complexing agents.¹⁴³

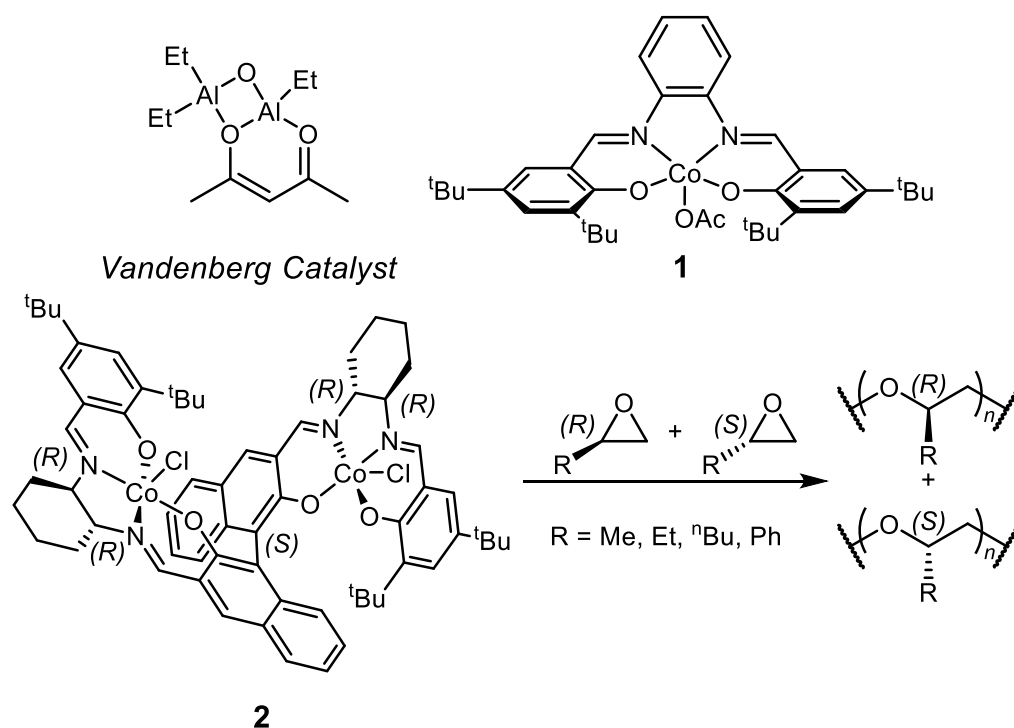


Scheme 53: Self-solvation of a potassium counter ion by a PEO-backbone, leading to a “penultimate effect” that affects the reactivity of the active chain end, depending on the number of monomer units incorporated thus far.

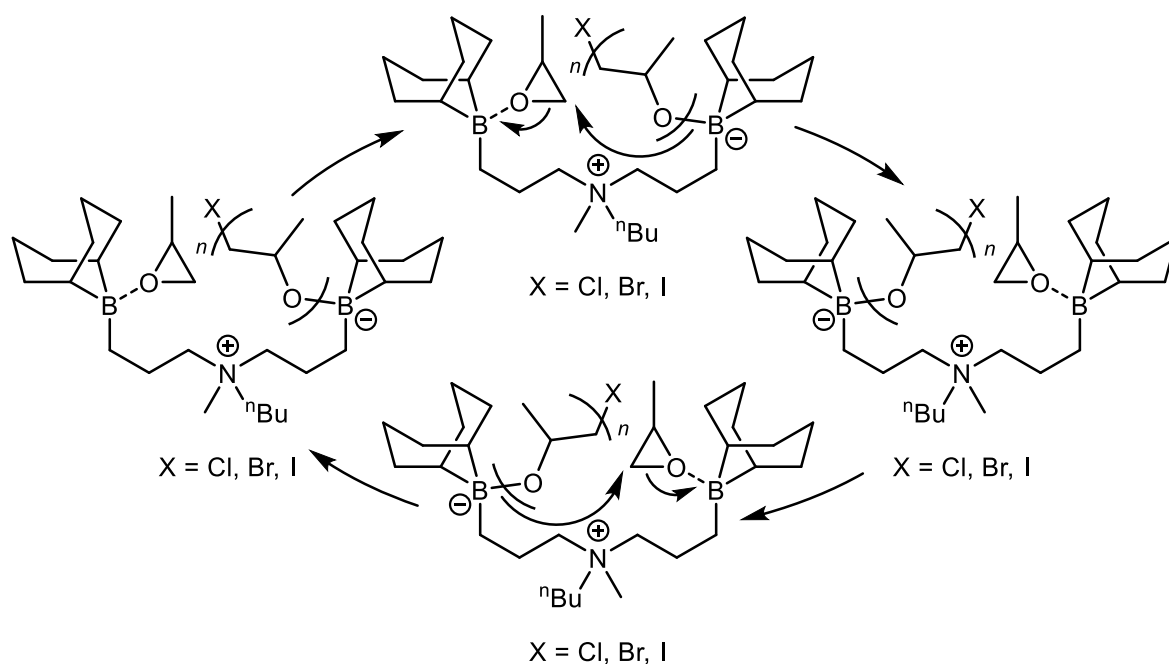
3.2.2. Coordination Polymerization

Due to the above stated intriguing material properties, high-molecular-weight polyethers would be of great interest for industrial, medical or pharmaceutical applications. Yet, molar masses exceeding $50\,000\text{ g}\cdot\text{mol}^{-1}$ remain out of grasp for the traditional, oxyanionic approach (*vide supra*). Hence, intensive research efforts have been focused on developing well-defined catalysts, to pursue a coordination – insertion-based polymerization mechanism that would enable polyether syntheses to break free of their limitations. These efforts have excellently been reviewed in literature,¹⁴⁴ which is why concise highlights shall avail at this point. Typically, catalysts employed in this type of polymerization are composed of an organometallic, and a protic compound. This generates an active M-X-bond, that is incorporated in often multinuclear structures, while also non-associated catalysts have been reported. Generally, the catalyst is designed to fulfil the purpose of monomer activation, and ideally induce stereoselectivity *via* the formation of suitable (chiral) environments. In most cases, di- and trivalent metals like calcium, zinc or aluminium are used, as the need for Lewis acidity is obvious. One might tend to the assumption, that the same rationale of design as used in the polymerization of vinyl monomers might be applicable here; however, there are some peculiarities that distinguish the ROP of epoxides from the polymerization of vinyl-bearing monomers, that need to be considered when designing novel catalysts. During the initiation and propagation, the oxygen atom of the monomer will enter bond-formation with the metal, resulting in a bond of significant σ -character. The monomer is then ring-opened by a nucleophilic attack of the initiator or the active chain-end, respectively. Together with amides and amide-alkoxides, catalysts based on alkaline earth metals are amongst the most active systems for EO. They feature a broad range of activity (0 – 50 °C), which lies below the melting point of PEO. This tremendously increases industrial relevance, as now the technique of dispersion polymerization becomes feasible. Here, the formed polymer will directly precipitate and can simply be filtered off at the end of the reaction, which results in little to no catalyst contamination. Calcium-based catalysts, that are mostly object of patent literature, proved to be particularly effective for EO polymerization.¹⁴⁵ Considering the fact, that EO has a higher propensity to form complexes compared to PO, this fact becomes readily conceivable as calcium exhibits a weaker coordination with epoxides. Furthermore,

this also explains why calcium-based complexes are ineffective for PO polymerization: the monomer activation is simply not strong enough, leading to a low reaction rate. Yet, for EO, calcium catalysts reported in literature are able to produce 1800 g PEO per gram calcium, which excludes the necessity of further purification.¹⁴⁵ Other important examples include the so-called *Vandenberg Catalyst*, which is comprised of a mixture of AlEt₃, 0.5 eq. of H₂O and 0.5 eq. of acetylacetonate (Scheme 54), and was developed as early as 1960.¹⁴⁶ This represented the first example of a catalytic system, that later delivered PPO of over 550 000 g·mol⁻¹ on an industrial scale, while the polymers even featured some degree of isotacticity.¹⁴⁷ Yet, hitherto, neither the underlying mechanism nor the catalyst structure itself have been conclusively elucidated. Salient work by *Coates* et al. was published in 2005, where a cobalt(III)-salicylidine-based catalyst succeeded in the synthesis of purely isotactic PPO (Scheme 54, compound **1**, > 99 % *mm*-triad placement, M_n over 250 000 g·mol⁻¹, $D_M = 1.5 - 2.5$).^{22a} However, clarifying the polymerization mechanism revealed that the active species was not the homogeneously dissolved, but rather the non-dissolved fraction of the catalyst. In the solid-state, the catalyst possessed a pseudo-*C*₂-symmetry which placed the cobalt-centers at a favourable distance of 713 pm, enabling a bimetallic polymerization mechanism in a chiral environment. This permitted the authors to design a fully homogeneous congener of this catalyst, while maintaining the bimetallic motif envisioned before (Scheme 54, compound **2**).^{22b} Indeed, this catalyst succeeded in the polymerization of a range of monosubstituted epoxides (Scheme 54, R = Me, Et, ⁿBu, Ph), performing at TOFs of up to 30 000 h⁻¹, while maintaining extraordinary stereoselectivity (> 98 % *mm*-triad placement). This system was further improved by the same group, and their findings have concisely been reviewed in literature.^{22c, d, 148} Only recently, *Wu* et al. have developed the first highly active metal-free ROP of PO and EO, that reached molar masses exceeding 10⁶ g·mol⁻¹ for PPO with good control over polydispersities ($D_M = 1.07 - 1.33$).¹⁴⁹ Chain-extension experiments, as well as kinetic analyses furthermore suggested a living character of this polymerization. The authors employed a bifunctional catalyst with two borane-based moieties on the two sides as Lewis acidic monomer activators, while the center featured a quaternary ammonium halide as initiating site (Scheme 55). This catalyst displayed high activity even at low catalyst loadings of 5 ppm, and represents the most active, metal-free approach to generate high molecular weight polyethers to date.



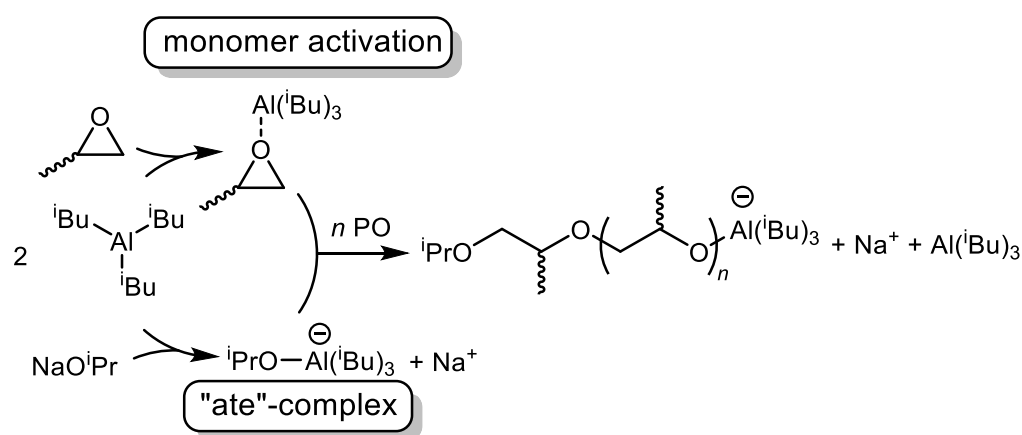
Scheme 54: Top left: Proposed structure of the Vandenberg Catalyst. Top right: cobalt-salicylidine-based catalyst, capable of producing isotactic PPO ($M_n > 250\,000\text{ g}\cdot\text{mol}^{-1}$). Bottom: improved version of **1**, now fully homogeneous and capable of stereoselectively polymerizing a range of monosubstituted epoxides, if a racemic mixture of **2** is applied.



Scheme 55: Catalytic cycle of the first highly active metal-free ROP of PO, as proposed by *Wu* and co-workers. The Lewis acidic boron-derived moieties act as monomer activator, while the quaternary ammonium halide in the center acts as initiating site. Scheme adapted from literature.¹⁴⁹

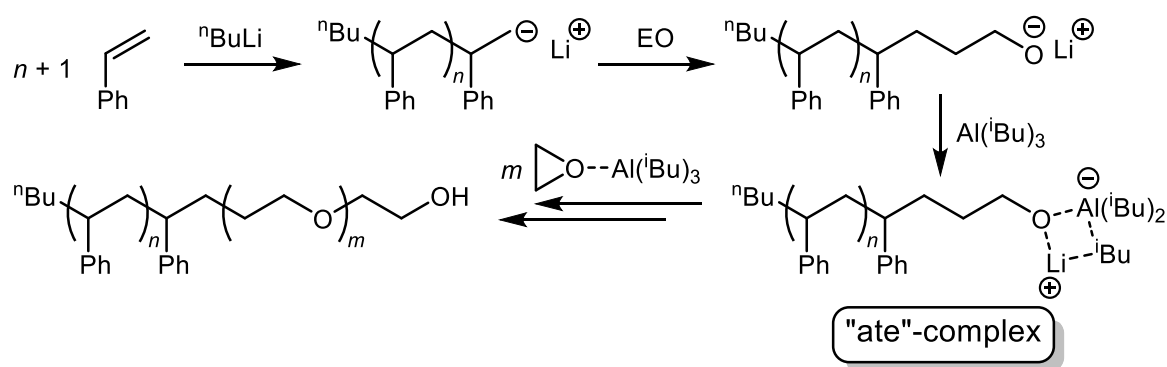
3.2.3. Activated Monomer Mechanism

Much like the activated monomer mechanism introduced in chapter 1.1.4.1, the epoxide is activated with a LA, which increases the electron deficiency at the α -carbon adjacent to the heterocyclic oxygen. Subsequently, the monomer is ring-opened by a weak nucleophile, initiating polymerization, which then propagates *via* the nucleophilic attack of the active chain-end on another activated monomer. Strictly speaking, this places the described mechanism in the context of Lewis Pair chemistry, and might thus also be regarded as a type of Lewis Pair Polymerization. However, as this method was developed as an improvement of the already existing oxyanionic process, even without the LA-activated monomer, most of the systems still display polymerization activity towards several epoxides, albeit with lower activity and/or control. A conclusive review of systems is provided in literature,¹⁵⁰ which is why here only the general concepts and distinct features will be highlighted. In 2004, *Deffieux* et al. reported the fast and efficient polymerization of PO using a catalytic system comprised of an alkali metal and a trialkylaluminium-species (Scheme 56).¹⁵¹ This enabled the authors to synthesize PPO with a molecular weight of 170 000 g·mol⁻¹ ($\bar{D}_M = 1.34$) in under 2 h. The polymer exhibited exclusive head-to-tail-linkages with no apparent stereoselectivity. This increase in polymerization activity and little side-reactions, can be reasoned by the interaction of the alkyl-aluminium-species with the propagating chain-end. The LA hereby attenuates the basicity of the secondary alkoxide *via* coordination, reducing the commonly encountered transfer-to-monomer reaction. Mechanistic studies further revealed, that a LA/I-ratio of > 1 is mandatory, in order to ensure an efficient polymerization. This was attributed to the preceding



Scheme 56: Monomer activation mechanism employing triisobutyl-aluminium and weakly nucleophilic initiators for the polymerization of PO. Scheme adapted from literature.¹⁵¹

formation of an "ate"-complex, which acts as initiating species to ring-open the LA-activated monomer (Scheme 56). Generally, a strong monomer activation offers mitigation to several key issues of epoxide polymerization: the reactions can be conducted under mild conditions ($-30\text{ }^{\circ}\text{C}$ – r.t.), while weak nucleophiles and propagating species ensure a narrow molecular weight distribution. Also, drastic increases of polymerization rates were observed, which enabled *Carlotti et al.* in 2010 to polymerize EO using lithium-salts, generating copolymers with poly(styrene) and poly(isoprene) in a one-pot procedure (Scheme 57).¹⁵² Furthermore, as demonstrated in literature, this approach broadened the accessible monomer range of epoxides to BO and 1,2-hexylene oxide, while also displaying a functional group tolerance in the polymerization of ECH.¹⁵³

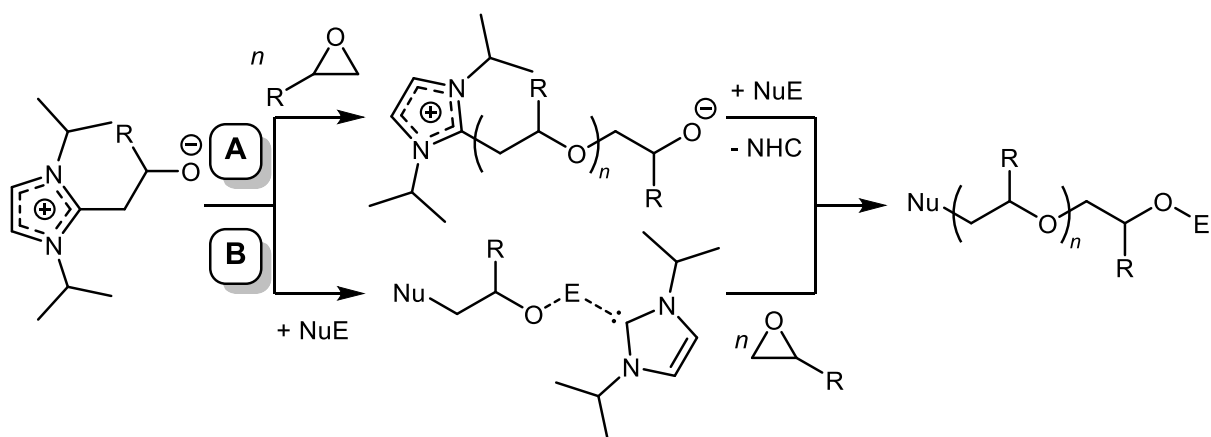


Scheme 57: One-pot synthesis of PS-*b*-PEO copolymers, enabled by the activated monomer approach *via* the formation of an "ate"-complex with a lithium-based catalyst.

3.2.4. N-Heterocyclic Carbenes

Ever since the emergence of NHCs in 1991,¹⁵⁴ they have been established as an incredibly versatile class of organic compounds, finding applications in a multitude of catalytic transformations or ligand chemistry. Of course, polymer chemistry is no exception to that, and the application of NHCs as organocatalysts in macromolecular chemistry has also been reviewed.¹⁵⁵ For the ROP of epoxides, however, NHCs so far fell short of their usual performance. Nevertheless, EO polymerization was established in 2009 by *Taton et al.*, which succeeded in the synthesis of α,ω -bifunctional PEG, without the occurrence of cyclic species.¹⁵⁶ The mechanism hereby proceeded *via* a nucleophilic attack of the NHC on the monomer, generating a zwitterionic species. The authors then proposed two possible ways of propagation: either the generated zwitterion will directly participate in chain-extension (activated

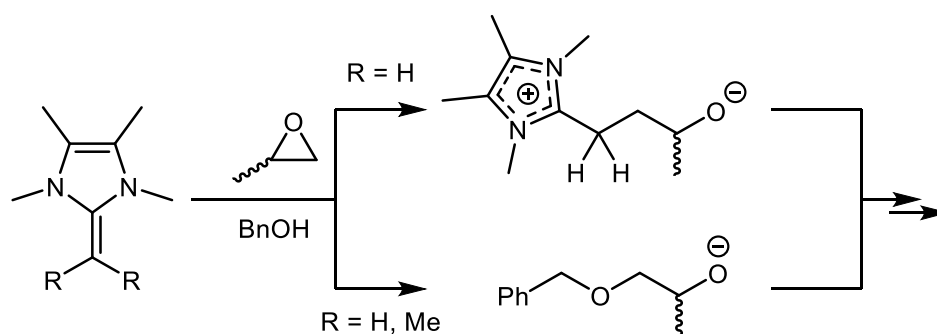
monomer mechanism, Scheme 58, **A**), and the termination agent (comprised of a nucleophile and an electrophile (NuE)) will terminate the chain ends, liberating the NHC in the final step of the polymerization. The second pathway proposed, that the NHC acts as a catalyst (chain-end activation, Scheme 58, **B**). Here, NuE will act as a chain regulator, which directly resubstitutes the NHC at the zwitterion, and subsequent propagation will form the already α,ω -functionalized polymer. Using this approach, azide-functionalized PEG could be synthesized, that possesses potential applications in click-chemistry. Furthermore, block-copolymers with PCL were also feasible, as NHC display a pronounced ability to polymerize cyclic esters (*vide supra*). Finally, in 2010, the same group extended their approach to PO.¹⁵⁷ However, conversions remained below 40 % despite prolonged reaction times of 3 days, while also displaying allyl-terminated species if the molecular weight exceeded 4500 g·mol⁻¹.



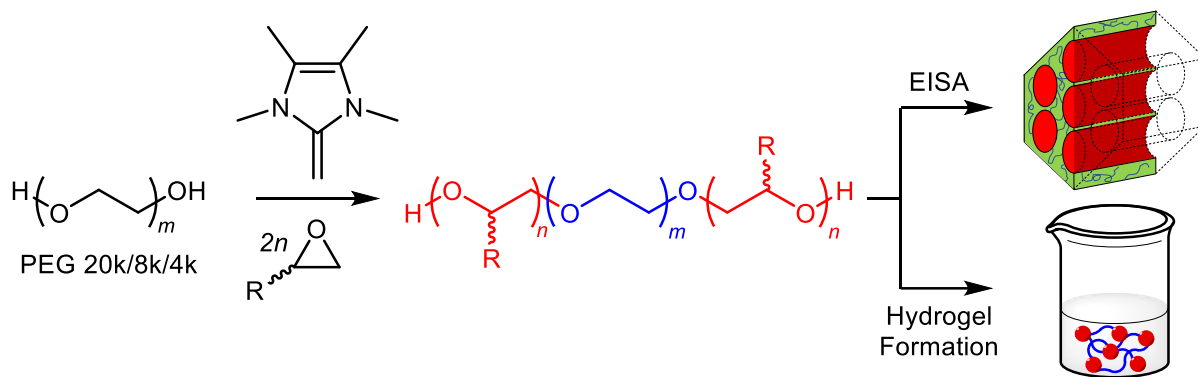
Scheme 58: NHC-catalyzed ROP of (substituted) epoxides. The initial zwitterion is formed *via* the nucleophilic attack of the NHC on the respective monomer. Pathway A represents a monomer activated mechanism, where the zwitterionic species directly participates in chain-extension, until it is finally terminated. In pathway B, the chain-end-activated mechanism, NuE directly resubstitutes the NHC, after which propagation proceeds to form the α,ω -bifunctional polyether.

3.2.5. N-Heterocyclic Olefins

To the best of the author's knowledge, the application of NHOs in polyether synthesis *via* the ROP of epoxides is limited to our group. Established in 2015 by *Naumann, Thomas* and *Dove*, a system comprised of several NHOs and benzyl alcohol (BnOH), succeeded in the preparation of well-defined PPO (88 %, 68 h, M_n up to 12 000 g·mol⁻¹, $D_M < 1.06$, TON up to 2200).^{8a} The key to this extraordinarily well-controlled reaction was the subtle adjustment of the NHO's structure to feature a dimethyl substitution on the exocyclic carbon atom (Scheme 59). This would preclude the nucleophilic attack of the NHO on the BnOH-activated monomer, which would otherwise lead to a zwitterionic polymerization resulting in high-molecular weight impurities – a reactivity, that would later be exploited, resulting in the publication presented in this chapter, and was recently highlighted elsewhere.^{9b} This approach proved to be suitable to synthesize well-defined amphiphilic triblock copolymers, using PO or BO as monomers, and PEG of varying molecular weight as macroinitiator (Scheme 60).^{8b} Furthermore, owing to the Poisson-like molar mass distribution ($D_M < 1.03$) of the resulting copolymers, these could be used as structure-directing agents (SDAs) in an evaporation-induced self-assembly (EISA) process to prepare mesoporous carbon materials. Notably, depending on the number of repeating units of PO in the copolymer, the SDAs could be tailored towards precise mesoporous structures. Only recently, PPO-*b*-PEO-*b*-PPO triblock copolymers prepared by the same technique were applied to form hydrogels (Scheme 60).¹⁹ These hydrogels possessed remarkable robustness compared to commercially available “pluronic”, that are comprised of PEO-*b*-PPO-*b*-PEO copolymers. Again, attributable to the length of the PPO-block, the robustness of the hydrogels could be tailored. Mechanistically,



Scheme 59: Well-controlled preparation of PPO using NHOs and BnOH as initiator. Depicted is the initial active species, after the first ring-opening step. The upper pathway occurs with NHOs bearing no substitution on the exocyclic carbon, and leads to zwitterion formation and high-molecular weight impurities. If a dimethyl substitution is featured on the exocyclic carbon, the lower pathway is exclusively addressed.

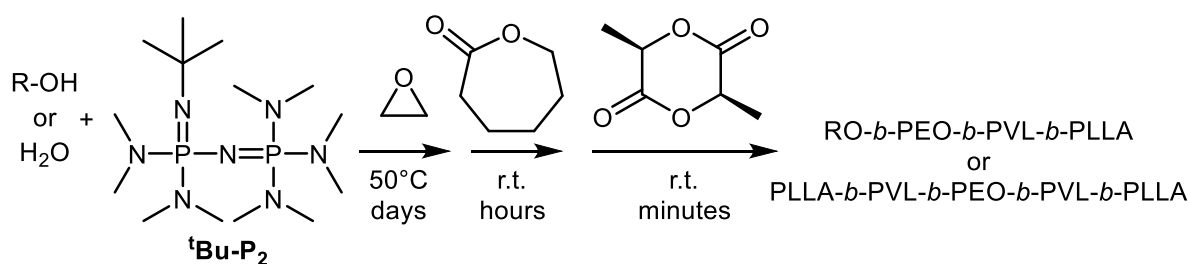


Scheme 60: Synthetic approach to so-called "reverse Pluronics[®]", consisting of a PPO-*b*-PEO-*b*-PPO triblock copolymer. Applications include the preparation of mesoporous carbon materials (top) and hydrogels in water (bottom). R = Me or Et.

the above-described systems all operate *via* an anionic process, where the NHO activates the initiator, which then performs a nucleophilic attack on the monomer, leading to ring-opening and initiation.

3.2.6. Phosphazenes

Owing to their high basicity and low nucleophilicity, phosphazenes provide sufficient reactivity to act as deprotonating agents for epoxides, as shown for EO in 1994 by *Möller* and co-workers.¹⁵⁸ Applying the phosphazene ^tBu-P₄ (Figure 7, left), the authors achieved over 90 % isolated yield in 48 h, applying various alcohols (methanol, 1-octanol, pentaerythritol) as initiators. Molar masses reached up to 6500 g·mol⁻¹ with good control ($\mathcal{D}_M < 1.13$). In 2014, *Hadjichristidis* et al. applied the relatively mild ^tBu-P₂ to successfully prepare tri- (BnOH as initiator) and pentablock (H₂O as initiator) terpolymers from CL and *L*-Lactide (Scheme 61).¹⁵⁹ Hereby, chain transfer reactions were absent and terpolymers could be generated with narrow PDIs ($\mathcal{D}_M = 1.10$). However, ^tBu-P₂ displayed an attenuated reactivity towards EO, prolonging reaction times to 2 d for the initial EO polymerization. Indeed, only the strongest commercially available phosphazene ^tBu-P₄ features enough basicity to polymerize epoxides other than EO.⁷ Also, despite representing a metal-free procedure, phosphazenes exhibit high cytotoxicity and their high price limits industrial applications. Nevertheless, the protonated versions of phosphazenes embody soft counter-ions with a low ion-pair association propensity. Hence, they were employed to break up lithium aggregates with alkoxides, enabling a switch from carbanionic to oxyanionic polymerization mechanisms and allowing for the preparation of copolymers derived from styrene, EO and 1-ethoxyethyl glycidyl ether.¹⁶⁰ Also, another mechanistic switch was possible with



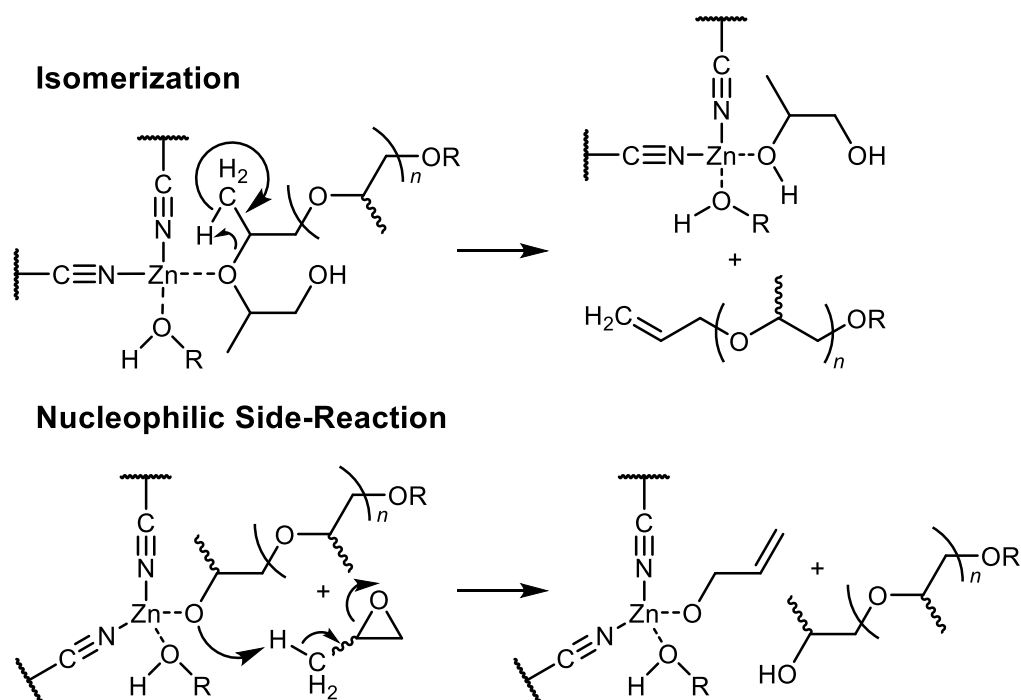
Scheme 61: One-pot approach to tri- and pentablock terpolymers, using phosphazenes as organocatalyst.

phosphazenes, as shown by *Zhao* and co-workers:¹⁶¹ after anionic ROP of EO or BO, the applied phosphazene was neutralized by adding diphenyl phosphate (DPP), which then acted as acidic catalyst for the ROP of CL, VL or trimethylenecarbonate. However, the authors observed a retardation effect of the phosphazanium-DPP salt on ester polymerization.

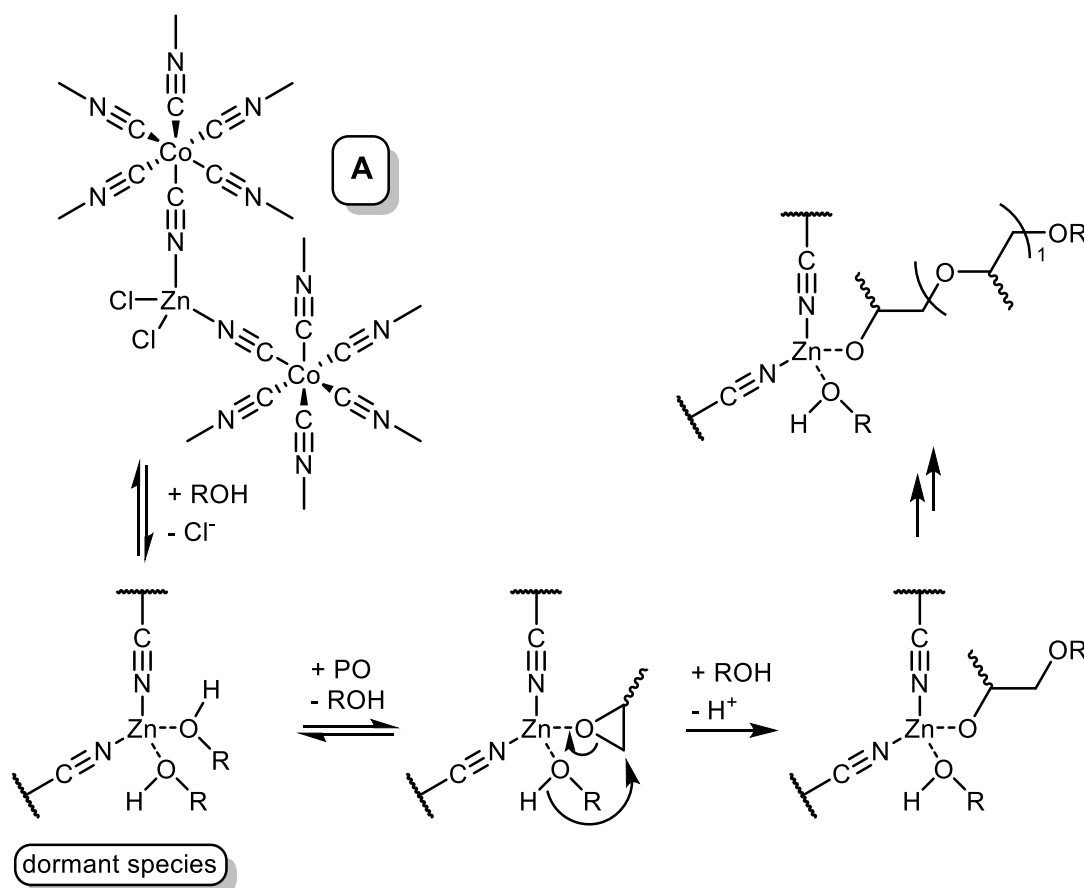
3.2.7. Double Metal Cyanide Catalysis

Double Metal Cyanide (DMC) catalysis has first been reported in 1966 by *Johnston* as a method to synthesize high-quality polyols for polyurethane synthesis.¹⁶² Continuous research and development in this field led to low catalyst loadings of 15 – 50 ppm, which makes further purification of the resulting polymer unnecessary.¹⁶³ Yet, this catalyst system mostly prevails in industry and patent literature, with little significance in the scientific community. This is attributable to its arduous synthesis, harsh reaction conditions (high temperatures and pressures) and the fact, that even the catalyst structure itself remains elusive and difficult to analyse; these catalysts are highly insoluble and the crystal structure strongly depends on the preparation procedure.¹⁶⁴ A proposed structure of a DMC catalyst is depicted in Scheme 63, **A**. The mechanism hereby proceeds *via* the formation of a dormant site, realized by a ROH-triggered ligand exchange (Scheme 63).¹⁶⁵ The monomer will then coordinate to the metal center of the dormant site ensuing its activation, and is subsequently ring-opened by the ROH-species. The thus generated active chain-end will then perform a nucleophilic attack on another activated monomer to propagate the polymerization. Side-reactions are embodied by isomerization and a nucleophilic reaction; however, compared to alkali metal hydroxide initiated ROP of PO, this issue has been significantly improved (DMC: 0.003 mequiv./g polymer vs. KOH: 0.04 – 0.10 mequiv./g polymer, Scheme 62).^{165b} Furthermore, a rapid intermolecular chain transfer located at the active metal center ensures a narrow molecular weight distribution of the ensuing polymer (Scheme 63).

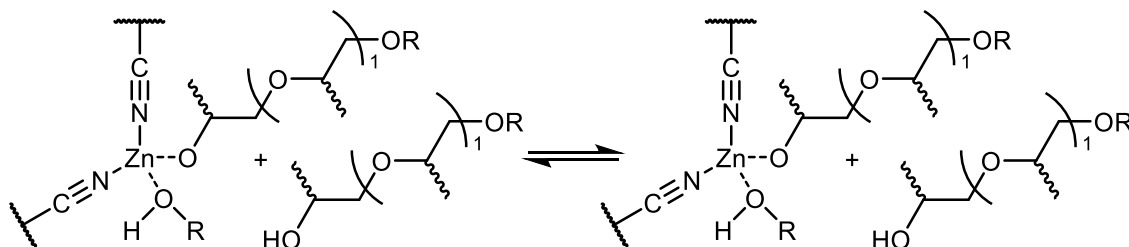
Yet, one of the major drawbacks that thwarts the establishment of DMC catalysts on a large industrial scale, is the fact that protic species cannot terminate the active chain end. Thus, no functionalization *via* terminating agents is possible, and strongly desired EO-capped polyols remain out of reach for this catalyst class. Instead, a mixture of unreacted PPO and highly ethoxylated PPO or PEO homopolymer is formed. Furthermore, owing to the slow monomer coordination to the catalyst, a pronounced induction period ranging from about 20 min to several hours can be observed. Still, once polymerization takes place, the reaction rate exceeds that of anionic ROP.¹⁶³ Also, when strongly coordinating initiators are used, this will preclude monomer coordination and hence quench reactivity, just as is also the case for alkaline species, that deactivate the catalyst's surface. Another interesting characteristic of these catalysts is the fact, that they display a lower reactivity towards EO than PO.¹⁶⁶ Since the rate-determining step is the coordination of the monomer to the catalyst, it can readily be reasoned that the electron-rich PO will more readily accomplish coordination to the Lewis acidic catalyst center, than EO will. DMC catalysts have accomplished the copolymerization of epoxides with CO₂, where a CO₂-fraction of up to 68 % could be reached, with moderately controlled molar masses



Scheme 62: Proposed side-reactions present with DMC-catalysed ROP of epoxides.^{165b}



Intermolecular Chain Transfer



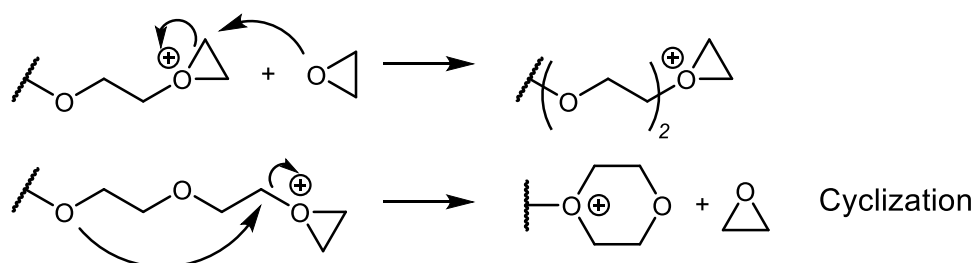
Scheme 63: Proposed polymerization mechanism according to literature, including intermolecular chain transfer ensuring a narrow PDI.^{165a}

($\bar{D}_M = 2.3 - 3.3$).¹⁶⁷ Also, the copolymerization of PO with maleic anhydride (MA) was successfully established, preparing almost alternating copolymers for a MA/PO-ratio ≥ 1 ($M_n = 3000 \text{ g}\cdot\text{mol}^{-1}$, $\bar{D}_M = 1.35 - 1.54$) and a high catalytic productivity of 10 kg polymer per gram catalyst.¹⁶⁸

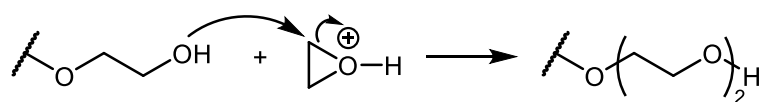
3.2.8. Cationic Systems

The cationic ROP of heterocycles has been well-understood and -reviewed ever since 1985.¹⁶⁹ However, the applicability for polyether synthesis *via* ROP of epoxides is limited, as cyclic species caused by back-biting reactions can hardly be avoided. Two general mechanisms govern the cationic ROP, one being the activated chain-end (ACE), while the other is the activated monomer (AM) mechanism (Scheme 64). In ACE-based systems, the monomer performs a nucleophilic attack on a carbon atom at the activated chain-end, leading to propagation. However, as nucleophilic oxygen atoms are also located along the polymer backbone, inter- and intramolecular chain transfer reactions are an indomitable feature in such ACE-controlled cationic polymerizations. In fact, the PEO chain exhibits a higher basicity than the EO monomer, resulting in concurrent macrocyclization side-reactions alongside propagation.^{169b} Hence, no end-group control can be achieved using this approach. On the other hand, the AM mechanism allows for significant better control, owing to several facts.¹⁷⁰ Firstly, the active centers (i.e. the cationic charges) are located on the monomer, while the polymer chain remains neutral. Hence, a significant decrease of side-reactions can be observed. Furthermore, the formation of cyclic oligomers can also be avoided when applying alcohols as initiators. Also, if a high monomer over alcohol ratio is employed while the instantaneous monomer concentration is kept low (i.e. *via* the slow addition of monomer), this will further improve control over the reaction. The AM-approach was for example employed in 1995 by *Biedron* et al. to synthesize well-defined telechelic oligodiols of PO and ECH.¹⁷¹

Activated Chain-End (ACE)



Activated Monomer (AM)



Scheme 64: Applicable mechanisms for the cationic ROP of epoxides, together with abundantly encountered cyclization reactions when employing the ACE mechanism.

3.3. Publications

One of the most severe limitations in epoxide polymerization is the almost indomitable occurrence of transfer-to-monomer reactions. This side-reaction impedes control over the polymerization and drastically restricts molar masses of polymers derived from substituted epoxides. Furthermore, a significant drop in reactivity is observed for epoxides with larger substituents, which sharply narrows the range of accessible monomers. Hence, considerable research efforts have been invested in order to overcome, or at least mitigate these issues. This resulted in elaborate catalysts, that far exceed established industrial processes in terms of activity, stereoselectivity and molar masses of the resulting polymers. Yet, they lack industrial relevance, as their often-arduous synthesis and instability when subjected to oxygen or water can only be considered or realized under laboratory conditions. Thus, both industry and science are in dire demand for a catalytic system with ready availability, that could alleviate at least some of the issues described above. As NHOs have already been established as suitable organocatalyst for PO polymerizations where transfer-to-monomer reactions are suppressed,^{8a} it was now targeted to overcome the molar mass limitations caused by slow polymerization kinetics and remaining side-reactions. Hereby, dual catalysis was reasoned to be a suitable approach, as the monomer activation achieved by a LA would proposedly ensue a faster polymerization. Hence, several NHO/LA-combinations were screened in the polymerization of PO, and a suitable LP was found. As the LP-mediated polymerization proceeded in a notably exothermic manner, subsequent reactions were conducted in dilution at -36 °C to increase the control and preclude monomer evaporation. Intriguingly, this method unhinged the molar mass limitations for PO, succeeding in the preparation of ultra-high molecular weight PPO with molar masses up to 10⁶ g·mol⁻¹. Furthermore, the catalytic setup was extended to also encompass BO and AGE, and random copolymers with AGE have been prepared. Notably, no transfer-to-monomer was observed in all cases. Thus, after establishing the extremely well-controlled PO polymerization with NHOs, now an NHO/LA-based system for LPP with ready availability was developed, that succeeded in preparing ultra-high molecular weight PPO.

3rd Publication:

P. Walther, A. Krauss, S. Naumann*, *Angew. Chem. Int. Ed.* **2019**, *58*, 10737-10741; *Angew. Chem.* **2019**, *131*, 10848-10852.

Ring-Opening Polymerization

International Edition: DOI: 10.1002/anie.201904806

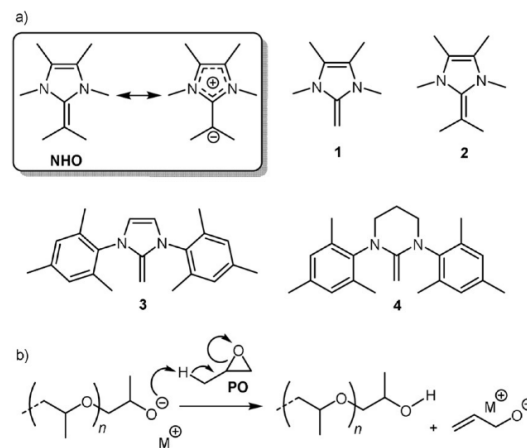
German Edition: DOI: 10.1002/ange.201904806

Lewis Pair Polymerization of Epoxides via Zwitterionic Species as a Route to High-Molar-Mass Polyethers

Patrick Walther, Annabelle Krauß, and Stefan Naumann*

Abstract: A dual catalytic setup based on *N*-heterocyclic olefins (NHOs) and magnesium bis(hexamethyldisilazide) ($\text{Mg}(\text{HMDS})_2$) was used to prepare poly(propylene oxide) with a molar mass (M_n) $> 500\,000\text{ g mol}^{-1}$, in some cases even $> 10^6\text{ g mol}^{-1}$, as determined by GPC/light scattering. This is achieved by combining the rapid polymerization characteristics of a zwitterionic, Lewis pair type mechanism with the efficient epoxide activation by the Mg^{II} species. Transfer-to-monomer, traditionally frustrating attempts at synthesizing polyethers with a high degree of polymerization, is practically removed as a limiting factor by this approach. NMR and MALDI-ToF MS experiments reveal key aspects of the proposed mechanism, whereby the polymerization is initiated via nucleophilic attack by the NHO on the activated monomer, generating a zwitterionic species. This strategy can also be extended to other epoxides, including functionalized monomers.

It remains a major challenge to prepare high-molar-mass polyethers via ring-opening polymerization (ROP) of substituted epoxides such as propylene oxide (PO).^[1] Transfer reactions (Scheme 1) pose the main difficulty in this context, most blatantly so for simple metal alkoxide catalysts.^[2] Here, the anionic polymerization is not only impractically slow, but molecular weights are also severely capped (typically $< 10\,000\text{ g mol}^{-1}$) and control over the end groups is limited. Application of crown ethers or phosphazene-type bases accelerates the reaction, but this still entails significant or even increased transfer rates.^[3,4] In this regard, the application of organocatalysts was a significant improvement; employment of *N*-heterocyclic carbenes (NHCs) as demonstrated by Taton^[5] and, later, of *N*-heterocyclic olefins (NHOs) by some of us^[6,7] enabled the well-controlled preparation of poly(propylene oxide) (PPO) with designed end groups and highly defined molecular weight distribution (down to $D_M \leq 1.03$).^[7] While convenient as well as metal- and solvent-free, these methods still displayed limitations; PPO with $M_n > 12\,000\text{ g mol}^{-1}$ was not reported in these cases. Perhaps tellingly, the few studies describing the preparation of truly high-molecular-weight PPO resort to dual catalytic, cooperative setups. Elegant work by Carlotti, Deffieux,^[8,9] and



Scheme 1. a) Mesomeric structure and employed NHOs. b) Transfer-to-monomer as a frequently encountered side reaction.

Coates^[10] can be understood as early examples for this concept (M_n up to $150\,000\text{ g mol}^{-1}$). Very recently a dual catalytic approach using phosphazenes and triethylborane was used to prepare PPO with M_n up to $200\,000\text{ g mol}^{-1}$.^[11,12]

In the following, it will be detailed how zwitterionic polymerization, a mechanism well established in organopolymerization chemistry,^[13–16] and the monomer-activating Lewis acidity of Mg^{II} combine to provide a powerful tool for the generation of polyethers with exceptionally high molecular weight.

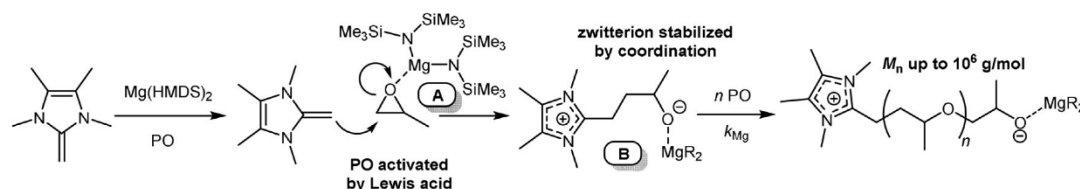
NHOs (Scheme 1), which are identical to the so-called deoxy-Breslow intermediates frequently encountered in NHC catalysis,^[17] possess an electron-rich, polar olefinic bond.^[18–20] The mesomeric structure suggests latent carbanion-like behavior and NHOs were indeed found to be powerful nucleophiles and strong bases,^[21–25] displaying a base/nucleophile dualism familiar from NHC organopolymerization.^[26–28]

These properties already surfaced when NHOs were first employed to polymerize PO;^[6] apart from anionic polymerization, a minor fraction of the monomer was consumed via a zwitterionic pathway (Figure S4). Importantly, the latter mechanism yielded polyether with a higher degree of polymerization than that found for the dominant anionic process, thus hinting at a promising approach for high-molar-mass polyether.

Crucially, however, the presence of -OH functionalities is required to activate the monomer for ring opening,^[6,29,30] resulting in a situation where deprotonation (entailing anionic polymerization) always prevails. Indeed, reactions in the absence of alcohol initiator did not enforce zwitterionic

[*] P. Walther, A. Krauß, Dr. S. Naumann
Institute of Polymer Chemistry
University of Stuttgart
Pfaffenwaldring 55, 70569 Stuttgart (Germany)
E-mail: stefan.naumann@ipoc.uni-stuttgart.de

Supporting information and the ORCID identification number(s) for the author(s) of this article can be found under:
<https://doi.org/10.1002/anie.201904806>.



Scheme 2. Investigated polymerization of PO via a cooperative NHO/Mg(HMDS)₂ setup. R = HMDS.

polymerization but rather resulted in only negligible conversion.^[6]

This prompted us to investigate metal-based Lewis acids (LAs) for the purpose of tailored epoxide activation without introducing protic moieties. Focusing on hard, oxophilic LAs, it was found that the simplest LAs, such as LiCl, MgCl₂, MgI₂, ZnI₂ or YCl₃, did not entail meaningful amounts of polyether when applied together with NHO **1** in bulk reactions with PO (Table S2). This dramatically changed when a Mg^{II} species with two hexamethyldisilazide ligands was employed instead (Mg(HMDS)₂, Scheme 2). When a fivefold molar excess was used relative to NHO **1** and 1000 equiv of PO, the reaction was complete in less than 5 minutes at room temperature (Table 1, entry 1). The polymerization was conducted in a pressure tube and noticeably exothermic; ¹H NMR spectroscopy showed quantitative monomer consumption while GPC analysis (CHCl₃, vs. PS standards) revealed a high *M_n* of 61 000 g mol⁻¹ (*D_M* = 1.47). The high molar mass was substantiated by light scattering (see the Supporting Information), which revealed that a correction factor of 0.55 has to be applied to provide a more realistic description of the polyether molecular weights. Reactions in the presence of benzyl alcohol failed to yield any polyether under these conditions.

For better investigation, the polymerization was slowed down by cooling and dilution. When pentane was applied along with a 5 M concentration of PO at -36 °C (glove box freezer), the reactions proceeded gently; quantitative conversion and very similar polymer properties were achieved without the need for special reaction vessels (entry 2). To map out the limits of this catalyst system, variations of the reaction parameters were tested. Lowering the NHO loading to 0.02 mol% still resulted in quantitative monomer consumption, while the observed molar mass of the isolated polyether increased significantly (entries 3–5). The obtained molar masses and the required reaction time were clearly dependent on the proportion of Mg(HMDS)₂ present, with regards to both the excess of the LA relative to the NHO and the LA/monomer ratio.

While monomer consumption was much slower than that described for previous examples, the polymerization still proceeded in a well-behaved manner with reasonably controlled molecular weight distribution (*D_M* = 1.1–1.3, Figure 1 and Figure S5). Interestingly, in all cases a pronounced induction period can be observed, indicative of the slow formation of zwitterions (see discussion below). PPO with the highest molar mass is obtained for a NHO/LA ratio of 1:10, marking a very high *M_n* of 520 000 g mol⁻¹. The corresponding 1:20 ratio results in an expected faster reaction and lower

Table 1: Polymerization of PO, using **1**/Mg(HMDS)₂ as the catalyst system. [PO] = 5 M in pentane. LA = Mg(HMDS)₂.

Entry	1 /LA/PO	<i>t</i> [h]	<i>T</i> [°C]	Conv. ^[a] [%]	<i>M_n</i> [g mol ⁻¹] (<i>D_M</i>) ^[b]
1 ^[c]	1:5:1000	5 min	rt	> 99	61 000 (1.47)
2	1:5:1000	4	-36	> 99	55 000 (1.21)
3	1:2.5:5000	384	-36	> 99	420 000 (1.57)
4	1:10:5000	81	-36	> 99	520 000 (1.24)
5	1:20:5000	24	-36	> 99	210 000 (1.25)
6	1:5:1000	45 min	60	> 99	48 000 (2.1)

[a] Determined via ¹H NMR analysis. [b] Determined from GPC (CHCl₃, PS calibration) corrected by factor 0.55. [c] Bulk polymerization.

molar mass (*M_n* = 210 000 g mol⁻¹), suggesting an improved but still low initiation efficiency. Conversely, a lower LA loading (1:2.5) entails a much slower reaction, which, however, still reaches a conversion of > 99%. The molar mass of the isolated polyether in the latter case is slightly lower than that found for NHO/LA = 1:10, which is tentatively attributed to the minute occurrence of transfer-to-monomer as a result of the very low concentration of Mg(HMDS)₂. Indeed, the presence of this specific LA^[31] seems crucial to achieving high *M_n*, since similar compounds behave very differently (see below). It was also possible to accelerate the polymerization by applying elevated temperatures (compare entries 2 and 6, Table 1).

The above findings indicate that a zwitterionic polymerization mechanism is indeed operative. To verify this, NMR and MALDI-ToF MS investigations were conducted. ¹H NMR spectroscopy revealed the striking impact of the presence of Mg(HMDS)₂ on the polymerization system. While the spectrum of a 1:1 mixture (C₆D₆, ambient) of NHO **1** and PO showed practically no difference relative to spectra of these compounds alone (Figure S6), the corresponding 1:1 solution of Mg(HMDS)₂ and PO displayed a significant low-field shift of the methine and methylene signals of the monomer ($\Delta\delta$ (methine) = 0.58 ppm). Furthermore, the set of signals typically observed for Mg(HMDS)₂ (arising from the presence of monomeric and dimeric magnesium silazide species, Figure S7) is transformed into only a single peak for the -Si-CH₃ moieties (Figure S8).^[32] Taken together, this suggests the formation of complex **A** from PO and the LA (Scheme 2), which will transfer electron density from the epoxide to the metal and thus activate the monomer for nucleophilic attack and subsequent ring opening. Not surprisingly, neither NHO alone nor the LA alone can initiate polymerization on a timescale comparable to that of their combined reaction, underlining the gained coopera-

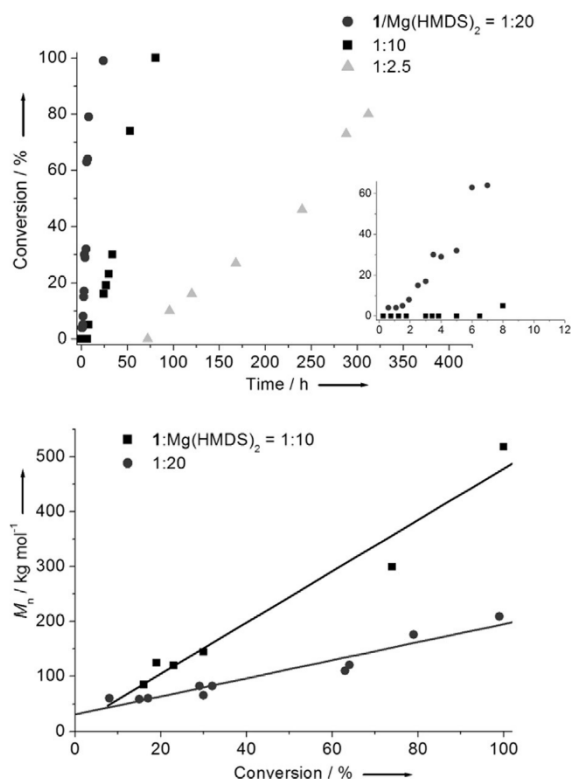


Figure 1. Conversion vs. time and M_n vs. conversion for PO polymerization using different 1/LA ratios. For reaction conditions, see Table 1, entries 3–5.

tivity effects. Notably, neither KHMDS nor LiHMDS showed similar activation of PO and coherently polymerizations failed or delivered low molar masses (Table S3).

Low-molar-mass samples prepared for MALDI-ToF MS analysis allowed for calculation of the end groups, a central piece of evidence for the existence of the proposed zwitterionic species. It was found that the PPO formed by the action of 1/Mg(HMDS)₂ is indeed terminated by NHO-derived moieties (Figure 2). Only a single polymer population is observed and the experimental mass is in excellent agreement with that calculated. The absence of allyl-related signals in the ¹H NMR spectrum of the sample investigated by MALDI-ToF MS (Figure S10) complements this observation. Notably, NHO-derived termini have also been identified when NHO **3** was employed (Figures S13 and S14). These findings are the same, regardless of whether Na⁺ was added during matrix preparation or not; the zwitterionically derived polyether molecules are inherently cationized.

In summary, these findings indicate that the cooperative, zwitterionic mechanism proposed (Scheme 2) is most likely correct. We have shown unambiguously that the NHO directly adds to the monomer, thereby initiating the polymerization under formation of zwitterions (**B**). Also, all evidence supports that Mg(HMDS)₂ activates the monomer (**A**) but does not start monomer consump-

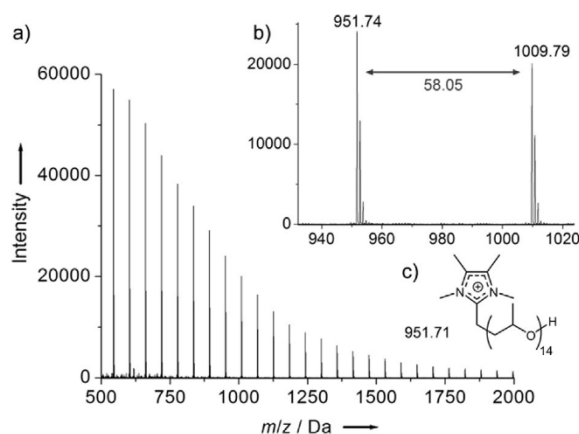


Figure 2. a) MALDI-ToF mass analysis of PPO prepared by 1/Mg-(HMDS)₂ (see the Supporting Information for details), b) expansion, and c) calculated mass of NHO-terminated and -cationized PPO. 1/Mg(HMDS)₂/PO ratio of 1:5:20 (0.25 M in pentane).

tion itself; it does not act as a base in this specific context. It can be argued plausibly that the role of the magnesium species extends beyond simple activation of the epoxide. Three compounds compete for coordination to the Lewis acid: Apart from the monomer, for which significant interaction has been shown (see above), these include the NHO itself and the propagating oxyanion. Complexation of the NHO depletes the polymerization setup of free initiator. Low initiation efficiencies would result, which is exactly what is observed (see Table 1 and Table 2). Indeed, ¹H NMR experiments (1:1) at room temperature (Figure S6) and at variable temperatures between –40 °C and 20 °C (Figure S9) reveal complex formation between olefin and Mg(HMDS)₂; no dissociation can be observed and the concentration of free NHO must be very low indeed under polymerization conditions (low temperature, excess of Mg^{II}). Regarding the propagating oxyanion and the magnesium Lewis acid, observation in situ is challenging but stabilization of the anion by coordination is more than probable (**B**, Scheme 2). Relevantly, this reduces the reactivity of the oxyanion, potentially mitigating its propensity for side reactions. The propagating species can thus be understood as a oxyanion/Mg(HMDS)₂ Lewis pair, placing the proposed mechanism in the context of

Table 2: Polymerization of several epoxides, using Mg(HMDS)₂ in combination with different NHOs. 5 M in pentane. LA = Mg(HMDS)₂.

No.	NHO	NHO/LA/M	M	t [h]	T [°C]	Conv. [%] ^[a]	M_n [kg mol ⁻¹] (\mathcal{M}_n) ^[b]
1	2	1:20:5000	PO	141	–36	>99	1.400 (1.55)
2	2	1:20:5000	PO	2	rt	83	340 (1.99)
3	3	1:5:1000	PO	96	–36	>99	280 (2.3)
4	4	1:5:1000	PO	96	–36	>99	450 (2.2)
5 ^[c]	1	1:5:1000	BO	72	–36	>99	21 (2.1)
6 ^[c]	1	1:20:1000	BO	2	60	89 ^[c]	6.9 (2.5)
7	1	1:5:1000	AGE	0.5	rt	>99	310 (1.95)
8	1	1:5:1000	AGE	72	–36	>99	880 (1.65)

[a] Determined via ¹H NMR analysis. [b] Determined from GPC (CHCl₃, PS calibration) corrected by factor 0.55. [c] Bulk polymerization.

Lewis pair polymerization (LPP),^[33,34] as recently reviewed by Chen,^[35] for which also NHO-derived examples exist.^[36,37]

Hence, a triple role is proposed for Mg(HMDS)₂. Firstly, activation of the epoxide enables zwitterion formation and efficient propagation. Secondly, complexation of the NHO entails a high effective ratio of monomer to initiator. Thirdly, coordination of the oxyanion suppresses transfer-to-monomer, as the propagating species is rendered less basic. The combination of all three effects seems necessary to obtain the high conversion and high polyether molar masses described in this study. A detailed polymerization mechanism, including the conceivable formation of spirocycles,^[29,38] is found in the Supporting Information (Figure S15).

The propensity to form zwitterions will also depend on the chemical structure of the NHO, with the ability to stabilize the positive charge, steric congestion, and double-bond polarization as important factors.^[29,39,40] Thus, several other NHOs were employed in the same setup. Application of **2**, a compound with higher proton affinity and more pronounced steric encumbrance than **1**,^[39] gave PPO with even higher molar masses (Table 2, entry 1). The exceptionally high M_n of $1.4 \times 10^6 \text{ g mol}^{-1}$ most probably originates from a very low initiation efficiency, nonetheless providing full monomer conversion and a reasonably controlled molecular weight distribution ($\bar{D}_M = 1.55$). Polymerization at room temperature is faster, yet less controlled, delivering PPO with a reduced, if still substantial molar mass (entry 2), fully in line with the observations made earlier. Polymerization also succeeded when *N*-aryl-bearing compounds **3** and **4** were employed. Monomer consumption was slower and less controlled than found for **1**, but the reaction still proceeded to full conversion and gave very high M_n (entries 3 and 4). Notably, the activation of the epoxide monomer is strong enough to enable a saturated, non-imidazole NHO (**4**) to polymerize PO, in sharp contrast to the metal-free setup,^[6] highlighting the key role played by the LA in this catalytic system. Overall, however, it is obvious that NHO **1** is the most suitable initiator among the investigated NHOs. This can be attributed to its minimal steric congestion, high double-bond polarization, and ability to aromatize upon zwitterion formation.^[39] In combination with its very simple structure and ease of preparation, compound **1** can thus be considered the ideal partner to the equally well-available Mg(HMDS)₂^[31] for the preparation of high-molar-mass PPO.

To investigate the monomer scope accessible for **1**/Mg(HMDS)₂, other epoxide monomers were screened. 1,2-Butylene oxide (BO) was also found to be polymerizable by this setup, but to a significantly reduced degree when compared to PO (Table 2, entries 5 and 6), mirroring the behavior of NHO-based BO organopolymerization.^[7] Reactions had to be conducted without solvent to achieve practicable speed of conversion, and even then the obtained M_n was almost an order of magnitude lower than that received for PO under identical conditions. It should be considered that these molar masses ($7000\text{--}21\,000 \text{ g mol}^{-1}$) are still substantial, especially when compared to those achieved with the established polymerization techniques.^[1] In contrast to BO, allyl glycidyl ether (AGE) displayed fast and exothermic conversion in bulk at ambient temperatures, comparable to

PO and enabling the rapid generation of the corresponding homopolymer with a very high M_n (entries 7 and 8). Copolymerization of AGE and PO is likewise possible, generating a random copolymer with no pronounced gradient as indicated by ¹H/¹³C NMR analysis and a PO/AGE ratio matching the monomer feed (Figures S16 and S17, and Table S3 for a more complete list of polymerizations). As documented, the olefinic bond of the monomer remains intact and allyl isomerization is not detectable; the application of such functionalized olefins thus enables the preparation of polyether structures with very high molar mass and suitable sites for subsequent cross-linking or other derivatizations. As one such future use, PO-based elastomers for low-temperature applications can be imagined; indeed, such materials have been commercialized (service range: -60 to $>200^\circ\text{C}$) for which high- M_n polyether was employed.^[41,42] Current research in our lab aims to revive this type of material.

In conclusion, a new approach to access high-molar-mass PPO ($M_n > 0.5 \times 10^6 \text{ g mol}^{-1}$) has been developed. This succeeded by employing Lewis pair polymerization via zwitterions based on nucleophilic *N*-heterocyclic olefins in cooperation with Mg(HMDS)₂ as an epoxide-activating Lewis acid. While this system enables a high turnover per NHO (TON up to 5000) and practicable reaction times, an increase of initiation efficiency is envisioned to further promote the usefulness of this setup.

Acknowledgements

We gratefully acknowledge funding by the Deutsche Forschungsgemeinschaft (German Research Foundation, DFG), project number 358283783 (CRC 1333) and project NA 1206/2.

Conflict of interest

The authors declare no conflict of interest.

Keywords: cooperative effects · homogeneous catalysis · magnesium · ring-opening polymerization · zwitterions

How to cite: *Angew. Chem. Int. Ed.* **2019**, *58*, 10737–10741
Angew. Chem. **2019**, *131*, 10848–10852

- [1] J. Herzberger, K. Niederer, H. Pohlit, J. Seiwert, M. Worm, F. R. Wurm, H. Frey, *Chem. Rev.* **2016**, *116*, 2170.
- [2] G. Odian, *Principles of Polymerization*, 4th ed., Wiley-Interscience, New York, **2004**, pp. 548–553.
- [3] O. Rexin, R. Mülhaupt, *J. Polym. Sci. Part A* **2002**, *40*, 864.
- [4] R. P. Quirk, G. M. Lizarraza, *Macromol. Chem. Phys.* **2000**, *201*, 1395.
- [5] J. Raynaud, W. N. Ottou, Y. Gnanou, D. Taton, *Chem. Commun.* **2010**, *46*, 3203.
- [6] S. Naumann, A. W. Thomas, A. P. Dove, *Angew. Chem. Int. Ed.* **2015**, *54*, 9550; *Angew. Chem.* **2015**, *127*, 9686.
- [7] A. Balint, M. Papendick, M. Clauss, C. Müller, F. Giesselmann, S. Naumann, *Chem. Commun.* **2018**, *54*, 2220.
- [8] C. Billouard, S. Carloti, P. Desbois, A. Deffieux, *Macromolecules* **2004**, *37*, 4038.

- [9] A. Labbé, S. Carloti, C. Billouard, P. Desbois, A. Deffieux, *Macromolecules* **2007**, *40*, 7842.
- [10] P. C. B. Widger, S. M. Ahmed, G. W. Coates, *Macromolecules* **2011**, *44*, 5666.
- [11] Y. Chen, J. Shen, S. Liu, J. Zhao, Y. Wang, G. Zhang, *Macromolecules* **2018**, *51*, 8286.
- [12] C.-J. Zhang, H.-Y. Duan, L.-F. Hu, C.-H. Zhang, X.-H. Zhang, *ChemSusChem* **2018**, *11*, 4209.
- [13] L. Guo, D. Zhang, *J. Am. Chem. Soc.* **2009**, *131*, 18072.
- [14] E. J. Shin, H. A. Brown, S. Gonzalez, W. Jeong, J. L. Hedrick, R. M. Waymouth, *Angew. Chem. Int. Ed.* **2011**, *50*, 6388; *Angew. Chem.* **2011**, *123*, 6512.
- [15] Y. Zhang, E. Y.-X. Chen, *Angew. Chem. Int. Ed.* **2012**, *51*, 2465; *Angew. Chem.* **2012**, *124*, 2515.
- [16] H. A. Brown, R. M. Waymouth, *Acc. Chem. Res.* **2013**, *46*, 2585.
- [17] B. Maji, M. Horn, H. Mayr, *Angew. Chem. Int. Ed.* **2012**, *51*, 6231; *Angew. Chem.* **2012**, *124*, 6335.
- [18] R. D. Crocker, T. V. Nguyen, *Chem. Eur. J.* **2016**, *22*, 2208.
- [19] M. M. D. Roy, E. Rivard, *Acc. Chem. Res.* **2017**, *50*, 2017.
- [20] K. Powers, C. Hering-Junghans, R. McDonald, M. J. Ferguson, E. Rivard, *Polyhedron* **2016**, *108*, 8.
- [21] S. Kronig, P. G. Jones, M. Tamm, *Eur. J. Inorg. Chem.* **2013**, 2301.
- [22] A. Fürstner, M. Alcarazo, R. Goddard, C. W. Lehmann, *Angew. Chem. Int. Ed.* **2008**, *47*, 3210; *Angew. Chem.* **2008**, *120*, 3254.
- [23] Y.-B. Wang, Y.-M. Wang, W.-Z. Zhang, X.-B. Lu, *J. Am. Chem. Soc.* **2013**, *135*, 11996.
- [24] P. Walthers, S. Naumann, *Macromolecules* **2017**, *50*, 8406.
- [25] P. Walthers, W. Frey, S. Naumann, *Polym. Chem.* **2018**, *9*, 3674.
- [26] M. Fèvre, J. Pinaud, Y. Gnanou, J. Vignolle, D. Taton, *Chem. Soc. Rev.* **2013**, *42*, 2142.
- [27] S. Naumann, A. P. Dove, *Polym. Chem.* **2015**, *6*, 3185.
- [28] B. Maji, M. Breugst, H. Mayr, *Angew. Chem. Int. Ed.* **2011**, *50*, 6915; *Angew. Chem.* **2011**, *123*, 7047.
- [29] M. Al Ghamdi, L. Cavallo, L. Falivene, *J. Phys. Chem. C* **2017**, *121*, 2730.
- [30] For a recent study on activation of epoxides via H-bond donors, see: P. Yingcharoen, C. Kongtes, S. Arayachukiat, K. Suvarnapunya, S. V. C. Vummaleti, S. Wannakao, L. Cavallo, A. Poater, V. D'Elia, *Adv. Synth. Catal.* **2018**, *455*, 304.
- [31] Mg(HMDS)₂ is commercially available. For preparation, see: J. F. Allan, K. W. Henderson, A. R. Kennedy, *Chem. Commun.* **1999**, 1325.
- [32] M. Westerhausen, *Inorg. Chem.* **1991**, *30*, 96.
- [33] S. Naumann, P. B. V. Scholten, J. A. Wilson, A. P. Dove, *J. Am. Chem. Soc.* **2015**, *137*, 14439.
- [34] Y. Bai, J. He, Y. Zhang, *Angew. Chem. Int. Ed.* **2018**, *57*, 17230; *Angew. Chem.* **2018**, *130*, 17476.
- [35] M. Hong, J. Chen, E. Y.-X. Chen, *Chem. Rev.* **2018**, *118*, 10551.
- [36] Q. Wang, W. Zhao, J. He, Y. Zhang, E. Y.-X. Chen, *Macromolecules* **2017**, *50*, 123.
- [37] Q. Wang, W. Zhao, S. Zhang, J. He, Y. Zhang, E. Y.-X. Chen, *ACS Catal.* **2018**, *8*, 3571.
- [38] J. Raynaud, C. Absalon, Y. Gnanou, D. Taton, *Macromolecules* **2010**, *43*, 2814.
- [39] R. Schuldt, J. Kästner, S. Naumann, *J. Org. Chem.* **2019**, *84*, 2209.
- [40] S. Naumann, K. Mundsinger, L. Cavallo, L. Falivene, *Polym. Chem.* **2017**, *8*, 5803.
- [41] D. A. Berta, E. J. Vandenberg in *Handbook of Elastomers* (Eds.: A. K. Bhowmick, H. L. Stephens), Marcel Dekker, New York, **2001**, Chapter 25.
- [42] R. C. Ferrier, S. Pakhira, S. E. Palmon, C. G. Rodriguez, D. J. Goldfeld, O. O. Iyiola, M. Chwatko, J. L. Mendoza-Cortes, N. A. Lynd, *Macromolecules* **2018**, *51*, 1777.

Manuscript received: April 17, 2019

Accepted manuscript online: May 17, 2019

Version of record online: June 27, 2019

Supporting Information

Experimental

Starting materials and catalyst synthesis

\pm Propylene oxide (PO, TCI Chemicals, > 99.0 % (GC)), \pm Butylene oxide (BO, TCI Chemicals, > 99.0 % (GC)) and Allyl glycidyl ether (AGE, Sigma-Aldrich, \geq 99 %) were dried over CaH_2 , and subsequently distilled (in case of AGE under static vacuum ($1 \cdot 10^{-3}$ mbar), otherwise ambient pressure). After degassing the clear liquids with two cycles of freeze-pump-thaw, the monomers were stored under protective conditions inside the glove box (LabMaster, MBraun, Germany, freezer, -36 °C). LiHMDS (Sigma Aldrich, powder, > 97 %), KHMDS (Sigma Aldrich, 95 %), $\text{Mg}(\text{HMDS})_2$ (synthesized according to literature-known procedure²⁰) and $\text{Mg}(\text{TFSI})_2$ (Sigma-Aldrich) were used as received and stored inside the glove box under exclusion of light. The solvents used in polymerization reactions were taken from a solvent purification system (MBraun, Germany), and stored under protective conditions (glove box) over molecular sieves (3 Å). NHO **1**,^{2c, 8a, 10} **2**,^{2c, 99, 134} **3**^{6, 76} and **4**^{6, 76} (Figure S1) were prepared according to literature-known procedures. Identity was confirmed via $^1\text{H}/^{13}\text{C}$ NMR, for full characterization see cited references. A schematic synthetic route is provided below (Figure S2).

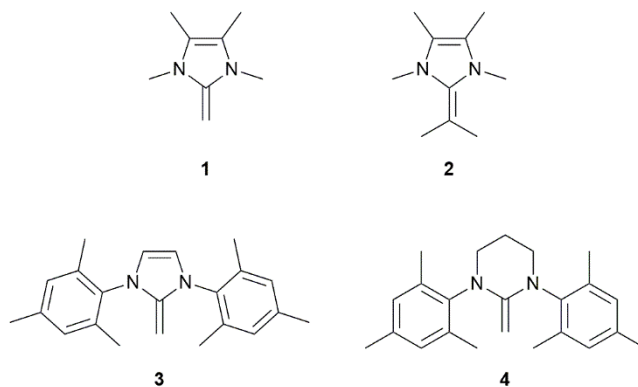


Figure S15. NHOs applied in this study.

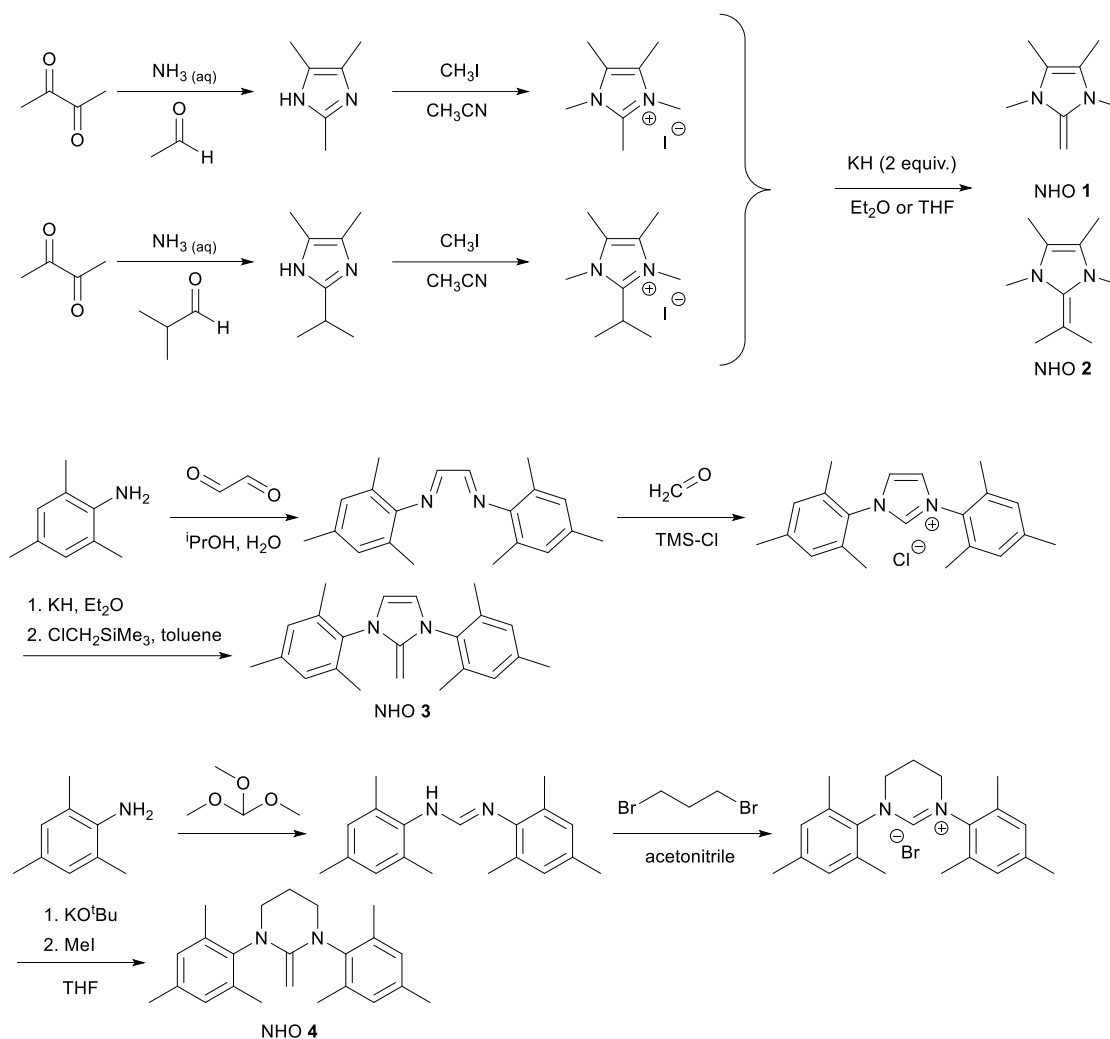


Figure S16. Schematic synthesis of NHOs 1-4.

General Polymerization Procedures

The polymerization setups were assembled inside the glove box. Reactions at elevated temperature were then transferred into pressure tubes, and subsequently stirred at the stated temperature outside the glove box (pre-heated oil bath), while reactions at ambient temperature and -36 °C were carried out inside the glove box or in the glove box freezer, respectively. The polymerizations were quenched by dissolving the residue in wet chloroform. Conversion of PO was determined by means of proton NMR spectroscopy (CDCl₃), monitoring the $-\underline{CH}-\underline{CH}_2-\text{O}-$ signals of the respective monomer ($\delta = 3.0 - 2.4$ ppm) and the resulting polymer ($\delta = 3.6 - 3.3$ ppm). For other monomers, the same signals were monitored, which were slightly shifted to $\delta = 3.1 - 2.5$ ppm (monomer, AGE), $\delta = 3.7 - 3.4$ ppm (polymer, AGE) or $\delta = 2.9 - 2.4$ ppm (monomer, BO) and $\delta = 3.7 - 3.2$ ppm (polymer, BO). To exclude any undesired polymerization, solid and liquid components were premixed in separate vials until the reaction was started by combining both mixtures. In case of reactions performed in the glove box freezer,

the premixed components were kept separately inside the freezer for approx. 30 min, prior to mixing them and starting the reaction.

Characterization and Analysis

A *Bruker* Avance III 400 spectrometer was used to record NMR spectra (^{13}C , ^1H). Variable temperature NMR (^1H) was conducted in the -40°C to 20°C temperature range. The chemical shifts are reported relative to reference peaks of the respective deuterated solvents. Molar masses were determined by means of GPC measurements in CHCl_3 and in dimethylacetamide (DMAc). For CHCl_3 GPC (40°C , poly(styrene) standard, calibrated from $800 - 2\,000\,000\text{ g}\cdot\text{mol}^{-1}$), a *PSS* SDV $5\ \mu\text{m}$ $8*50\text{mm}$ guard column, three *PSS* SDV $100\,000\ \text{\AA}$ $5\ \mu\text{m}$ $8*50\text{mm}$ columns and an *Agilent* 1200 Series G1362A detector (RI) were employed. Samples were prepared with a concentration of $c = 2.5\text{ mg}\cdot\text{mL}^{-1}$, and the measurements were conducted with a flow-rate of $1\text{ mL}\cdot\text{min}^{-1}$. For a more realistic estimation of the true PPO molar masses, the results obtained from this calibration relative to poly(styrene) were corrected by a factor determined from a GPC setup with light-scattering detector (see below). The correction parameter was determined from several high-molar mass samples with $\bar{D}_M < 2.0$ (Table S3) and was found to be 0.55. All data given in the manuscript are corrected by this light-scattering-derived factor. Regarding GPC multiangle laser light scattering (GPC-MALLS) measurements, the mobile phase consisted of THF ($T = 30^\circ\text{C}$). An *Agilent* Infinity 1260 system was equipped with linear M styrene – divinylbenzene – copolymer network columns (50 mm guard column, $2*300\text{ mm}$ separation column) manufactured by *PSS Polymer Standards Service*, a *PSS* SECcurity UV and RI detector. The MALLS detector applied consisted of a *PSS* SLD 7000/BI-MwA unit measuring at 657 nm. Calibration was conducted against poly(styrene) standards ($500 - 2\,500\,000\text{ g}\cdot\text{mol}^{-1}$). To determine the absolute molecular weights, the dn/dc value was previously determined by measuring a serial dilution of poly(propylene oxide) in THF ($c = 0.5 - 15\text{ mg}\cdot\text{mL}^{-1}$), using a *PSS* DnDc 1260 detector at 620 nm and $T = 30^\circ\text{C}$ (see Figure S3).

For measurements conducted in dimethylacetamide (DMAc, 40°C), calibration was achieved using poly(ethylene oxide) standards ($25\,000 - 1\,000\,000\text{ g}\cdot\text{mol}^{-1}$). An *Agilent* GPC-system 1260 infinity setup consisting of a 50 mm guard column, one 300 mm *Agilent* “mixed B” column filled with polar, modified silica and a RI detector was applied. The mobile phase consisted of DMAc with $5\text{ g}\cdot\text{L}^{-1}$ LiBr added, in which the samples were dissolved for three days and subsequently filtered using $0.2\ \mu\text{m}$ PTFE syringe-filters. The flow rate applied was $0.75\text{ mL}\cdot\text{min}^{-1}$, while the sample concentration amounted to $2\text{ mg}\cdot\text{mL}^{-1}$.

MALDI-ToF MS analyses were measured with a *Bruker* Autoflex III (337 nm, reflector mode). The sample-preparation consisted of mixing the matrix solution (2,5-dihydroxybenzoic acid, 5 mg/mL in THF), polymer solution (10 mg/mL in THF) and, if needed, a solution of

sodium trifluoromethanesulfonate (0.1 M in 90% acetone, 10% water), applying a ratio of 2:1:2. Polystyrene standards were used for calibration.

GPC-MALLS correction

Table S12: Comparison of CHCl₃ GPC (PS standards) raw data and corrected results based on GPC-MALLS, as well as DMAc GPC (PEO standards). Monomer = propylene oxide if not stated otherwise.

NHO	NHO/Mg/M	<i>t</i> [h]	<i>T</i> [°C]	Conv. ^[a] [%]	<i>M_n</i> (PDI)	<i>M_{n,corr.}</i> ^[b]	<i>M_n</i>
					(CHCl ₃ , PS) [g·mol ⁻¹]	(DMAc, PEO) [g·mol ⁻¹]	
1	1:5:1100	5 min	r.t.	> 99	942 000 (1.24)	518 000	125 000
1	1:5:1000	0.5	-36	> 99	832 000 (1.66)	458 000	134 000
1	1:5:1000	4	-36	> 99	767 000 (1.57)	422 000	49 000
1	1:5:1000	72	-36	> 99	621 000 (1.99)	342 000	51 000
2	1:20:5000	2	r.t.	83	380 000 (1.25)	209 000	100 000
2	1:20:4000	96	-36	94	100 000 (1.21)	55 000	37 000
4	1:5:1000	96	r.t.	> 99	110 000 (1.47)	61 000	25 000
1 ^[c]	1:5:1000	2	r.t.	> 99	563 000 (1.95)	310 000	insoluble

[a]: determined by ¹H NMR analysis (400 MHz, CDCl₃); [b]: correction factor of 0.55 applied; [c]: Monomer = AGE.

Dn/Dc determination

Sample ID: Polypropylene oxide in THF
Concentration #1: 4.850e-01

Temperature = 30.0 °C
Intensity = 80%

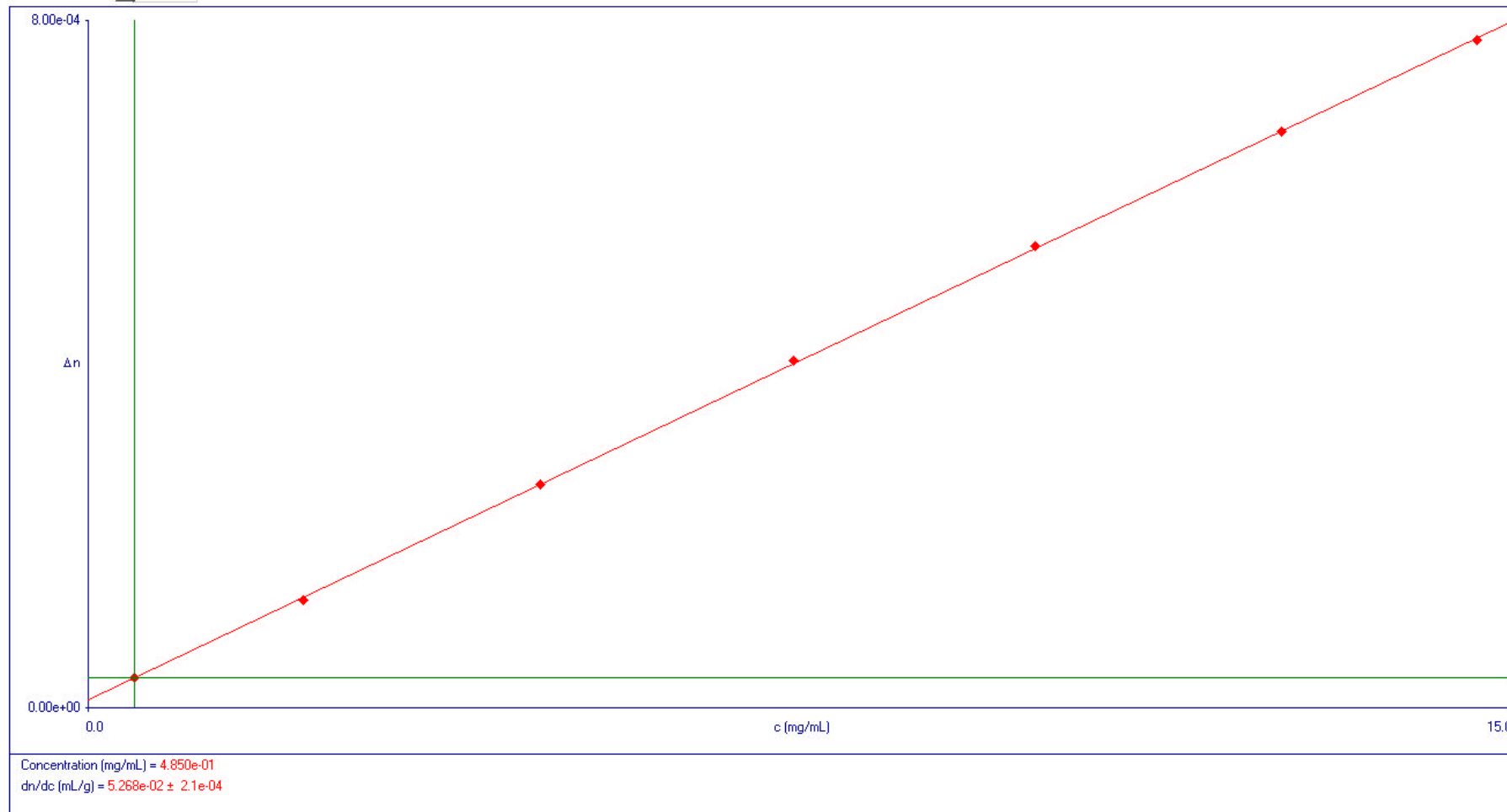


Figure S17: Serial dilution to obtain dn/dc (THF, 30°C, $c = 0.5 - 15 \text{ mg}\cdot\text{mL}^{-1}$).

Previous work and this work

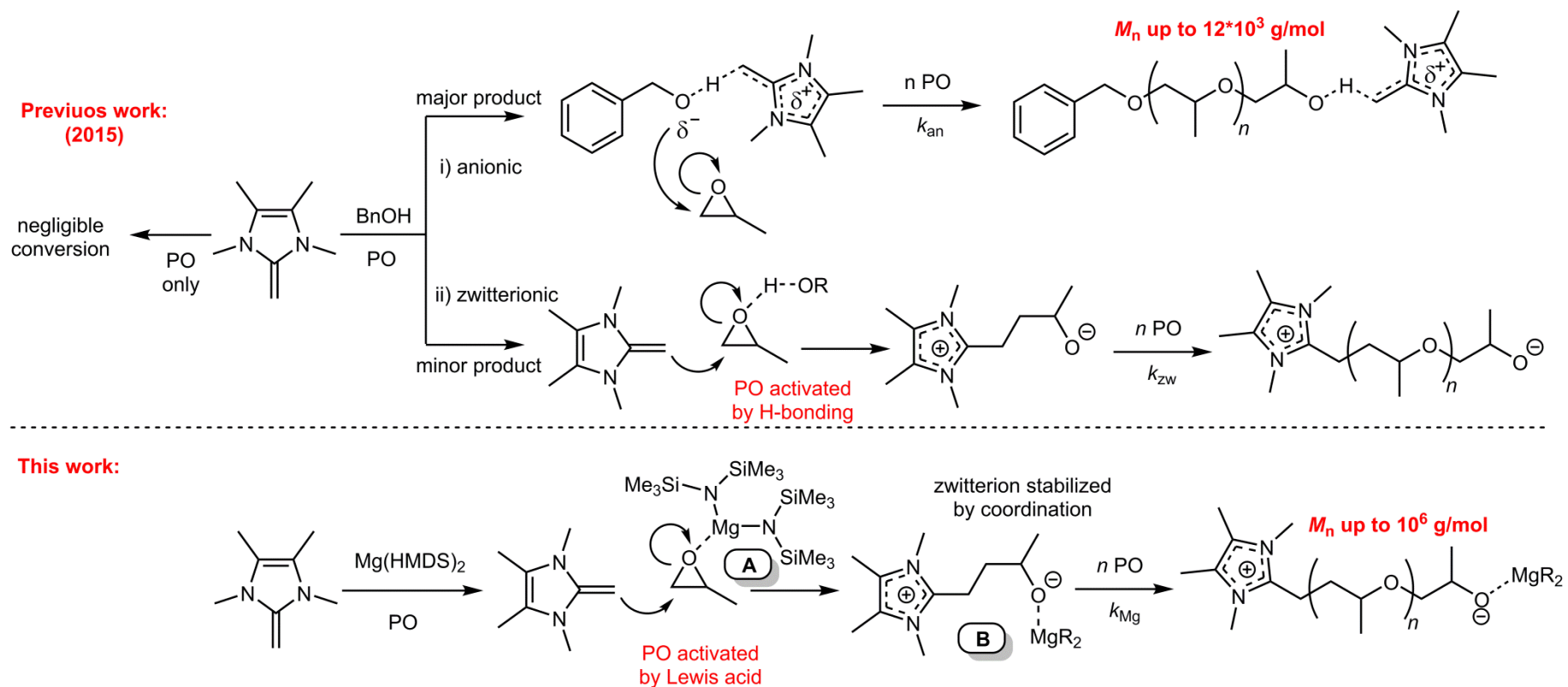


Figure S18. Top: Reaction scheme for the NHO-based, metal-free polymerization of PO in the presence of alcohol initiator, mainly resulting in anionic polymerization of the monomer.^[2] Bottom: Cooperative NHO/ $Mg(HMDS)_2$ polymerization of PO via monomer activation resulting in a zwitterionic Lewis pair polymerization.

Screening of different Lewis Acids

Table S13. Reactions using NHO 1/MX_n/PO in a 1:5:1000 ratio (bulk).

Entry	MX _n	<i>t</i> [h]	<i>T</i> [°C]	Conv. ^[a] [%]
1	MgCl ₂	24	80	-
2	MgI ₂	24	80	-
3	LiCl	24	80	-
4	ZnI ₂	24	80	< 5
5	YCl ₃	24	80	< 5

^[a] Determined via ¹H NMR spectroscopy.

Representative GPC analysis

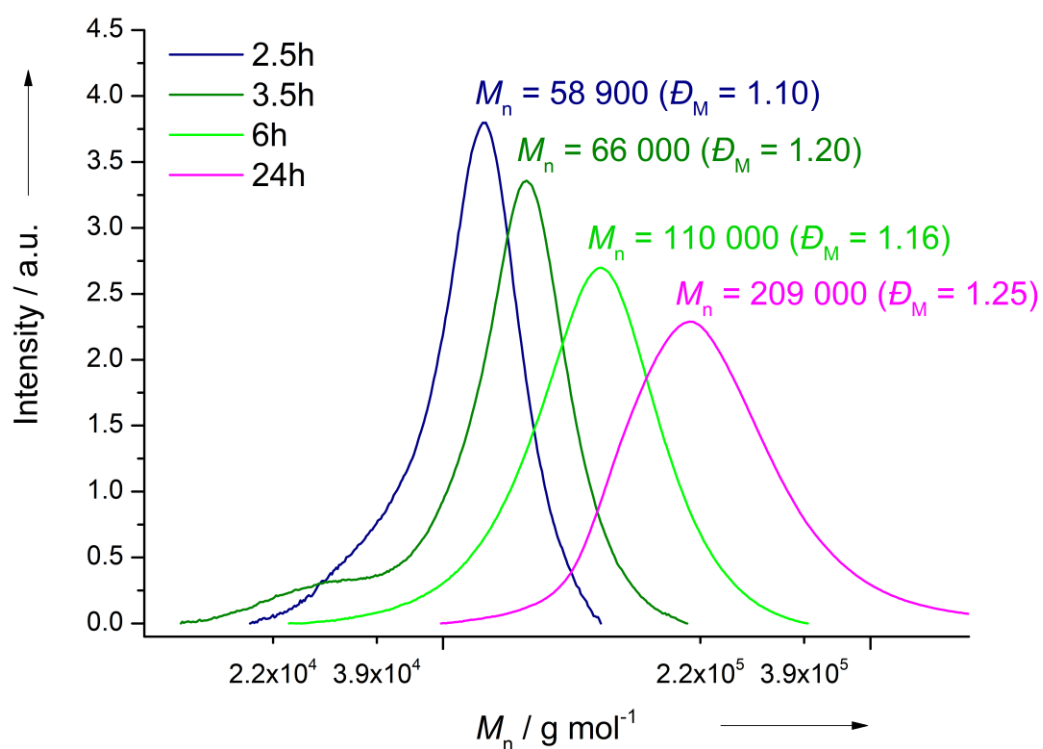


Figure S19. GPC traces of 1/Mg(HMDS)₂/PO = 1:20:5000. For reaction conditions see Table 1, entry 5.

^1H NMR investigation of polymerization setup

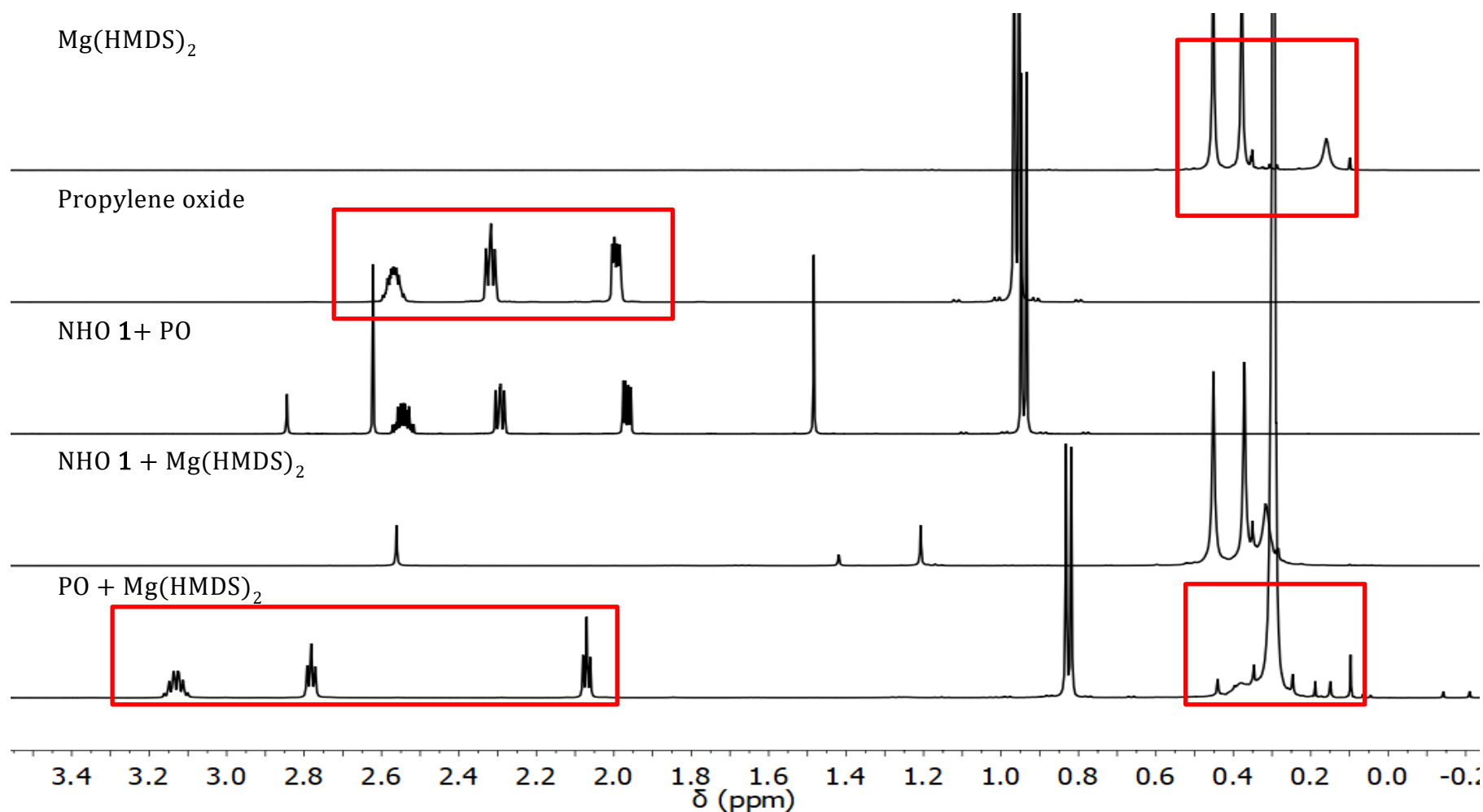


Figure S20. ^1H NMR (C_6D_6 , 400 MHz, ambient) of $\text{Mg}(\text{HMDS})_2$, propylene oxide and NHO 1 and combinations thereof (all mixtures were prepared with a 1:1 molar ratio of their components). Note the distinct shift of the PO-derived signals and the characteristic change of the peak pattern attributable to $\text{Mg}(\text{HMDS})_2$, see also Figure S7 and S8.

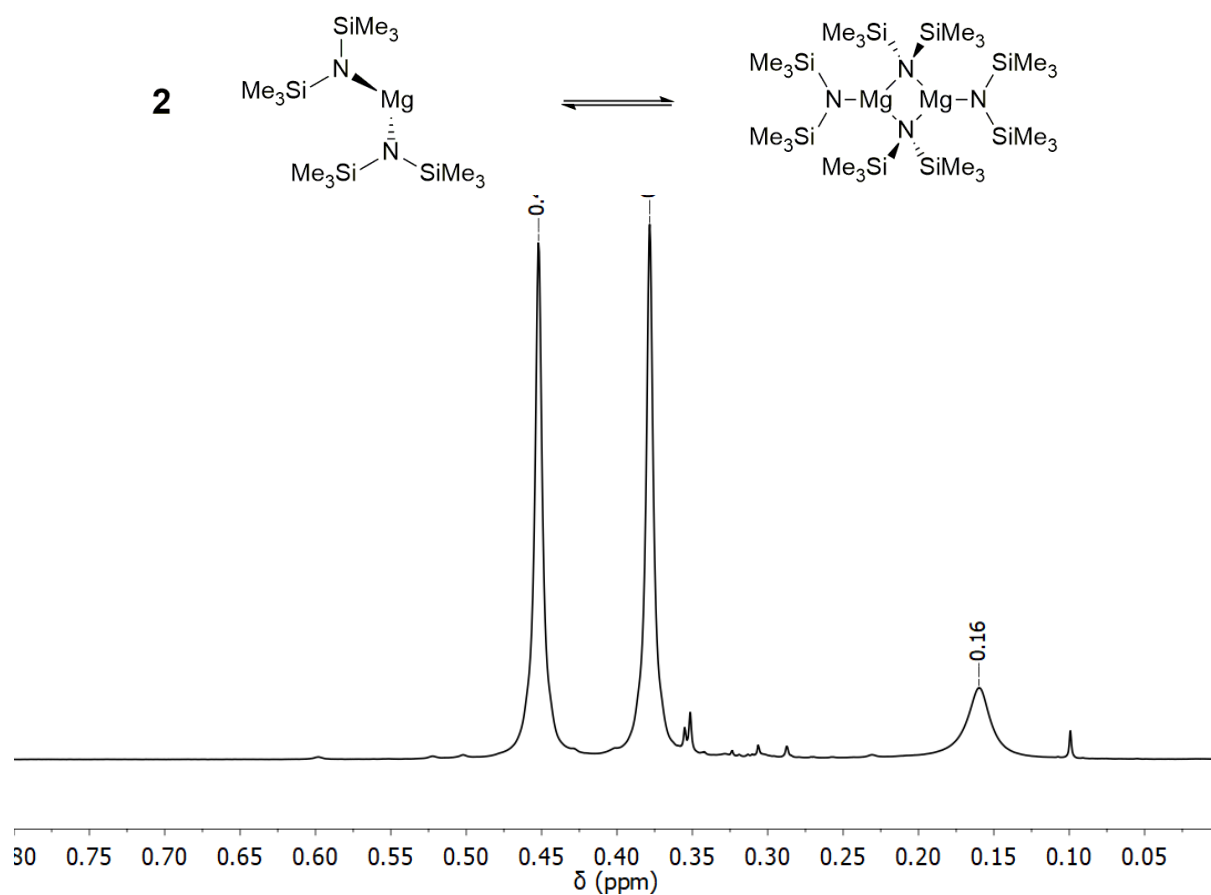


Figure S21. ^1H NMR (C_6D_6 , 400 MHz, ambient) of $\text{Mg}(\text{HMDS})_2$. Literature proposes the distinct signal pattern to originate from an equilibrium of dimeric and monomeric structures.^{20, 172}

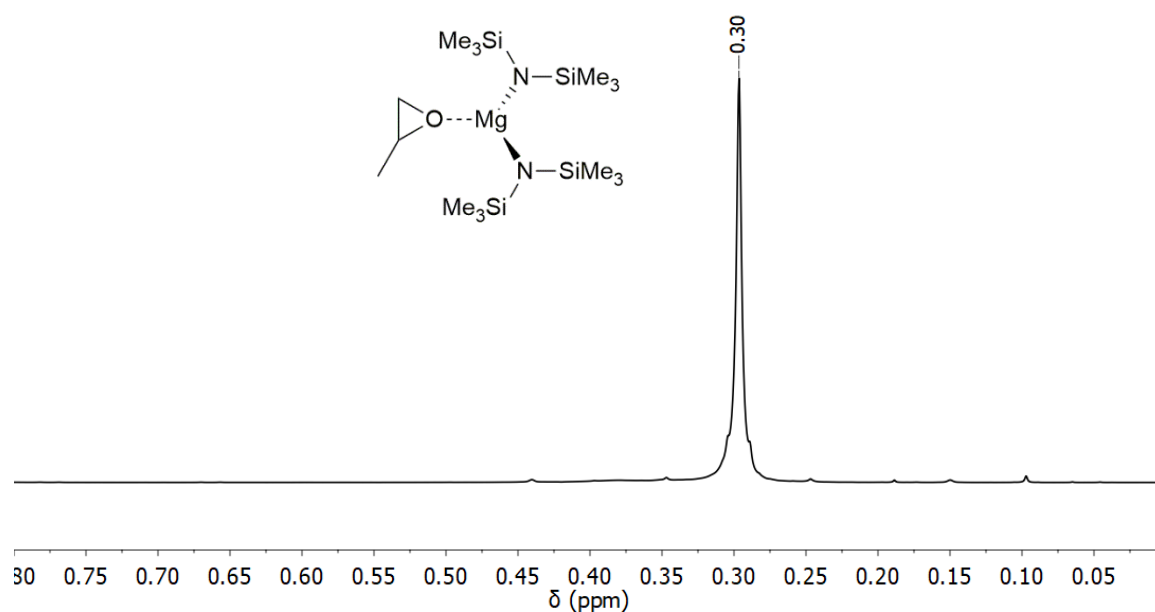


Figure S22. ^1H NMR (C_6D_6 , 400 MHz, ambient, see Figure S6 for full spectrum) of $\text{Mg}(\text{HMDS})_2 + \text{PO}$ (ratio: 1:1). Only one singlet appears, indicating the formation of a monomeric magnesium species. Complexation by PO is proposed to rationalize this observation.

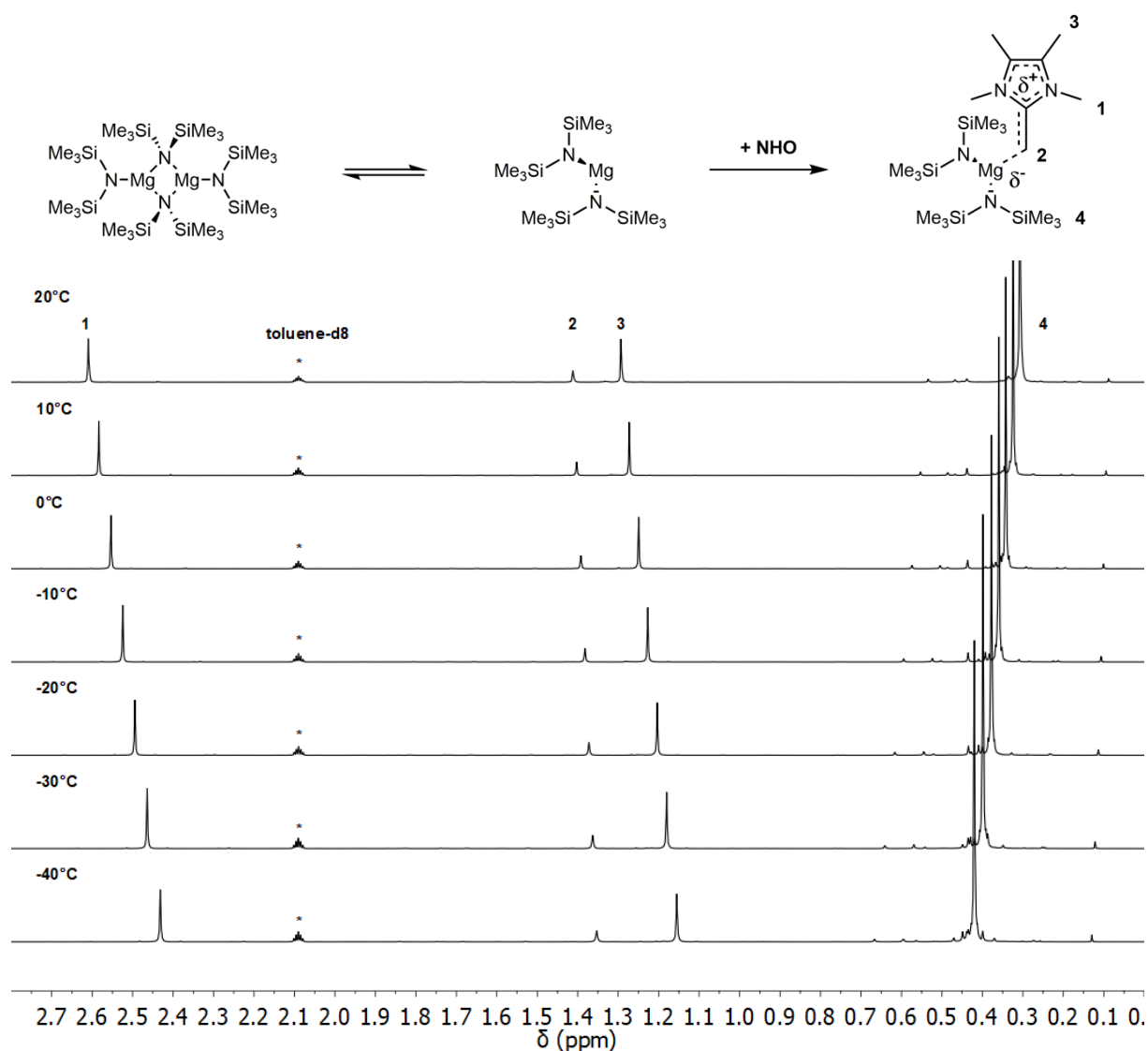
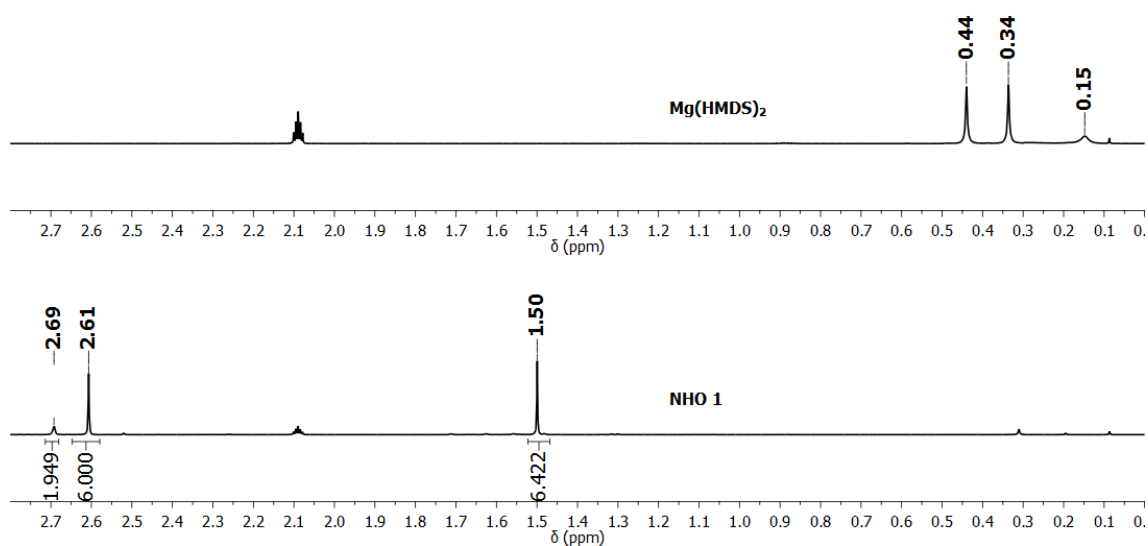
^1H NMR binding study of NHO/ $\text{Mg}(\text{HMDS})_2$ 

Figure S23. Above: ^1H NMR (400 MHz, toluene- d_8) of NHO **1** and $\text{Mg}(\text{HMDS})_2$ at various temperatures. The sample was prepared in a 1:1 molar ratio of both components ($[\mathbf{1}] = 0.05$ mol/L). Below: Note the stark difference for analysis of NHO and $\text{Mg}(\text{HMDS})_2$ alone.



Samples prepared for MALDI-ToF MS analysis

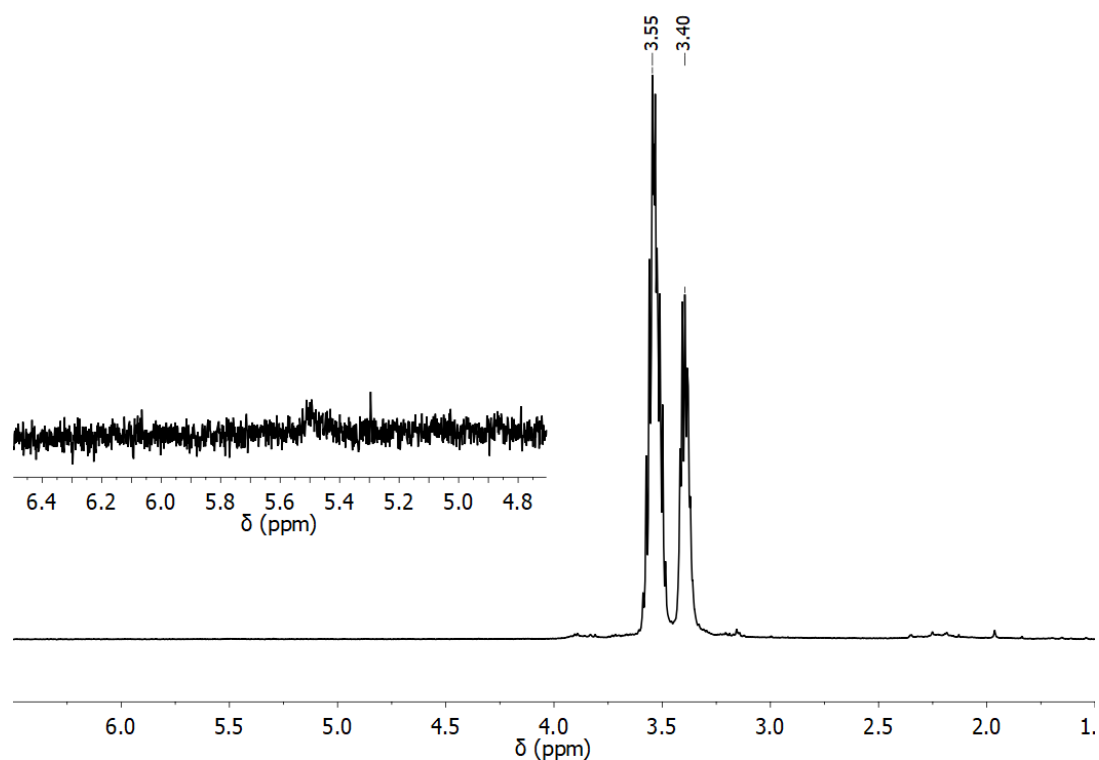


Figure S24. Detail from ^1H NMR (CDCl_3 , 400 MHz, ambient) of poly(propylene oxide), synthesized by applying a ratio of $\text{NHO 1}/\text{Mg}(\text{HMDS})_2/\text{PO} = 1:5:25$. No olefinic protons resulting from allylic end groups originating from transfer-to-monomer are present.

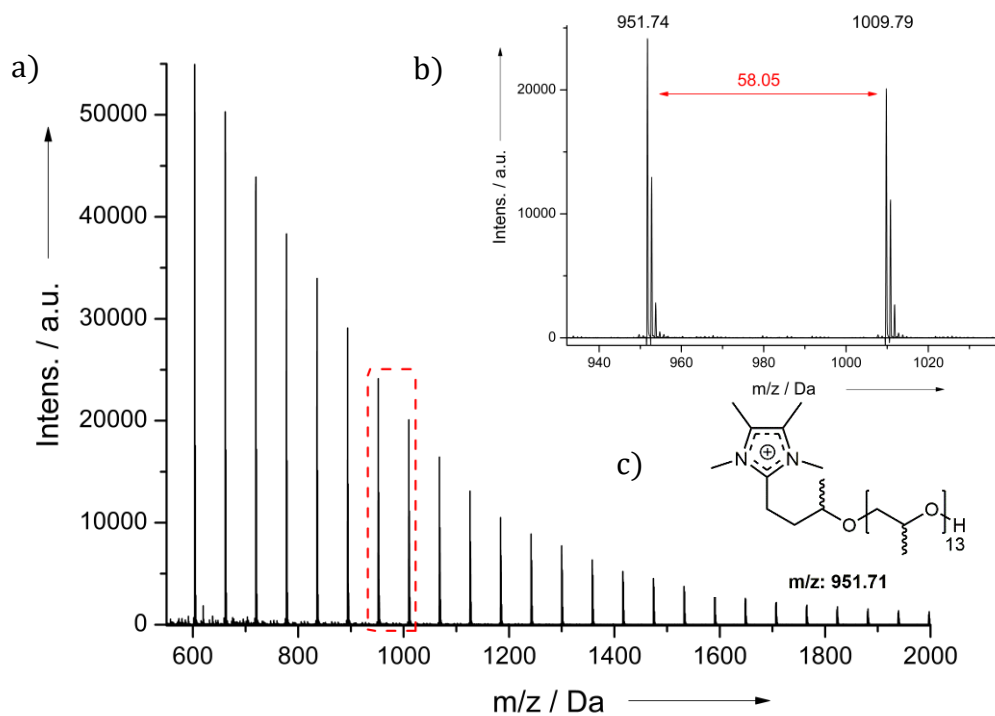


Figure S25. MALDI-ToF MS analysis of poly(propylene oxide) derived from a polymerization using $\text{NHO 1}/\text{Mg}(\text{HMDS})_2/\text{PO}$ in a ratio of 1:5:20 (0.25 M in *n*-pentane). Na^+ was added during matrix preparation.

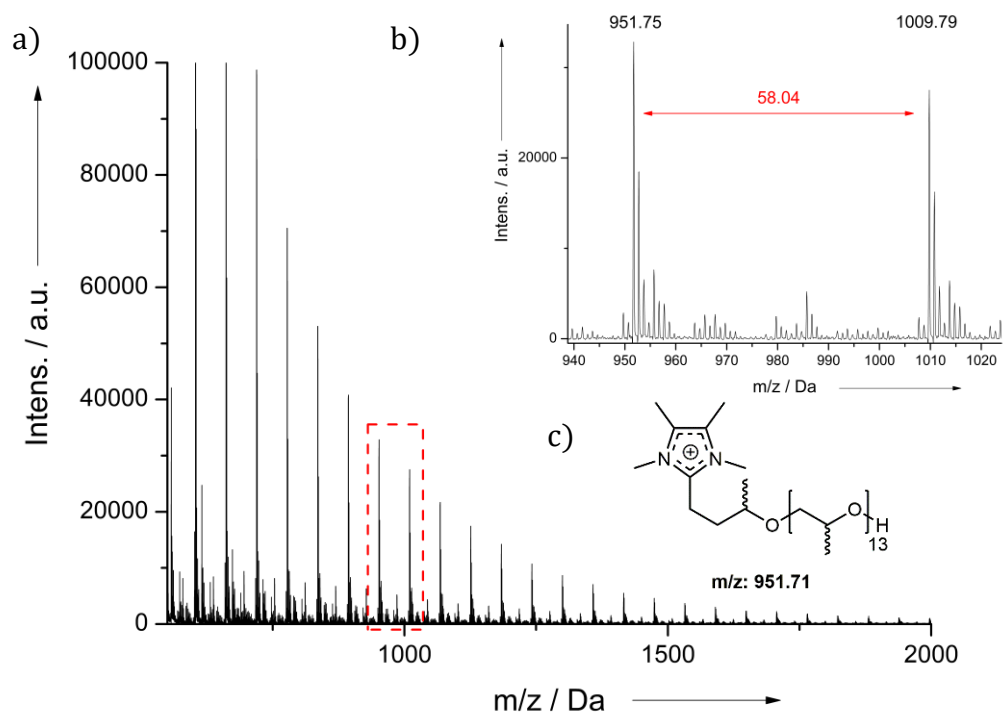


Figure S26. MALDI-ToF MS analysis of poly(propylene oxide) derived from a polymerization using NHO 1/Mg(HMDS)₂/PO in a ratio of 1:5:20 (0.25 M in *n*-pentane). No Na⁺ was added during matrix preparation.

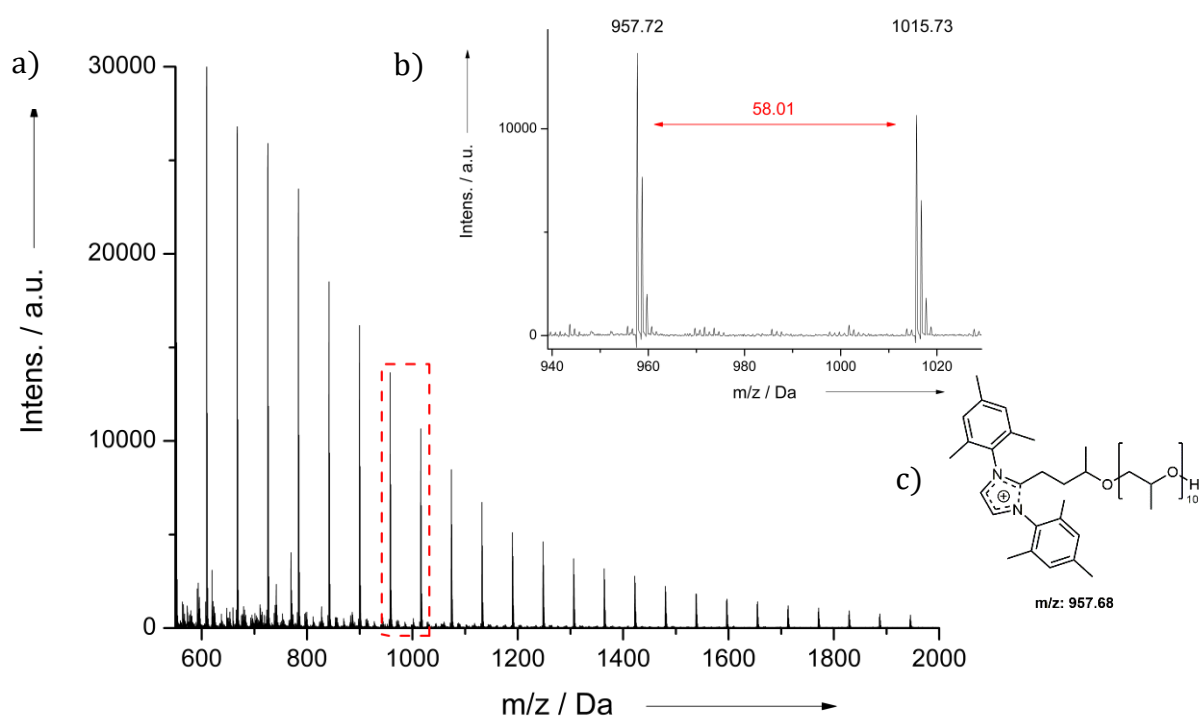


Figure S27. MALDI-ToF MS analysis of poly(propylene oxide) derived from a polymerization using NHO 3/Mg(HMDS)₂/PO in a ratio of 1:5:20 (0.25 M in *n*-pentane). Na⁺ was added during matrix preparation.

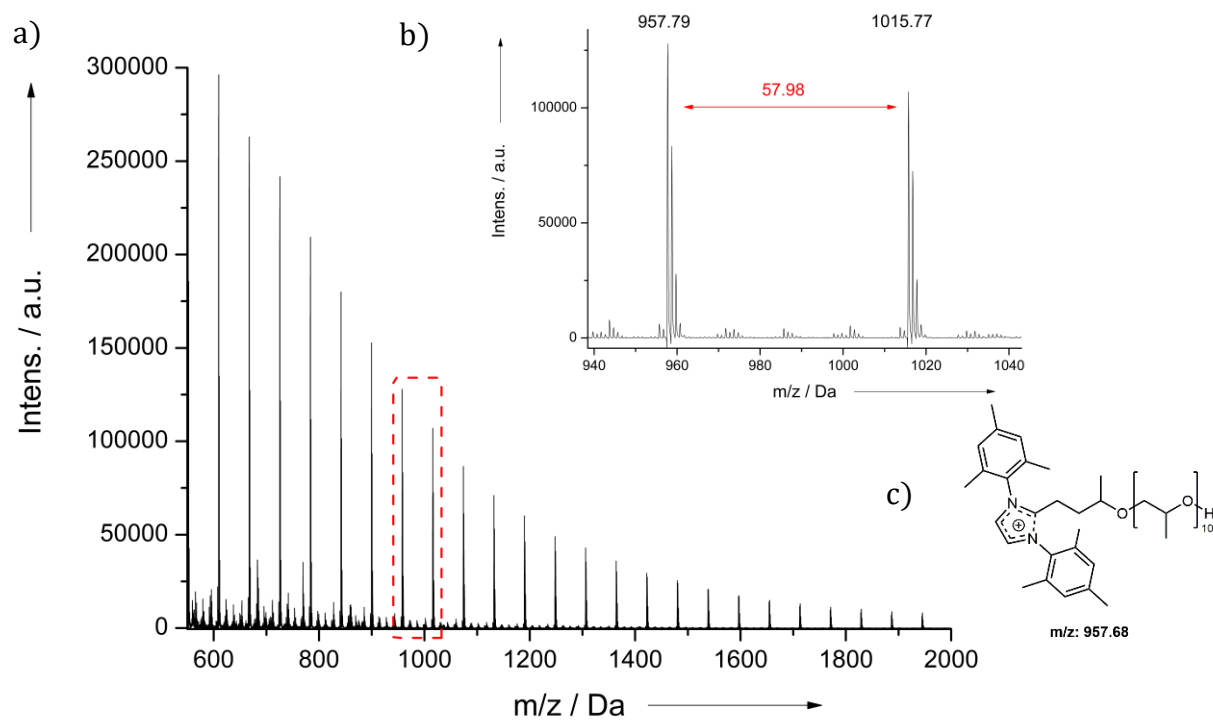


Figure S28. MALDI-ToF MS analysis of poly(propylene oxide) derived from a polymerization using NHO 3/Mg(HMDS)₂/PO in a ratio of 1:5:20 (0.25 M in *n*-pentane). No Na⁺ was added during matrix-preparation.

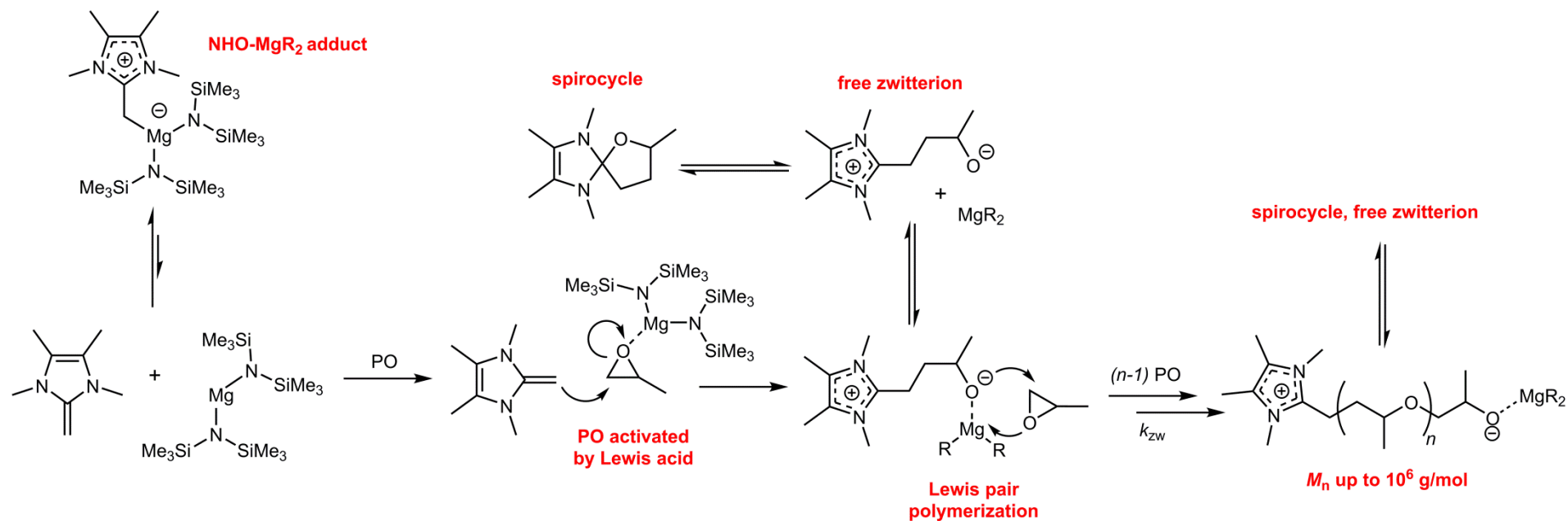


Figure S29. Proposed polymerization mechanism, including conceivable side reactions. The impact of the Lewis acid component seems to be on three different levels. a) A reduction of the concentration of free NHO (=initiator) by complexation; b) activation of the monomer, increasing its susceptibility for nucleophilic attack and ring-opening; c) mitigation of the reactivity of the propagating oxyanion by coordination, potentially explaining the suppression of transfer to monomer as side reaction. Propagation thus occurs via a Lewis pair. The formation of spirocycles, as proposed by Taton^[10] and Falivene^[11] for NHC- or NHO-mediated PO polymerization, cannot be ruled out and might constitute an alternative mechanism for elimination of side reactions. R = -N(SiMe₃)₂.

¹H NMR investigation of PO/AGE copolymerization

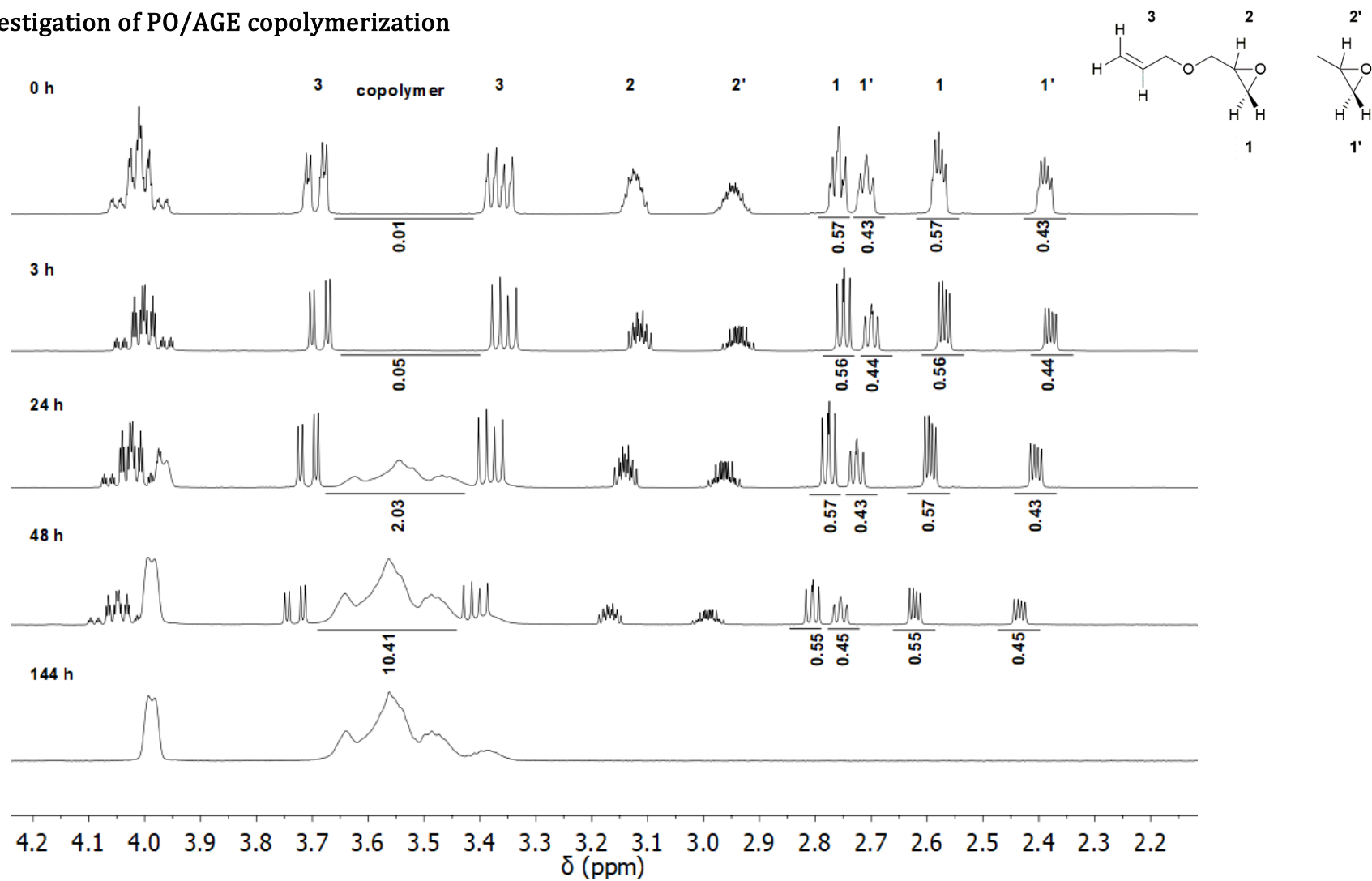


Figure S30. ¹H NMR (CDCl₃, 400 MHz, ambient) of samples drawn from a PO/AGE copolymerization setup (NHO 1/Mg(HMDS)₂/PO/AGE = 1:5:900:1100, 10 M in *n*-pentane, -36°C, 72 h, $M_n = 450.000 \text{ gmol}^{-1}$ ($\bar{D}_M = 1.75$)).

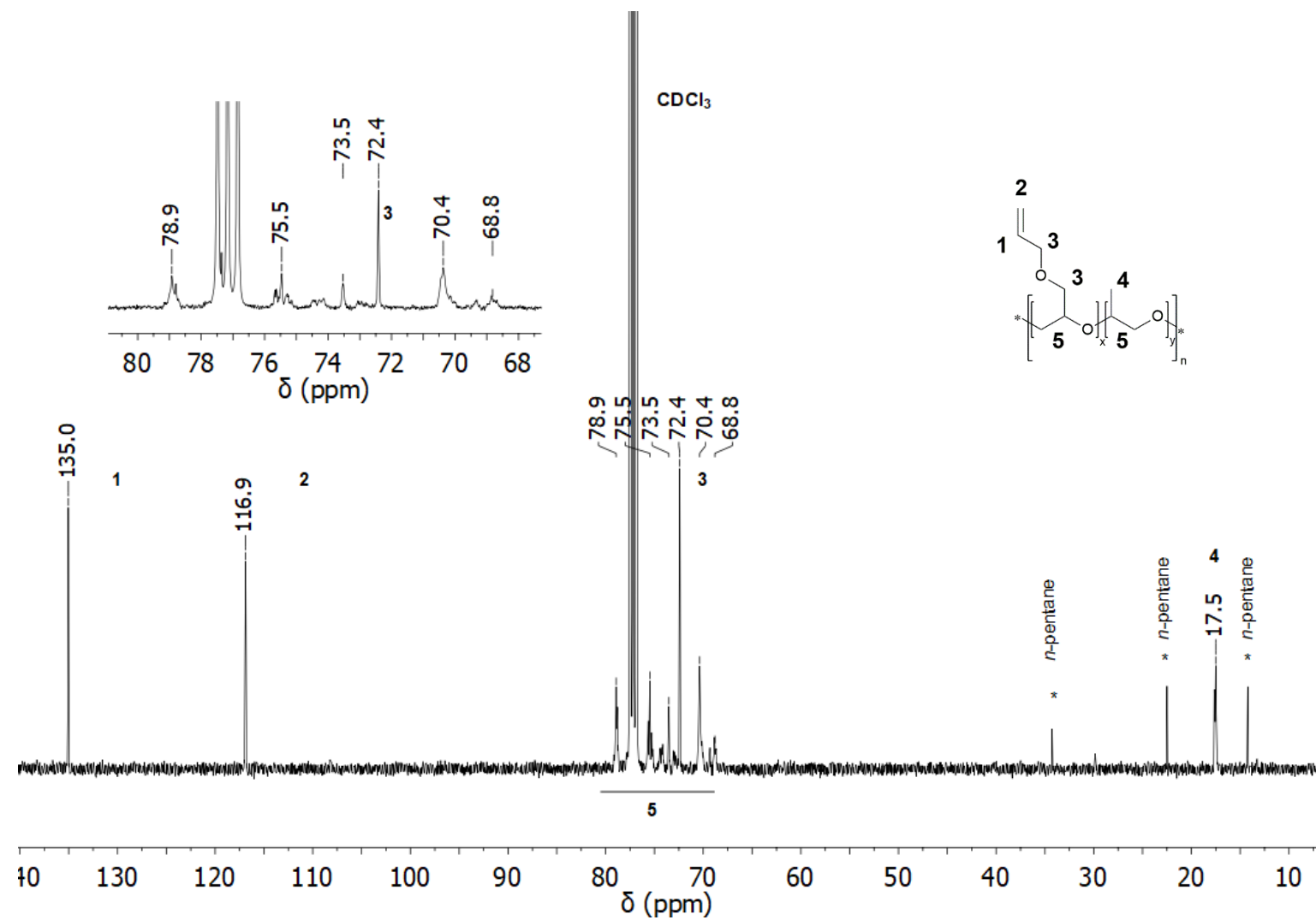


Figure S31. ^{13}C NMR analysis (CDCl_3 , 101 MHz, ambient) of the synthesized copolymer resulting from PO and AGE (NHO 1/Mg(HMDS)₂/PO/AGE = 1:5:900:1100, 10 M in n -pentane, -36°C . 72 h, $M_n = 450.000 \text{ g mol}^{-1}$ ($D_M = 1.75$)).

¹³C NMR analysis of high-molecular weight poly(propylene oxide)

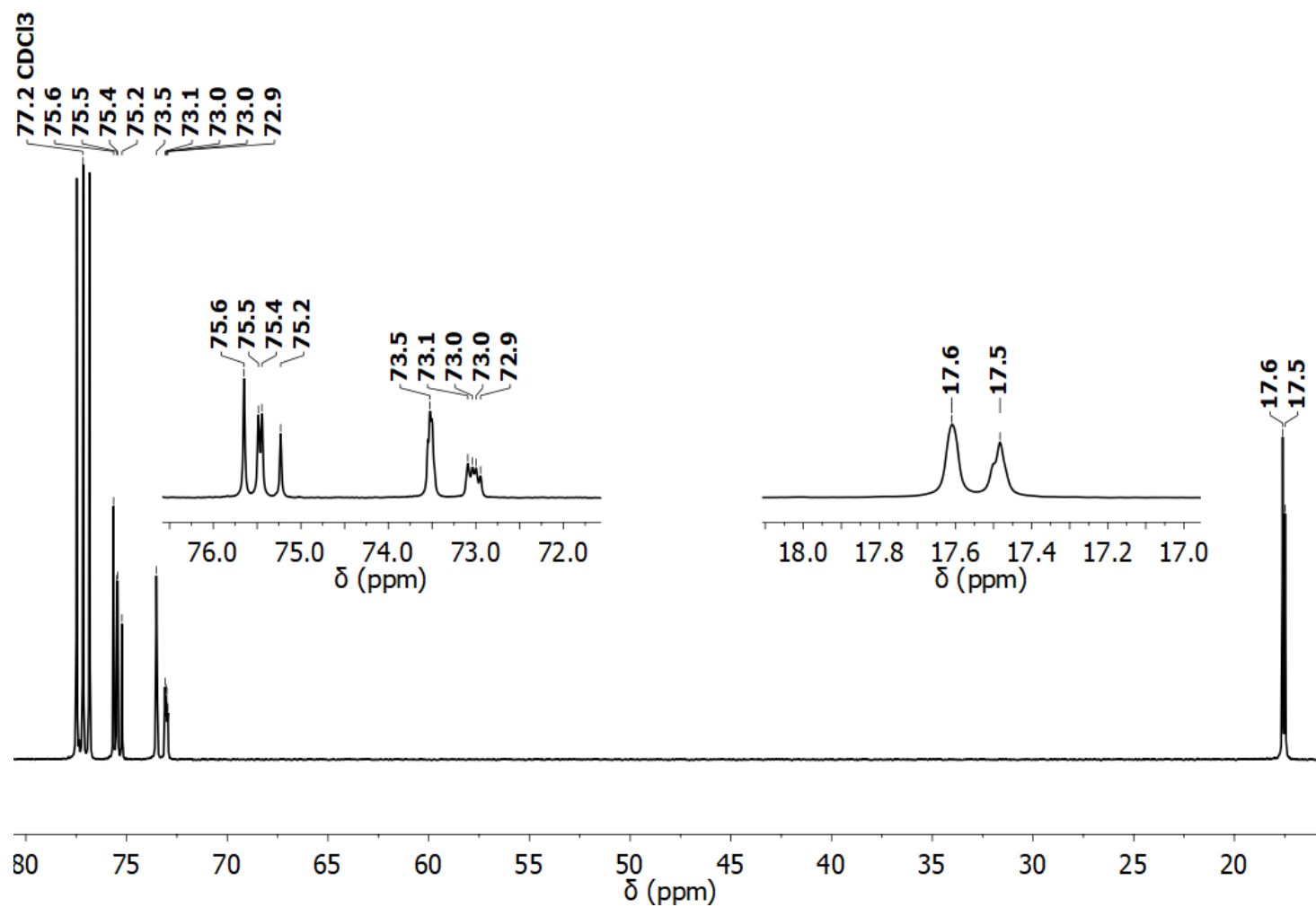


Figure S32: ¹³C NMR (101 MHz, CDCl₃) of high-molecular weight poly(propylene oxide), including details of relevant areas. Solely signals belonging to AAA (BBB) units are present, which suggests a highly regioselective Head-to-Tail (HT) propagation mechanism.

Additional polymerization examples

Table S14. Polymerization of different monomers (Mon), with different Lewis Acids and NHOs. [Mon] = 5M unless noted otherwise.

NHO	LA	Monomer	NHO/MX _n /Mon	<i>t</i> [h]	<i>T</i> [°C]	Conv. ^[a] [%]	<i>M_n</i> (<i>D_M</i>) ^[b] [g·mol ⁻¹]	<i>M_{n,corr.}</i>
1	Mg(HMDS) ₂	BO	1:5:1000	72	-36	> 99	38400 (2.1)*	21100
1	Mg(HMDS) ₂	BO	1:5:1000	96	r.t.	45	11000 (4)*	6100
1	Mg(HMDS) ₂	BO	1:20:1000	2	60	89	12500 (2.5)*	6900
1	Mg(HMDS) ₂	AGE	1:5:1000	0.5	r.t.	> 99	563000 (1.95)	309700
1	Mg(HMDS) ₂	AGE	1:5:1000	4	60	> 99	64300 (5)	35400
1	Mg(HMDS) ₂	AGE	1:5:1000	72	-36	> 99	1.6·10 ⁻⁶ (1.65)	880000
2	Mg(HMDS) ₂	PO	1:5:5000	48	r.t.	> 99	380000 (2.5)	209000
2	Mg(HMDS) ₂	PO	1:20:5000	141	-36	> 99	2.6·10 ⁻⁶ (1.55)	1.4·10 ⁻⁶
3	Mg(HMDS) ₂	PO	1:5:1000	96	-36	> 99	500000 (2.3)	275000
4	Mg(HMDS) ₂	PO	1:5:1000	96	-36	> 99	810000 (2.2)	446000
1	LiHMDS	PO	1:5:1000	72	r.t.	-	-	-
1	KHMDS	PO	1:5:1000	72	r.t.	90	5200 (1.43)	2900
1	Mg(TFSI) ₂	PO	1:5:1000	96	r.t.	60	80000 (1.63)	44000

*: bulk reactions; ^[a] determined via ¹H NMR; ^[b] determined via GPC (CHCl₃), raw data and light-scattering-corrected results.

References

- [1] M. Westerhausen, *Inorg. Chem.* **1991**, *30*, 96-101.
- [2] S. Naumann, A. W. Thomas, A. P. Dove, *Angew. Chem. Int. Ed.* **2015**, *54*, 9550-9554; *Angew. Chem.* **2015**, *127*, 9686-9690.
- [3] U. Gruseck, M. Heuschmann, *Chem. Ber.* **1987**, *120*, 2053-2064.
- [4] S. Naumann, D. Wang, *Macromolecules* **2016**, *49*, 8869-8878.
- [5] S. Kronig, P. G. Jones, M. Tamm, *Eur. J. Inorg. Chem.* **2013**, *2013*, 2301-2314.
- [6] H. Quast, M. Ach, M. K. Kindermann, P. Rademacher, M. Schindler, *Chem. Ber.* **1993**, *126*, 503-516.
- [7] K. Powers, C. Hering-Junghans, R. McDonald, M. J. Ferguson, E. Rivard, *Polyhedron* **2016**, *108*, 8-14.
- [8] P. Walther, W. Frey, S. Naumann, *Polym. Chem.* **2018**, *9*, 3674-3683.
- [9] A. I. Ojeda-Amador, A. J. Martínez-Martínez, G. M. Robertson, S. D. Robertson, A. R. Kennedy, C. T. O'Hara, *Dalton Transactions* **2017**, *46*, 6392-6403.
- [10] J. Raynaud, C. Absalon, Y. Gnanou, D. Taton, *Macromolecules* **2010**, *43*, 2814.
- [11] M. Al Ghamdi, L. Cavallo, L. Falivene, *J. Phys. Chem. C* **2017**, *121*, 2730.

4. Appendix

4.1. References

- (1) A. Duda, A. Kowalski, T. Endo, F. Ganachaud, S. Boileau, F. F. Stewart, E. S. Peterson, P. J. Dijkstra, R. Hoogenboom, J. Roda, M. R. Buchmeiser, O. Coulembier, P. Dubois, O. Dechy-Cabaret, B. Martin-Vaca, D. Bourissou, H. Keul, J. Penelle, A. P. Dove, A. Heise, C. J. Duxbury, A. R. A. Palmans, *Handbook of Ring-Opening Polymerization*, Wiley-VCH, Weinheim, **2009**.
- (2) a) S. Naumann, F. G. Schmidt, W. Frey, M. R. Buchmeiser, *Polym. Chem.* **2013**, *4*, 4172; b) S. Naumann, P. B. Scholten, J. A. Wilson, A. P. Dove, *J. Am. Chem. Soc.* **2015**, *137*, 14439-14445; c) S. Naumann, D. Wang, *Macromolecules* **2016**, *49*, 8869-8878; d) M. M. D. Roy, E. Rivard, *Acc. Chem. Res.* **2017**, *50*, 2017-2025.
- (3) M. Hong, J. Chen, E. Y. Chen, *Chem. Rev.* **2018**, *118*, 10551-10616.
- (4) P. Walther, S. Naumann, *Macromolecules* **2017**, *50*, 8406-8416.
- (5) M. Hong, E. Y. Chen, *Nat. Chem.* **2016**, *8*, 42-49.
- (6) P. Walther, W. Frey, S. Naumann, *Polym. Chem.* **2018**, *9*, 3674-3683.
- (7) J. Herzberger, K. Niederer, H. Pohlit, J. Seiwert, M. Worm, F. R. Wurm, H. Frey, *Chem. Rev.* **2016**, *116*, 2170-2243.
- (8) a) S. Naumann, A. W. Thomas, A. P. Dove, *Angew. Chem. Int. Ed.* **2015**, *54*, 9550-9554; *Angew. Chem.* **2015**, *127*, 9686-9690; b) A. Balint, M. Papendick, M. Clauss, C. Müller, F. Giesselmann, S. Naumann, *Chem. Commun.* **2018**, *54*, 2220-2223.
- (9) a) P. Walther, A. Krauss, S. Naumann, *Angew. Chem. Int. Ed.* **2019**, *58*, 10737-10741; *Angew. Chem.* **2019**, *131*, 10848-10852; b) P. Walther, C. Vogler, S. Naumann, *Synlett* **2020**, *31*, 641-647.
- (10) U. Gruseck, M. Heuschmann, *Chem. Ber.* **1987**, *120*, 2053-2064.
- (11) a) Y. B. Wang, Y. M. Wang, W. Z. Zhang, X. B. Lu, *J. Am. Chem. Soc.* **2013**, *135*, 11996-12003; b) Y.-B. Jia, Y.-B. Wang, W.-M. Ren, T. Xu, J. Wang, X.-B. Lu, *Macromolecules* **2014**, *47*, 1966-1972; c) K.-M. Wang, S.-J. Yan, J. Lin, *Eur. J. Org. Chem.* **2014**, *2014*, 1129-1145; d) M. Blumel, J. M. Noy, D. Enders, M. H. Stenzel, T. V. Nguyen, *Org. Lett.* **2016**, *18*, 2208-2211; e) R. D. Crocker, T. V. Nguyen, *Chem. Eur. J.* **2016**, *22*, 2208-2213; f) A. Iturmendi, N. Garcia, E. A. Jaseer, J. Munarriz, P. J. Sanz Miguel, V. Polo, M. Iglesias, L. A. Oro, *Dalton Trans* **2016**, *45*, 12835-12845; g) S. Naumann, A. W. Thomas, A. P. Dove, *ACS Macro Lett.* **2016**, *5*, 134-138; h) V. B. Saptal, B. M. Bhanage, *ChemSusChem* **2016**, *9*, 1980-1985.
- (12) R. Schuldt, J. Kästner, S. Naumann, *J. Org. Chem.* **2019**, *84*, 2209-2218.
- (13) a) A. Duda, S. Penczek, *Macromol. Chem. Phys.* **1996**, *197*, 1273-1283; b) K. N. Houk, A. Jabbari, H. K. Hall Jr., C. Alemán, *J. Org. Chem.* **2008**, *73*, 2674-2678; c) M. Hong, E. Y. Chen, *Angew. Chem. Int. Ed.* **2016**, *55*, 4188-4193; *Angew. Chem.* **2016**, *128*, 4260-4265; d) M. Hong, X. Tang, B. S. Newell, E. Y. X. Chen, *Macromolecules* **2017**, *50*, 8469-8479; e) N. Zhao, C. Ren, H. Li, Y. Li, S. Liu, Z. Li, *Angew. Chem. Int. Ed.* **2017**, *56*, 12987-12990; *Angew. Chem.* **2017**, *129*, 13167-13170; f) J. B. Zhu, E. M. Watson, J. Tang, E. Y. Chen, *Science* **2018**, *360*, 398-403.
- (14) a) J. Schaefer, *Macromolecules* **1969**, *2*, 533-537; b) C. Price, M. K. Akkapeddi, B. T. DeBone, B. C. Furie, *J. Am. Chem. Soc.* **1972**, *94*, 3964-3971; c) J. Wu, Z. Shen, *J. Polym. Sci., Part A: Polym. Chem.* **1990**, *28*, 1995-1997; d) K. Mortensen, W. Brown, J. Erling, *Macromolecules* **1994**, *27*, 5654-5666.
- (15) T. R. Hoare, D. S. Kohane, *Polymer* **2008**, *49*, 1993-2007.
- (16) a) Y. Meng, D. Gu, F. Zhang, Y. Shi, H. Yang, Z. Li, C. Yu, B. Tu, D. Zhao, *Angew. Chem. Int. Ed.* **2005**, *44*, 7053-7059; *Angew. Chem.* **2005**, *43*, 7215-7221; b) X. Qian, H. Li, Y. Wan, *Microporous Mesoporous Mater.* **2011**, *141*, 26-37; c) P. Li, Y. Song, Q.

- Lin, J. Shi, L. Liu, L. He, H. Ye, Q. Guo, *Microporous Mesoporous Mater.* **2012**, *159*, 81-86; d) T. Y. Ma, L. Liu, Z. Y. Yuan, *Chem. Soc. Rev.* **2013**, *42*, 3977-4003.
- (17) M. M. Doeff, *J. Electrochem. Soc.* **1999**, *146*, 2024-2028.
- (18) A. Sosnik, D. Cohn, *Biomaterials* **2004**, *25*, 2851-2858.
- (19) F. Markus, J. R. Bruckner, S. Naumann, *Macromol. Chem. Phys.* **2020**, *221*, 1900437.
- (20) M. Westerhausen, *Inorg. Chem.* **1991**, *30*, 96-101.
- (21) a) Q. Wang, W. Zhao, J. He, Y. Zhang, E. Y. X. Chen, *Macromolecules* **2017**, *50*, 123-136; b) Y. Chen, J. Shen, S. Liu, J. Zhao, Y. Wang, G. Zhang, *Macromolecules* **2018**, *51*, 8286-8297; c) S. Liu, T. Bai, K. Ni, Y. Chen, J. Zhao, J. Ling, X. Ye, G. Zhang, *Angew. Chem. Int. Ed.* **2019**, *58*, 15478-15487; *Angew. Chem.* **2019**, *43*, 15624-15633; d) Q. Wang, W. Zhao, S. Zhang, J. He, Y. Zhang, E. Y. X. Chen, *ACS Catal.* **2018**, *8*, 3571-3578.
- (22) a) K. L. Peretti, H. Ajiro, C. T. Cohen, E. B. Lobkovsky, G. W. Coates, *J. Am. Chem. Soc.* **2005**, *127*, 11566-11567; b) W. Hirahata, R. M. Thomas, E. B. Lobkovsky, G. W. Coates, *J. Am. Chem. Soc.* **2008**, *130*, 17658-17659; c) P. C. B. Widger, S. M. Ahmed, G. W. Coates, *Macromolecules* **2011**, *44*, 5666-5670; d) M. I. Childers, J. M. Longo, N. J. Van Zee, A. M. LaPointe, G. W. Coates, *Chem. Rev.* **2014**, *114*, 8129-8152.
- (23) a) J. Penelle, G. Clarebout, I. Balikdjian, *Polym. Bull.* **1994**, *32*, 395-401; b) A. Benlahouès, B. Brissault, S. Boileau, J. Penelle, *Macromol. Chem. Phys.* **2018**, 1700463; c) R. H. Grubbs, E. Khosravi, *Handbook of Metathesis, Vol. 3: Polymer Synthesis*, Wiley-VCH Verlag GmbH, Weinheim, **2015**; d) W. Kuran, *Prog. Polym. Sci.* **1998**, *23*, 919-992.
- (24) a) Z. Jedlinski, M. Kowalczyk, P. Kurcok, *Macromolecules* **1991**, *24*, 1218-1219; b) Y. Shen, Z. Shen, Y. Zhang, K. Yao, *Macromolecules* **1996**, *29*, 8289-8295.
- (25) B. M. Chamberlain, M. Cheng, D. R. Moore, T. M. Ovitt, E. B. Lobkovsky, G. W. Coates, *J. Am. Chem. Soc.* **2001**, *123*, 3229-3238.
- (26) a) F. S. Dainton, K. J. Ivin, *Nature* **1948**, *162*, 705-707; b) F. S. Dainton, K. J. Ivin, *Q. Rev. Chem. Soc.* **1958**, *12*, 61; c) A. V. Tobolsky, A. Rembaum, A. Eisenberg, *J. Polym. Sci.* **1960**, *45*, 347-366; d) J. P. van Hook, A. V. Tobolsky, *J. Polym. Sci.* **1958**, *33*, 429-445; e) A. V. Tobolsky, A. Eisenberg, *J. Am. Chem. Soc.* **1959**, *81*, 780-782.
- (27) C. W. Bielawski, R. H. Grubbs, *Prog. Polym. Sci.* **2007**, *32*, 1-29.
- (28) a) A. Duda, A. Kowalski, S. Penczek, H. Uyama, S. Kobayashi, *Macromolecules* **2002**, *35*, 4266-4270; b) S. A. Vysokomolekulyarnye Soedineniya, A. A., B. V. Lebedev, E. G. Kiparisova, *Vysokomol. Sedin., Ser. A* **1983**, *25*, 1679 - 1685.
- (29) S. Penczek, K. Matyjaszewski, *J. polym. sci., Polym. symp.* **1976**, *56*, 255-269.
- (30) H.-J. Kreß, W. Stix, W. Heitz, *Macromol. Chem. Phys.* **1984**, *185*, 173-191.
- (31) F. Korte, W. Glet, *J. Polym. Sci. Pol. Lett.* **1966**, *4*, 685-689.
- (32) a) H. Jacobson, W. H. Stockmayer, *J. Chem. Phys.* **1950**, *18*, 1600-1606; b) J. A. Semlyen, *Ring-chain equilibria and the conformations of polymer chains in Mechanisms of Polyreactions - Polymer Characterization. Advances in Polymer Science, Vol. 21*, Springer, Berlin, Heidelberg, **1976**, pp. 41-75.
- (33) A. Duda, *Polimery* **1998**, *43*, 135-144.
- (34) K. Matyjaszewski, S. Słomkowski, S. Penczek, *J. Polym. Sci., Part A: Polym. Chem.* **1979**, *17*, 2413-2422.
- (35) a) P. J. Flory, *J. Am. Chem. Soc.* **1940**, *62*, 1561-1565; b) P. J. Flory, in *Principles of Polymer Chemistry*, Cornell University Press, Ithaca, NY, **1953**, p. 336.
- (36) J.-M. Raquez, P. Degée, R. Narayan, P. Dubois, *Macromolecules* **2001**, *34*, 8419-8425.
- (37) S. Penczek, P. Kubisa, R. Szymanski, *Macromol. Rapid Commun.* **1991**, *12*, 77-80.

- (38) a) A. Deffieux, S. Boileau, *Macromolecules* **1976**, *9*, 369 - 371; b) S. Słomkowski, *Polymer* **1986**, *27*, 71-75.
- (39) S. Penczek, P. Kubisa, K. Matyjaszewski, *Adv. Polym. Sci.* **1980**, *37*, 52.
- (40) S. Penczek, *J. Polym. Sci., Part A: Polym. Chem.* **2000**, *38*, 1919-1933.
- (41) a) K. S. Kazanskii, A. A. Solovyanov, S. G. Entelis, *Eur. Polym. J.* **1971**, *7*, 1421-1433; b) L. Wilczek, J. P. Kennedy, *Polym. J.* **1987**, *19*, 531-538; c) A. Duda, S. Penczek, *Makromol. Chem., Macromol. Symp.* **1991**, *47*, 127-140; d) A. Duda, S. Penczek, *Macromol. Rapid Commun.* **1994**, *15*, 559-566; e) T. Biela, A. Duda, *J. Polym. Sci., Part A: Polym. Chem.* **1996**, *34*, 1807-1813.
- (42) A. Duda, S. Penczek, *Macromol. Rapid Commun.* **1995**, *16*, 67-76.
- (43) a) C. K. Williams, *Chem. Soc. Rev.* **2007**, *36*, 1573-1580; b) A. K. Sutar, T. Maharana, S. Dutta, C. T. Chen, C. C. Lin, *Chem. Soc. Rev.* **2010**, *39*, 1724-1746.
- (44) S. Kobayashi, H. Uyama, *J. Polym. Sci., Part A: Polym. Chem.* **2002**, *40*, 192-209.
- (45) a) R. K. Sadhir, R. M. Luck, *Expanding Monomers. Synthesis, Characterization, and Applications*, CRC Press, Florida, **1992**; b) W. Choi, F. Sanda, T. Endo, *Macromolecules* **1998**, *31*, 9093-9095.
- (46) T. Endo, K. Suga, *J. Polym. Sci., Part A: Polym. Chem.* **1989**, *27*, 1831-1842.
- (47) A. Simakova, C. Arnoux, K. Matyjaszewski, *Polimery* **2017**, *62*, 262-271.
- (48) I. S. Chung, K. Matyjaszewski, *Macromolecules* **2003**, *36*, 2995-2998.
- (49) M. R. Buchmeiser, *Chem. Rev.* **2000**, *100*, 1565-1604.
- (50) a) M. R. Buchmeiser, *Macromol. Rapid Commun.* **2019**, *40*, 1800492; b) M. R. Buchmeiser, *Chemistry* **2018**, *24*, 14295-14301; c) M. R. Buchmeiser, *Polymer Reviews* **2016**, *57*, 15-30; d) M. R. Buchmeiser, *Immobilization of Olefin Metathesis Catalysts in Olefin Metathesis* (Ed.: K. Grela), **2014**; e) F. Ziegler, J. Teske, I. Elser, M. Dyballa, W. Frey, H. Kraus, N. Hansen, J. Rybka, U. Tallarek, M. R. Buchmeiser, *J. Am. Chem. Soc.* **2019**, *141*, 19014-19022; f) I. Elser, J. Groos, P. M. Hauser, M. Koy, M. van der Ende, D. Wang, W. Frey, K. Wurst, J. Meisner, F. Ziegler, J. Kästner, M. R. Buchmeiser, *Organometallics* **2019**, *38*, 4133-4146; g) M. J. Benedikter, R. Schowner, I. Elser, P. Werner, K. Herz, L. Stöhr, D. A. Imbrich, G. M. Nagy, D. Wang, M. R. Buchmeiser, *Macromolecules* **2019**, *52*, 4059-4066.
- (51) a) R. R. Schrock, *Acc. Chem. Res.* **1986**, *19*, 342-348; b) J. O. Krause, M. T. Zarka, U. Anders, R. Weberskirch, O. Nuyken, M. R. Buchmeiser, **2003**, *42*, 5965-5969; *Angew. Chem.* **2003**, *115*, 6147-6151; c) E. Despagnet-Ayoub, T. Ritter, *N-Heterocyclic Carbenes as Ligands for Olefin Metathesis Catalysts in N-Heterocyclic Carbenes in Transition Metal Catalysis* (Ed.: F. Glorius), Springer Berlin Heidelberg, Berlin, Heidelberg, **2007**, pp. 193-218.
- (52) G. N. Lewis, *Valence and the Structure of Atoms and Molecules*, The Chemical Catalog Company, Inc., New York, **1923**.
- (53) a) H. Yamamoto, *Lewis Acids in Organic Synthesis*, Wiley-VCH, Weinheim, **2000**; b) F. A. Cotton, G. Wilkinson, C. A. Murillo, *Advanced Inorganic Chemistry*, 6th ed., Wiley, Toronto, **1999**.
- (54) a) G. C. Welch, L. Cabrera, P. A. Chase, E. Hollink, J. D. Masuda, P. Wei, D. W. Stephan, *Dalton Trans.* **2007**, 3407-3414; b) G. C. Welch, R. R. San Juan, J. D. Masuda, D. W. Stephan, *Science* **2006**, *314*, 1124-1126; c) P. Spies, G. Erker, G. Kehr, K. Bergander, R. Frohlich, S. Grimme, D. W. Stephan, *Chem. Commun.* **2007**, 5072-5074; d) G. C. Welch, D. W. Stephan, *J. Am. Chem. Soc.* **2007**, *129*, 1880-1881; e) P. A. Chase, G. C. Welch, T. Jurca, D. W. Stephan, *Angew. Chem. Int. Ed.* **2007**, *46*, 8050-8053; *Angew. Chem.* **2007**, *119*, 8196-8199; f) J. S. McCahill, G. C. Welch, D. W. Stephan, *Angew. Chem. Int. Ed.* **2007**, *46*, 4968-4971; *Angew. Chem.* **2007**, *119*, 5056-5059.

- (55) a) D. W. Stephan, *Science* **2016**, *354*, 1248-1257; b) D. Chen, J. Klankermayer, H. Berke, Y. Jiang, X. Yang, C. Jiang, S. Chakraborty, A. Landwehr, Z. Lu, H. Ye, H. Wang, L. Greb, J. Paradies, W. Uhl, E.-U. Würthwein, E. L. Kolychev, E. Theuergarten, M. Tamm, S. Khan, M. Alcarazo, P. Knochel, K. Karaghiosoff, S. Manolikakes, A. E. Ashley, D. O'Hare, T. H. Warren, G. Erker, E. Y. Chen, D. Wass, A. Amgoune, G. Bouhadir, D. Bourissou, *Frustrated Lewis Pairs II: Expanding The Scope, Vol. 334*, Springer-Verlag, Berlin, Heidelberg, **2013**.
- (56) Y. Zhang, G. M. Miyake, E. Y. Chen, *Angew. Chem. Int. Ed.* **2010**, *49*, 10158-10162; *Angew. Chem.* **2010**, *122*, 10356-10360.
- (57) a) R. F. Childs, D. L. Mulholland, A. Nixon, *Can. J. Chem.* **1982**, *60*, 801-808; b) R. F. Childs, D. L. Mulholland, A. Nixon, *Can. J. Chem.* **1982**, *60*, 809-812.
- (58) a) V. Gutmann, *Coord. Chem. Rev.* **1976**, *18*, 225-255; b) U. Mayer, V. Gutmann, W. Gerger, *Monatsh. Chem.* **1975**, *106*, 1235-1257; c) M. A. Beckett, G. C. Strickland, J. R. Holland, K. Sukumar Varma, *Polymer* **1996**, *37*, 4629-4631.
- (59) H. Bohrer, N. Trapp, D. Himmel, M. Schleep, I. Krossing, *Dalton Trans.* **2015**, *44*, 7489-7499.
- (60) A. R. Jupp, T. C. Johnstone, D. W. Stephan, *Dalton Trans.* **2018**, *47*, 7029-7035.
- (61) S. G. Lias, J. F. Liebman, R. D. Levin, *J. Phys. Chem. Ref. Data* **1984**, *13*, 695-808.
- (62) G. Wilke, H. Martin, R. Mülhaupt, H. H. Brintzinger, *Ziegler Catalysts - Recent Scientific Innovations and Technological Improvements*, Springer-Verlag, Weinheim, **1995**.
- (63) T. C. Johnstone, G. Wee, D. W. Stephan, *Angew. Chem. Int. Ed.* **2018**, *57*, 5881-5884; *Angew. Chem.* **2018**, *130*, 5983-5986.
- (64) S. J. Geier, D. W. Stephan, *J. Am. Chem. Soc.* **2009**, *131*, 3476-3477.
- (65) Y. Zhang, G. M. Miyake, M. G. John, L. Falivene, L. Caporaso, L. Cavallo, E. Y. Chen, *Dalton Trans.* **2012**, *41*, 9119-9134.
- (66) J. He, Y. Zhang, L. Falivene, L. Caporaso, L. Cavallo, E. Y. X. Chen, *Macromolecules* **2014**, *47*, 7765-7774.
- (67) W. Nzahou Ottou, E. Conde-Mendizabal, A. Pascual, A.-L. Wirotius, D. Bourichon, J. Vignolle, F. Robert, Y. Landais, J.-M. Sotiropoulos, K. Miqueu, D. Taton, *Macromolecules* **2017**, *50*, 762-774.
- (68) X. Wang, Y. Zhang, M. Hong, *Molecules* **2018**, *23*, 442-453.
- (69) M. G. Knaus, M. M. Giuman, A. Pothig, B. Rieger, *J. Am. Chem. Soc.* **2016**, *138*, 7776-7781.
- (70) T. Xu, E. Y. Chen, *J. Am. Chem. Soc.* **2014**, *136*, 1774-1777.
- (71) J. Chen, E. Y. X. Chen, *Isr. J. Chem.* **2015**, *55*, 216-225.
- (72) H. Zhang, Y. Nie, X. Zhi, H. Du, J. Yang, *Chem. Commun.* **2017**, *53*, 5155-5158.
- (73) N. von Seggern, T. Schindler, S. Naumann, *Biomacromolecules* **2020**, *21*, 2661-2669.
- (74) R. Gompper, H. Schaefer, *Chem. Ber.* **1967**, *100*, 591-604.
- (75) a) *Base Catalysts for Organopolymerization in Organic Catalysis for Polymerisation* (Eds.: A. P. Dove, H. Sardon, S. Naumann), The Royal Society of Chemistry, Cambridge, **2018**, pp. 121-197; b) S. Naumann, *Chem. Commun.* **2019**, *55*, 11658-11670.
- (76) K. Powers, C. Hering-Junghans, R. McDonald, M. J. Ferguson, E. Rivard, *Polyhedron* **2016**, *108*, 8-14.
- (77) B. Radziszewski, *Chem. Ber.* **1882**, *15*, 1493-1496.
- (78) M. M. Hansmann, P. W. Antoni, H. Pesch, *Angew. Chem. Int. Ed.* **2020**, *59*, 5782-5787; *Angew. Chem.* **2020**, *132*, 5831-5836.
- (79) H. Zhou, R. Zhang, X.-B. Lu, *Adv. Synth. Catal.* **2019**, *361*, 326-334.

- (80) J. Meisner, J. Karwounopoulos, P. Walther, J. Kästner, S. Naumann, *Molecules* **2018**, *23*, 432.
- (81) B. Maji, H. Mayr, *Angew Chem Int Ed Engl* **2012**, *51*, 10408-10412; *Angew. Chem.* **2012**, 10554-10558.
- (82) R. Breslow, *J. Am. Chem. Soc.* **1958**, *80*, 3719-3726.
- (83) J. Nakayama, K. Akimoto, Y. Sugihara, *Tetrahedron Lett.* **1998**, *39*, 5587-5590.
- (84) W. Li, N. Yang, Y. Lyu, *J. Org. Chem.* **2016**, *81*, 5303-5313.
- (85) H. Zhou, G.-X. Wang, X.-B. Lu, *Asian Journal of Organic Chemistry* **2017**, *6*, 1264-1269.
- (86) H. Zhou, R. Zhang, S. Mu, H. Zhang, X. B. Lu, *ChemCatChem* **2019**, *11*, 5728-5732.
- (87) L. H. Finger, J. Guschlbauer, K. Harms, J. Sundermeyer, *Chemistry* **2016**, *22*, 16292-16303.
- (88) C. Hering-Junghans, I. C. Watson, M. J. Ferguson, R. McDonald, E. Rivard, *Dalton Trans* **2017**, *46*, 7150-7153.
- (89) M. Blumel, R. D. Crocker, J. B. Harper, D. Enders, T. V. Nguyen, *Chem. Commun.* **2016**, *52*, 7958-7961.
- (90) U. Kaya, U. P. Tran, D. Enders, J. Ho, T. V. Nguyen, *Org. Lett.* **2017**, *19*, 1398-1401.
- (91) D. Mandal, S. Chandra, N. I. Neuman, A. Mahata, A. Sarkar, A. Kundu, S. Anga, H. Rawat, C. Schulzke, K. R. Mote, B. Sarkar, V. Chandrasekhar, A. Jana, *Chemistry* **2020**, *26*, 5951-5955.
- (92) A. El-Hellani, J. Monot, R. Guillot, C. Bour, V. Gandon, *Inorg. Chem.* **2013**, *52*, 506-514.
- (93) Y. Wang, M. Y. Abraham, R. J. Gilliard, D. R. Sexton, P. Wei, G. H. Robinson, *Organometallics* **2013**, *32*, 6639-6642.
- (94) W. H. Lee, Y. F. Lin, G. H. Lee, S. M. Peng, C. W. Chiu, *Dalton Trans.* **2016**, *45*, 5937-5940.
- (95) C. Hering-Junghans, P. Andreiuk, M. J. Ferguson, R. McDonald, E. Rivard, *Angew. Chem. Int. Ed.* **2017**, *56*, 6272-6275; *Angew. Chem.* **2017**, *129*, 6368-6372.
- (96) E. Hupf, F. Kaiser, P. A. Lummis, M. M. D. Roy, R. McDonald, M. J. Ferguson, F. E. Kuhn, E. Rivard, *Inorg. Chem.* **2020**, *59*, 1592-1601.
- (97) P. P. Ponti, J. C. Baldwin, W. C. Kaska, *Inorg. Chem.* **1979**, *18*, 873-875.
- (98) H. Schumann, M. Glanz, J. Winterfeld, H. Hemling, N. Kuhn, H. Bohnen, D. Bläser, R. Boese, *J. Organomet. Chem.* **1995**, *493*, C14-C18.
- (99) S. Kronig, P. G. Jones, M. Tamm, *Eur. J. Inorg. Chem.* **2013**, *2013*, 2301-2314.
- (100) D. A. Imbrich, W. Frey, S. Naumann, M. R. Buchmeiser, *Chem. Commun.* **2016**, *52*, 6099-6102.
- (101) a) M. Iglesias, A. Iturmendi, P. J. Sanz Miguel, V. Polo, J. J. Perez-Torrente, L. A. Oro, *Chem. Commun.* **2015**, *51*, 12431-12434; b) A. Iturmendi, N. Garcia, E. A. Jaseer, J. Munarriz, P. J. Sanz Miguel, V. Polo, M. Iglesias, L. A. Oro, *Dalton Trans.* **2016**, *45*, 12835-12845.
- (102) I. C. Watson, A. Schumann, H. Yu, E. C. Davy, R. McDonald, M. J. Ferguson, C. Hering-Junghans, E. Rivard, *Chemistry* **2019**, *25*, 9678-9690.
- (103) W. H. Carothers, G. L. Dorough, F. J. v. Natta, *J. Am. Chem. Soc.* **1932**, *54*, 761-772.
- (104) a) C. Jerome, P. Lecomte, *Adv Drug Deliv Rev* **2008**, *60*, 1056-1076; b) S. Dutta, W.-C. Hung, B.-H. Huang, C.-C. Lin, *Recent Developments in Metal-Catalyzed Ring-Opening Polymerization of Lactides and Glycolides: Preparation of Poly(lactides), Polyglycolide, and Poly(lactide-co-glycolide) in Synthetic Biodegradable Polymers* (Eds.: B. Rieger, A. Künkel, G. W. Coates, R. Reichardt, E. Dinjus, T. A. Zevaco), Springer Berlin Heidelberg, Berlin, Heidelberg, **2012**, pp. 219-283; c) P. Lecomte, C.

- Jérôme, *Recent Developments in Ring-Opening Polymerization of Lactones in Synthetic Biodegradable Polymers* (Eds.: B. Rieger, A. Künkel, G. W. Coates, R. Reichardt, E. Dinjus, T. A. Zevaco), Springer Berlin Heidelberg, Berlin, Heidelberg, **2012**, pp. 173-217; d) A.-C. Albertsson, I. K. Varma, *Biomacromolecules* **2003**, *4*, 1466-1486.
- (105) A.-M. Carnival, J. Halleux, G. G.-Q. Chen, D. M. Wiles, C. Jerome, P. Lecomte, P. A. M. Lips, P. J. Dijkstra, P. J. Halley, A. J. Varma, D. Plackett, T. M. Keenan, S. W. Tanenbaum, J. P. Nakas, J.-F. Zhang, X. Sun, K. Dean, L. Yu, G. Scott, M. Bhattacharya, R. L. Reis, V. Correlo, L. Boesel, S. Matumura, G. Madras, D. M. Wiles, G. Scott, S. Guilbert, P. Feuilloley, H. Bewa, V. Bellon-Maurel, *Biodegradable Polymers for Industrial Applications*, Woodhead Publishing Limited, Cambridge, **2005**.
- (106) A. Kowalski, A. Duda, S. Penczek, *Macromol. Rapid Commun.* **1998**, *19*, 567-572.
- (107) a) M. C. Tanzi, P. Verderio, M. G. Lampugnani, M. Resnati, E. Dejana, E. Sturani, *J. Mater. Sci. Mater. Med.* **1994**, *5*, 393-396; b) T. Yamada, D.-Y. Jung, R. Sawada, T. Tsuchiya, *J. Biomed. Mater. Res. B Appl. Biomater.* **2008**, *87B*, 381-386.
- (108) A. Stjerndahl, A. F. Wistrand, A.-C. Albertsson, *Biomacromolecules* **2007**, *8*, 937-940.
- (109) P. Degée, P. Dubois, R. Jérôme, S. Jacobsen, H.-G. Fritz, *Macromol. Symp.* **1999**, *144*, 289-302.
- (110) W. M. Stevels, M. J. K. Ankoné, P. J. Dijkstra, J. Feijen, *Macromolecules* **1996**, *29*, 8296-8303.
- (111) a) M. H. Chisholm, C.-C. Lin, J. C. Gallucci, B.-T. Ko, *Dalton Trans.* **2003**, 406-412; b) B.-T. Ko, C.-C. Lin, *J. Am. Chem. Soc.* **2001**, *123*, 7973-7977.
- (112) a) H. Ma, J. Okuda, *Macromolecules* **2005**, *38*, 2665-2673; b) H. Ma, T. P. Spaniol, J. Okuda, *Angew. Chem. Int. Ed.* **2006**, *45*, 7818-7821; *Angew. Chem.* **2006**, *118*, 7982-7985.
- (113) a) L. R. Rieth, D. R. Moore, E. B. Lobkovsky, G. W. Coates, *J. Am. Chem. Soc.* **2002**, *124*, 15239-15248; b) A. P. Dove, V. C. Gibson, E. L. Marshall, H. S. Rzepa, A. J. P. White, D. J. Williams, *J. Am. Chem. Soc.* **2006**, *128*, 9834-9843.
- (114) a) A. Amgoune, C. M. Thomas, J.-F. Carpentier, *Macromol. Rapid Commun.* **2007**, *28*, 693-697; b) A. Amgoune, C. M. Thomas, S. Ilinca, T. Roisnel, J.-F. Carpentier, *Angew. Chem. Int. Ed.* **2006**, *45*, 2782-2784; *Angew. Chem.* **2006**, *118*, 2848-2850.
- (115) T. M. Ovitt, G. W. Coates, *J. Polym. Sci., Part A: Polym. Chem.* **2000**, *38*, 4686-4692.
- (116) Z. Zhong, P. J. Dijkstra, J. Feijen, *J. Am. Chem. Soc.* **2003**, *125*, 11291-11298.
- (117) F. Nederberg, E. F. Connor, M. Möller, T. Glauser, J. L. Hedrick, *Angew. Chem. Int. Ed.* **2001**, *40*, 2712-2715; *Angew. Chem.* **2001**, *113*, 2784-2787.
- (118) a) B. G. G. Lohmeijer, R. C. Pratt, F. Leibfarth, J. W. Logan, D. A. Long, A. P. Dove, F. Nederberger, J. Choi, C. Wade, R. M. Waymouth, J. L. Hedrick, *Macromolecules* **2006**, *39*, 8574-8583; b) R. C. Pratt, B. G. G. Lohmeijer, D. A. Long, R. M. Waymouth, J. L. Hedrick, *J. Am. Chem. Soc.* **2006**, *128*, 4556-4557.
- (119) A. P. Dove, R. C. Pratt, B. G. Lohmeijer, R. M. Waymouth, J. L. Hedrick, *J. Am. Chem. Soc.* **2005**, *127*, 13798-13799.
- (120) a) G. W. Nyce, T. Glauser, E. F. Connor, A. Möck, R. M. Waymouth, J. L. Hedrick, *J. Am. Chem. Soc.* **2003**, *125*, 3046-3056; b) S. Csihony, D. A. Culkin, A. C. Sentman, A. P. Dove, R. M. Waymouth, J. L. Hedrick, *J. Am. Chem. Soc.* **2005**, *127*, 9079-9084; c) N. E. Kamber, W. Jeong, S. Gonzalez, J. L. Hedrick, R. M. Waymouth, *Macromolecules* **2009**, *42*, 1634-1639.
- (121) W. Jeong, J. L. Hedrick, R. M. Waymouth, *J. Am. Chem. Soc.* **2007**, *129*, 8414-8415.

- (122) G. W. Nyce, S. Csihony, R. M. Waymouth, J. L. Hedrick, *Chem. Eur. J.* **2004**, *10*, 4073-4079.
- (123) U. Hiroshi, K. Shiro, *Chem. Lett.* **1993**, *22*, 1149-1150.
- (124) a) I. van der Meulen, M. de Geus, H. Antheunis, R. Deumens, E. A. J. Joosten, C. E. Koning, A. Heise, *Biomacromolecules* **2008**, *9*, 3404-3410; b) J. Cai, B. S. Hsiao, R. A. Gross, *Polym. Int.* **2009**, *58*, 944-953; c) J. Engel, A. Cordellier, L. Huang, S. Kara, *ChemCatChem* **2019**, *11*, 4983-4997.
- (125) D. Mecerreyes, R. Jérôme, P. Dubois, *Novel Macromolecular Architectures Based on Aliphatic Polyesters: Relevance of the "Coordination-Insertion" Ring-Opening Polymerization* in *Adv. Polym. Sci., Vol. 147*, Springer-Verlag, **1999**.
- (126) J. Liu, L. Liu, *Macromolecules* **2004**, *37*, 2674-2676.
- (127) P. Degée, P. Dubois, R. Jérôme, *Macromol. Chem. Phys.* **1997**, *198*, 1973-1984.
- (128) D. Patel, S. T. Liddle, S. A. Mungur, M. Rodden, A. J. Blake, P. L. Arnold, *Chem. Commun.* **2006**, 1124-1126.
- (129) P. L. Arnold, I. J. Casely, Z. R. Turner, R. Bellabarba, R. B. Tooze, *Dalton Trans.* **2009**, 7236-7247.
- (130) Y. A. Chang, R. M. Waymouth, *Polym. Chem.* **2015**, *6*, 5212-5218.
- (131) E. Piedra-Aroni, C. Ladavière, A. Amgoune, D. Bourissou, *J. Am. Chem. Soc.* **2013**, *135*, 13306-13309.
- (132) A. Pietrangelo, S. C. Knight, A. K. Gupta, L. J. Yao, M. A. Hillmyer, W. B. Tolman, *J. Am. Chem. Soc.* **2010**, *132*, 11649-11657.
- (133) a) H. Quast, M. Ach, M. K. Kindermann, P. Rademacher, M. Schindler, *Chem. Ber.* **1993**, *126*, 503-516; b) S. Kronig, P. G. Jones, M. Tamm, *Eur. J. Inorg. Chem.* **2013**, *2013*, 2301-2314.
- (134) H. Quast, M. Ach, M. K. Kindermann, P. Rademacher, M. Schindler, *Chem. Ber.* **1993**, *126*, 503-516.
- (135) a) M. Hans, J. Lorkowski, A. Demonceau, L. Delaude, *Beilstein J. Org. Chem.* **2015**, *11*, 2318-2325; b) C. E. Knappke, J. M. Neudorfl, A. J. von Wangelin, *Org. Biomol. Chem.* **2010**, *8*, 1695-1705; c) K. Hirano, S. Urban, C. Wang, F. Glorius, *Org. Lett.* **2008**, *11*, 1019-1022; d) M. Iglesias, D. J. Beetstra, J. C. Knight, L.-L. Ooi, A. Stasch, S. Coles, L. Male, M. B. Hursthouse, K. J. Cavell, A. Dervisi, I. A. Fallis, *Organometallics* **2008**, *27*, 3279-3289.
- (136) T. Dudev, C. Lim, *J. Am. Chem. Soc.* **1998**, *120*, 4450-4458.
- (137) A. Wurtz, *Ann. Chim. Phys.* **1863**, *69*, 317-355.
- (138) A. Deffieux, S. Boileau, *Polymer* **1977**, *18*, 1047-1050.
- (139) a) A. Stolarzewicz, D. Neugebauer, Z. Grobelny, *Macromol. Chem. Phys.* **1995**, *196*, 1295-1300; b) A. Stolarzewicz, D. Neugebauer, J. Grobelny, *Macromol. Rapid Commun.* **1996**, *17*, 787-793.
- (140) R. G. Pearson, *J. Am. Chem. Soc.* **1963**, *85*, 3533-3539.
- (141) C. A. Finch, *Anionic Polymerisation to Cationic Polymerisation* in *Encyclopedia of Polymer Science and Engineering, Vol. 2* (Eds.: H. F. Mark, N. M. Bikales, C. G. Overberger, G. Menges), Wiley-Interscience, New York, **1985**.
- (142) N. Platzner, *Encyclopedia of Polymer Science and Engineering, Vol. 2*, Wiley-Interscience, New York, **1986**.
- (143) C. Price, *Acc. Chem. Res.* **1974**, *7*, 294-301.
- (144) I. Dimitrov, C. B. Tsvetanov, *High-Molecular-Weight Poly(ethylene oxide) in Polymer Science: A Comprehensive Reference, Vol. 4*, **2012**, pp. 551-569.
- (145) G. L. Goeke, F. J. Karol, *Process for Preparing Olefin Oxide Polymerization Catalysts by Aging the Catalysts* **1980**, U.S. 4193892 A.
- (146) E. J. Vandenberg, *J. Polym. Sci.* **1960**, *47*, 486-489.

- (147) D. A. Berta, E. J. Vandenberg, in *Handbook of Elastomers* (Eds.: A. K. Bhowmick, H. L. Stephens), Marcel Dekker, New York, **2001**, pp. 683-697.
- (148) J. W. Kramer, D. S. Treitler, E. W. Dunn, P. M. Castro, T. Roisnel, C. M. Thomas, G. W. Coates, *J. Am. Chem. Soc.* **2009**, *131*, 16042–16044.
- (149) G.-W. Yang, Y.-Y. Zhang, R. Xie, G.-P. Wu, *Angew. Chem. Int. Ed.* **2020**, DOI: 10.1002/anie.202002815; *Angew. Chem.* **2020**, DOI: 10.1002/ange.202002815.
- (150) A.-L. Brocas, C. Mantzaridis, D. Tunc, S. Carlotti, *Prog. Polym. Sci.* **2013**, *38*, 845-873.
- (151) C. Billouard, S. Carlotti, P. Desbois, A. Deffieux, *Macromolecules* **2004**, *37*, 4038-4043.
- (152) V. Rejsek, P. Desbois, A. Deffieux, S. Carlotti, *Polymer* **2010**, *51*, 5674-5679.
- (153) a) S. Carlotti, A. Labbé, V. Rejsek, S. Doutaz, M. Gervais, A. Deffieux, *Macromolecules* **2008**, *41*, 7058-7062; b) A.-L. Brocas, M. Gervais, S. Carlotti, S. Pispas, *Polym. Chem.* **2012**, *3*, 2148-2155.
- (154) A. J. Arduengo, R. L. Harlow, M. Kline, *J. Am. Chem. Soc.* **1991**, *113*, 361-363.
- (155) M. Fèvre, J. Pinaud, Y. Gnanou, J. Vignolle, D. Taton, *Chem. Soc. Rev.* **2013**, *42*, 2142-2172.
- (156) J. Raynaud, C. Absalon, Y. Gnanou, D. Taton, *J. Am. Chem. Soc.* **2009**, *131*, 3201-3209.
- (157) J. Raynaud, W. N. Ottou, Y. Gnanou, D. Taton, *Chem. Commun.* **2010**, *46*, 3203-3205.
- (158) B. Eßwein, N. M. Steidl, M. Möller, *Macromol. Rapid Commun.* **1996**, *17*, 143-148.
- (159) J. Zhao, D. Pahovnik, Y. Gnanou, N. Hadjichristidis, *Polym. Chem.* **2014**, *5*, 3750-3753.
- (160) A. A. Toy, S. Reinicke, A. H. E. Müller, H. Schmalz, *Macromolecules* **2007**, *40*, 5241-5244.
- (161) J. Zhao, D. Pahovnik, Y. Gnanou, N. Hadjichristidis, *Macromolecules* **2014**, *47*, 3814-3822.
- (162) H. R. Johnson, *Method of Making a Polyether Using a Double Metal Cyanide Complex Compound* **1966**, U.S. 3278459.
- (163) M. Ionescu, *Chemistry and Technology of Polyols for Polyurethanes*, Rapra Technology, **2005**.
- (164) Y. J. Huang, G. R. Qi, L. S. Chen, *Appl. Catal., A* **2003**, *240*, 263-271.
- (165) a) Y.-J. Huang, X.-H. Zhang, Z.-J. Hua, S.-L. Chen, G.-R. Qi, *Macromol. Chem. Phys.* **2010**, *211*, 1229-1237; b) I. Kim, J.-T. Ahn, C. S. Ha, C. S. Yang, I. Park, *Polymer* **2003**, *44*, 3417-3428.
- (166) K. S. Clement, L. L. Walker, R. M. Wehmeyer, R. H. Whitmarsh, D. C. Molzahn, W. P. Dianis, D. E. Laycock, J. W. Weston, R. J. Elwell, *Polymerization of Ethylene Oxide Using Metal Cyanide Catalysts* **2002**, U.S. 6642423.
- (167) a) R.-J. Wei, X.-H. Zhang, Y.-Y. Zhang, B.-Y. Du, Z.-Q. Fan, G.-R. Qi, *RSC Adv.* **2014**, *4*, 3188-3194; b) D. J. Darensbourg, M. J. Adams, J. C. Yarbrough, *Inorg. Chem.* **2001**, *40*, 6543-6544.
- (168) Z. Hua, G. Qi, S. Chen, *J. Appl. Polym. Sci.* **2004**, *93*, 1788-1792.
- (169) a) S. Penczek, P. Kubisa, K. Matyjaszewski, J. P. Kennedy, *Cationic Ring-Opening Polymerization: 2. Synthetic Applications*, Springer-Verlag, Berlin, **1985**; b) K. Matyjaszewski, M. Möller, *Polymer Science: A Comprehensive Reference*, Elsevier Science, Amsterdam, **2012**.
- (170) S. Penczek, P. Kubisa, R. Szymański, *Makromol. Chem., Macromol. Symp.* **1986**, *3*, 203-220.

- (171) T. Biedron, K. Brzezinska, P. Kubisa, S. Penczek, *Polym. Int.* **1995**, *36*, 73-80.
- (172) A. I. Ojeda-Amador, A. J. Martínez-Martínez, G. M. Robertson, S. D. Robertson, A. R. Kennedy, C. T. O'Hara, *Dalton Trans.* **2017**, *46*, 6392-6403.